DIPOP
DIFFERENTIAL POSITIONING PACKAGE FOR THE GLOBAL POSITIONING SYSTEM

P. VANICEK
G. BEUTLER
A. KLEUSBERG
R. B. LANGLEY
R. SANTERRE
D. E. WELLS

August 1985

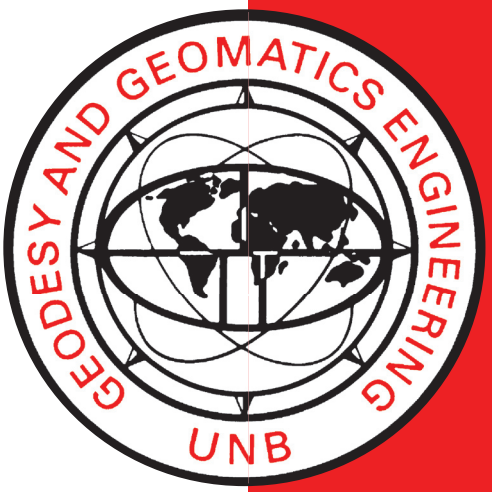

TECHNICAL REPORT
NO. 115

PREFACE

In order to make our extensive series of technical reports more readily available, we have scanned the old master copies and produced electronic versions in Portable Document Format. The quality of the images varies depending on the quality of the originals. The images have not been converted to searchable text.

DIPOP: DIFFERENTIAL POSITIONING PACKAGE FOR THE GLOBAL POSITIONING SYSTEM

P. Vanícek
G. Beutler
A. Kleusberg
R.B. Langley
R. Santerre
D.E. Wells

Department of Surveying Engineering
University of New Brunswick
P.O. Box 4400
Fredericton, N.B.
Canada
E3B 5A3

August 1985
Latest Reprinting February 1994

FOREWORD

This technical report is the final contract report prepared for the Geodetic Survey of Canada (GSC) under the terms of contract DSS No. OST83-00353 (DSS File No. 24ST.23244-3-4574). The Scientific Authority at GSC for this contract was Dr. Demitris Delikaraoglou. The Principal Investigator (Project Coordinator) was Petr Vanicek with Richard Langley and David Wells as co-Principal Investigators.

Parts of the work reported herein were funded by two Natural Sciences and Engineering Research Council of Canada (NSERC) Strategic Research Grants (Nos. G0757 - Marine Geodesy, and G1488 - Marine Geodesy Applications), two NSERC Operating Grants (Nos. A8452 - Applications of Radio Interferometry in Geodesy and Geodynamics, and A1219 - Arctic Navigation/Satellite Positioning), and an NSERC International Scientific Exchange Award (No. IS-0112) to support the visit of Gerhard Beutler, who was on leave of absence from his University. Support under the New Technology Employment program of Employment and Immigration Canada also contributed to this work.

We wish to acknowledge gratefully the diverse assistance we have received from Dr. D. Delikaraoglou. Mr. R. Moreau, Recherche Territoriale, Ministère de l'Energie et des Ressources, Québec, was instrumental in arranging for us to have access to the data from the Québec experiment (section 5.2.2). We also wish to thank Ms. W. Wells for her, as usual, flawless word processing of this report.

TABLE OF CONTENTS

Table of Contents

LIST OF FIGURES

LIST OF TABLES

SYMBOL CONVENTION

A_o, A_1, A_2,... : receiver clock coefficients (offset, linear drift, quadratic drift, ...)

A_X : design matrix of station coordinates

A_Λ : design matrix of nuisance parameters

n_{ij}^k : single difference ambiguity parameters

$n_{ij}^{k\ell}$: double difference ambiguity parameters

n : ambiguity parameters in general

N : normal matrix $(A^T P_\ell A)$

N_{XX} : normal matrix for station coordinates

$N_{X\Lambda}$: normal matrix for station coordinates and nuisance parameters

$N_{\Lambda\Lambda}$: normal matrix for nuisance parameters

Λ : nuisance parameters {n, α, σ, ...} in general

o^k : particular satellite orbital elements

o : orbital elements in general

$\vec{R}$: station position coordinates

$\vec{r}$: satellite coordinates

P_ℓ : weight matrix of observations

P_X : a priori weight matrix for station coordinates

P_Λ : a priori weight matrix for nuisance parameters

U_X : right-hand side of the normal equation for station coordinates $(A_X^T P_\ell W)$

U_Λ : right-hand side of the normal equation for nuisance parameters $(A_\Lambda^T P_\ell W)$

W : misclosure vectors

X : all station coordinates $\{\vec{R}_1, \vec{R}_2, \ldots, \vec{R}_n\}$

V : residuals

ε : noise

ϕ : phase of a signal carrier; latitude

λ : wavelength of carrier; longitude

h : height above reference ellipsoid

H^o : orthometric height

$\Delta\tilde{\rho}_{ij}^{k}$: observed single difference

$\Delta\rho_{ij}^{k}$: computed single difference

$\Delta^2\tilde{\rho}_{ij}^{k\ell}$: observed double difference

$\Delta^2\rho_{ij}^{k\ell}$: computed double difference

$V^{k\ell}$: double difference residuals

$\Delta_I^2\rho_{ij}^{k\ell}$: ionospheric refraction for double difference

$\Delta_T^2\rho_{ij}^{k\ell}$: tropospheric refraction for double differnce

$\dot{\rho}_i^{\ell}$: range rate (station i satellite ℓ)

ρ_i^j : range from station i to satellite j

$\Delta t^{k\ell}$: synchronization error of satellite clock ℓ with respect to satellite clock k

ΔT_{ij} : synchronization error of receiver clock j with respect to receiver clock i

$\vec{e}_i^{\,k}$: unit vector station i, satellite k

$\vec{r}^{\,j}$: position vector of satellite position S^j

$\vec{R}_i$: position vector of ground station P_i

$\vec{\rho}_i^{\,j}$: range vector from $\vec{R}_i$ to $\vec{r}^{\,j}$. ρ_i^j is the length of $\vec{\rho}_i^{\,j}$

c : velocity of light in a vacuum

1. INTRODUCTION

According to the terms of this contract, we were supposed to address the following problems:

(i) existing temporal and spatial correlations and correlations between different kinds of GPS observables;

(ii) practical methodology and algorithm structure for implementing these correlations;

(iii) degree of elaboration of the force field required to achieve a given accuracy of orbital arcs of a given length, and detailed evaluation of the different options of orbital bias modelling;

(iv) different approaches suitable for resolving the ambiguities inherent in GPS carrier phase measurements;

(v) software performance under real conditions, i.e., processing real data from different GPS receivers such as the Macrometer™ V-1000, Texas Instruments TI-4100, and possibly SERIES.

These problems were to be addressed in part by means of software implemented on the HP 1000 minicomputer.

To use the HP 1000, we found it necessary to substantially modify the existing program VECA (see Langley et al. [1984]). The VECA program was originally designed for the UNB mainframe computer and consequently difficult to transplant economically onto the HP 1000. The other reason for the modification was the necessity for the program to cope with data collected by different types of receivers. These data are available in vastly different formats and structures.

To avoid having to change the basic philosophy of the software every time a new development comes about, we had decided first to define what an ideal GPS-geodetic-differential-positioning software package should do. This we have done in Chapter 2.

Another decision was taken, also at the beginning of the contractual period, to structure the software so that it would consist of three basic units: a set of preprocessors, the main processor, and a postprocessor. Each particular type of receiver would have a special preprocessor developed for it, while the main processor and the postprocessor would be common to all types of receivers. The two preprocessors developed under the auspices of this contract, one for the Macrometer™ V-1000 and one for

the TI-4100 receivers, are described in section 3.2. Section 3.3 is devoted to the main processor, while the postprocessor is described in section 3.5.

Problems (iii) and (iv) required by the contract were tackled in the first report [Beutler et al., 1984] submitted earlier during the life of this contract. Here we only expose the overall strategy for dealing with biases in the model (section 3.4.1) and summarize our findings (in sections 3.4.2 and 3.4.3).

Concerning contract item (iii), we have gone as far as we thought was required for the double difference mode (cf. section 3.4.2 and Beutler et al. [1984]). Optimal modelling of orbital biases for single difference and range modes, if desired, would possibly require some additional work.

We feel that we have solved the ambiguity problem (item (iv)) adequately by adopting a two-stage elimination process (first step within the preprocessing stage, second step during the main processing). A comparative performance of this part of the algorithm is investigated in a separate paper [Vaníček et al., 1985] appended to this report (Appendix B). Our ambiguity results should be now systematically compared with those obtained by Geodetic Survey of Canada, who use a different algorithm in their software.

Correlations, spatial as well as temporal, between GPS observations (contract item (i)) remain a problem. We have investigated the effect of mathematical correlations on resulting positions, and found it to be relatively unimportant (cf. Chapter 4). We feel that physical correlations will probably be appreciably more significant. Their estimation and modelling, however, was far beyond our capabilities under this contract. In Chapter 4, we outline a theoretical approach which, we believe, would lead to a formulation of a covariance model for GPS observables. The architecture of DIPOP's main processor was designed to allow a relatively easy implementation of a nondiagonal weight matrix of the observations (contract item (ii)) once its elements can be analytically generated from a meaningful covariance model.

Item (v) of the contract is addressed in Chapter 5, where we describe the data processing and results from three different campaigns involving the Macrometer™ V-1000 and TI-4100 receivers. For the user of our software to get the most comprehensive view of the data processing and the results,

the postprocessor (section 3.5) was designed in such a way as to output every possible piece of information one may wish to have. Many of these pieces are, however, optional and as such may be suppressed in the output.

The software performs well with real data giving numerically identical results with the "old" Macrometer™ programs PRMAC3 and PRMNET for the IBM [Beutler, 1984], wherever a direct comparison is possible. The speed of processing has dramatically increased compared to the VECA transplanted from the mainframe computer. Preprocessors tailored to other types of GPS receivers may be added to the software as new types become available.

We feel that we have succeeded in producing a tool capable of processing in a "user-friendly" manner data acquired in the field on a routine basis. This tool may be developed further along the individual lines as described above to bring it closer to the ideal GPS software. It also will be capable of helping to solve some of the remaining scientific questions.

Throughout this report, we use the term "session" to describe that part of a field campaign which is characterized by a unique (non-overlapping) set of nuisance parameters (biases). In all the developed software, dates are denoted by the modified Julian dates (MJD) (except for the TI-4100 preprocessor, where the GPS timing in Z-count [Wells et al., 1981] is used internally), and individual satellites are referred to by the part of the P-code (PRN) they transmit.

For those readers who are interested in the more intimate details of the software described here, Technical Memorandum 6 [Santerre et al., 1985] is available which describes the inner workings of the program. Technical Memorandum 6 also contains the user's guide for the program.

2. IDEAL SOFTWARE FOR GEODETIC APPLICATIONS OF GPS

To a major extent, the architecture of GPS software is determined by the way in which the GPS observations were collected. In order to discuss the ideal (or even merely desirable) characteristics of GPS software, we must first look carefully at the observing strategy which will generate the data the software would be designed to handle. If we are to consider "ideal" software, its usefulness must not be limited to the present development phase of GPS.

In this chapter we look at the implications on GPS observing and processing strategies of the advent of the full GPS satellite constellation, and of plentiful relatively inexpensive receivers.

2.1. Present and Future Observing Strategies

Present GPS observing strategies have evolved while there have been two severe limitations (the incomplete satellite constellation, and scarce, expensive receivers) on the quantity of GPS data available. Both these limitations will be removed over the next few years, as the full GPS constellation is completed and as the competition between receiver manufacturers, for the considerable GPS market, works to decrease the cost and increase the availability of receivers. Let us look at the impact of each of these limitations on present observing strategies, and the impact of their removal on future strategies.

First we introduce the concept of an observing "session." In this section we define an observing session as the occupation of a single station by a specific receiver for a time span over which GPS signals are received continuously. If two receivers are being used at different stations, then the baseline observing session is the time span over which GPS signals are received continuously and simultaneously by both receivers. This latter agrees in practice with the definition of "session" given in the Introduction and used elsewhere in the report: That part of an observing campaign characterized by a unique set of biases. Since everywhere else we implicitly work with baselines, the distinction made here is unnecessary.

The present limited constellation of prototype GPS satellites provides coverage for only a few hours per day, and usually with fewer satellites

available at any instant than will be the case when the full constellation is implemented. The limited daily time span has provided a natural break between observing sessions so that, so far, GPS data has been provided in convenient discretized "clumps." In most cases, the short duration of daily GPS coverage has precluded travel between stations, so that usually only one observing session per receiver per day is scheduled (or one baseline observing session per receiver pair per day).

GPS has been shown to be cost-effective in comparison with other space-based or terrestrial techniques, even today with the limited constellation and with presently available receivers. However, in comparison with predictions for the next few years, GPS receivers have been scarce and costly to purchase, lease, or rent. Therefore, in most cases, the minimum receiver complement (that is two, for baseline measurements) has been used. This has resulted in another convenient limitation to the data.

So far, a typical GPS survey has involved the measurement of one baseline per day, requiring two receivers. Some networks have been surveyed using three (see section 5.2.2), and occasionally more receivers [Bock et al., 1984], and splitting the daily GPS coverage into two sessions, with a middle gap for travel between stations. However, in these cases, the "baseline-by-baseline" mentality has persisted in planning the observing strategy and handling the data. A better three-receiver observing strategy has been proposed [Snay, 1985].

Once the full constellation is in place, however, and much less expensive GPS receivers are plentifully available, observing strategies will no longer be limited to the baseline-by-baseline approach. In fact the limitation may come from what data processing strategies are feasible. In order to contrast the present practice with what will soon be possible, let us examine two of the many possible future observing strategies.

One possible strategy which leads to simple logistics and simple data processing is the "star" strategy. In this case a few stations are selected as "monitor" stations and are continuously occupied. The other network points are briefly occupied by "roving" receivers. Only rover-to-monitor baselines are used in the network adjustment. Our results [Beutler et al., 1984] have shown that better results are achieved if all baselines are taken into account.

Another strategy which is not so simple logistically, but which allows incorporation of all possible station interconnections into the network adjustment, is the "rolling balloon" strategy. Assuming we have 24-hour GPS satellite coverage, n receivers available (e.g., $10 < n < 100$), and a network of u stations to be surveyed (e.g., $10\ n < u < 100\ n$). Then the rolling balloon observations would start at one "end" or along one boundary of the network and would move receivers to advanced stations in such a way that the receivers are always as closely spaced to each other as possible. This can be simply visualized as an enormous (compressible) balloon rolling over the network--the area of contact between the balloon and the network at any instant defining the extent of receiver distribution.

One rolling balloon receiver deployment strategy would be to transport receivers from stations uncovered behind the balloon to stations about to be covered by the balloon. This would mean that some fraction of the n receivers would always be in the process of being transported, or "rolled." Appendix A considers this problem for an idealized network geometry.

This strategy ignores an important point made by Snay [1985]. If a station is occupied only once, any set-up errors (miscentring, wrong height above mark) will be undetected. Only if each station is occupied at least three times will such set-up errors be uniquely attributable (assuming no more than one set-up per station has an error). This requirement in effect triples the receiver transportation logistics problem. Perhaps the above strategy could be modified by having receivers transported in three stages through the rolling balloon coverage. The star strategy suffers even more severely in the event of a set-up error at a monitor site.

2.2 Present and Future Data Processing Strategies

The basic GPS observations, be they code pseudoranges or carrier phase, are biased ranges. The challenge in processing GPS data is in how best to handle the biases in order to extract the true ranges. The biases originate from a small number of sources:

- imperfect clocks in both satellites and receivers;
- ionospheric and tropospheric delays;
- cycle ambiguities, in the case of carrier phase observations;
- orbit errors.

Several approaches can be taken to deal with these biases. If a bias

has a stable, well understood structure, it can be modelled, estimated, and removed from the data either through preprocessing (ambiguities), or estimated together with the station coordinates as nuisance parameters (tropospheric delay scaling, orbit biases). In some cases, additional observations can be used, either to directly measure the bias (ionospheric delay), or to derive a model for the bias (tropospheric delay). Finally, if a bias is perfectly linearly correlated across different data sets, it can be eliminated by differencing the data sets (clock biases).

This last approach warrants further discussion. The double differencing technique (differencing across satellites, to eliminate receiver clock biases, and across receivers, to eliminate satellite clock biases) works well. However, it introduces some mathematical correlations in the data which are not easy to take into account (see Chapter 4).

If r receivers continuously and simultaneously track s satellites, then there are $r(r - 1)\, s(s - 1)/4$ possible double difference data series which can be formed, only $(r - 1)\,(s - 1)$ of which will be independent. However, if there is a break in the data from any one of the four data series used to form a double difference, then data from the other three series are ignored for the duration of the break as well. Such breaks, if frequent enough, will tend to reduce the interdependence between double difference data series.

Let us illustrate this with a rather pathological case (see Figure 2.1). Assume simultaneous GPS (undifferenced) data series are observed at three stations (i, j, k) from four satellites (1, 2, 3, 4) for four hours. Assume also that, due to equipment, operator, or signal shading problems, one eighth of the data are lost (in convenient one-hour chunks as shown). The resulting "independent" double difference data series (inside the dashed square) suffer 50% data loss. The right column and bottom row which, in the case of no data loss, could be mathematically derived from these "independent" data series, can now be so derived only for half the valid data therein. They are no longer linearly dependent. From the physical point of view, since the satellite geometry changes with time, the data loss will result in different geometrical configurations being used for each of the three baselines, so we should expect that here too the linear dependence of the third baseline on the other two will be reduced. In the extreme, all $r(r - 1)\, s(s - 1)/4$ double difference series may be

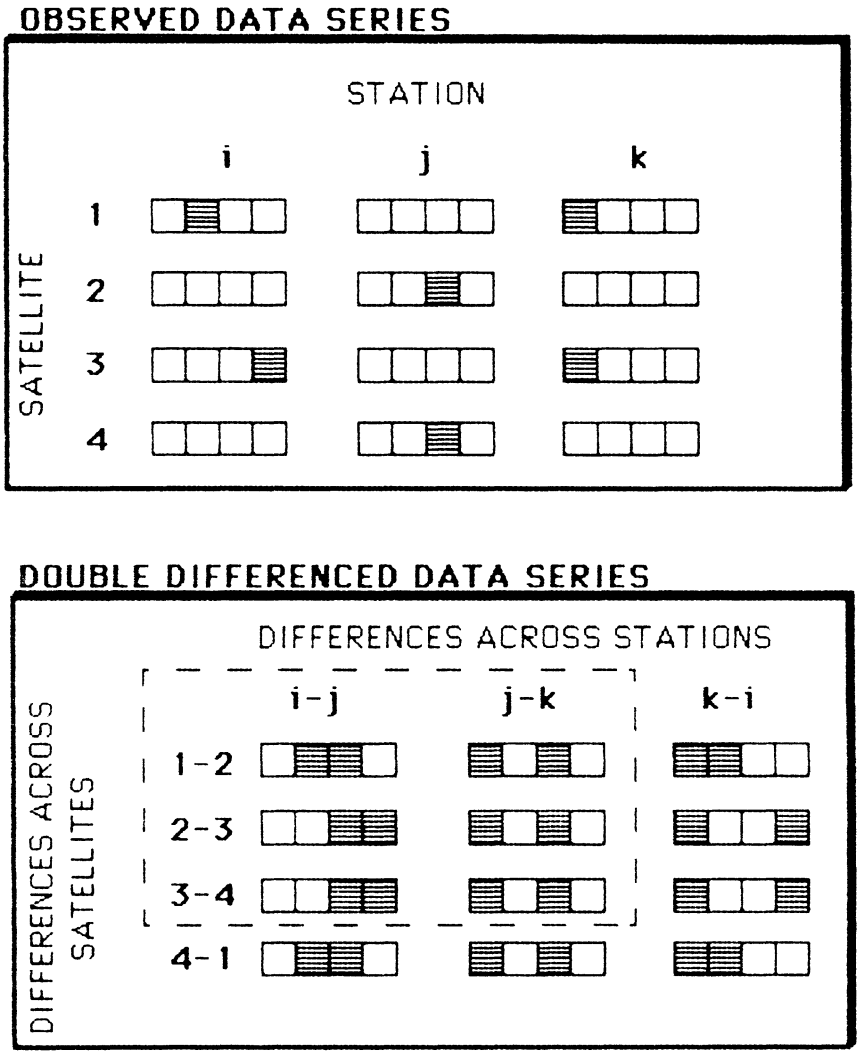

FIGURE 2.1

Effect of data loss on double differences.

independent.

In any case, even with the present baseline-by-baseline observing techniques, it is not always simple to decide how best to form the double differences. A multi-receiver campaign under 24-hour GPS coverage, and incorporating the triple set-ups at each station discussed in section 2.1, will involve many receiver moves and many possibilities for data breaks. The star strategy would come closest to maintaining the present baseline-by-baseline approach but, as discussed, is not without problems. It is worth while considering whether alternatives to double differencing can be devised, which will be as effective in handling clock biases. In particular, can the nuisance parameter approach be taken?

If we have phase measurements from s satellites at r receivers (i.e., r×s time series $\phi(t)$), to form the "traditional" single differences we subtract the time series between pairs of stations (eliminating the influence of satellite clock errors). This reduces the number of time series from rv×s to (r - 1)s.

If, instead, we were to introduce as nuisance parameters s time series of satellite clock bias parameters, one such time series for each satellite clock, the effect should similar. More specifically, consider the (simplified) observation equation:

$$\rho_i^j(t_k) = |r^j(t_k) - R_i| + \Delta t^j(t_k) - \Delta T_i(t_k) \quad , \tag{2.1}$$

where Δt^j represents the satellite clock error, and ΔT_i the receiver clock error, both with respect to GPS system time. In the differencing approach, we subtract two such equations from different stations i, in which case the $\Delta t^j(t_k)$ term (which is independent of i) disappears. In the nuisance parameter estimation approach, we solve for independent values of $\Delta t^j(t_k)$ for each t_k, using observations from all stations i. (Note, if we were to explicitly eliminate the nuisance parameters from the normal equations, we would, in effect, return to the differencing approach.) The advantage of the nuisance parameter approach is that we can then work with "raw" phase measurements, and not have the complicated bookkeeping and correlation problems involved in processing differenced observations.

Similarly for double differences--instead of differencing between satellites, and (in the "traditional" method) reducing the number of

observational time series from (r - 1)s to (r - 1)(s - 1) (eliminating the influence of the receiver pair differential clock errors)--we could introduce instead r time series of receiver clock bias parameters.

We lose nothing from the degrees of freedom point of view. In the differencing approach we reduce the same number of observation time series as we add in the nuisance parameter estimation. And our flexibility is vastly improved. For example, merely by fiddling with the a priori weights on these nuisance parameter time series we can enforce the equivalent of single difference or double difference (and "partial" differencing) very easily. Also, by introducing some kind of serial correlation function (i.e., smoothing the nuisance parameter time series), we can effectively vary our model for these clocks from something that is considered completely uncorrelated (an independent nuisance parameter for each satellite and each receiver at each time epoch) to something having strong serial correlation over lengthy periods (equivalent to using a model with only a few nuisance parameters such as a truncated power series in time).

This would mean that one algorithm, with options on the nuisance parameter weighting and serial correlation, would effectively duplicate the phase, single, and double difference algorithms.

This approach would make it imperative to process all the observations from one epoch in one step. It would, however, place no limitations on which of the many possible observing strategies was used, the selection of which could then be made on other grounds (logistics, cost, time, etc.).

One of the complications in GPS data processing is the amount of data that may have to be processed; the collection rate for some types of receivers (e.g., TI-4100) is very high. Although each data point contributes to the solution, there must exist a rate optimal from the combined point of view of accuracy, computing cost, and observing time. Are the 60 data points used by Macrometer™ V-1000 the universally best count? What is the trade-off between observing time and the number of observations? These questions should be addressed in a systematic way.

3 DIFFERENTIAL POSITIONING PROGRAM - DIPOP

The present version of DIPOP consists of preprocessing units, the main processor and a postprocessor (Figure 3.1).

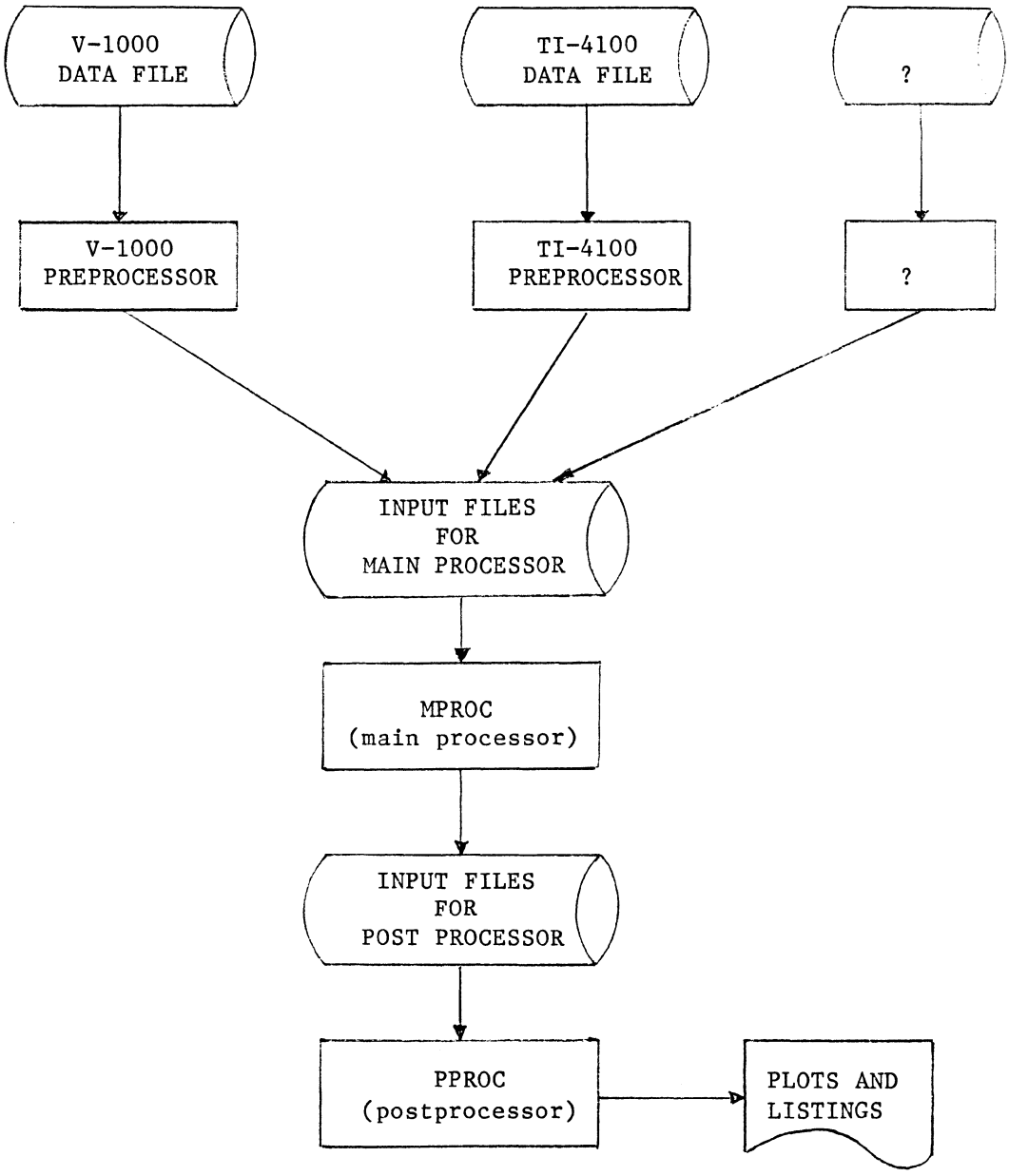

Figure 3.1. General program structure.

This structure has been chosen to deal with the differences in observation records and ephemeris representation of different types of receivers. The dedicated preprocessors (which may consist of several programs) take the observation and ephemeris data as provided for the different GPS types of receivers and create a standardized input file for the main processor. The preprocessing includes (not necessarily all items in every preprocessor):

- data decoding;
- detection of gross errors;
- data reduction;
- computation of either single or double differences;
- estimation of the accuracy of the observations;
- detection of cycle slips and estimation of the number of cycles jumped;
- computation of satellite coordinates in the CT system.

At present, separate preprocessors exist for the Macrometer™ V-1000 single frequency (see section 3.2.1) and TI-4100 dual frequency (see section 3.2.2) observations. For every observation epoch the preprocessors write one record into the main processor input file. The format of these records is described in Santerre et al. [1985].

These preprocessed data records provide the link to the main processor (MPROC). The MPROC program (see section 3.3) performs essentially a sequential least-squares adjustment with nuisance parameter elimination on demand. Parameter elimination has been employed to reduce the memory requirement. Nevertheless, all information needed to recompute the eliminated parameters at the end is stored on disk during processing. The main processor stores the results of each sequence of the sequential adjustment in the postprocessor input file.

The postprocessor (PPROC) then produces alphanumerical and graphical presentations of the results (see section 3.5). Each of the units shown in Figure 3.1 is complemented by an interactive program to set up command files for preprocessors, main processor, and postprocessor (see section 3.1). For details, see Santerre et al. [1985].

3.1 Operator Dialogue

For each of the four parts of our DIPOP package (Macrometer™ preprocessor, Texas Instruments preprocessor, main adjustment processor, and postprocessor) the operator will have to supply a variety of input data. The approach we have taken in each case is to store this data on a disc file, and to provide operator dialogue software which allows editing of the data on file. The files are coded ASCII files, however, so that utilities such as the HP Edit 1000 and HP File Manager can be used to list, archive, or edit the files independent of our software.

The architecture of the dialogue software is similar to that which we have used in the past for VECA. The software is command-driven rather than menu-driven or forms-driven. An earlier experience with attempting forms-driven dialogue software on the HP 1000, using the HP 2648A features, convinced us that it is not an effective route to take: such software is opaque and incomprehensible, inflexible and hard to modify, and device dependent.

It is our feeling that the development of menu-driven or forms-driven dialogue software would be more effectively and efficiently developed on a powerful personal computer (for example, the Apple Macintosh) for which menus and forms can easily be programmed. Such a computer could be interfaced as a terminal to the HP system, and would serve as the "front end" for complex software systems such as DIPOP. We propose that consideration be given to this alternative in future development.

The operator dialogue for each of the four packages is documented in the Operator's Guide (Appendix B).

3.2 Preprocessors

3.2.1 Macrometer™ V-1000 Preprocessor

To reflect the form of the observation record (see Santerre et al. [1985]), the preprocessor for the Macrometer™ V-1000 is composed of four different parts: program TRNTF; program MACPR; program PREMA; and program MACLN. The interaction between these parts is summarized by the flow chart in Figure 3.2. The description of each program is given in the next pages. Listings of the programs and their subroutines and a user's guide have been presented by Santerre et al. [1985]. The activity of the preprocessor is controlled by a command file created by the user interactively.

3.2.1.1 Program TRNTF

The program TRNTF is the HP 1000 version of program TRNSNEW originally written by G. Beutler [1984] for the IBM computer. Because of the size of this program and the memory capacity of the HP 1000 RTE-IVB, TRNTF is split into eight segments (RDFIL, SETUP, TRNT1, TRANS, TRNT2, TRNT3, TRNT4, and ORBIN) and uses the extended memory area (EMA) for large variables. The subroutines are stored in the files &T1LIB and &T2LIB. The data structure also differs slightly from the original IBM version.

TRNTF approximates the orbits of GPS satellites defined by the Macrometer™ T-files. The principle of the approximation is the following: User specifies the time interval in which he wants to approximate the orbits of all GPS satellites. All satellite positions in this time interval are extracted from the T-file by subroutine RDTFL or RDTFQ. Using these positions as "observations," an orbit improvement process is invoked, where the orbits are generated by numerical integration with the subroutines of the Bernese Intlib-library. For short arcs (typically less than 6 hours corresponding to one half of a revolution), a simple force field (e.g., J2, J3, J4 terms of the earth's gravitational field, lunar and solar attraction) may be used in the computations. The results of these orbit determinations, i.e., the coefficients of the polynomial approximation of the exact solutions for all the satellites in the T-file during the requested time interval as well as orbital elements given for a specific time, are then stored in the output file. This disc-file (T-A) is subsequently used to obtain observation misclosures. The above process,

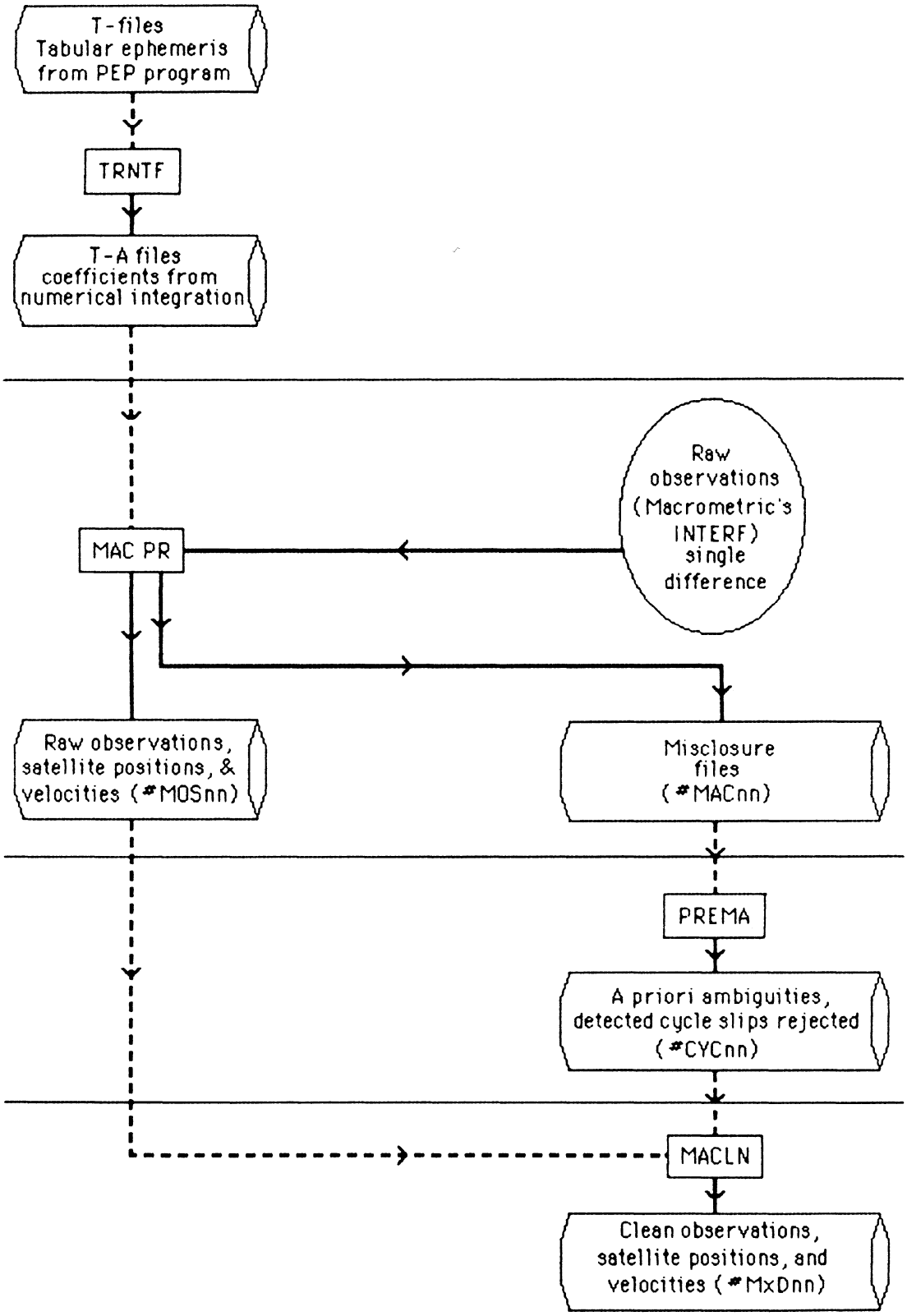

FIGURE 3.2
Macrometer™ V-1000 preprocessor flow chart.

i.e., the orbit determination for a specific time interval plus storage of the result in the T-A file, is done for all the observation periods of the observation campaign in one TRNTF program run (the results being stored in one T-A file). The program MACPR will find the required orbital arc by comparing the time of the first observation with the beginning of the interval given in the T-A file.

3.2.1.2 Program MACPR

The program MACPR creates two files. (a) The first file (#MOSnn) contains the raw observations from the INTERF's Macrometric program (read from a tape) and satellite positions and velocities from the T-A file(s). This file is used eventually to make a part of the final file assembled for the main processor. The evaluation of the positions and velocities is done as follows: One of the subroutines of the program (RDTAF) finds in the T-A file the right orbital arc commensurate with the time of the first observation. Then the program extracts the coefficients of numerical integration and computes the satellite positions and velocities in the quasi-inertial system (defined by the mean rotation axis and the direction to the vernal point) at the time of observation (given in UTC). Then subroutine EDEFS transforms these positions into the conventional terrestrial (CT) system. Because we need to compute the satellite position (in the CT system) at the time of transmission, i.e.,

$$\vec{r}^{\,j}(t-\rho/c) = \vec{r}^{\,j}(t) - \rho_i^j/c \times \dot{\vec{r}}^{\,j}(t) \quad , \tag{3.1}$$

where

t is the reception time

c is the velocity of light in a vacuum,

the velocity vectors $\dot{\vec{r}}$ are also transformed (subroutine TOPEF) into the CT system.

(b) The second file (#MACnn) contains the misclosures computed from the raw observations and the a priori information on the station and satellite positions. This file is analysed subsequently by the program PREMA. The predicted values of ranges for this analysis take into account neither the tropospheric and ionospheric corrections nor the antenna

heights.

Throughout, the convention "observation for the ith satellite 2nd station minus observation for the ith satellite 1st station" is used.

3.2.1.3 Program PREMA

The programme PREMA is an interactive programme to approximate both single and double differences by algebraic polynomials. This approximation allows us to reject bad observations, to obtain a priori values for the ambiguities, and to detect, if possible, existing cycle slips.

(a) In the first step, the single difference preprocessing, we analyse the value of misclosures from the #MACnn file:

$$\varepsilon_{ij}^{k} = \Delta\tilde{\rho}_{ij}^{k} - \Delta\rho_{ij}^{k} \tag{3.2}$$

for each satellite k separately. Here $\Delta\tilde{\rho}_{ij}^{k}$ are the "measured" single differences and $\Delta\rho_{ij}^{k}$ are the theoretical values of single differences computed using approximate orbits and a priori station coordinates.

We now distinguish two cases:

(i) If there are no breaks (cycle slips) in the data: We fit, in the least-squares sense, the ε_{ij}^{k} (separately for each satellite) by low degree algebraic polynomial:

$$P(t) = \sum_{\ell=0}^{q} p_{\ell}\, t^{\ell} \quad , \tag{3.3}$$

where t is a time interval defined as "time of observation" minus a "reference time" which might be, for example, the mid-point of an observing session. The time t can be expressed in any convenient unit; e.g., hours, minutes, seconds, epoch number. The degree q, of the polynomial, typically chosen is between 4 and 6.

(ii) If there are m_b breaks (cycle slips) in the data for, say, satellite k: The total observation period is divided into m_b "break-free" subintervals I_m, $m=1,2,\ldots,m_b$. The ε_{ij}^{k} are now fitted by the following piecewise continuous function:

$$\tilde{P}(t) = \tilde{p}_{om} + \sum_{\ell=1}^{q} \tilde{p}_{\ell}^{k}\, t^{\ell}, \; t \in I_m; \quad m=1,2,\ldots,m_b \quad . \tag{3.4}$$

(b) This first step is followed by the double difference

preprocessing. Here we analyse the so-called double differences, $\Delta\rho^{\ell}_{ij} - \Delta\rho^{k}_{ij}$, forming the following misclosures:

$$E^{\ell k}_{ij} = (\Delta\tilde{\rho}^{\ell}_{ij} - \Delta\rho^{\ell}_{ij}) - (\Delta\tilde{\rho}^{k}_{ij} - \Delta\rho^{k}_{ij}),\ \ell \neq k,\ i \neq j \quad . \qquad (3.5)$$

The polynomial fitting is then identical with that for the single differences.

So far, we have tacitly assumed that the division of an observation period into break-free subintervals for each satellite k is known a priorily. This, however, is not always the case. Such breaks are often not detected at the time of observation, and a close examination of the data at this preprocessing stage is necessary to detect them. Although completely automatic break detection and removal software could be developed, we opted for an interactive preprocessing program (similar to that available with the Macrometric software) using a computer graphics package and the mathematical tools given in the preceding paragraph. A brief description of the use of this program follows.

To begin with, it is assumed that a "new subinterval" begins if one or more zeroes are encountered in the observation series of a satellite. A fit using eqn. (3.4) is performed, and the residuals are displayed on a terminal screen. The operator can then redefine the interval boundaries and reject outliers. This process may be repeated, at the user's discretion, until a satisfactory selection is found. Operator action may also be necessary as zeros in the data do not always mean a break, and breaks are not always accompanied by zero values. A careful examination of the residuals, however, will usually reveal all such breaks.

Essentially the same procedure is repeated with the double differences in the second step. At this stage it is usually easy to detect any data breaks (cycle slips) present. Normally, the estimated values of slipped cycles

$$(n^{k\ell}_{ij})_m = (\tilde{p}_{o1} - \tilde{p}_{om})/(\lambda/2),\ m = 2,3,\ldots,m_b \qquad (3.6)$$

are close to integer numbers. If, moreover, the estimated r.m.s. errors of the $n^{k\ell}_{ij}$ are much smaller than 1, it is safe to remove the breaks by correcting the double difference "observations" in the m_b subintervals by adding to them the values $(n^{k\ell}_{ij})_m \cdot (\lambda/2)$. Actually, the half-cycle slips found in the double differences are applied to one of the two single

differences forming the particular double difference series. Which of the single differences has to be corrected follows from inspecting all the input series in the vicinity of the break. Then, processing all the corrected data together shows the success (or the failure) of the process.

In a double-difference observable, the cycle ambiguity is the difference between two single-difference ambiguities. Therefore, in order to determine the ambiguities, the single-difference ambiguity of one of the satellites is set equal to zero for the duration of the observing session. This satellite is referred to as a "reference satellite" (see section 3.3). Normally we choose the one most observed in a session to be the "reference satellite."

The analysis of the double-difference should be used whenever there are breaks detected because it allows a surer evaluation of cycle slips; double differences are much less affected by clock errors. For example, if the satellite in channel #4 is chosen as the "reference satellite" and a break occurs at all the channels simultaneously, then the results $n_{ij}^{k\ell}$ will be added to the non-reference satellite double difference series for satellites in channels 1, 2, and 3, and subtracted for satellites in channels 5 and 6. These results are stored on files (#CYCnn) used by the last program of the preprocessor.

One would expect that this mode of preprocessing might fail if the $\Delta\rho_{ij}^{k}$ were only very poor approximations of the correct range differences $\Delta\tilde{\rho}_{ij}^{k}$. Tests have shown, however, that even for the longest baselines analysed, station offsets of up to 500 m and orbital errors of the order of a few kilometres did not seem to render this approach invalid. An a priori introduced bias of 500 m and several kilometre biases in the ephemerides did not have any measurable effect on either the recovered ambiguities or the a posteriori variance factor.

The above described preprocessing is done using a modification of program DPLOT [Davidson, 1984], available on the HP 1000 for interactive plotting of ASCII data files on either the HP-7470 plotter or the Cybernex 1012 graphics terminal. Program DPLOT was modified to allow interactive usage, and renamed GPSPL. Adaptations were made to produce plots with a minimum of operator intervention. The ability to create plots on the screen for interactive processing, or on paper for a permanent record, was

particularly attractive.

3.2.1.4 Program MACLN

Program MACLN is designed to take files #CYCnn, assembled by PREMA (containing all the information on cycle slips, ambiguities, and rejected observations), and #MOSnn, assembled by MACPR (containing raw single differences and satellite position information), and assemble the "final" observation file (#MxDnn) for the main processor MPROC. This resulting file may contain either single differences (#MSDnn), double differences (#MDDnn), or triple differences (#MTDnn) as specified by the user.

3.2.2 TI-4100 Preprocesor

The output of the Texas Instruments TI-4100 consists of records containing the ephemerides of the GPS satellites and of observation records at the predefined measurement rate. This statement is based on the data presently available at UNB for analysis. The TI-4100 processor may be programmed to output additional information [Texas Instruments, 1984].

An observation record at local time t includes the following measurements on the received GPS signal:

- P-code phase: $p(t)$
- carrier frequency: $\dot{\phi}(t)$ (3.7)
- carrier phases at $t - \Delta t$ and $t + \Delta t$: $\phi(t \pm \Delta t)$,

where Δt is a small, known time interval (not to be confused with satellite clock synchronization error). These observations are provided on both L1 and L2 carrier signals and for up to four satellites simultaneously. A typical measurement rate is $(3 \text{ sec})^{-1}$ resulting in about 200,000 carrier and P-code observations for an observation time of five hours. For differential positioning involving two receivers, this figure becomes almost 400,000. The reduction of this large amount of data to a manageable size and the evaluation of the satellite orbits from ephemerides is done in the preprocessing software TEXIN, described in section 3.2.2.1.

The other goal of the data preprocessing is to find discontinuities in the carrier phase observations (cycle slips) and to determine the corresponding integer number of jumped cycles. This is done in the program PRETI, described in section 3.2.2.2. For a detailed description, see Santerre et al. [1985].

The activity of the preprocessor is controlled by a command file created by the user interactively.

3.2.2.1 Program TEXIN

Each of the observations mentioned in the previous section is transmitted in an encoded form [Texas Instruments, 1984]. We assume in the sequel that the observation records have been decoded properly to yield P-code phase in seconds of the current GPS week and carrier phase and frequency in units of cycles and cycles per second respectively. All observations are time tagged with readings of the receiver clock.

This receiver (local) clock may or may not be synchronized with GPS time [Texas Instruments, 1982]. If the TI-4100 receiver has already determined its time offset with respect to GPS time, this offset will be transmitted in the observation records as an integral number of 20 msec (the fundamental unit of the TI-4100 time frame). In the preprocessing software, this offset is applied to the local clock readings to yield observation time tags close to GPS time. If the TI-4100 has not yet determined its time offset, the first P-code phase observations of a session are used together with the signal propagation delay to compute the approximate GPS time t_R of signal reception:

$$t_R = p(t) + \delta t \quad , \tag{3.8}$$

where

$p(t)$ = P-code phase observed at local time t

δt = signal propagation delay, computed from satellite ephemerides and approximate station coordinates.

The computed time offset

$$0 = t_R - t \tag{3.9}$$

is truncated to an integer multiple of 20 msec (to remain within the time frame of the TI-4100) and applied to all observation time tags. Computations related to synchronization and time offset determination are done in the subroutine SNCRO. In the following we shall assume that all receiver time readings t are corrected for the time offset.

The next step in preprocessing, subroutine CHECK, is primarily designed to eliminate gross errors in the observations. The carrier

frequency observation at time t is compared to the difference between carrier phase at $t + \Delta t$ and $t - \Delta t$, divided by $2\Delta t$. If the discrepancy is larger than 10% (of the observed carrier frequency), the observation record is eliminated. The same is done if the discrepancy between the P-code phases observed on L1 and L2 is larger than 1 msec. Once the observation record passes these checks, the difference between the P-code phases on L1 and L2 is used to correct the L1 value for dispersive refraction delay. The carrier phase observations of the L1 and L2 signals at $t + \Delta t$ and $t - \Delta t$ are furthermore corrected for the receiver frequency offset of 6 kHz in L1 and -7.6 kHz in L2 [Texas Instruments, 1984].

The sequence of observations after this subprogram is sketched in Figure 3.3. A sequence like this exists for every active pseudo-channel of the TI-4100.

At this point in preprocessing, we still have about 240,000 carrier and P-code observations for an observing period of 5 hours from two receivers. To further reduce the amount of data, it has been decided to compress the observations of a certain time interval ΔT to a "normal point observation" for the middle of the interval ΔT (not to be confused with receiver synchronization error). A simple way of producing these pseudo-observations is to fit some function of time to the observations in ΔT and to take the function value at the centre of ΔT to be the pseudo-observation. If the number of observations in ΔT exceeds the number of parameters in the function, a least-squares fit may be done which provides additionally a measure of the closeness of the fitted function to the data. One particular kind of easy-to-handle function is an algebraic polynomial, which has been chosen to approximate the observation time series in a least-squares sense:

$$\tilde{p}(t_j) = \sum_{i=0}^{N_p} A_i^p (t_j - t_o)^i + V^p(t_j) \quad , \tag{3.10}$$

$$\tilde{\phi}_k(t_j) = \sum_{i=0}^{N_{\phi_k}} A_i^{\phi_k} (t_j - t_o)^i + V^{\phi_k}(t_j) \quad , \tag{3.11}$$

A_i^p and $A_i^{\phi_k}$ are unknown polynomial coefficients; t_o denotes the normal

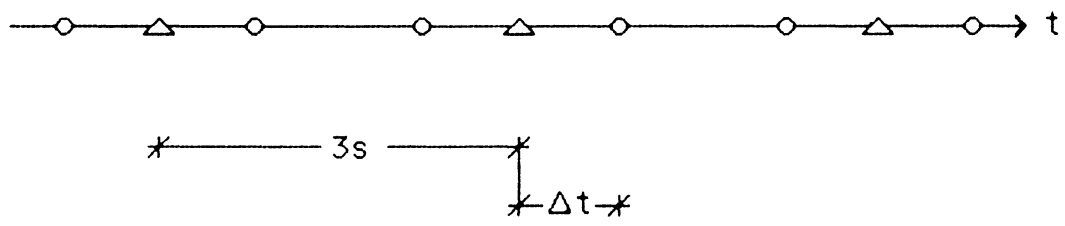

○ Carrier phase L1 and L2

△ P-code phase on L1, corrected for dispersive refraction delay

FIGURE 3.3
Observation sequence after subroutine CHECK.

point epoch, N_p and N_{ϕ_k} denote the order of the polynomial, and the approximation interval is given by

$$t_o - \frac{\Delta T}{2} \leq t_j < t_o + \frac{\Delta T}{2} \quad . \tag{3.12}$$

The last equation holds for carrier phases on both frequencies f_k, k=1,2. The least-squares solution for the normal points is given by:

$$\hat{p}(t_o) = \hat{A}_o^p \pm \hat{\sigma}_o^p \tag{3.13}$$

$$\hat{\phi}_k(t_o) = \hat{A}_o^{\phi_k} \pm \hat{\sigma}_o^{\phi_k} \tag{3.14}$$

with

$$\hat{\sigma}_o^p = \frac{1}{\sqrt{n}} \hat{\sigma}^p$$

$$\hat{\sigma}_o^{\phi_k} = \frac{1}{\sqrt{n}} \hat{\sigma}^{\phi_k} \quad ,$$

where n is the number of observations in the interval (3.12). The estimated variances of the observations

$$(\hat{\sigma}^p)^2 = (n - N_p - 1)^{-1} \sum_{i=0}^{N_p} (V^p(t_j))^2 \tag{3.15}$$

$$(\hat{\sigma}^{\phi_k})^2 = (n - N_{\phi_k} - 1)^{-1} \sum_{i=0}^{N_{\phi_k}} (V^{\phi_k}(t_j))^2 \tag{3.16}$$

are representative of the "goodness" of the approximations (3.10) and (3.11). This goodness depends on the polynomial degree N, the length of the approximation interval ΔT, and the smoothness of the data to be approximated. For our purpose, it is desirable to have the approximation interval as long as possible to achieve an effective data reduction. In order to find a suitable combination of N and ΔT and to investigate the smoothness of the carrier phase and P-code phase data, several polynomial approximations for varying ΔT and N have been tested. Some of the results are discussed below.

Figure 3.4 shows residuals $V^{\phi}_{1}(t)$ of carrier phase observations with two different receivers for the same time interval. The approximation interval is one hour and the degree of the polynomial is 3. At first glance, it is quite obvious that there is a high degree of correlation between the residuals of different pseudo-channels (trackers) of a receiver. Furthermore, it can be seen that the spectrum of the residuals is quite different for the two receivers. The high correlation between different pseudo-channels indicates that the residuals are dominated by errors in the receiver oscillator (receiver clock) because these are common to all receiver channels.

The difference between the spectra of the residuals of the two receivers may be due to differences in performance of the Cesium frequency standards connected to the receivers. The figures shown are representative of all observation sessions of the 1984 Ottawa campaign (see section 5.3): the high frequency noise always appears in connection with the FTS Cesium clock, whereas the low frequency variations are typical of the receiver connected to the HP Cesium clock. The possible reasons for the different noise structures will not be discussed here. Due to the rather high frequency noise in the FTS Cesium, a reasonably accurate polynomial fit to the carrier phase data was impossible, even for short approximation intervals. On the other hand, the high positive correlation between different channels suggests that the difference between two channels might be approximated with a higher accuracy.

Figure 3.5 shows residuals from a polynomial fit to differences in carrier phase observations on channels one and two. The original observations were the same as in the previous analysis, and the degree of the approximating polynomial is three. Compared to Figure 3.4 we see a reduction in the amplitude of the residual signal by a factor of five. This holds for the residuals of both receivers and, moreover, now no difference in spectrum is visible. The signals shown in this figure reflect mainly variations in the satellite oscillators, refraction, and short period orbit variations. Correlation between the residual series of the two receivers is obvious, although not very pronounced.

The role of differential dispersive refraction in GPS carrier phase observations becomes apparent when we compare the residuals of carrier

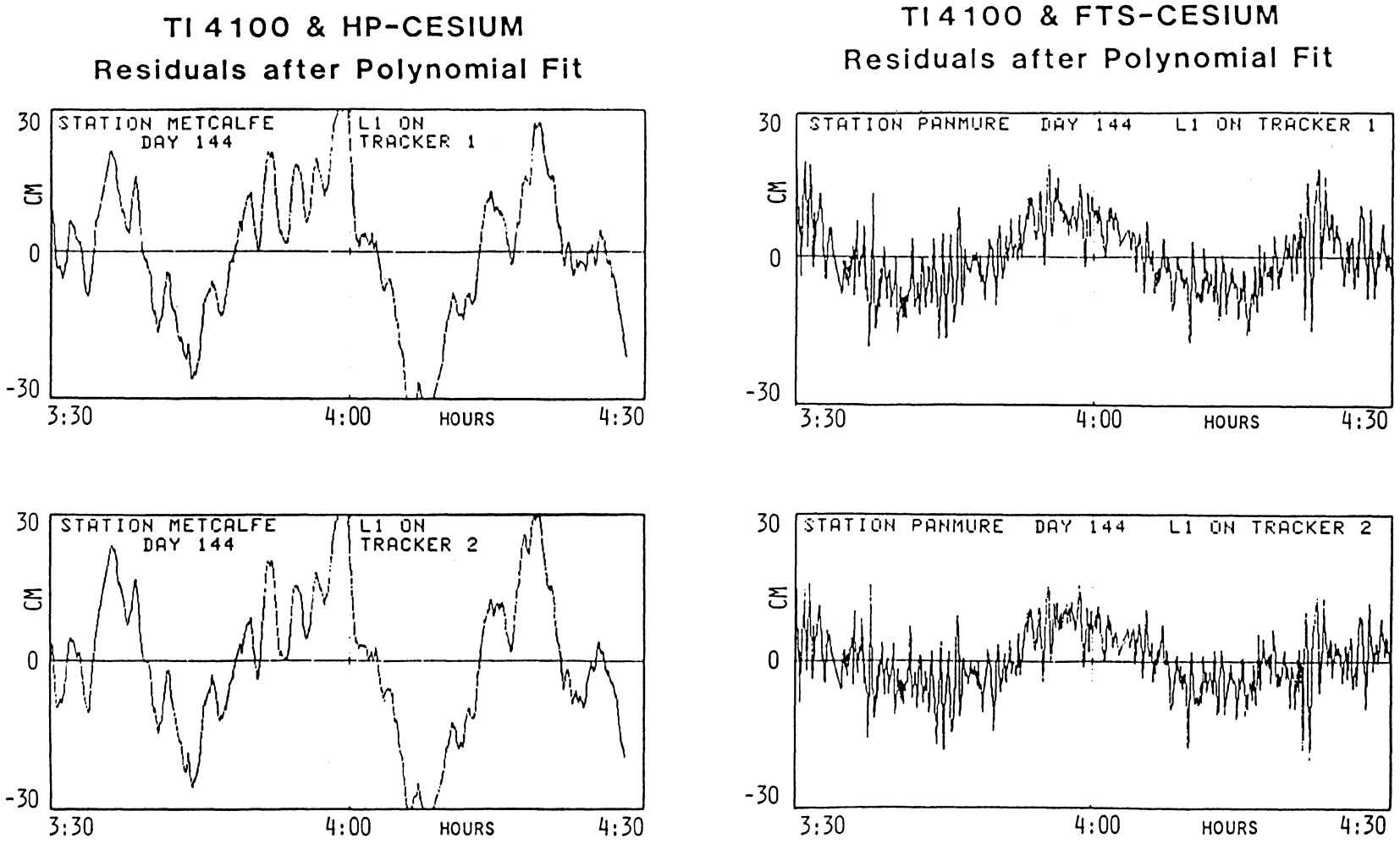
TI 4100 & HP-CESIUM
Residuals after Polynomial Fit
STATION METCALFE
DAY 144
L1 ON
TRACKER 1
30
CM
0
-30
3:30
4:00
HOURS
4:30
TI 4100 & FTS-CESIUM
Residuals after Polynomial Fit
STATION PANMURE DAY 144 L1 ON TRACKER 1
STATION METCALFE
DAY 144
L1 ON
TRACKER 2
STATION PANMURE DAY 144 L1 ON TRACKER 2

FIGURE 3.4

Comparison between
Phase Differences at two Stations

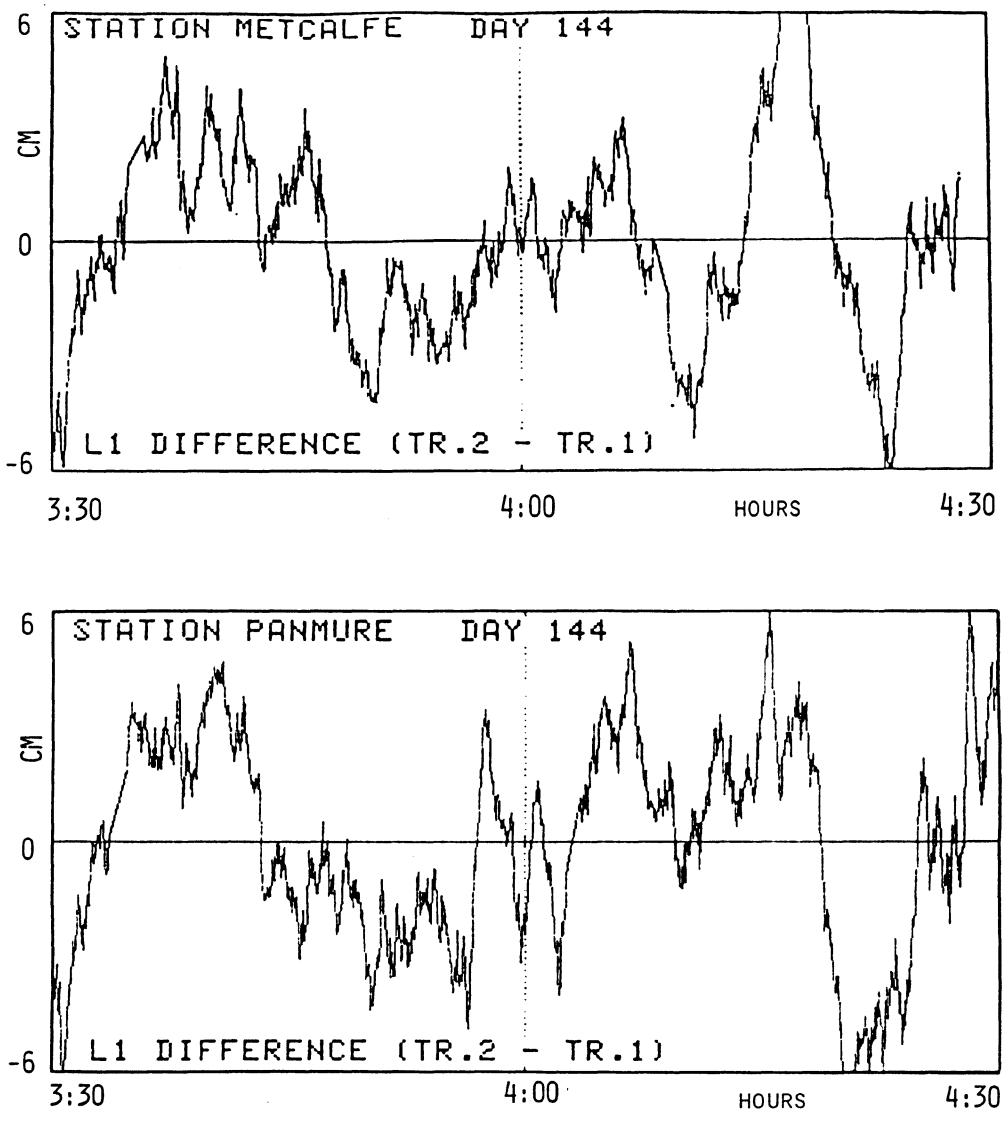

FIGURE 3.5

Residuals after 3rd-order polynomial fit.

phase differences on L1 to those on L2 (see Figure 3.6). Every peak in the L1 signal repeats itself amplified in the L2 signal.

A more detailed look at the residuals of a third-order polynomial fit over 4 minutes is provided in Figure 3.7. The amplitude range is now ± 2 cm, and the length of the residual series is only four minutes. It can be seen that, at this scale, typical signal variations are ± 1 cm over periods of 1 minute. No systematic variations of higher frequency seem to be present. These characteristics were also found in the analysis of the carrier phase observations of the other sessions.

Based on these findings, it was decided to compute one minute normal point observations for differences between the carrier phases observed in up to four pseudo-channels of the TI-4100. Additionally, for the first pseudo-channel, a normal point observation for the carrier phase is computed. The latter will be less accurate due to the noise level in the original phase observations (cf. Figure 3.4). The degree of the approximating polynomial is always three. The procedure is illustrated in Figure 3.8.

Taking the difference between carrier phase observations seems at present to be the most simple and straightforward way to get rid of the local oscillator errors (clock errors). If, after the preprocessing, the carrier phases are needed rather than carrier phase differences, they can be recomputed as a linear combination of the preprocessor output (cf. Figure 3.8). The reduced observation data set for two receivers and five hours observation time consists now of 7200 normal point observation.

As will be seen below, in differential positioning with carrier phase observations, the primary use of P-code phase is the determination of the satellite position from ephemerides. Assuming a satellite velocity of 4 km/s, roughly a tenth of a microsecond accuracy is needed to provide an internal precision better than a millimetre in the orbit computation. The short period distortions due to the variations in local receiver oscillator are clearly smaller than a nanosecond (cf. Figure 3.4). Therefore the computation of one minute normal point pseudo-observations for P-code phase is straightforward.

If the estimated error σ_{ϕ_k} of either the carrier phase or carrier phase differences (cf. eqn. (3.14)) is greater than a tenth of a carrier cycle, the observations of that particular normal point interval ΔT are

Comparison between Phase Differences on L1 and L2 (same Station)

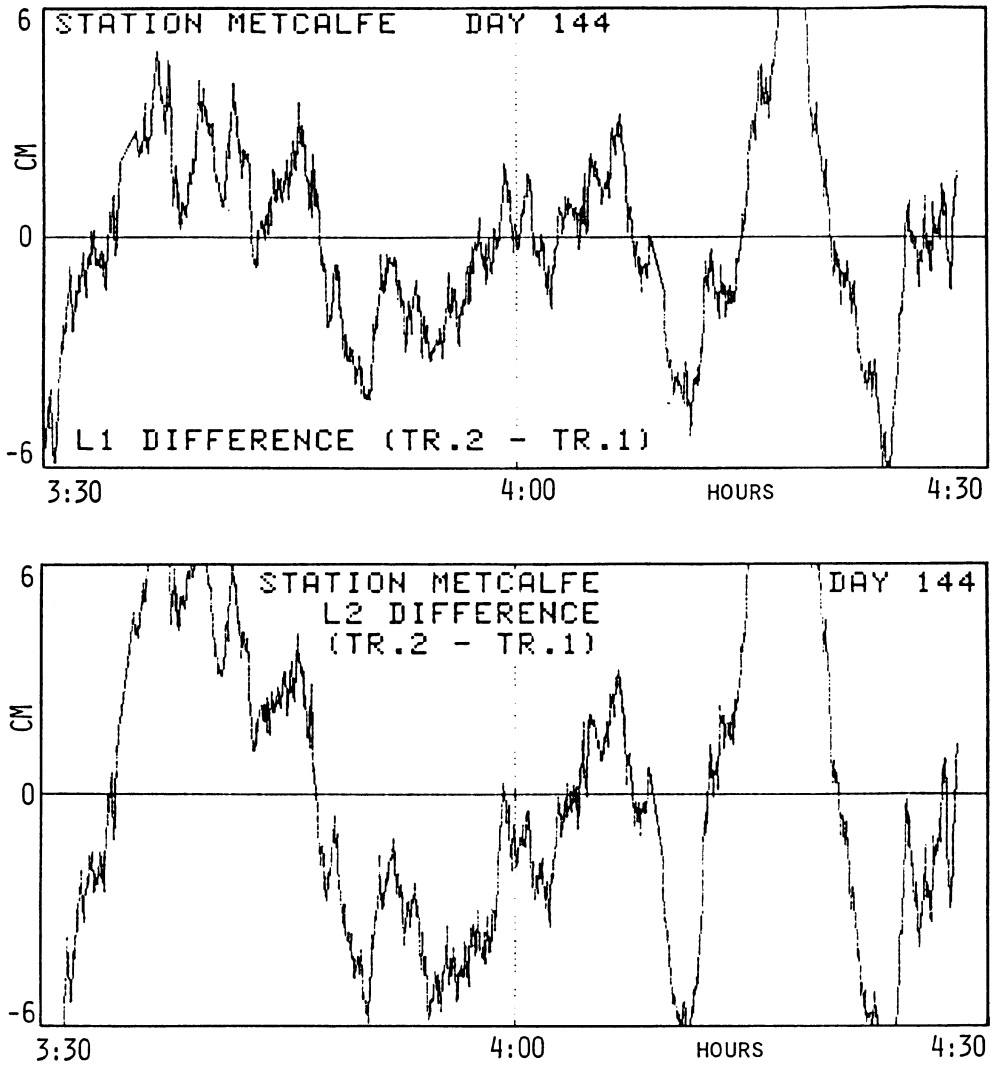

FIGURE 3.6

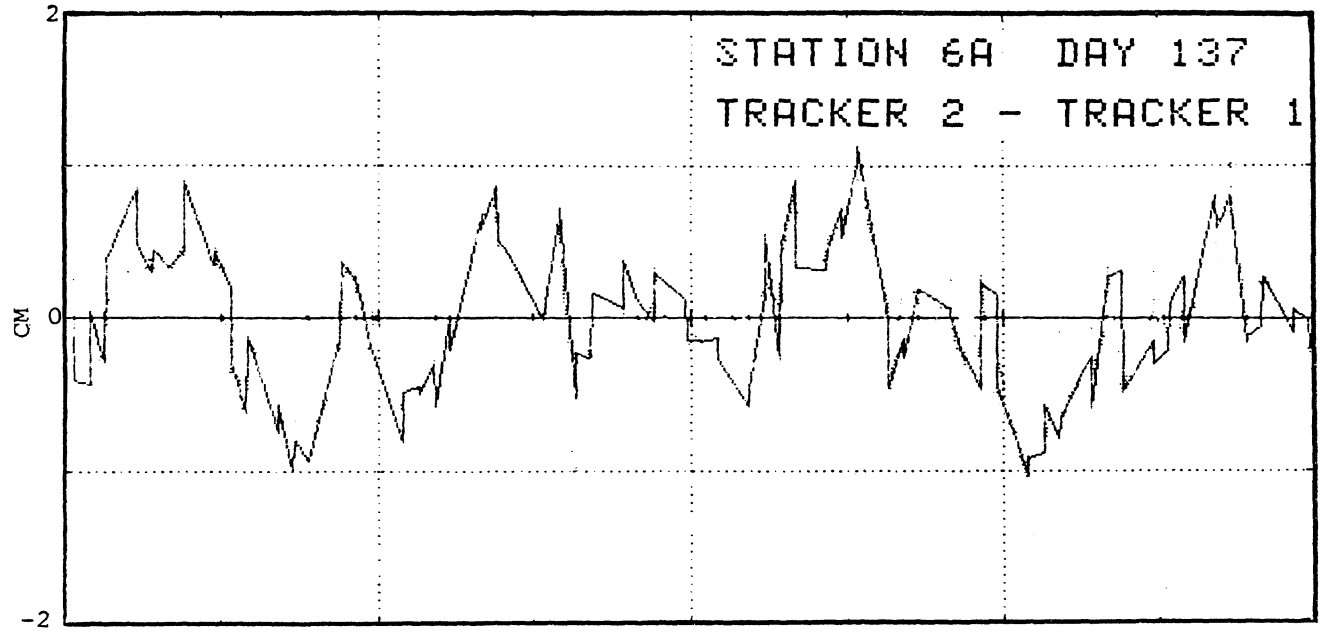

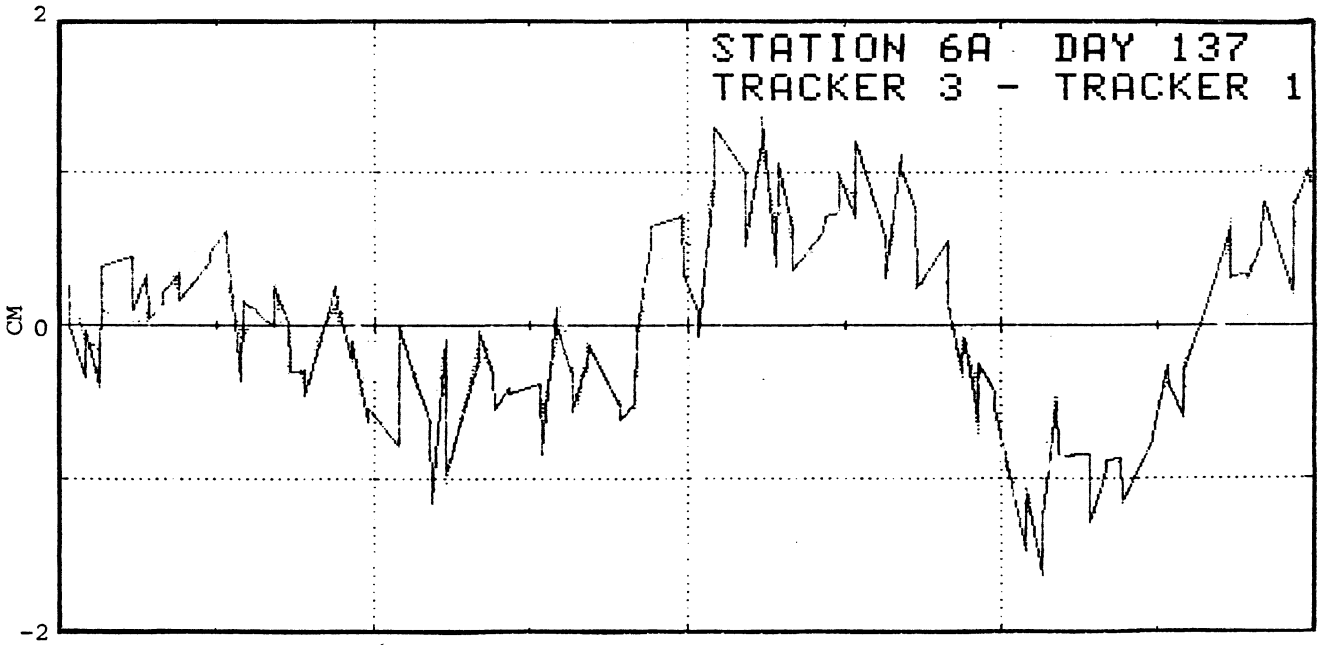

FIGURE 3.7

Residuals of 3rd-order polynomial fit over 4 minute span.

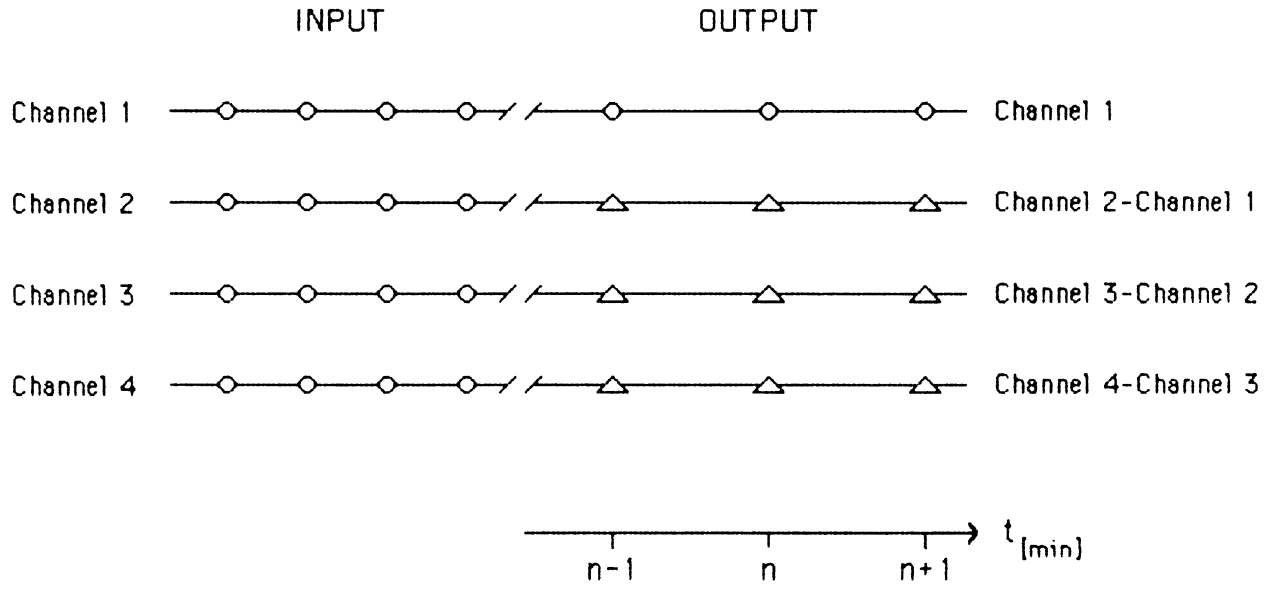

○ Carrier phase

△ Carrier phase difference

FIGURE 3.8
Scheme of carrier phase normal points.

rejected.

The computations described above are performed in subroutines RESTO, CADIF, and NOPNT (see Figure 3.9).

The next step in preprocessing is the evaluation of the satellite coordinates pertaining to the carrier phase normal point observations. The P-code phase observed on a signal at time t is the reading of the satellite's clock at the time of transmission of that signal. That means that, after correcting the P-code phase for the offset between satellite time and GPS time, it can be used for the evaluation of satellite coordinates from the GPS ephemerides record transmitted in the message. Subroutine FINDE selects the best available ephemerides, based on the Ephemerides Reference Time; subroutine CLKAN evaluates the parameters describing the satellite clock offset from GPS time; and subroutine SATOR finally computes CT coordinates of the satellite at transmission time. For further processing, the corrected P-code phases are also transformed into biased ranges by subroutine PSRAN.

The results of the preprocessor TEXIN, consisting of

(a) normal point observations for carrier phases and carrier phase differences on L1 and L2;

(b) normal point observations for P-code biased ranges;

(c) estimated variances for (a) and (b);

(d) satellite coordinates corresponding to the normal point observations;

are stored on disk for further processing.

3.2.2.2 Program PRETI

If for any reason the continuous phase counting in the receiver is interrupted, the carrier phase observation will show a temporal discontinuity. These data breaks can be removed by adding or subtracting an integer number of carrier cycles to all observations after the discontinuity.

Program TEXIN (section 3.2.2.1) produces for every observing receiver a reduced observation record containing carrier phase differences between receiver channels. The program PRETI reads two of these records, one for each of two receivers, and forms double differences by matching the time tags and differencing the single phase differences once more. Naturally, the two records have to contain observations with common time tags, i.e.,

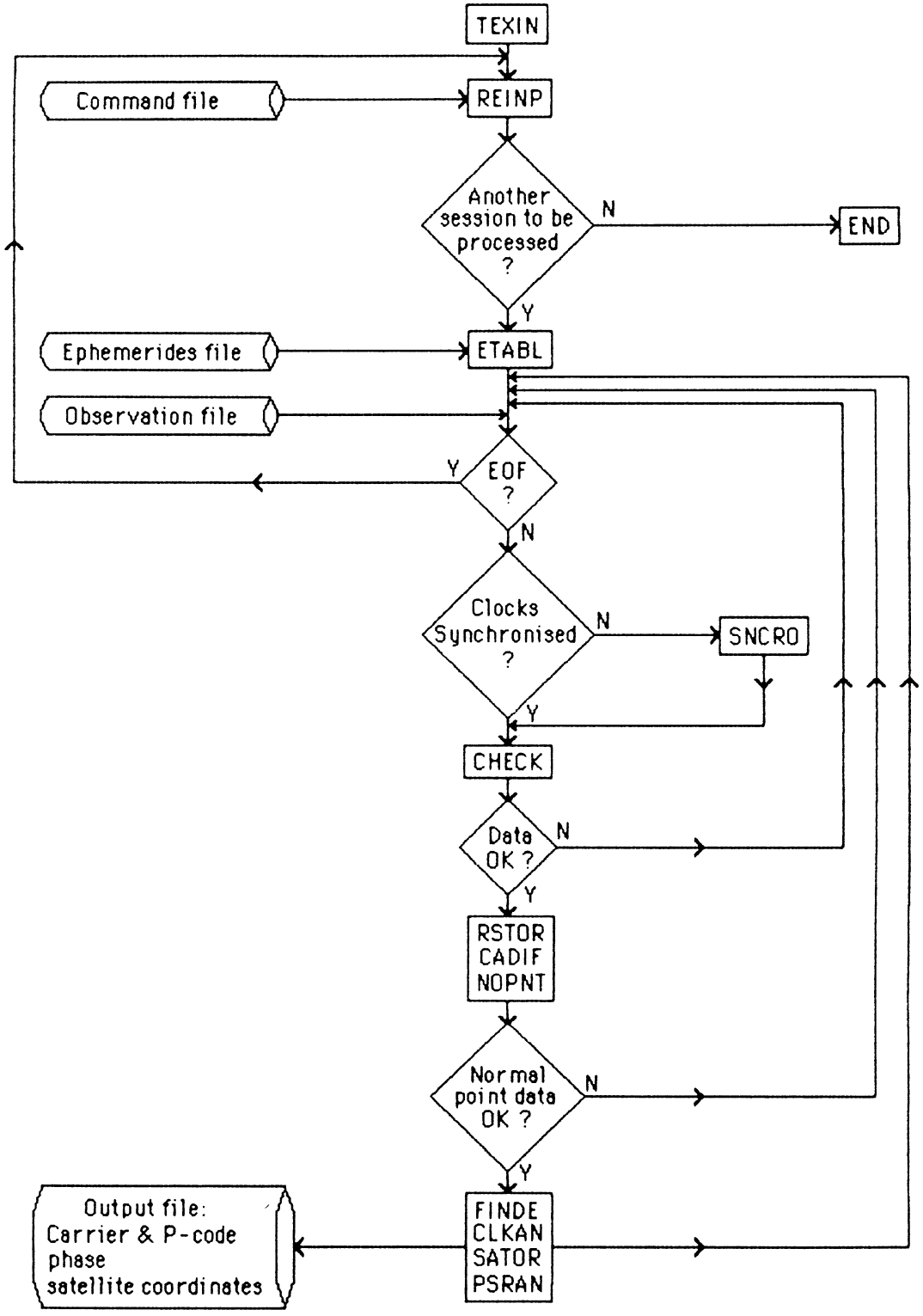

FIGURE 3.9
TI-4100 preprocessor flow chart.

simultaneous observations.

The new time series of carrier phase double differences still contain differences of the above described discontinuities. Program PRETI finds and removes these discontinuities from the measurements and writes for every epoch an observation record onto the input file for the main processor.

To find the cycle slips, program PRETI forms carrier phase double difference misclosures with respect to the approximate station coordinates. If the difference in misclosure between two subsequent epochs is larger than a predefined threshold, the program interprets the integer part of this difference as a cycle slip and removes it from all subsequent observations on this particular signal. At the beginning of an observation session, this procedure also removes the main portion of the carrier phase ambiguity.

3.3 Main Processor

The main processor MPROC consists essentially of the least-squares filter. Figure 3.10 shows the block diagram of the program. The subroutines used are listed in Appendix C. For a detailed description, see Santerre et al. [1985].

The main processor is controlled by the main processor command file created by the front end. This file contains the following general information:

(a) Reference ellipsoid (a, f^{-1}).

(b) The name of the file which contains the a priori station coordinates and their standard deviations (or weight matrix). The first record of this file indicates in which coordinate system this information is.

(c) Epoch at which we wish to evaluate nuisance parameters.

(d) Epoch at which we wish to evaluate station coordinates.

For each session, this file contains the following additional information:

(a) The observation file name.

(b) A priori standard deviation of the observations (from preprocessing).

(c) Heights of antennas above the survey marks (no horizontal eccentricity is allowed for).

(d) Number of clock parameters to be evaluated and their a priori standard deviations. (These standard deviations reflect the quality of the clock used and the care taken in the synchronization in the field.)

(e) Option to evaluate or not the ambiguities at the very beginning; (because the "clean" observation file contains only a priori values of the ambiguities, they have to be estimated once more; option: 1≡yes). If the estimated values for the ambiguities are close to integers, the observation file can be re-processed to create a new observation file with integer ambiguities enforced. At this stage, the re-evaluation of the ambiguities is not required; option: 0≡no).

Each session is analysed separately. The scene is first set by going through the following points: The observations, satellite positions, and velocities for each epoch are read from the corresponding file (subroutine RDRCF). This subroutine recognizes the observation type by the tag at the beginning of each record. At the first epoch, the antenna heights above

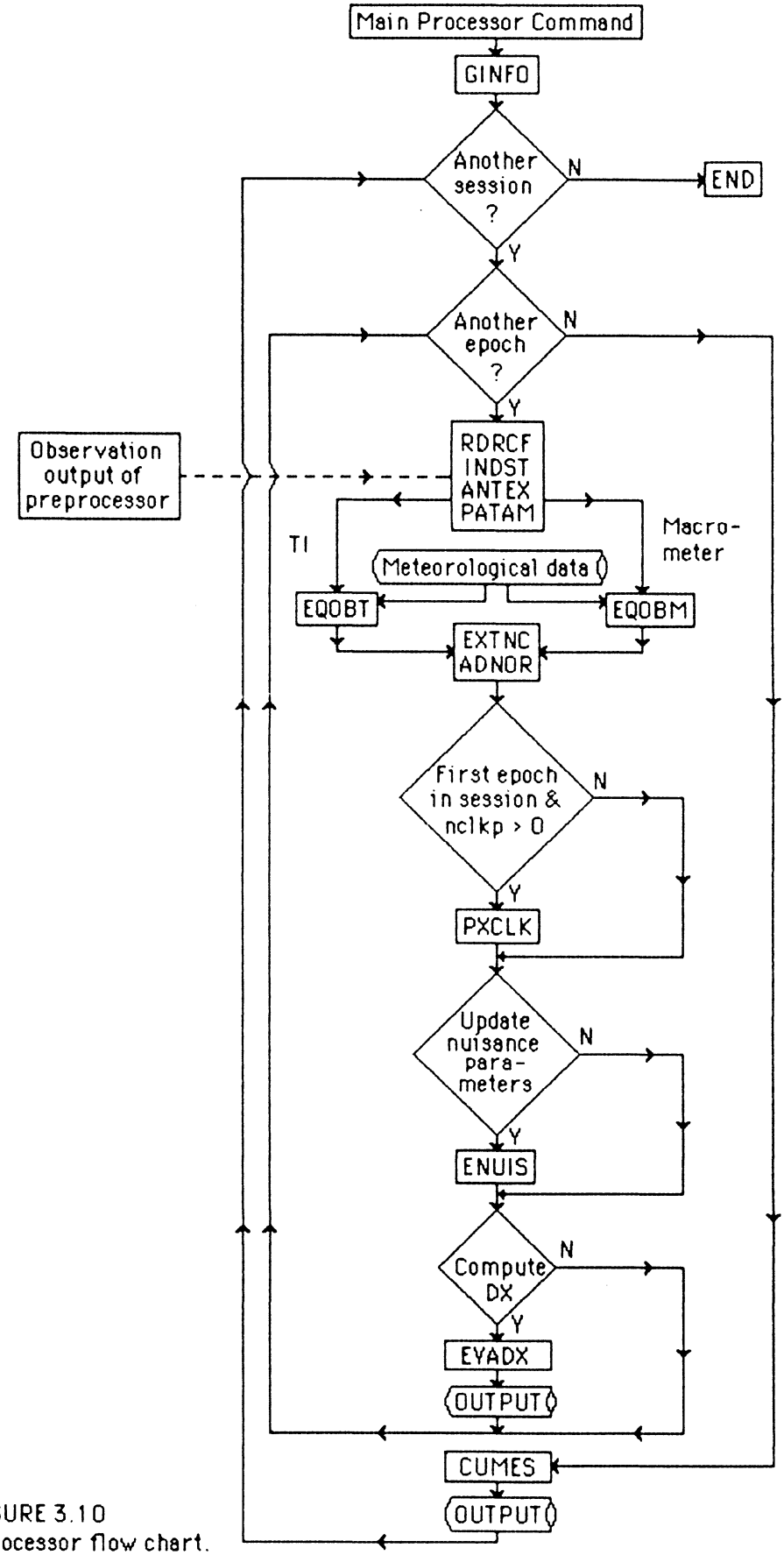

FIGURE 3.10
The main processor flow chart.

the survey markers are converted into CT coordinates.

The a priori weight matrix of the clock parameters (offset or offset and drift for one particular session) is set, if the user wishes to evaluate these. No a priori weights are given to the ambiguities, the reason being that it is not possible to adequately estimate the uncertainties of a priori values of these ambiguities for all types of receivers. If the ambiguities are to be evaluated, the order in which the satellites appear has to be kept by the computer to correctly set the appropriate components of the design matrix relative to these ambiguities.

Then tropospheric and ionospheric corrections, the misclosure, and one column of the design matrix are computed for each observation. Note that here we deal with the conventional "exact" misclosure vector of a least-squares adjustment, corrected for delays, cycle slips, and antenna height. Hence they are bound to be different from those in the #MACnn file as described in section 3.2.1.2. This processing is done by subroutines for the TI double difference observations and for the Macrometer™ double difference observations. The observation equations used for double differences are:

$$V^{k\ell} = \Delta^2\rho^{k\ell}_{ij} - (+\dot{\rho}^{\ell}_{i} - \dot{\rho}^{k}_{i})\Delta T_{ij} + \frac{\lambda}{2} n^{k\ell}_{ij} - \Delta^{2\tilde{}}\rho^{k\ell}_{ij} \quad , k\neq\ell_1,\ i\neq j \ , \qquad (3.17)$$

where

$\Delta^2\rho^{k\ell}_{ij}$ is the computed double difference

$\Delta^{2\tilde{}}\rho^{k\ell}_{ij}$ is the observed double difference

$\dot{\rho}^{\ell}_{i}$ is the range rate (station i satellite ℓ)

ΔT_{ij} is the synchronization error of receiver clock j with respect to receiver clock i.

λ is the wave length of the carrier

$n^{k\ell}_{ij}$ is the double difference ambiguity (parameter)

Equation (3.17) is merely eqn. (6) (part A of Beutler et al. [1984]) rewritten with the symbol convention adopted for this report.

The partial derivatives for the station coordinates read:

$$\frac{\partial \Delta^2 \rho_{ij}^{k\ell}}{\partial \vec{R}_i} = \vec{e}_i^{\ell} - \vec{e}_i^{k} \; ; \quad \frac{\partial \Delta^2 \rho_{ij}^{k\ell}}{\partial \vec{R}_j} = - \vec{e}_j^{\ell} + \vec{e}_j^{k} \; ; \tag{3.18}$$

where

$$\Delta^2 \rho_{ij}^{k\ell} = \Delta \rho_{ij}^{\ell} - \Delta \rho_{ij}^{k}$$

$$\Delta \rho_{ij}^{k} = \rho_j^k - \rho_i^k$$

$$\rho_j^k = |\vec{r}^k - \vec{R}_j| \quad .$$

Because ΔT can be expressed as

$$\Delta T = A_o + A_1 (t - t_o) \tag{3.19}$$

the partial derivatives for the clock coefficients (receiver j relative to receiver i) are:

$$\frac{\partial \Delta^2 \rho_{ij}^{k\ell}}{\partial A_o} = \dot{\rho}_i^{\ell} - \dot{\rho}_i^{k} \tag{3.20}$$

$$\frac{\partial \Delta^2 \rho_{ij}^{k\ell}}{\partial A_1} = (\dot{\rho}_i^{\ell} - \dot{\rho}_i^{k}) \; (t - t_o) \; ; \tag{3.21}$$

where t is the observation time; t_o is a reference time.

For the Macrometer™ double difference observations, the clock offset and drift are estimated on demand. For the TI-4100, the unknown "ΔT" does not appear explicitly in the observation equation (cf. section 3.2.2), and clock bias is thus not estimated.

The partial derivatives for double difference ambiguities are given by:

$$\frac{\partial \Delta^2 \rho_{ij}^{k\ell}}{\partial n_{ij}^{k}} = - \frac{\lambda}{2} \; ; \quad \frac{\partial \Delta^2 \rho_{ij}^{k\ell}}{\partial n_{ij}^{\ell}} = \frac{\lambda}{2} \quad . \tag{3.22}$$

These are also valid for the single difference ambiguities: the evaluation of single difference ambiguities (for the non-reference satellites) is done

with respect to the reference satellite in the double difference ambiguity mode.

In the present version of MPROC we have not implemented any subroutine dealing with orbital bias estimations, because no improvement would have ensued for the campaigns we have had data for (the longest baseline being 66 km) and because of the memory requirements to solve for 6 Keplerian elements for 6 satellites. This will be remedied when the RTE-6/VM operating system is in place. These subroutines are, however, implemented in all VECA, PRMAC3, and PRMNET programs.

The least-squares filtering is done along the same lines as in VECA [Langley et al., 1984]. The equations are spelled out in section 3.4.1. The nuisance parameters (clock coefficients and ambiguities) can be evaluated on demand by the subroutine ENUIS which evaluates eqn. (3.70). Station coordinates can be evaluated at any time during a session on demand from eqn. (3.69). Results, i.e., corrections to the a priori station coordinates, are stored on disc to be read by the postprocessor to produce printout and plots. The same process is employed epoch by epoch until the end of the session is reached unless interrupted by the operator.

At the end of a session, the arrays $S^{(n-1)}$, $R^{(n-1)}$ (eqns. (3.61) and (3.62)) are accumulated, and the matrices M_i^{-1}, $M_i^{-1}U_\Lambda i$, and $M_i^{-1}O_i^T$ computed (subroutine CUMES) and stored on disc to allow the recomputation of the nuisance parameters with the final estimates of $\hat{X}$ (eqns. (3.44) and (3.55)).

The same is repeated session after session. One of the characteristics of the main processor is that the nuisance parameters which are not common to more than one session are removed before the beginning of the processing of the next session (cf. section 3.4.1). This permits us to keep the dimensions of the array $R^{(n-1)}$ (eqn. (3.52)) relatively small, even though it contains all the information on nuisance parameters. For example, the Ottawa Macrometer™ campaign in the summer of 1983 consisted of 4 stations and 21 observation sessions. The number of unknowns with a standard algorithm equals to 117 (3 coordinates × 4 stations) + (5 double difference ambiguities × 21 sessions). With the algorithm developed here, the number of unknowns is kept to a maximum of 17 (4 stations × 3 coordinates + 5 double difference ambiguities) all through the network adjustment. This eliminates the need for the segmentation of the program and no array has to be put in the extended memory area (EMA).

At the end of the processing of all the sessions, the final array $S^{(n-1)}$ (eqn. (3.61)) is stored on disc. This is to facilitate the evaluation of the covariance matrix of station coordinates (eqn. (3.53)) and the re-evaluation of the covariance matrix of the nuisance parameters (eqns. (3.54) and (3.55)). This approach also gives the possibility to continue the processing starting with the new estimates of station coordinates and $S^{(n-1)}$ playing the role of the a priori P_x matrix for the new station coordinates. This information (new coordinates and new a priori P_x matrix) is stored on disc. To restart the processing, the operator will only have to enter the name of this disc file the way he did it at the beginning of the processing (see item (b) on the general information above).

The evaluation of residuals $\hat{V}$ is done only on demand by a second run of MPROC as follows: they are computed as the misclosure vector

$$\hat{V}^{k\ell} = - [\Delta^{2\tilde{}}\rho_{ij}^{k\ell} - \Delta^{2}\rho_{ij}^{k\ell}] \qquad (3.23)$$

where $\Delta^{2}\rho_{ij}^{k\ell}$ is the computed double difference with the final estimates of station coordinates and nuisance parameters.

3.4 Bias Elimination

The strategy for and implementation of an algorithm to evaluate/eliminate various biases (nuisance parameters) has been one of the major focal points of our research. Hence we have decided to devote the whole section to a description of our strategy and particulars concerning the individual families of biases.

3.4.1 Overall Strategy

For the derivations in this section, we divide the totality of all observations of a campaign into sessions (for definitions, see Introduction). In this context, a transition from one session to the next session is characterised by a complete change of all nuisance parameters, i.e., bias parameters (orbital, clock, atmospheric) and ambiguity parameters. Thus a session may last just a few hours but may also span a few days if common orbital biases are assumed for this time span.

After the observations of a session have been processed, the bias and ambiguity parameters pertaining to this session will be eliminated from the normal equations of the sequential least-squares adjustment to reduce storage space requirements in the main processor. The mathematics for parameter elimination (and recomputation) is given in section 3.4.1.1.

A session is divided into sequences. A sequence consists of all observations processed at the same time in the main processor. The sequence can be just one observation or may cover the complete session. Within a session, no bias parameters are eliminated, but the bias parameters may be evaluated after a certain specified number of sequences have been processed. The sequential processing within a session is described in section 3.4.1.2.

3.4.1.1 Elimination session by session

Utilizing the above structure in the observation equations, we can organize the design matrix for the observations of n sessions in the following way:

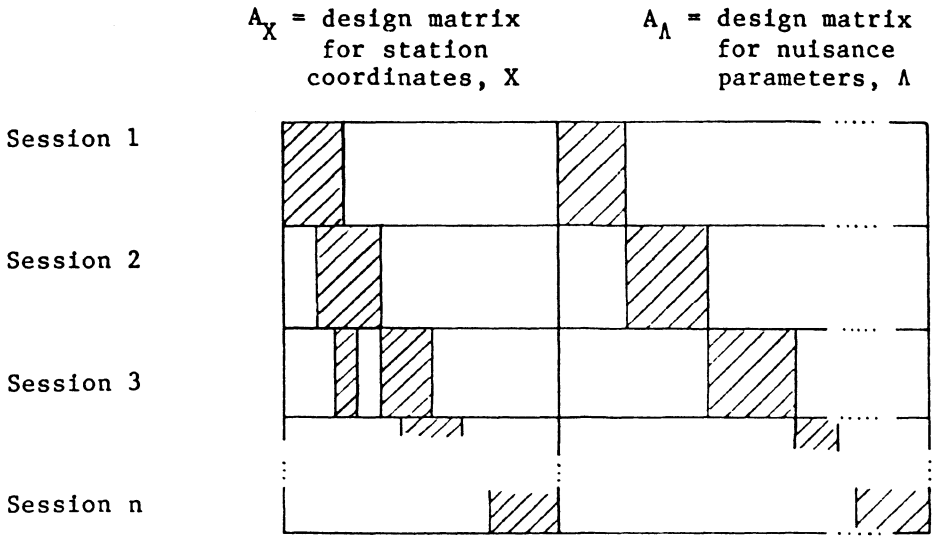

$$A = [A_X,\ A_\Lambda] = \begin{bmatrix} A_{X_1} & A_{\Lambda_1} & 0 & & 0 \\ A_{X_2} & 0 & A_{\Lambda_2} & & \\ & & & & \\ A_{X_n} & 0 & & & A_{\Lambda_n} \end{bmatrix} \qquad (3.24)$$

If we assume zero correlation between the observations of different sessions, we obtain a block diagonal weight matrix for the observations:

$$P_\ell = \mathrm{diag}(P_{\ell_1},\ P_{\ell_2},\ \ldots,\ P_{\ell_n}) \quad , \qquad (3.25)$$

and the least-squares normal equations are:

$$\begin{bmatrix} N_{XX} & N_{X\Lambda} \\ N_{\Lambda X} & N_{\Lambda\Lambda} \end{bmatrix} \cdot \begin{bmatrix} \hat{X} \\ \hat{\Lambda} \end{bmatrix} = \begin{bmatrix} U_X \\ U_\Lambda \end{bmatrix} \quad , \qquad (3.26)$$

where

$$N_{XX} = \sum_{i=1}^{n} A_{X_i}^T P_{\ell_i} A_{X_i} + P_X \quad , \qquad (3.27)$$

$$N_{\Lambda X} = \begin{bmatrix} A_{\Lambda_1}^T P_{\ell_1} A_{X_1} \\ A_{\Lambda_2}^T P_{\ell_2} A_{X_2} \\ \\ A_{\Lambda_n}^T P_{\ell_n} A_{X_n} \end{bmatrix} , \tag{3.28}$$

$$N_{X\Lambda} = N_{\Lambda X}^T , \tag{3.29}$$

$$N_{\Lambda\Lambda} = \mathrm{diag}(A_{\Lambda_1}^T P_{\ell_1} A_{\Lambda_1} + P_{\Lambda_1}, A_{\Lambda_2}^T P_{\ell_2} A_{\Lambda_2} + P_{\Lambda_2}, \ldots, A_{\Lambda_n}^T P_{\ell_n} A_{\Lambda_n} + P_{\Lambda_n}), \tag{3.30}$$

and

$$U_X = \sum_{i=1}^{n} A_{X_i}^T P_{\ell_i} W_i , \tag{3.31}$$

$$U_\Lambda = \begin{bmatrix} A_{\Lambda_1}^T P_{\ell_1} W_1 \\ A_{\Lambda_2}^T P_{\ell_2} W_2 \\ \\ A_{\Lambda_n}^T P_{\ell_n} W_n \end{bmatrix} , \tag{3.32}$$

with the misclosure vectors W_i, i=1,n, and a priori weight matrices P_X and P_{Λ_i}, i=1,n, for the unknowns. The inverse of the partitioned normal equation matrix can be written as (see, e.g., Vaníček and Krakiwsky [1982]):

$$\begin{bmatrix} N_{XX} & N_{X\Lambda} \\ \\ N_{\Lambda X} & N_{\Lambda\Lambda} \end{bmatrix}^{-1} = \begin{bmatrix} C_{XX} & C_{X\Lambda} \\ \\ C_{\Lambda X} & C_{\Lambda\Lambda} \end{bmatrix} , \tag{3.33}$$

with

$$C_{XX} = (N_{XX} - N_{X\Lambda}\, N_{\Lambda\Lambda}^{-1}\, N_{\Lambda X})^{-1} \quad ,$$

$$C_{X\Lambda} = -C_{XX}\, N_{X\Lambda}\, N_{\Lambda\Lambda}^{-1} = C_{\Lambda X}^{T} \quad , \tag{3.34}$$

$$C_{\Lambda\Lambda} = N_{\Lambda\Lambda}^{-1} + N_{\Lambda\Lambda}^{-1}\, N_{\Lambda X}\, C_{XX}\, N_{X\Lambda}\, N_{\Lambda\Lambda}^{-1} \quad .$$

Denoting:

$$N_i = A_{X_i}^{T}\, P_{\ell_i}\, A_{X_i} \quad ,$$

$$O_i = A_{X_i}^{T}\, P_{\ell_i}\, A_{\Lambda_i} \quad ,$$

$$M_i = A_{\Lambda_i}^{T}\, P_{\ell_i}\, A_{\Lambda_i} + P_{\Lambda_i} \quad , \tag{3.35}$$

$$U_{X_i} = A_{X_i}^{T}\, P_{\ell_i}\, W_i \quad ,$$

$$U_{\Lambda_i} = A_{\Lambda_i}^{T}\, P_{\ell_i}\, W_i \quad ,$$

and using eqns. (3.27) to (3.34), we get the following expressions for the first two covariance matrices (3.34):

$$C_{XX} = \Big(\sum_{i=1}^{n} N_i + P_X - \sum_{i=1}^{n} O_i\, M_i^{-1}\, O_i^{T}\Big)^{-1}$$

$$= \Big(\sum_{i=1}^{n} \{N_i - O_i\, M_i^{-1}\, O_i^{T}\} + P_X\Big)^{-1} \quad , \tag{3.36}$$

$$C_{X\Lambda} = -\, C_{XX}[O_1\, M_1^{-1},\ O_2\, M_2^{-1},\ \ldots,\ O_n\, M_n^{-1}] \quad . \tag{3.37}$$

By means of eqns. (3.36) and (3.37), we obtain from (3.26) and (3.33) the least-squares estimates for the station coordinates X after n sessions:

$$\hat{X}^{(n)} = C_{XX} \cdot U_X + C_{X\Lambda} \cdot U_\Lambda$$

$$= \Big(\sum_{i=1}^{n} \{N_i - O_i M_i^{-1} O_i^T\} + P_X \Big)^{-1} \Big(\sum_{i=1}^{n} U_{X_i} - \sum_{i=1}^{n} O_i M_i^{-1} U_{\Lambda_i} \Big)$$

$$= \Big(\sum_{i=1}^{n} \{N_i - O_i M_i^{-1} O_i^T\} + P_X \Big)^{-1} \sum_{i=1}^{n} \{U_{X_i} - O_i M_i^{-1} U_{\Lambda_i}\} \qquad (3.38)$$

The change in $\hat{X}$ from session (n-1) to session n,

$$\delta\hat{X}^{(n)} = \hat{X}^{(n)} - \hat{X}^{(n-1)} \quad , \qquad (3.39)$$

is obtained from (3.38) as:

$$\delta\hat{X}^{(n)} = \Big(\sum_{i=1}^{n} \{N_i - O_i M_i^{-1} O_i^T\} + P_X \Big)^{-1} \sum_{i=1}^{n} \{U_{X_i} - O_i M_i^{-1} U_{\Lambda_i}\}$$

$$- \Big(\sum_{i=1}^{n-1} \{N_i - O_i M_i^{-1} O_i^T\} + P_X \Big)^{-1} \sum_{i=1}^{n-1} \{U_{X_i} - O_i M_i^{-1} U_{\Lambda_i}\}$$

which can be rewritten as:

$$\delta\hat{X}^{(n)} = \Big(\sum_{i=1}^{n} \{N_i - O_i M_i^{-1} O_i^T\} + P_X \Big)^{-1} \big(\{U_{X_n} - O_n M_n^{-1} U_{\Lambda_n}\} - \{N_n - O_n M_n^{-1} O_n^T\} \hat{X}^{(n-1)} \big). \qquad (3.40)$$

The solution $\hat{X}^{(n)} = \hat{X}^{(n-1)} + \delta\hat{X}^{(n)}$ is based on:

- the previous solution $\hat{X}^{(n-1)}$;
- the accumulated reduced normal equation matrix:

$$\sum_{i=1}^{n} \{N_i - O_i M_i^{-1} O_i^T\} + P_X \; ;$$

- the change in reduced normal equation matrix from session n-1 to session n: $N_n - O_n M_n^{-1} O_n^T$;
- the observations of session n imbedded in U_{X_n} , U_{Λ_n}.

The estimates for the nuisance parameters do not appear explicitly in eqn. (3.40); if these values are desired, they can be evaluated after the final solution for X has been obtained.

From eqn. (3.26) we get:

$$N_{XX} \cdot \hat{X} + N_{X\Lambda} \cdot \hat{\Lambda} = U_X$$
$$N_{\Lambda X} \cdot \hat{X} + N_{\Lambda\Lambda} \cdot \hat{\Lambda} = U_\Lambda \quad , \tag{3.41}$$

with

$$\hat{\Lambda} = \begin{bmatrix} \hat{\Lambda}_1 \\ \hat{\Lambda}_2 \\ \\ \hat{\Lambda}_n \end{bmatrix} \quad ,$$

$$U_X = \sum_{i=1}^{n} U_{X_i} \quad , \tag{3.42}$$

$$U_\Lambda = \begin{bmatrix} U_{\Lambda_1} \\ U_{\Lambda_2} \\ \\ U_{\Lambda_n} \end{bmatrix}$$

The second of eqns. (3.41) gives the least-squares estimate

$$\hat{\Lambda} = N_{\Lambda\Lambda}^{-1} \cdot [U_\Lambda - N_{\Lambda X} \cdot \hat{X}] \tag{3.43}$$

for Λ where $\hat{X}$ is the final estimate for the station coordinates X. Realizing the special structure of $N_{\Lambda\Lambda}$ (cf. eqn. (3.30), we can rewrite eqn. (3.43) separately for each session i as:

$$\hat{\Lambda}_i = M_i^{-1}(U_{\Lambda_i} - O_i^T \hat{X}) \quad . \tag{3.44}$$

If a recomputation of the $\hat{\Lambda}_i$ with eqn. (3.44) is desired, the matrix products $M_i^{-1} U_{\Lambda_i}$ and $M_i^{-1} O_i^T$ are to be stored during the sequential processing of the observations of the subsequent sessions. After the final

solution $\hat{X}$ for X has been obtained, these matrix products are used in eqn. (3.44) for the evaluation of $\hat{\Lambda}_i$.

During the sequential solution for $\hat{X}$ with eqn. (3.40), the squared weighted sum of the residuals has to be updated. From eqn. (3.24) we get:

$$V = \begin{bmatrix} V_1 \\ V_2 \\ \\ V_n \end{bmatrix} = \begin{bmatrix} A_{X_1} \\ A_{X_2} \\ \\ A_{X_n} \end{bmatrix} \hat{X} + \begin{bmatrix} A_{\Lambda_1} \cdot \hat{\Lambda}_1 \\ A_{\Lambda_2} \cdot \hat{\Lambda}_2 \\ \\ A_{\Lambda_n} \cdot \hat{\Lambda}_n \end{bmatrix} - \begin{bmatrix} W_1 \\ W_2 \\ \\ W_n \end{bmatrix} . \tag{3.45}$$

Because of eqn. (3.25), we obtain after the nth session,

$$(V^T P_\ell V)^{(n)} = \sum_{i=1}^{n} V_i^T P_{\ell_i} V_i \quad . \tag{3.46}$$

With eqn. (3.44), V_i can be written as:

$$V_i = A_{X_i} \cdot \hat{X} + A_{\Lambda_i} M_i^{-1} (U_{\Lambda_i} - O_i^T \hat{X}) - W_i$$

$$= (I - A_{\Lambda_i} M_i^{-1} A_{\Lambda_i}^T P_{\ell_i})(A_{X_i} \cdot \hat{X} - W_i) \ , \tag{3.47}$$

resulting in:

$$V_i^T P_{\ell_i} V_i = (A_{X_i} \cdot \hat{X} - W_i)^T (P_{\ell_i} - P_{\ell_i} A_{\Lambda_i} M_i^{-1} A_{\Lambda_i}^T P_{\ell_i})(A_{X_i} \cdot \hat{X} - W_i). \tag{3.48}$$

With definitions (3.35) and some elementary operations we arrive at:

$$V_i^T P_{\ell_i} V_i = \hat{X}^T (N_i - O_i M_i^{-1} O_i^T) \hat{X} - 2(U_{X_i}^T - U_{\Lambda_i}^T M_i^{-1} O_i^T) \hat{X}$$

$$+ W_i^T P_{\ell_i} W_i - U_{\Lambda_i}^T M_i^{-1} U_{\Lambda_i} \quad .$$

Using (3.38) we get from (3.46)

$$(V^T P_\ell V)^{(n)} = \sum_{i=1}^{n} (W_i^T P_{\ell_i} W_i - U_{\Lambda_i}^T M_i^{-1} U_{\Lambda_i}) - \hat{X}^{(n)^T} \sum_{i=1}^{n} (N_i - O_i M_i^{-1} O_i^T) \hat{X}^{(n)} \quad (3.49)$$

Comparing (3.49) for (n-1) and for n we compute for the increment:

$$\delta(V^T P_\ell V)^{(n)} = (V^T P_\ell V)^{(n)} - (V^T P_\ell V)^{(n-1)} \quad (3.50)$$

$$\begin{aligned} \delta(V^T P_\ell V)^{(n)} = {} & (W_n^T P_{\ell_n} W_n - U_{\Lambda_n}^T M_n^{-1} U_{\Lambda_n}) \\ & - \hat{X}^{(n-1)^T} (U_{X_n} - O_n M_n^{-1} U_{\Lambda_n}) \\ & - \hat{X}^{(n)^T} \{(U_{X_n} - O_n M_n^{-1} U_{\Lambda_n}) - (N_n - O_n M_n^{-1} O_n^T) X^{(n-1)}\} . \end{aligned} \quad (3.51)$$

The matrices on the right-hand side of (3.51) are the same as those in eqn. (3.40) for the updating of the unknown vector X.

For the covariance matrix C of the unknowns after the processing of n sessions, we derive from eqn. (3.33) by further partitioning:

$$C^{(n)} = \left[\begin{array}{c|ccc} C_{XX} & C_{X\Lambda_1} & C_{X\Lambda_2} & C_{X\Lambda_n} \\ \hline C_{\Lambda_1 X} & C_{\Lambda_1\Lambda_1} & C_{\Lambda_1\Lambda_2} & \\ C_{\Lambda_2 X} & C_{\Lambda_2\Lambda_1} & C_{\Lambda_2\Lambda_2} & \\ & & & \\ C_{\Lambda_n X} & & & C_{\Lambda_n\Lambda_n} \end{array}\right]^{(n)} . \quad (3.52)$$

Inspection of eqns. (3.34) through (3.37) gives the following explicit expressions for the submatrices in eqn. (3.52):

$$C_{XX}^{(n)} = \left(\sum_{i=1}^{n} \{N_i - O_i M_i^{-1} O_i^T\} + P_X \right)^{-1} \quad , \tag{3.53}$$

$$C_{\Lambda_i X}^{(n)} = - M_i^{-1} O_i^T C_{XX}^{(n)} \quad \text{for } i \leq n \quad , \tag{3.54}$$

$$= \text{undefined for } i > n \quad ,$$

$$C_{\Lambda_i \Lambda_i}^{(n)} = M_i^{-1} + M_i^{-1} O_i^T C_{XX}^{(n)} O_i M_i^{-1} \quad \text{for } i \leq n \quad , \tag{3.55}$$

$$= \text{undefined for } i > n \quad ,$$

$$C_{\Lambda_i \Lambda_j}^{(n)} = M_i^{-1} O_i^T C_{XX}^{(n)} O_j M_j^{-1} \quad \text{for } i \leq n \text{ and } j \leq n \quad , \tag{3.56}$$

$$= \text{undefined for } i > n \text{ or } j > n \; .$$

If a recomputation of the complete covariance matrix (3.52) is desired after the final estimate for X has been evaluated, the matrices M_i^{-1} and $M_i^{-1} O_i^T$ have to be stored during the sequential processing of the observation sessions.

3.4.1.2 Elimination within one session

From the preceeding session (n-1) we know the least-squares estimates for the station coordinates, $\hat{X}^{(n-1)}$, and their covariance matrix, $C_{XX}^{(n-1)}$. The observation equations for session n can be written (cf. (3.24)):

$$A_{X_n} X + A_{\Lambda_n} \Lambda_n = W_n + V_n, \; P_{\ell_n} \quad . \tag{3.57}$$

In this subsection we will deal always with quantities related to session n. Thus we omit the subscript n and denote the session (if absolutely necessary for clarification) by a superscript n. Subscripts will be used to identify sequences within the nth session.

We rewrite eqn. (3.57) as:

$$\left[\begin{array}{c|c} A_{X_1} & A_{\Lambda_1} \\ A_{X_2} & A_{\Lambda_2} \\ A_{X_k} & A_{\Lambda_k} \end{array}\right] \left[\begin{array}{c} X \\ \Lambda \end{array}\right] = \left[\begin{array}{c} W_1 + V_1 \\ W_2 + V_2 \\ W_k + V_k \end{array}\right] \quad , \tag{3.58}$$

and we assume that the sequences have been chosen in such a manner that observations of different sequences are uncorrelated.

$$P_\ell = \mathrm{diag}(P_{\ell_1}, P_{\ell_2}, \ldots, P_{\ell_k}) \quad . \tag{3.59}$$

Equations (3.58) and (3.59) lead to the normal equations for the qth sequence in the nth session:

$$\begin{bmatrix} \sum_{i=1}^{q} A_{X_i}^T P_{\ell_i} A_{X_i} + S^{(n-1)} + P_X & \sum_{i=1}^{q} A_{X_i}^T P_{\ell_i} A_{\Lambda_i} \\ \sum_{i=1}^{q} A_{\Lambda_i}^T P_{\ell_i} A_{X_i} & \sum_{i=1}^{q} A_{\Lambda_i}^T P_{\ell_i} A_{\Lambda_i} + P_\Lambda \end{bmatrix} \cdot \begin{bmatrix} X \\ \Lambda \end{bmatrix} =$$

$$= \begin{bmatrix} \sum_{i=1}^{q} A_{X_i}^T P_{\ell_i} W_i + R^{(n-1)} \\ \sum_{i=1}^{q} A_{\Lambda_i} P_{\ell_i} W_i \end{bmatrix} \quad . \tag{3.60}$$

$S^{(n-1)}$ is the accumulated reduced normal equation matrix with respect to X of the previous (n-1) sessions and $R^{(n-1)}$ is the corresponding right hand side.

$$S^{(n-1)} = \sum_{k=1}^{n-1} (N_k - O_k M_k^{-1} O_k^T) \quad , \tag{3.61}$$

$$R^{(n-1)} = \sum_{k=1}^{n-1} (U_{X_k} - O_k M_k^{-1} U_{\Lambda_k}) \quad . \tag{3.62}$$

The dimension of X is always 3 times the number of observing stations, whereas the number of nuisance parameters will be increasing during a

session, e.g., if new cycle slip ambiguities are to be included. The actual dimension of Λ in an adjustment sequence q will be denoted by p.

Denoting now:

$$
\begin{aligned}
N_{XX}^{q} &= \sum_{i=1}^{q} E_i , \quad E_i = A_{X_i}^{T} P_{\ell_i} A_{X_i} , \\
N_{X\Lambda}^{pq} &= \sum_{i=1}^{q} F_i^{p} , \quad F_i^{p} = A_{X_i}^{T} P_{\ell_i} A_{\Lambda_i}^{p} , \\
N_{\Lambda\Lambda}^{pq} &= \sum_{i=1}^{q} G_i^{p} , \quad G_i^{p} = A_{\Lambda_i}^{pT} P_{\ell_i} A_{\Lambda_i}^{p} , \\
U_{X}^{q} &= \sum_{i=1}^{q} H_i , \quad H_i = A_{X_i}^{T} P_{\ell_i} W_i , \\
U_{\Lambda}^{pq} &= \sum_{i=1}^{q} J_i^{p} , \quad J_i^{p} = A_{\Lambda_i}^{pT} P_{\ell_i} W_i ,
\end{aligned}
\tag{3.63}
$$

where $A_{\Lambda_i}^{p}$ is the matrix of the first p columns of A_{Λ_i}, we rewrite eqn. (3.60) as:

$$
\begin{bmatrix} N_{XX}^{q} + S^{(n-1)} + P_X & N_{X\Lambda}^{pq} \\ N_{\Lambda X}^{pq} & N_{\Lambda\Lambda}^{pq} + P_{\Lambda}^{p} \end{bmatrix} \begin{bmatrix} \hat{X} \\ \hat{\Lambda}^{p} \end{bmatrix} = \begin{bmatrix} U_{X}^{q} + R^{(n-1)} \\ U_{\Lambda}^{pq} \end{bmatrix} \tag{3.64}
$$

$\hat{\Lambda}^{p}$ consists of the first p nuisance parameters and P_{Λ}^{p} is the corresponding a priori weight matrix.

We then obtain the least-squares solution of eqn. (3.64) in the qth sequence:

$$
\hat{X}^{q} = (N_{XX}^{q} + P_X + S^{(n-1)})^{-1}(U_{X}^{q} + R^{(n-1)} - N_{X\Lambda}^{pq}\,\hat{\Lambda}^{pq}) , \tag{3.65}
$$

$$\hat{\Lambda}^{pq} = (N_{\Lambda\Lambda}^{pq} + P_{\Lambda}^{p})^{-1}(U_{\Lambda}^{pq} - N_{\Lambda X}^{pq}\,\hat{X}^{q}) \quad . \tag{3.66}$$

Realizing that

$$\hat{X}^{(n-1)} = (S^{(n-1)} + P_X)^{-1}\,R^{(n-1)} \quad , \tag{3.67}$$

and denoting

$$\delta\hat{X}^{nq} = \hat{X}^{q} - \hat{X}^{(n-1)} \quad , \tag{3.68}$$

we derive from (3.65)

$$\delta\hat{X}^{nq} = (N_{XX}^{q} + P_X + S^{(n-1)})^{-1}(U_X^q - N_{X\Lambda}^{pq}\,\hat{\Lambda}^{pq} - N_{XX}^{q}\,\hat{X}^{(n-1)}) \tag{3.69}$$

This equation relates the least-squares estimate for the station coordinates in the qth sequence of the nth session to the current estimate for the first p nuisance parameters, $\hat{\Lambda}^{pq}$, and the estimated station coordinates, $\hat{X}^{(n-1)}$ at the end of the (n-1)st session.

Combining eqns. (3.65) and (3.66), we obtain the explicit formula for $\hat{\Lambda}^{pq}$:

$$\begin{aligned}\hat{\Lambda}^{pq} = {} & (N_{\Lambda\Lambda}^{pq} + P_{\Lambda}^{p} - N_{\Lambda X}^{pq}(N_{XX}^{q} + P_X + S^{(n-1)})^{-1}N_{X\Lambda}^{pq})^{-1} \\ & \cdot (U_{\Lambda}^{pq} - N_{\Lambda X}^{pq}(N_{XX}^{q} + P_X + S^{(n-1)})^{-1}(U_X^q + R^{(n-1)}) \quad .\end{aligned} \tag{3.70}$$

Equation (3.70) can be used from time to time to update the estimate for the nuisance parameters Λ^{p}. Between these updates, the best available estimate for Λ^{p} can be used to replace $\hat{\Lambda}^{pq}$ in eqn. (3.69) and to evaluate $\delta\hat{X}^{nq}$ approximately.

It should be noted here that immediately after an update of Λ^{pq} with eqn. (3.70) and an evaluation of eqn. (3.69), the effect of prior approximations is eliminated.

3.4.2 Orbital Bias Elimination

The main processor requires the components of the position and velocity vectors of the satellites for each observation epoch. If an orbit improvement is to be attempted as discussed below, the mean Keplerian elements corresponding to the position and velocity vectors must also be provided for the processor.

The position and velocity vectors and the mean Keplerian elements are obtained from auxiliary programs. For processing Macrometer™ data, TRNTF (cf. section 3.2.1) has been written. This program approximates the orbits of GPS satellites, starting with the orbits represented by the Macrometer™ T-files. The T-file ephemerides are used as a priori values in an orbit improvement process using numerical integration. The output of program TRNTF consists of the coefficients of a high-order (typically, 10th) polynomial approximation of the orbit over a short arc, typically less than 6 hours, and orbital elements for a specific epoch. The force field presently used in TRNTF consists of the zonal harmonics of the earth's gravitational field up to and including J_4 and the solar and lunar (central) gravitational fields.

The second part of the preprocessor (MACPR) evaluates, among other tasks, the polynomials to obtain consistent position and velocity components for each observation epoch (see section 3.2.1.3). This information, together with the Keplerian parameters, is passed to the main processor.

If the GPS broadcast ephemeris is used, such as in processing observations from the TI-4100, the ephemeris parameters are converted to position and velocity in the CT system by subroutine SATOR (see section 3.2.2.1) in the preprocessor for the TI data. Mean Keplerian elements for a certain epoch are also computed.

Perhaps the most serious impediment to achieving centimetre accuracies on baselines longer than several hundred kilometres is our imprecise knowledge of the orbits of the satellites. Although far less sensitive to orbit uncertainty than point positioning, baseline determination using the phase difference observable is still limited in accuracy by orbit error.

How sensitive is the phase-difference technique to an error, $\vec{dr}$, in the geocentric position of a satellite, $\vec{r}$? If we ignore all other effects except geometry, the unambiguous phase recorded at station 1 for a

particular satellite is:

$$\rho_1 = |\vec{\rho}_1| \quad , \tag{3.71}$$

where

$$\vec{\rho}_1 = \vec{r}_1 - \vec{R}_1 \quad , \tag{3.72}$$

with $\vec{R}_1$ being the true geocentric position vector of station 1 and $\vec{r}_1$ the true geocentric position vector of the satellite. For the same satellite observed from station 2 at the same instant,

$$\vec{\rho}_2 = \vec{r}_2 - \vec{R}_2 \quad , \tag{3.73}$$

since wavefronts that arrive at the receivers at the same instant, depart the satellite at different times, $\vec{r}_1$ and $\vec{r}_2$, will in general be different, with $|\vec{r}_2 - \vec{r}_1| < 80$ m. The baseline vector is

$$\vec{B} = \vec{R}_2 - \vec{R}_1 \quad .$$

The single difference observable is

$$\Delta\rho = \rho_2 - \rho_1 = (\vec{\rho}_2 \cdot \vec{\rho}_2)^{1/2} - (\vec{\rho}_1 \cdot \vec{\rho}_1)^{1/2} \quad . \tag{3.74}$$

Let us now suppose that we have only approximate position for the satellite equal to $\vec{r}_1 + d\vec{r}$ and $\vec{r}_2 + d\vec{r}$. We then have

$$\begin{aligned} \Delta\rho = {} & [(\vec{\rho}_2 + d\vec{r} - d\vec{R}_2) \cdot (\vec{\rho}_2 + d\vec{r} - d\vec{R}_2)]^{1/2} \\ & - [(\vec{\rho}_1 + d\vec{r} - d\vec{R}_1) \cdot (\vec{\rho}_1 + d\vec{r} - d\vec{R}_1)]^{1/2} \quad , \end{aligned} \tag{3.75}$$

where $d\vec{R}_1$ and $d\vec{R}_2$ are the movements to the position vectors of stations 1 and 2 so that

$$\vec{R}_i + d\vec{R}_i \tag{3.76}$$

yields the displaced position of station i. The corresponding baseline vector is therefore

$$\vec{B} + d\vec{B} = \vec{R}_2 - \vec{R}_1 + d\vec{R}_2 - d\vec{R}_1 \quad . \tag{3.77}$$

Expanding (3.75) we have

$$\begin{aligned} \Delta\rho = {} & [\vec{\rho}_2 \cdot \vec{\rho}_2 + 2\vec{\rho}_2 \cdot (d\vec{r} - d\vec{R}_2) + (d\vec{r} - d\vec{R}_2) \cdot (d\vec{r} - d\vec{R}_2)]^{1/2} \\ & - [\vec{\rho}_1 \cdot \vec{\rho}_1 + 2\vec{\rho}_1 \cdot (d\vec{r} - d\vec{R}_1) + (d\vec{r} - d\vec{R}_1) \cdot (d\vec{r} - d\vec{R}_1)]^{1/2} \ , \end{aligned} \tag{3.78}$$

which we can write as

$$\begin{aligned} \Delta\rho = {} & \rho_2 [1 + 2\frac{\vec{\rho}_2}{\rho_2^2} \cdot (d\vec{r} - d\vec{R}_2) + \frac{1}{\rho_2^2} (d\vec{r} - d\vec{R}_2) \cdot (d\vec{r} - d\vec{R}_2)]^{1/2} \\ & - \rho_1 [1 + 2\frac{\vec{\rho}_1}{\rho_1^2} \cdot (d\vec{r} - d\vec{R}_1) + \frac{1}{\rho_1^2} (d\vec{r} - d\vec{R}_1) \cdot (d\vec{r} - d\vec{R}_1)]^{1/2} \ . \end{aligned} \tag{3.79}$$

Expanding the square roots and discarding terms which are the products of differentials, we get

$$\begin{aligned} \Delta\rho &= \rho_2 [1 + \frac{\vec{\rho}_2}{\rho_2^2} \cdot (d\vec{r} - d\vec{R}_2)] - \rho_1 [1 + \frac{\vec{\rho}_1}{\rho_1^2} \cdot (d\vec{r} - d\vec{R}_1)] \\ &= \rho_2 - \rho_1 + (\frac{\vec{\rho}_2}{\rho_2} - \frac{\vec{\rho}_1}{\rho_1}) \cdot d\vec{r} - \frac{\vec{\rho}_2}{\rho_2} \cdot d\vec{R}_2 + \frac{\vec{\rho}_1}{\rho_1} \cdot d\vec{R}_1 \quad . \end{aligned} \tag{3.80}$$

Now, $\rho_2 - \rho_1 = \Delta\rho$, so

$$(\frac{\vec{\rho}_2}{\rho_2} - \frac{\vec{\rho}_1}{\rho_1}) \cdot d\vec{r} = \frac{\vec{\rho}_2}{\rho_2} \cdot d\vec{R}_2 - \frac{\vec{\rho}_1}{\rho_1} \cdot d\vec{R}_1 \quad . \tag{3.81}$$

Since we are only interested in the baseline vector as a relative position vector, with no loss in generality we can set $d\vec{R}_2 = \vec{0}$, so that

$$d\vec{R}_1 = - d\vec{B} \quad , \tag{3.82}$$

and

$$(\frac{\vec{\rho}_2}{\rho_2} - \frac{\vec{\rho}_1}{\rho_1}) \cdot d\vec{r} = \frac{\vec{\rho}_1}{\rho_1} \cdot d\vec{B} \quad . \tag{3.83}$$

In order to simplify this equation, we introduce the approximation

$$\rho_1 \simeq \rho_2 = \rho \quad , \tag{3.84}$$

where ρ is the approximate range from either station 1 or 2 to the satellite. We then have

$$\frac{1}{\rho}(\vec{\rho}_2 - \vec{\rho}_1) \cdot d\vec{r} = \frac{\vec{\rho}_1}{\rho} \cdot d\vec{B} \quad , \tag{3.85}$$

or

$$\vec{B} \cdot d\vec{r} = \vec{\rho}_1 \cdot d\vec{B} \quad . \tag{3.86}$$

Equation (3.86) is a useful expression for studying the effects of orbit errors on baseline estimates. Here, however, we will only consider a crude order of magnitude effect for which we can approximate eqn. (3.86) as

$$|\vec{B}||d\vec{r}| \doteq \rho|d\vec{B}| \quad , \tag{3.87}$$

or

$$\frac{dB}{B} = \frac{dr}{\rho} \quad . \tag{3.88}$$

This is the expression we have been seeking. It relates the error dB incurred in estimating a baseline of length B as a result of an error dr in the assumed position of the satellite. This relationship has been obtained by others, for example, by Bauersima [1983], but has not been derived in the form shown here in an English language publication.

The minimum and maximum ranges for the GPS satellites are approximately 20,200 and 25,800 km respectively. Rounding the lower figure down to 20,000 km gives us a pessimistic value for the relative uncertainty in baseline length estimation of 5×10^{-8} dr(m). If the orbit uncertainty is 200 m, the relative baseline accuracy would be about 10 parts per

million (ppm). This amounts to 60 cm on a baseline of length 60 km. The actual error would be somewhat less since we took a pessimistic value for the range. More importantly, in an actual determination a number of satellites well distributed on the sky would be observed. Since the orbit errors of different satellites in different parts of the sky would tend to be random, the baseline error would average to a smaller value. Baselines derived from double or triple difference observations would be similarly affected.

What is the accuracy of presently available GPS orbits? Information on GPS orbits is readily available from at least four sources with differing degrees of accuracies. These sources are (i) the Prediction Bulletin of the Goddard Space Flight Center (GSFC), (ii) the predicted ephemerides broadcast by the GPS satellites themselves, (iii) the orbits computed by the U.S. DoD Naval Surface Weapons Center (NSWC), and (iv) orbits computed by Litton Aero Service for the users of Macrometers.

The orbits contained in the GSFC bulletin are computed well in advance of their time of use and satellite positions computed from these orbits could be in error by the order of kilometres. Such orbits should only be used for the prediction of alerts.

The GPS satellites broadcast a predicted ephemeris based on historical and near real-time tracking by the U.S. DoD and predicted for the following 24-hour period. These orbits are uploaded into the satellites at least once per day during the present test phase. To our knowledge, no detailed study on the accuracy of these orbits has been published. However, satellite positions computed from these orbits are predicted to have a user equivalent range error of 1.5 to 4 metres [van Dierendonck et al., 1980]. Anderle [1984] states that the combined effect of satellite clock and position error on pseudo-range measurements is 6 m. Presumably this is an r.m.s. measure and does not include biases which may be approximately constant during a pass segment.

A further indication of the accuracy of the broadcast ephemeris is provided by the results of the Ottawa test of the TI-4100 reported in Chapter 5. The repeatability in baseline length of better than 1 ppm implies (cf. eqn. (3.88)) an average orbit accuracy at the worst of about 20 m. Since other errors contribute to the 1 ppm uncertainty, the orbits could have an accuracy significantly greater than 20 m. In any case, it

appears that the broadcast ephemeris is suitable for 1 ppm relative positioning. However, three cautions are in order: (i) the ephemeris must be fresh, i.e., used for the one-hour period for which it was intended and ideally be within a few hours of upload, (ii) the ephemeris should not be used near the times when the GPS control segment makes the weekly satellite momentum dumps, and (iii) in the future, the full-accuracy broadcast ephemeris may not be available to all GPS users.

The orbits computed by NSWC are also based on tracking by the GPS control segment and are available to qualified users on a delayed basis. The accuracy of satellite positions determined from these orbits is believed to be in the range of 20 to 30 m. As these orbits are derived from historical data rather than new real-time data, one would expect the orbits to be of higher accuracy. A detailed comparison of the broadcast and precise ephemeris awaits a future study.

Litton Aero Service also provides precise ephemerides to its customers. The accuracy of these orbits is probably equivalent to those of NSWC. Macrometer™ T-files are based on NSWC or Litton orbits.

King et al. [1984] have reported on the interferometric determination of satellite orbits using receivers at the three stations of the POLARIS VLBI network: Westford, MA, Richmond, FL, and Fort Davis, TX. They obtained formal orbit (r.m.s.) errors of 3 to 5 m (rms).

We have developed our software to take advantage of any available orbits and to improve these orbits if necessary. Equation (3.88) shows that for short baselines the absolute sensitivity to orbit errors is small. However, for a given orbit accuracy, the baseline error grows with baseline length. For baselines longer than several hundred kilometres, the accuracy of an available ephemeris may be insufficient for many geodetic activities. Whereas the use of precise ephemerides computed from observations by a distant tracking network may buy some increase in accuracy; the highest baseline accuracies would be obtained if a tracking network in the vicinity of the baseline or baselines being measured is used. In fact, it is possible to use the same stations forming the baselines of interest to improve the satellite orbits. We have therefore looked at the problem of satellite orbit determination in some detail.

The determination of satellite orbits is an improvement process. One has at hand some orbital information and one wishes to improve the accuracy

of the orbits by removing the errors or biases contained therein. Algorithms to estimate orbital biases have been developed and widely used in the processing of Transit Doppler data. With some notable exception, these algorithms do not describe the orbits by physical parameters. For example, one technique is to parallely shift and rotate the orbit (used in the Transit processing program GEODOP). What usually results is a physically meaningless model in the sense that the resulting orbit is not a particular solution of the equations of motion of the satellite and is thus inherently imprecise. Nevertheless, such models may be useful in certain circumstances, e.g., when the orbit is observed from a small region [Kouba, 1985].

We have incorporated into our software an ability to estimate orbital biases in a purely physical way. Our method is outlined in Beutler et al. [1984] and Langley et al. [1984], and has been tested on an earlier IBM version of our software. Recapitulating briefly: the orbit of a satellite is a particular solution of a system of second-order differential equations:

$$\ddot{\vec{r}} = \vec{f}(t; \vec{r}, \dot{\vec{r}}, p_1, p_2, \ldots, p_n) \tag{3.89}$$

where $\vec{r} = \vec{r}(t)$ is the position of the satellite in an inertial reference frame, $\dot{\vec{r}}$ is the satellite's velocity, and $\ddot{\vec{r}}$, its acceleration. The parameters p_i define the various forces acting on the satellite: the gravitational fields, atmospheric drag, and radiation pressure. In order to obtain a particular solution of eqn. (3.87), we specify "initial" values of position and velocity. These values are best selected to correspond to the midpoint of the observation period, t_o. They are expressed in terms of osculating Keplerian elements:

$$\vec{r}(t_o) = \vec{r}(o_1, o_2, \ldots, o_6)$$

$$\dot{\vec{r}}(t_o) = \dot{\vec{r}}_o(o_1, o_2, \ldots, o_6) \quad , \tag{3.90}$$

where

o_1 = a, semimajor axis
o_2 = e, eccentricity
o_3 = i, inclination
o_4 = Ω, right ascension of the ascending node
o_5 = ω, argument of perigee
o_6 = T_o, time of perigee passage.

For our software, we are incorporating the ability to estimate all, or a subset, of the osculating elements at t_o. We have presumed the p_i to be known sufficiently well a priori.

Subroutine RPART, to be incorporated into the main processor (when our new operating system RTE-6/VM becomes operational), calculates the partial derivatives of a satellite position vector, $\vec{r}$, with respect to the orbital elements. The theoretical development of the necessary equations has been given in Langley et al. [1984]. The resulting estimates of the mean Keplerian parameters may be converted to position and velocity components to form a new ephemeris for the satellite. This process should, ideally, involve integration. At the moment, it does not.

How accurate should the force model be for providing orbits of a certain accuracy? Some theoretical studies have been undertaken in an attempt to answer these questions. The studies were performed using program TRNSNEW.

Starting with a Macrometer™ T-file spanning about four hours, orbits were generated using force fields of different degrees of precision. The following four cases were used:

(1) central field, radial force (GM = 3.986 0047 × 10^{14} m^3s^{-2});
(2) (1) plus the J_2 zonal harmonic (J_2 = 1082.627 × 10^{-6}, a_e=6378.140 km);
(3) (2) plus solar and lunar gravitation (GMS = 1.327 124 38 × 10^{20} m^3s^{-2}, GMM = 4.902 788 88 × 10^{12} m^3s^{-2});
(4) (3) plus the J_3 and J_4 zonal harmonics (J_3 = -2.536 × 10^{-6}, J_4 = -1.623 × 10^{-6}).

Numerical values for GM, J_2, J_3, and J_4 were taken from Lerch et al. [1979] and the values for the solar and lunar gravitation constants were taken from Beutler [1982]. The results of the analysis were presented in Beutler

et al. [1984]. A short summary will be given here.

The orbit generated assuming only the radial term of the earth's gravitational field departed from the T-file orbit by up to 600 m. The mean departure over the approximately four-hour period was about 280 m. The results for all the force fields are given in the following table:

TABLE 3.1

Trial	Force Field	Maximum Departure (m)	Mean Departure (m)	δ(dB/B) (ppm)
1	GM	583.2	277.9	14
2	GM, J_2	37.3	16.9	0.8
3	GM, J_2, GMS, GMM	9.8	5.3	0.3
4	GM, J_2, J_3, J_4, GMS, GMM	9.8	5.2	0.3

If we assume that the T-file orbits have an accuracy of about 30 m, then the mean departures represent the degradation in the orbits from going to simpler force models. We can convert this degradation to an equivalent baseline accuracy degradation using eqn. (3.88) and setting dr equal to the mean departure. These accuracy degradations are given in the above table. The values in the table indicate that the use of the J_3 and J_4 zonal harmonics yields only a small improvement in baseline accuracy at the 1 ppm level, whereas the inclusion of the J_2 zonal harmonic and the gravitational fields of the sun and moon is very significant. Clearly the use of the radial component of the earth's gravitation alone is quite insufficient if baseline accuracies of 1 ppm are the goal.

These results are confirmed by van Dierendonck et al. [1980], who present the following table of the approximate perturbing forces on the GPS satellites and the corresponding maximum excursion in satellite position after one hour.

TABLE 3.2

Force	Maximum Perturbing Acceleration (ms^{-2})	Maximum Excursion in one hour (m)
GM	5.6×10^{-1}	
J_2	5.3×10^{-5}	300
GMM	5.5×10^{-6}	40
GMS	3×10^{-6}	20
J_4	10^{-7}	0.6
Solar radiation pressure	10^{-7}	0.6
Higher-order gravity terms	10^{-8}	0.06
All other forces	10^{-8}	0.06

If relative position accuracy of 0.1 ppm or higher is required, more sophisticated force models must be used. We have begun to extend the present study to incorporate the smaller forces acting on the satellites. Figure 3.11 shows the radial, along track, and out-of-plane components of the difference between a 13-hour T-file orbit and that generated using a gravitational model complete to degree and order 4, GMM, GMS, and a simple model for solar radiation pressure. The maximum differences are less than 1 m. We are currently investigating their sources.

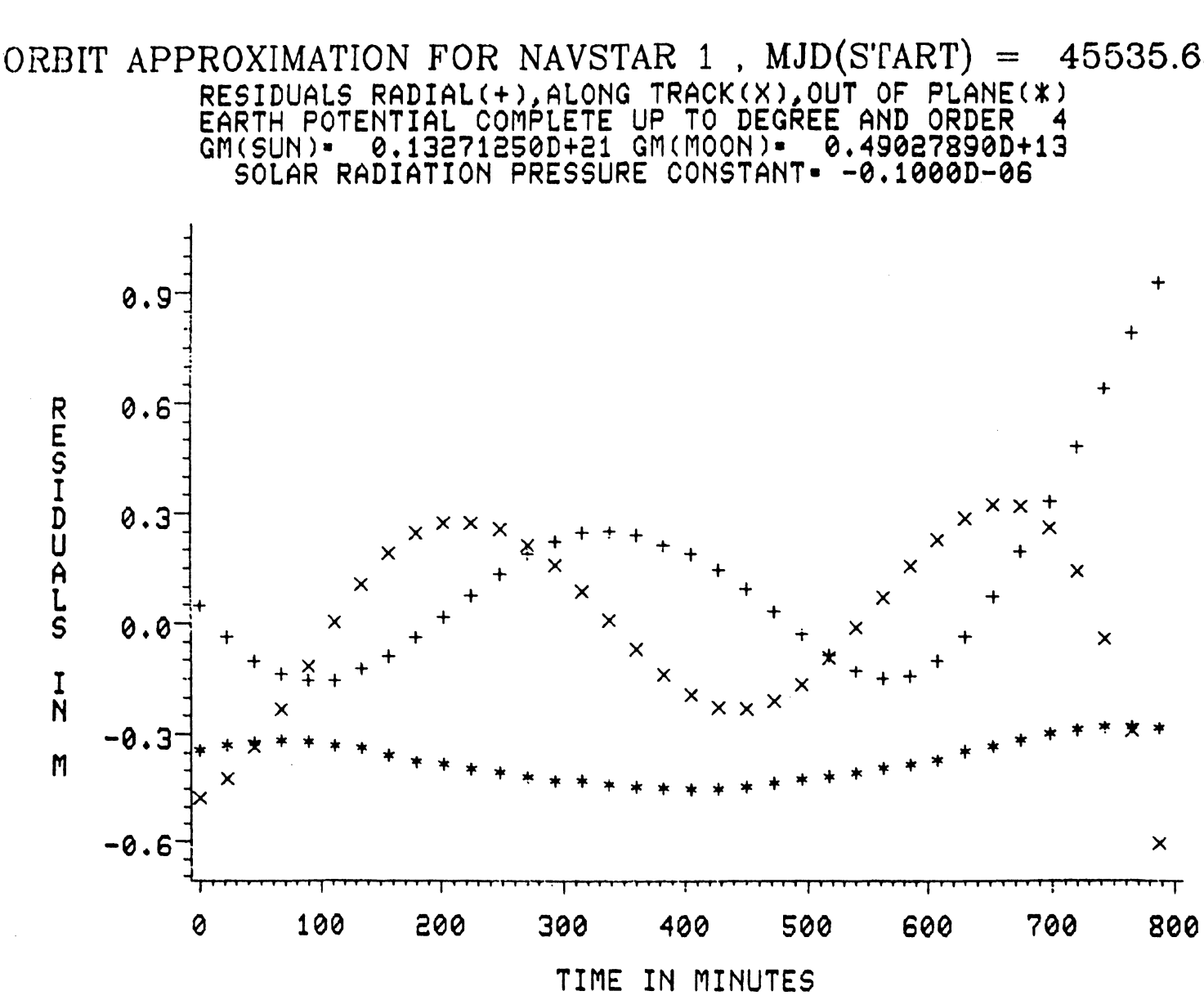

FIGURE 3.11
Difference between T-file orbit and generated orbit.

3.4.3 Ambiguity Elimination

The carrier phase ambiguity (see, e.g., Beutler et al. [1984]) is, by definition, an integer number. We are not aware of the existence of an efficient algorithm for simultaneous estimation of integer numbers (e.g., ambiguities) and real numbers (e.g., relative positions) in a least-squares adjustment. Therefore, in the present version of the software, ambiguities are estimated as real numbers, and then, if possible, constrained to the nearest integer in a second adjustment. Of course, this second adjustment is then not concerned with a parameter elimination in the sense of section 3.4.1; simply, the ambiguities are eliminated from the list of unknowns during the second adjustment.

This method works only for short baselines and single frequency carrier phase observations. To understand this we have to have a closer look at the appropriate observation equations.

The double difference observation equation for observations made at a single frequency f_m, may be written [Beutler et al., 1984] as:

$$\lambda_m \cdot \Delta^2 \tilde{\phi}^{k\ell}_{ijm} = \lambda_m \cdot n^{k\ell}_{ijm} - \Delta^2 \rho^{k\ell}_{ij} - \Delta^2_I \rho^{k\ell}_{ijm} - \Delta^2_T \rho^{k\ell}_{ij} \quad , \tag{3.91}$$

whereas the corresponding equation combining observations made at two frequencies, f_m and f_n, may be written (cf. Bauersima [1983]) as:

$$\frac{c^2}{f_m^2 - f_n^2} \left(\frac{\Delta^2 \tilde{\phi}^{k\ell}_{ijm}}{\lambda_m} - \frac{\Delta^2 \tilde{\phi}^{k\ell}_{ijn}}{\lambda_n} \right) = \frac{c^2}{f_m^2 - f_n^2} \left(\frac{n^{k\ell}_{ijm}}{\lambda_m} - \frac{n^{k\ell}_{ijn}}{\lambda_n} \right) - \Delta^2 \rho^{k\ell}_{ij} - \Delta^2_T \rho^{k\ell}_{ij} \tag{3.92}$$

In these somewhat simplified equations we have extended our symbol convention by using the indices m and n to denote quantities related to carriers L_m and L_n.

For single frequency observations on short baselines, the differential dispersive refraction is usually neglected (see section 3.4.4). For growing baseline length, the ionospheric refraction effects at the two stations decorrelate more and more and consequently, neglecting $\Delta^2_I \rho^{k\ell}_{ijm}$ distorts the model (eqn. (3.91) more and more. A direct result is that the real number estimates for the ambiguities are no longer close to integers. This effect is shown in Tables 3.3 and 3.4. They show the result of processing Macrometer™ V-1000 single frequency double difference data from the Ottawa test network (see section 5.2.1). The real number estimates for

```
BASELINE ANALYZED : PA       , MO

NUMBER OF OBSERVATIONS   =  221
MEAN ERROR OF UNIT WEIGHT=    0.0154 M

         OLD             NEW          DIFF.        +-

   1065091.466     1065091.438     -0.028      0.010
  -4354323.087    -4354322.894      0.193      0.004
   4522053.248     4522053.070     -0.177      0.005

ELLIPSOIDAL COORDINATES OF SECOND RECEIVER
------------------------------------------
LATITUDE  =  45 26 34.29297 +- 0.00015
LONGITUDE =- 76 15 18.81647 +- 0.00043
HEIGHT    =  90.901 M       +- 0.0050 M
LENGTH OF BASELINE(OLD)=           12843.7277 M
LENGTH OF BASELINE(NEW)=           12843.7331 M +- 0.0082 M

RESULTS FOR FILE-NR. 18 (NR OF OBS=108)
---------------------------------------

AMB. PARAMETER 1 =        22475.05 +-      0.10
AMB. PARAMETER 2 =        -2887.07 +-      0.06
AMB. PARAMETER 3 =        -2806.83 +-      0.14
AMB. PARAMETER 4 =        17214.96 +-      0.12

RESULTS FOR FILE-NR. 53 (NR OF OBS=113)
---------------------------------------

AMB. PARAMETER 1 =          444.05 +-      0.05
AMB. PARAMETER 2 =          345.05 +-      0.06
AMB. PARAMETER 3 =        24607.03 +-      0.09
AMB. PARAMETER 4 =          202.04 +-      0.07

RESULTS OF PROGRAM PRMAC-3 (PART 2)
-----------------------------------

FINAL ESTIMATION OF AMBIGUITIES
-------------------------------

AMB.NR.  1 =       22475
AMB.NR.  2 =       -2887
AMB.NR.  3 =       -2807
AMB.NR.  4 =       17215
AMB.NR.  5 =         444
AMB.NR.  6 =         345
AMB.NR.  7 =       24607
AMB.NR.  8 =         202

NUMBER OF OBSERVATIONS   =  221
MEAN ERROR OF UNIT WEIGHT=    0.0173 M

FINAL ESTIMATION OF RECEIVER COORDINATES
----------------------------------------

         OLD             NEW          DIFF.        +-

   1065091.466     1065091.440     -0.026      0.002
  -4354323.087    -4354322.894      0.192      0.004
   4522053.248     4522053.063     -0.184      0.004

ELLIPSOIDAL COORDINATES OF SECOND RECEIVER
------------------------------------------
LATITUDE  =  45 26 34.29279 +- 0.00007
LONGITUDE =- 76 15 18.81638 +- 0.00008
HEIGHT    =  90.897 M       +- 0.0054 M

LENGTH OF BASELINE(OLD)=           12843.7277 M
LENGTH OF BASELINE(NEW)=           12843.7273 M +- 0.0024 M
```

real number ambiguity result

estimated real number ambiguities

corresponding integer ambiguities

integer ambiguity result

TABLE 3.3

Short baseline results for integer ambiguities.

TABLE 3.4

Long baseline results for integer ambiguities.

```
BASELINE ANALYZED : ME       , MO

NUMBER OF OBSERVATIONS   =  413
MEAN ERROR OF UNIT WEIGHT=    0.0302 M

         OLD             NEW          DIFF.        +-

   1065091.466     1065091.326     -0.140      0.012
  -4354323.087    -4354322.933      0.153      0.006
   4522053.248     4522053.010     -0.237      0.006

ELLIPSOIDAL COORDINATES OF SECOND RECEIVER
------------------------------------------
LATITUDE  =  45 26 34.29134 +- 0.00020
LONGITUDE =- 76 15 18.82190 +- 0.00051
HEIGHT    =  90.867 M       +- 0.0072 M
LENGTH OF BASELINE(OLD)=           66268.7030 M
LENGTH OF BASELINE(NEW)=           66268.7833 M +- 0.0123 M

RESULTS FOR FILE-NR. 19 (NR OF OBS=117)
---------------------------------------

AMB. PARAMETER 1 =         1947.44 +-     0.07
AMB. PARAMETER 2 =         1645.85 +-     0.12
AMB. PARAMETER 3 =          620.36 +-     0.09
AMB. PARAMETER 4 =         1037.68 +-     0.08

RESULTS FOR FILE-NR. 25 (NR OF OBS=151)
---------------------------------------

AMB. PARAMETER 1 =        -2355.75 +-     0.09
AMB. PARAMETER 2 =         8125.52 +-     0.07
AMB. PARAMETER 3 =         3517.95 +-     0.08
AMB. PARAMETER 4 =         2114.72 +-     0.12
AMB. PARAMETER 5 =        -2424.28 +-     0.08

RESULTS FOR FILE-NR. 31 (NR OF OBS=145)
---------------------------------------

AMB. PARAMETER 1 =        -9833.71 +-     0.10
AMB. PARAMETER 2 =         5929.88 +-     0.09
AMB. PARAMETER 3 =        -4490.48 +-     0.10
AMB. PARAMETER 4 =        -6330.95 +-     0.12
AMB. PARAMETER 5 =       -10159.31 +-     0.08
```

the ambiguities on the 13 km Panmure-Morris baseline are close to integers (Table 3.3) and can be easily rounded off to the nearest whole number. This procedure clearly improves the internal precision of the estimated coordinates.

For the 66 km Metcalf-Morris baseline, the estimated real number ambiguities are not unambiguously close to particular integers (Table 3.4), and a new estimation of coordinates by rounding off the ambiguities to integers is also ambiguous.

If we now turn to the dual frequency carrier phase observations (eqn. (3.92)) and rewrite the ambiguity term for the GPS frequencies:

$$\frac{f_1}{f_2} = \frac{\lambda_2}{\lambda_1} = \frac{77}{60} \quad , \tag{3.93}$$

we obtain the following product of an integral part and a real part:

$$\frac{c^2}{f_1^2 - f_2^2} \left(\frac{N_{ij1}^{k\ell}}{\lambda_1} - \frac{N_{ij2}^{k\ell}}{\lambda_2}\right) = \frac{77}{2329} \lambda_1 (77N_{ij1}^{k\ell} - 60N_{ij2}^{k\ell}) \quad . \tag{3.94}$$

That equation states that the coefficient of the integer linear combination of the L1 and L2 ambiguities is by a factor of 2329/77 smaller than the corresponding coefficient in the single frequency observation eqn. (3.91). Consequently the left-hand side of eqn. (3.92) (the combination of L1 and L2 observations) would have to be $\sim$30 times more accurate than the single frequency observation in order to determine the integer ambiguity combination in eqn. (3.94) equally well.

Thus, on short baselines, the observation records of the TI-4100 can be processed first as two single frequency data records to determine the ambiguities $n_{ij1}^{k\ell}$ and $n_{ij2}^{k\ell}$ independently. If the real number estimates are unambiguously close to integers, they can be rounded off to that particular pair of integers. In a second adjustment, these integers are introduced as known quantities in eqn. (3.91).

This procedure does not work, however, for observations on long baselines. Therefore, on long baselines, carrier phase ambiguities for both single and dual frequency observations are estimated as real numbers only.

3.4.4 Other Biases

In addition to the orbital biases and the ambiguities, there are several other biases which affect the phase observables. These biases include satellite and receiver clock errors, phase delays in the receivers, phase delays due to the ionosphere and troposphere, and variations in the angular orientation of the earth from an assumed mean orientation. In the present version of our software, these biases are handled in different ways. Some are modelled, some are assumed small and ignored, and some cancel to a large degree when phases are combined in single or double differencing. Only receiver clock errors are currently removed by parameter estimation. But as a result of the formulation of the general scheme for removing nuisance parameters, outlined in section 3.4.1, DIPOP will have the facility to add additional error models with estimable free parameters.

Most of the biases and their effects on the observables have been discussed in our previous reports [Davidson et al., 1983; Langley et al., 1984; Beutler et al., 1984]. We indicate here only how these biases are handled in DIPOP.

3.4.4.1 Satellite clock errors

We can consider the effect of satellite clock errors on (i) observations and (ii) satellite positions obtained from the broadcast ephemeris.

Since we are concerned with the observation of phase, small errors in the epoch of a satellite clock are not important as far as observations are concerned. What is important is the frequency accuracy and stability of the satellite clock during the satellite pass. Since the satellite clocks are phase-locked to atomic frequency standards, we have assumed that the frequency accuracy and stability of the oscillators are such that they do not contribute measurably to a single difference observable.

The effect of satellite clock errors on the determination of satellite positions from the broadcast ephemeris is another matter. The phase of the P-code is used to determine the time of transmission of the signal (see section 3.2.2.1). This uncorrected time is in the time scale of the satellite which may differ from GPS time by as much as a few milliseconds. The broadcast message contains the offset between satellite time and GPS

time in the form of a clock polynomial and so can be used to correct the satellite time. A knowledge of satellite clock errors to 1 μs is sufficient to give ephemeris interpolation errors of less than a few millimetres.

3.4.4.2 Receiver clock errors

On the other hand, receiver clock errors may be important. In the single-difference observation equation [Beutler et al., 1984], there is a term: $(c - \dot{\rho}_i^k)\Delta t$, where c is the speed of light, $\dot{\rho}_i^k$ is the range rate at station i for satellite k at time t, and Δt is the synchronization error of receiver clock j with respect to receiver clock i. Although an attempt is made to synchronize the clocks in the two receivers at the time of the observations, the remaining synchronization error may be 1 μs or larger, affecting simple differences by 300 m or more. Furthermore, Δt may change with time.

Different options are possible for handling Δt in the processing of single-difference observations. These are discussed by Beutler et al. [1984]. The method we have adopted is to use the double-difference observations in which the bulk of the clock synchronization error is removed a priori. This is because the $c\Delta t$ term is common to the single-difference observations of the two satellites. The remaining term, $(\dot{\rho}_i^k - \dot{\rho}_i^\ell)\Delta t$, is at least a factor of 5×10^6 or so smaller than the term for the single-difference observations. It may still not be completely negligible, however. We therefore model the relative clock behaviour with a first-order polynomial (cf. eqn. (3.19)). The offset, A_0, and drift, A_1, are included as estimable nuisance parameters in the main processor software (cf. section 3.3). A separate polynomial is considered for each session.

We have performed tests with the Macrometer™ campaign observations to evaluate the improvement the clock parameter estimation can make. Some of these results are reported in Vaníček et al. [1985]. The most spectacular improvement being related to the baseline for which the antenna cable of one of the receivers was 30 m longer than the other one. The following table summarizes the results with and without clock offset parameter estimation for this particular case.

	No clock Offset Estimation	Clock Offset Estimation
Clock offset value	-	67 μsec ± 5 μsec
Mean error of unit weight	16 mm	3 mm
Average standard deviation of baseline component	4 mm	0.7 mm
Average of discrepancy from integer for ambiguity estimation	.3	.03
Change in baseline length	-	9 mm

3.4.4.3 Receiver phase delays

After being sensed by the receiving antenna, the satellite signal must follow a path through the preamplifier, antenna cabling, and receiver electronics before it is detected. This instrumental delay will contribute to the measured phase and computed phase differences. For the most part, this delay will be approximately constant and approximately the same for indentical receiver set-ups. However, there may be some variability due to temperature effects. In any case, the effect is of the same form as the relative clock behaviour and is absorbed in the estimation of the clock parameters.

3.4.4.4 Ionospheric delay

For TI-4100 observations, the ionospheric contribution to phase delay is effectively removed in the main processor. By using the observations at both L1 and L2 frequencies, we remove approximately 99% of the effect of the ionosphere. The residual ionospheric effect is ignored.

The Macrometer™ single-frequency observations are at present not corrected for the ionospheric effect. Some work has been done on modelling the effect of the ionosphere on the L1 signals [Abdullah, 1984; Beutler et al., 1984], but the results have not been completely satisfactory.

3.4.4.5 Tropospheric delay

The tropospheric delay is modelled in the main processor using

Hopfield's model [Hopfield, 1971]. Surface meteorological data for each station is contained in a file accessed by the main processor.

In the future, we plan to develop a simple parameterized model for the tropospheric delay. We will then include the zenith delay at each station as a nuisance parameter. Such parameter estimation may be combined with meteorological data including estimates of water vapour content from water vapour radiometers.

3.4.4.6 Earth's angular orientation

In order to get the satellite coordinates in the earth-fixed reference frame, they must be transformed by a number of rotation matrices. Two of these are the spin matrix, whose argument is sidereal time (functionally related to UT1), and the wobble matrix, whose arguments are the x and y coordinates of the pole. In the present version of the software, we use appropriate single mean values of UT1-UTC and the x and y coordinates of the pole for the whole time span of the observations.

The wobble and spin transformations are only made in the Macrometer™ preprocessor. The broadcast ephemeris used by the TI-4100 preprocessor is supposedly already in the earth-fixed frame.

In a future version of the software, we plan to have the Macrometer™ preprocessor directly access files of earth rotation data and to interpolate among the file entries to obtain values for the specific observation epochs.

3.5 Postprocessor

The basic decision we have made is that the presentation unit was going to be a baseline. Accordingly, the main output is a "baseline summary" printed for every selected baseline in the processed network. The baseline summaries are preceded by a "network summary" printout, which contains all the information pertinent to the whole network. The postprocessor is designed also to plot, as an option, a "position estimate history," as well as print (optionally) estimated observation residuals and estimated orbital biases. The list of subroutines used is given in Appendix C. A detailed description of the program can be found in Santerre et al. [1985].

3.5.1 Network summary

This summary is printed whether or not the observations were processed in a "network mode" or baseline by baseline. If only one baseline has been evaluated at a time, the summary simply lists the information pertaining to that baseline. The summary contains the following information:

(1) network name and location
(2) number of points in network and their numbers (names)
(3) duration of the observational campaign from ... to ....
(4) source of initial coordinates
(5) reference ellipsoid used (a, f^{-1})
(6) solution file name (prepared by the main processor)
(7) a posteriori variance factor ($\hat{\sigma}_o^2$)
(8) cross-correlations between points after adjustment which are larger (in absolute value) than a value ρ_o selected by the user (default value $\rho_o = 0.25$).

The network summary printout is followed by a sequence of baseline summaries for a subset of baselines selected by the user. (Default selection are those baselines which have been directly observed.)

3.5.2 Baseline summary

The following information is printed for every selected baseline:

(1) baseline name and location

(2) baseline is a part of ...(name... network (printed only if applicable)

(3) information pertaining to session #1:

(3.1) instruments: type and serial numbers

(3.2) observers

(3.3) observed from date..., hr..., min..., to date..., hr..., min...

(3.4) weather (general description)

(3.5) satellite nos..., ..., ..., used

(3.6) observing frequencies (L1, L2, both)

(3.7) elevation angle cutoff

(3.8) number of cycle slips detected

(3.9) general health of instruments

(3.10) source file names

(Information listed under (3) is repeated for each session that has contributed to the evaluation of herewith given positions.)

(4) source of ephemerides, their estimated accuracy, file name

(5) processing mode (ranges - P or C/A, single differences, double differences, triple differences, ...)

(6) tropospheric model used

(7) ionospheric model used (printed only if applicable)

(8) estimated ambiguities and their accuracies (optional)

(9) clock bias estimates and their accuracies (optional)

(10) atmospheric bias estimates (optional)

(11) special notices (optional).

Following the above baseline information, a summary of position determination for the first point is given below:

(12) point name (number)

(13) initial position estimates (ϕ, λ, h, H^o, N) and their standard deviations

(14) crosscorrelations larger (in absolute value) than a value ρ_1 selected by the user (default value $\rho_1 = 0.25$)

(15) final geodetic position estimates (ϕ, λ, h) and their standard deviations

(16) crosscorrelations larger (in absolute value) than a value ρ_2 selected by the user (default value $\rho_2 = 0.25$)

(17) final Cartesian position estimates (in the Conventional Terrestrial system) and their standard deviations

(18) crosscorrelations larger (in absolute value) than a value ρ_3 selected by the user (default value $\rho_3 = 0.25$).

Here comes the same positional information for the end point of the baseline, followed by results pertaining to the relative position of the two points:

(19) length of the baseline and its standard deviation

(20) baseline azimuth (degrees only--for plotting)

(21) initial position differences ($\Delta\phi$, $\Delta\lambda$, Δh) and their standard deviations

(22) crosscorrelations larger (in absolute value) than a value ρ_4 selected by the user (default value $\rho_4 = 0.25$)

(23) final geodetic position differences ($\Delta\phi$, $\Delta\lambda$, Δh) and their standard deviations

(24) crosscorrelations larger (in absolute value) than a value ρ_5 selected by the user (default value $\rho_5 = 0.25$)

(25) final Cartesian position differences Δx^{CT}, Δy^{CT}, Δz^{CT}) and their standard deviations

(26) crosscorrelations larger (in absolute value) than a value ρ_6 selected by the user (default value $\rho_6 = 0.25$).

3.5.3 Position estimate history

Upon request, the postprocessor would compile a file for plotting the evolution of the position or position difference determination. The plotting file contains the following information:

(1) $\phi(t_i)$ (or $\Delta\phi(t_i)$) for all instants t_i for which ϕ was determined

(2) $\lambda(t_i)$ (or $\Delta\lambda(t_i)$)

(3) $h(t_i)$ (or $\Delta h(t_i)$)

(4) $S(t_i)$, baseline length

(5) σ_ϕ, σ_λ, σ_h, σ_s (or $\sigma_{\Delta\phi}$, $\sigma_{\Delta\lambda}$, $\sigma_{\Delta h}$, σ_s) for the final solution

(6) times when orbital bias parameters were determined (updated)

(7) times when clock bias parameters were determined (updated)

(8) times when atmospheric bias parameters were determined (updated)--if applicable.

These data can then be plotted, for instance, as follows:

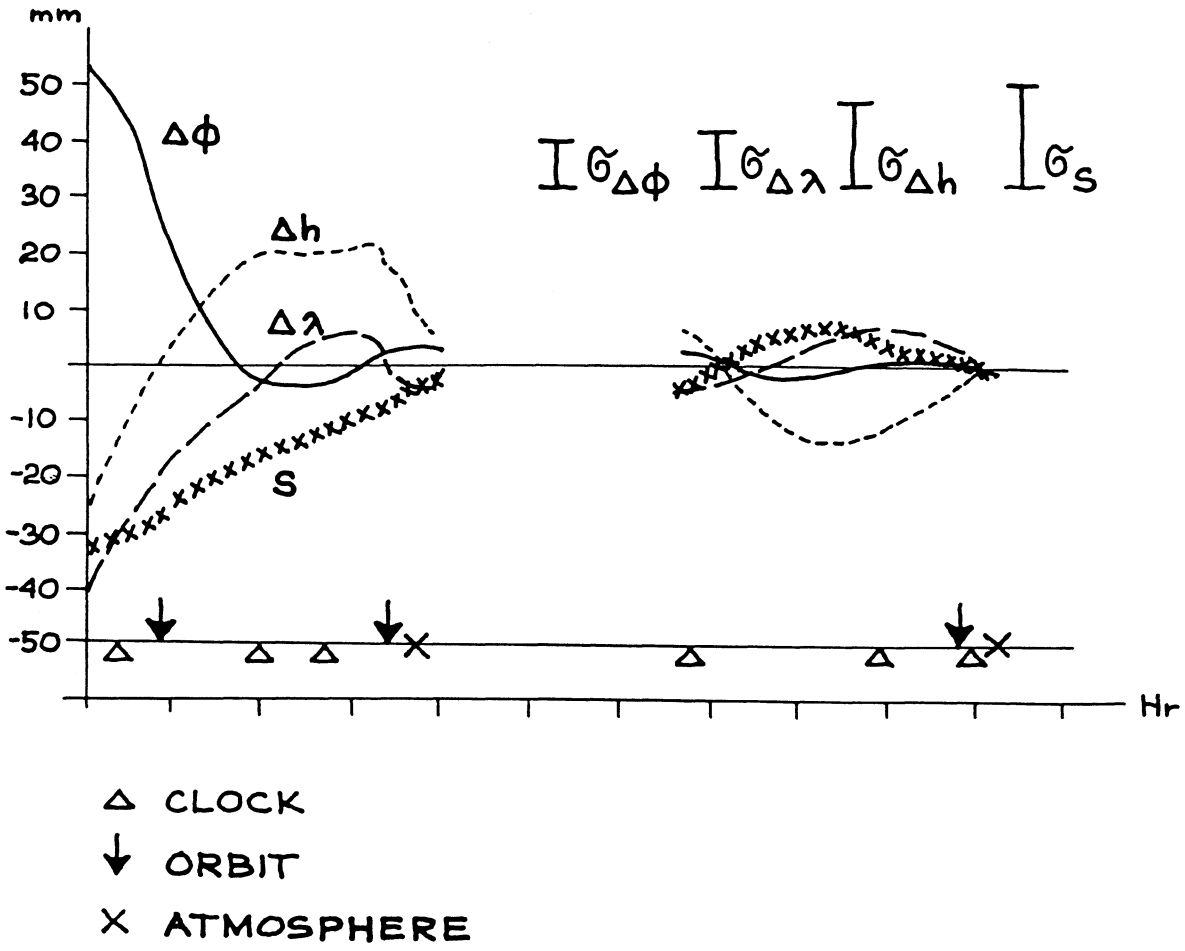

FIGURE 3.12

Position estimate history.

Actual implementation would depend on the available plotting facility.

3.5.4 Observation residuals and orbital biases

Upon request, the postprocessor will produce a file containing the time series of estimated observation residuals for the instants of acquisition, e.g., $\{\Delta^2\rho(t_i), t_i; i=1,n\}$. These may be desirable to study a possible systematic behaviour of or correlations among the observations.

The user may select to have yet another file prepared, that of the

estimated orbital biases and their covariance matrices. These data may be again desirable for further theoretical studies.

4. CORRELATIONS AMONG OBSERVATIONS

In this chapter we investigate the impact of mathematical correlations between double difference "observations" (section 4.1) to assess to what extent it is necessary to include these correlations in the main processor. The second section (4.2) describes one possible approach that can be used to investigate physical correlations and to model their effects.

4.1 Mathematical Correlations

To get some feeling as to how much the introduction of correlations may affect the results, we have adjusted the data from the Ottawa network (cf. Chapter 5) twice: once assuming no correlations among the observations (double differences collected by the Macrometer™ V-1000 receivers), and once taking into account the mathematical correlations caused by differencing the single differences. The origin, modelling, and effect of including these particular correlations were shown by Beutler et al. [1984] for adjustments in both modes: in the baseline by baseline mode, and in the network mode.

In both cases, the differences between the results in the two modes are significantly larger than the differences between uncorrelated and correlated modelling. The effect of introducing the mathematical correlations in the baseline mode is statistically insignificant (Table 4.1). The differences exceed 1σ in 33% of the cases. The distribution of these differences is clearly random with maximum absolute values being: 18.0 mm in the length of baselines, 8.0 mm in latitude, 14.0 mm in longitude, and 7.0 mm in height. The estimated standard deviations of results are generally smaller when correlation is not taken into account.

A similar story can be told about the two adjustments in the network mode (Table 4.2). The distribution of the differences appears once more to be random with magnitudes being, perhaps, even smaller than those obtained in the baseline mode. The standard deviations, again, increase slightly when the mathematical correlations are introduced.

Clearly, this particular mathematical correlation does not do much to improve the result. In taking the existing mathematical correlations only partially into account, the results are perhaps not surprising. We would, however, expect the results to be significantly more affected by existing

TABLE 4.1

Comparison of results with and without mathematical correlation.
(Baseline mode, real number cycle ambiguities.)

	$\Delta\phi$		$\Delta\lambda$		Δh		ℓ	
Baseline	Difference mm	Standard Deviation mm with / without	Difference mm	Standard Deviation mm with / without	Difference mm	Standard Deviation mm with / without	Difference mm / ppm	Standard Deviation mm with / without
PA-6A	3	4 / 4	1	7 / 8	1	5 / 5	2 / 0.1	6 / 7
MO-6A	-1	4 / 4	12	7 / 6	5	5 / 4	13 / 0.5	8 / 7
ME-6A	-6	5 / 5	0	9 / 9	-7	7 / 6	- 3 / - 0.1	11 / 11
PA-MO	0	5 / 5	- 1	8 / 9	2	5 / 5	1 / 0.1	8 / 8
ME-PA	-4	8 / 7	1	10 / 10	2	9 / 7	- 3 / - 0.1	13 / 11
ME-MO	8	7 / 6	-14	12 / 10	-3	9 / 7	18 / 0.3	14 / 12

TABLE 4.2

Comparison of results with and without mathematical correlation.
(Network mode, real number cycle ambiguities.)

	$\Delta\phi$		$\Delta\lambda$		Δh		ℓ	
Baseline	Difference mm	Standard Deviation mm with / without	Difference mm	Standard Deviation mm with / without	Difference mm	Standard Deviation mm with / without	Difference mm / ppm	Standard Deviation mm with / without
PA-6A	0	4 / 4	8	7 / 7	0	5 / 5	8 / 0.4	NOT AVAILABLE
MO-6A	-3	4 / 4	9	7 / 6	2	5 / 4	9 / 0.3	
ME-6A	-3	4 / 4	3	7 / 6	-2	5 / 4	-4 / -0.1	
PA-MO	2	not available	-1	not available	-2	not available	3 / 0.2	
ME-PA	-2		-5		-2		5 / 0.1	
ME-MO	0		-5		-4		6 / 0.1	

physical correlations due to atmospheric effects, orbital effects, and clock effects. These correlations are, unfortunately, for the most part unknown and would have to be investigated using some novel techniques. As a result, no correlations are accounted for in DIPOP, but the architecture is such that a non-diagonal weight matrix of observations can be implemented at a later stage.

4.2 Physical Correlations

Let us assume that we have s×p×l time series of measured phases $\phi^{S}_{P,L}(t)$, where s is the number of satellites S (simultaneously tracked by each receiver), p is the number of ground stations, and l is the number of carrier frequencies used (i.e., L equals either 1 or 2). Each time series can be written as:

$$\phi(t) = \phi^*(t) + m(t) + \varepsilon(t) \quad , \tag{4.1}$$

where $\phi^*(t)$ is the assumed correct value of the geometrical phase and m(t) includes the modelled value of both satellite and receiver clock offsets and drifts, the modelled values of tropospheric and ionospheric delays, and the modelled values of orbital biases. The term $\varepsilon(t)$ represents the noise due to measurement and model errors. It is the auto-correlation $C(\Delta t)$ of this noise in which we are interested.

Let us then take two simultaneous time series $\phi^{i}_{1}(t)$, $\phi^{i}_{2}(t)$ (forgetting, for the time being, about their dependence on the carrier) and construct the "single difference" (which we formerly called differential range [Vaníček et al., 1984]) series:

$$\Delta\phi^{i}_{12}(t) = \phi^{i}_{2}(t) - \phi^{i}_{1}(t) \quad . \tag{4.2}$$

This series also can be written as:

$$\Delta\phi^{i}_{12}(t) = \Delta\phi^{*i}_{12}(t) + \Delta m^{i}_{12}(t) + \Delta\varepsilon^{i}_{12}(t) \quad , \tag{4.3}$$

where the noise $\Delta\varepsilon^{i}_{12}(t)$ will have its own auto-correlation function $C_{\Delta\phi^{i}_{12}}(\Delta t)$ given as

$$C_{\Delta\phi_{12}^{i}}(\Delta t) = C_1^i(\Delta t) + C_2^i(\Delta t) - C_{12}^i(\Delta t) - C_{12}^i(-\Delta t) \quad , \tag{4.4}$$

where C_{12}^i is the cross-correlation function of ε_1^i and ε_2^i.

The double difference series is constructed as:

$$\begin{aligned} \Delta^2\phi_{12}^{ij}(t) &= \Delta\phi_{12}^{j}(t) - \Delta\phi_{12}^{i}(t) \\ &= \Delta^2\phi_{12}^{*ij}(t) + \Delta^2 m_{12}^{ij}(t) + \Delta^2\varepsilon_{12}^{ij}(t) \quad . \end{aligned} \tag{4.5}$$

Once more, the auto-correlation function $C_{\Delta^2\phi_{12}^{ij}}(\Delta t)$ of $\Delta^2\varepsilon_{12}^{ij}(t)$ is given as

$$C_{\Delta^2\phi_{12}^{ij}}(\Delta t) = C_{\Delta\phi_{12}^{j}}(\Delta t) + C_{\Delta\phi_{12}^{i}}(\Delta t) - C_{12}^{ij}(\Delta t) - C_{12}^{ij}(-\Delta t) \quad . \tag{4.6}$$

The main problem, indeed, is how to evaluate these auto-correlation functions and also the cross-correlation functions between two double difference series. The ideal situation would be to derive these from the known physical behaviour of the phase series. Failing this, one may wish to first get some understanding of the correlated behaviour of these series from actual data. Can thus observed phase series be analysed to yield these auto-correlation and cross-correlation functions?

It seems to us that this would be very difficult because the predominant feature of any of these series is the "position signal" and other signals, which we called above m(t), that would completely swamp the noise content $\varepsilon(t)$. Can we then model the signals and analyse the residuals? But modelling the signal is precisely what our software is doing anyway, so why not use the residuals obtained from our processor?

This can certainly be done, but there is one problem to be solved: The residuals coming from the least-squares estimation (such as the one implemented in our filter processor) are known to be artificially correlated because of the finite duration of the estimation process. Thus what one would see as auto- and cross-correlations of the residuals $V_{\Delta^2\phi}(t)$--or similarly $V_{\Delta\phi}(t)$ or $V_{\phi}(t)$--may be predominantly those imprinted by the filter. The question then is: How to disentangle the auto- and cross-correlations of the residuals into those inherent in the observed series and those imprinted by the filter?

We believe that this can be done by studying first the response of the filter for the particular satellite configuration and particular length of the observation series. This response can be studied by simulating perfect observations plus white noise, and getting the spectra and cross-spectra for the residuals obtained from this simulation. Then actually collected observation series can be processed by the same filter (same configuration and same series lengths) and new spectra and cross-spectra obtained for the real residuals. It is known [Godin, 1972] that a spectrum of a convolution of two series, the observations and the filter values, equals to the product of the spectra of the two series. By subtracting the former from the latter, we should then obtain the spectra and cross-spectra corresponding to the observed series, be they phases, single differences, or double differences. These spectra and cross-spectra can then be converted into auto- and cross-correlation functions (see e.g., Bendat and Piersol [1971]).

Once the auto- and cross-correlation functions are known and understood, an attempt should be made to produce an analytical covariance (correlation) model. Based on this model, it should not be overly difficult to devise an algorithm for generating a fully populated model weight matrix, where each element would be computed from a formula as needed.

5. EXPERIENCE WITH ACTUAL DATA

In order to verify the performance of DIPOP, we wished to process three sets of GPS data: the data collected using Macrometer™ V-1000 receivers on networks in the vicinity of Ottawa and Quebec City, and data collected using Texas Instruments TI-4100 receivers on the same Ottawa network. All of this data had been processed using previously developed software.

Our goal was only partially met. As usual under the pressure of contractual deadlines, there was no time left at the end of the contract period to put as much effort into the presentation of actual results as we would have liked to do. Consequently, the results presented here are not all in a uniform format. Moreover, the Quebec campaign data have been processed using the PRMAC3 and PRMNET IBM programs only. Since we have shown that DIPOP gives identical results to both of these programs, this omission makes no difference as to the numbers presented herein.

Concerning the camparison of our results with either the "ground truth" or other available GPS results, we have compared our Quebec results with both the ground truth and the results obtained using the Macrometrics software (see section 5.2.2). For the Ottawa test network, we have compared our results with the latest Geodetic Survey of Canada adjusted "ground truth" (D. McArthur, personal communication) (see section 5.4) and intercompared the results from the Macrometer™ and TI campaigns (see section 5.4).

5.1 How to Compare Results

5.1.1 Motivation

Many groups are and will be processing, in many different ways, various GPS data sets, related to a common test network. One example of such a network is the Ottawa Test Network (cf. sections 5.2.1 and 5.3).

In order that the results of these various investigations can be most easily compared, it would be very helpful if a common procedure for presenting the results could be agreed upon. The purpose of this section is to describe one such procedure.

The criteria upon which our procedure is based are:

(a) Any comparison should involve geocentric ellipsoidal rather than geocentric Cartesian coordinates, since the discrepancies can be more easily interpreted.

(b) The coordinate system used should be a CT system (we propose WGS72), rather than some versions of NAD27, to eliminate the problem of how to handle network distortions of the terrestrial NAD27 coordinates involved in any comparison, and also to be consistent with comparisons on other continents.

(c) Heights above the ellipsoid, rather than heights above the geoid (orthometric heights), must be used or else the ignored ellipsoid/geoid separation will show up as a scale difference in a comparison between "ground truth" and GPS coordinates.

(d) Differences in "ground truth" heights above the ellipsoid should be derived from $\Delta h = \Delta H^{O} + \Delta N$, where ΔH^{O} is the difference in orthometric height between stations, obtained from spirit levelling, and ΔN is the difference in geoid undulation between stations, obtained from a local geoid model. This procedure is likely to provide a much more accurate ΔN than differencing Transit Doppler-derived N values. A weighted combination procedure should be used to make the Doppler-derived N values and the local geoid-model-derived ΔN values consistent.

(e) A set of "ground truth" coordinates (ϕ, λ, H^{O}, N) for each network station should be adopted and used by all investigators. Any such set of coordinates should be clearly and uniquely labelled (perhaps by date). A document describing their determination with full covariance matrix information should be provided.

(f) Provision should be made in the comparison procedure to easily substitute a different set of "ground truth" coordinates, without major recomputations.

(g) Common tabular and graphical formats to represent the results should be adopted. These should be based on coordinate values, rather than coordinate differences, to eliminate the possibility of the reader interpreting the sign of such differences incorrectly.

5.1.2 Procedure

We propose that results be presented in terms of GPS-derived coordinate values, rather than the coordinate differences which actually

result from differential GPS data adjustments. We realize that we are thus adding something artificial which is not inherently in the results. However, the benefits in terms of clear presentation of comparative results more than offsets this apparent disadvantage.

We propose the following steps:

(a) Use only WGS72 coordinates in all that follows.

(b) Adopt a set of "ground truth" (TTG = terrestrial + geoid + Transit if available) coordinate values $(\phi, \lambda, H^{O}, N)_{TTG}$ for the network stations.

(c) Adopt (perhaps different) a priori coordinate values $(\phi, \lambda, h)_{A\ PRIORI}$ for the GPS determinations. These may be set equal to the TTG set above, but need not be. It is important that the two are identical in orientation and scale, but they may be translated by up to a few tens of metres. (This is because some differential baseline processing programs may hold one end of the baseline fixed. In such a case, the baseline solution vector will vary depending on this fixed position, due to design matrix dependence. Pessimistically, this may result in changes in the solution of order 1 mm for 20 metre translations of the fixed station.) Two sets of coordinate values are introduced to clearly separate the two different functions involved--the A PRIORI values are required to approximately locate the GPS coordinates on the earth. The TTG values are used for the comparison between GPS-derived and "ground truth" coordinate differences. Often they will be the same values in practice. However, if at a later time we wish to substitute different values for the original TTG values, we do not want to have to recompute the GPS-derived coordinate values.

(d) In the case of baseline determinations, one end of each baseline is considered the "reference" end. In the case of network determinations, one station in the network is considered the "reference" station. Translate the GPS coordinate values until the GPS-derived and TTG coordinates for such "reference" stations coincide. For the baseline case, this means translating the "free" end of the baseline by:

$$(\phi, \lambda, h)_{GPS(translated)} = (\phi, \lambda, h)_{TTG(ref)} + (\Delta\phi, \Delta\lambda, \Delta h)_{GPS}.$$

For the network case, this means translating GPS-derived coordinate values, for all stations except the reference station, by:

$$(\phi,\lambda,h)_{GPS(translated)} = (\phi,\lambda,h)_{GPS(solution)} + [(\phi,\lambda,h)_{A\ PRIORI(ref)} - (\phi,\lambda,h)_{TTG(ref)}] \ .$$

5.1.3 Tabular Presentations

Tabular presentations of the results should include:

(a) A listing of $(\phi,\ \lambda,\ h,\ H^{o},\ N)_{TTG}$ for all network stations, with (at least) standard deviations for each coordinate, and a description of how these values were derived (with references).

(b) A listing of $(\phi,\ \lambda,\ h)_{GPS(translated)}$ for the "free" ends in each baseline determination, or for the non-reference stations in a network solution. At least standard deviations for each coordinate should be provided, although full covariance matrix would be preferable. The particular assumptions, models, and techniques used to obtain the GPS results should, of course, be fully described in the text.

5.1.4 Graphical Presentations

Graphical presentations of the results should be provided for three cases. For baseline solutions, these should show how much various coordinates (e.g., "ground truth," various GPS solutions) differ for the "free" end of the baseline. For network solutions, these should show how much various coordinates differ for each "nonreference" station. In the case of figure misclosures, these should show how much the end point of the closed figure differs from the "reference" or start point, as determined by one or more sets of GPS baseline coordinate difference determinations.

We feel that in all three cases two plots should be provided:

(a) A plot in the $(\Delta\phi,\ \Delta\lambda)$ plane, scaled in millimetres, showing the azimuth of the baseline (or with an inset index figure in the case of network solution or figure misclosure). Each point on this plot should be surrounded by the one sigma relative confidence ellipse for the baseline (or with respect to the reference station for network or misclosure figures). The fact that this is a relative confidence

ellipse, not a position confidence ellipse, should be clearly explained in the text.

(b) A plot in the (Δh, Δs) plane, scaled in millimetres (also with an inset index figure in the case of network or figure misclosure). In the baseline case, the "Δs" axis is aligned to the baseline. In the network case, it is aligned to the vector from the "reference station." In the figure misclosure case, "Δs" represents the figure perimeter. Each point should also be surrounded by the one sigma confidence ellipse.

5.1.5 Examples

Tables 5.0(a), 5.0(b) and Figures 5.1 and 5.2 illustrate the recommended tables and plots for an actual case: Macrometer™ V-1000 results for the Ottawa Test Network from Valliant et al. [1985]. Other results appear elsewhere in this report.

5.2 Macrometer™ Experiments

We have used our new software package DIPOP to re-process data from an experiment involving Macrometer™ V-1000 Interferometric Surveyors. This experiment is the Ottawa area test conducted during the summer of 1983 by the Earth Physics Branch of the federal Department of Energy, Mines and Resources (EMR). We have previously discussed our processing of the data from this test using the dedicated Macrometer™ processing programs, PRMAC3 and PRMNET [Langley et al., 1984; Beutler et al., 1984]. Here we will give a very short description of the test and the results obtained using DIPOP. We will also compare our results with the newly adjusted coordinates of the Ottawa network determined from terrestrial and Transit observations [D. McArthur, personal communication].

We had also intended to process with DIPOP data from a second Macrometer™ experiment, the Québec City area test conducted by the Ministère de l'Energie et des Ressources du Québec in January 1984. However, these data are not presently in a form compatible with DIPOP. We therefore processed these data using the PRMAC3 and PRMNET programs. Since we have not previously reported our analysis of data from this experiment, we will give a somewhat more detailed account of the analysis.

TABLE 5.0(a)

Ground truth coordinates.

OTTAWA TEST NETWORK
Metcalfe - Panmure baseline
Macrometer™ V-1000 results using Macrometrics software
Results computed on NAD-27, ignoring geoid undulation (-3.4 m)
Results transformed to WGS-72, scaled down by 0.532 ppm,
Metcalfe coordinates fixed to ground truth values (Table 5.1)
Results expressed as Panmure coordinates, relative to Metcalfe as fixed station
Relative standard deviations (in parentheses) in millimetres

Data Set	Latitude North	Longitude East	Height above Ellipsoid	Chord length
Ground truth	45-20-18.847700 (0)	76-11-03.815900 (0)	113.650 (0)	57930.713 (0)
GPS Day 214	45-20-18.83317 (70)	76-11-03.82480 (137)	112.673 (89)	57930.818 (0)
GPS Day 220	45-20-18.83424 (52)	76-11-03.82471 (88)	112.644 (62)	57930.822 (0)
GPS Day 227	45-20-18.83522 (87)	76-11-03.82524 (101)	112.895 (92)	57930.840 (0)
GPS Day 228	45-20-18.83322 (97)	76-11-03.82021 (107)	112.718 (98)	57930.720 (0)
GPS mean	45-20-18.83396 (30)	76-11-03.82374 (52)	112.733 (113)	57930.718 (0)

TABLE 5.0(b)

Baseline results.

OTTAWA TEST NETWORK

Ground truth coordinates (February 1985 set)

WGS-72 (NWL-10F) ellipsoid used: a = 6378135.0 m, 1/f = 298.26

Standard deviations (in parentheses) not yet available

Horizontal coordinates from new adjustment (Feb 1985) of Ottawa 3D Test Adjustment

Orthometric heights from relevelling (August 1984)

Geometric heights (above ellipsoid) from Doppler observations

Reference: D. McArthur (personal communication)

Stn	Latitude North	Longitude East	Heights (m) Orthometric	Geoid	Geometric
6A	45-23-55.819611 (0)	75-55-20.635365 (0)	77.085 (0)	-39.96 (0)	37.13 (0)
7	45-23-55.154969 (0)	75-55-21.671856 (0)	76.629 (0)	-39.96 (0)	36.67 (0)
51	45-23-07.188485 (0)	75-56-36.445901 (0)	70.190 (0)	-39.96 (0)	30.23 (0)
Morris	45-26-34.326429 (0)	76-15-18.048791 (0)	89.605 (0)	-40.50 (0)	49.11 (0)
Panmure	45-20-18.847700 (0)	76-11-03.815900 (0)	153.946 (0)	-40.30 (0)	113.65 (0)
Metcalfe	45-14-34.026118 (0)	75-27-30.618371 (0)	102.730 (0)	-39.34 (0)	63.39 (0)
Renfrew	45-29-31.202627 (0)	76-42-31.644065 (0)	222.354 (0)	-40.42 (0)	181.93 (0)
Cataraqui	44-15-33.223263 (0)	76-34-24.251057 (0)	108.600 (0)	-40.90 (0)	67.67 (0)

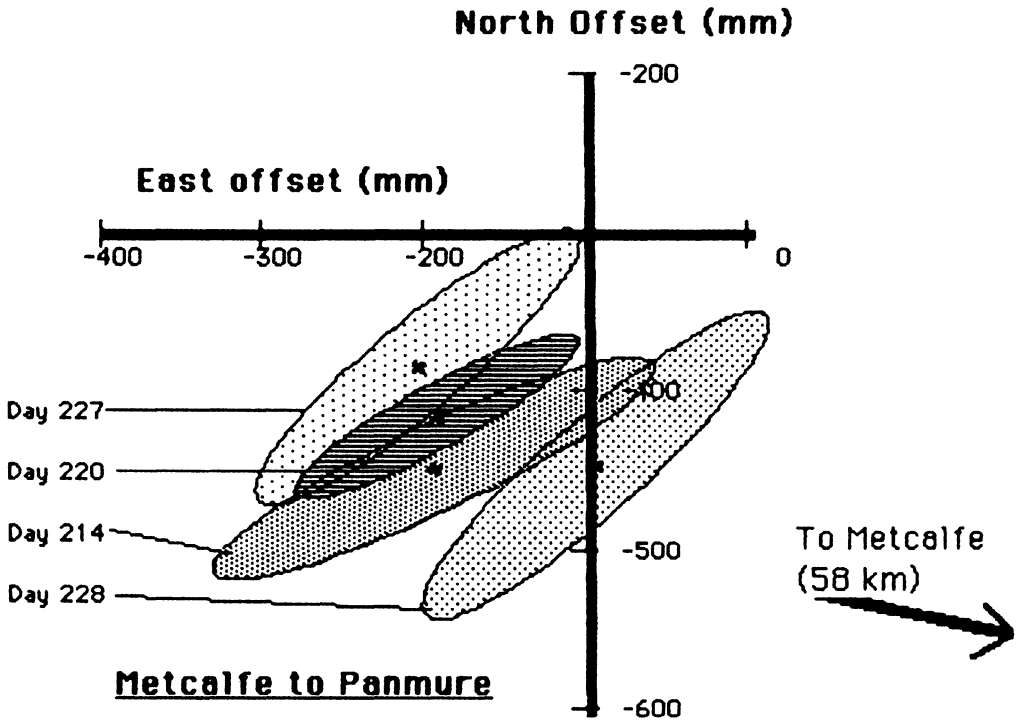

FIGURE 5.1

One sigma confidence ellipses of repeated GPS baseline determinations, plotted relative to"ground truth."

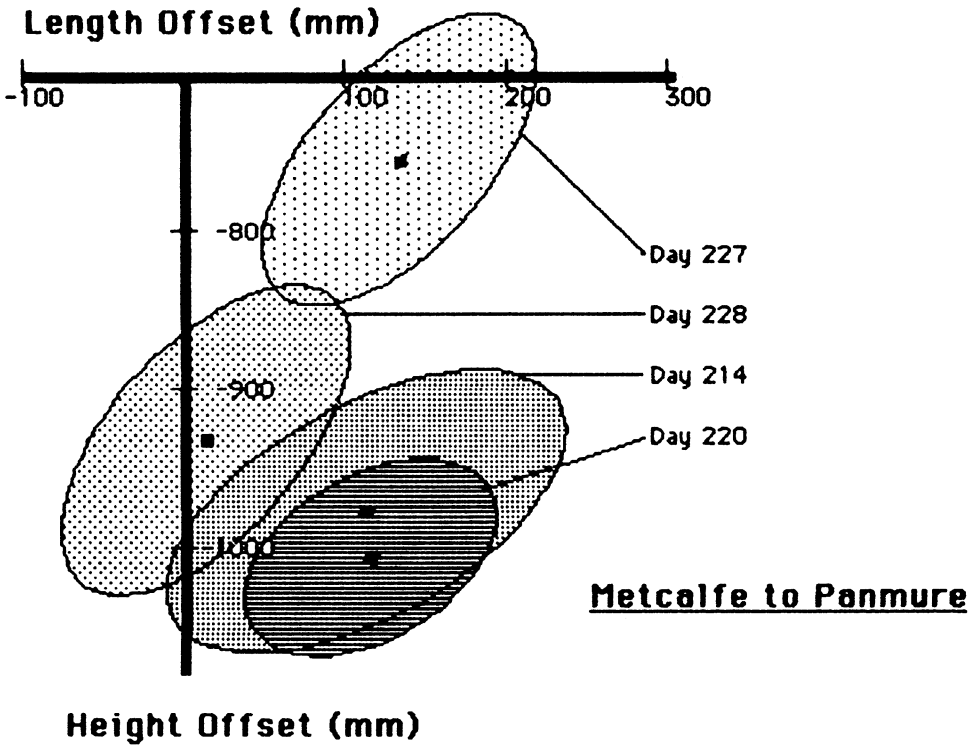

FIGURE 5.2

One sigma confidence ellipses of repeated GPS baseline determinations plotted in the vertical plane.

5.2.1 Ottawa Experiment

Between 19 July and 19 August 1983, the Earth Physics Branch of EMR conducted the first test in Canada of the Macrometer™. Two Macrometer™ V-1000 single frequency receivers were used to determine the baseline vectors between selected points of the Ottawa Test Network of the Surveys and Mapping Branch of EMR.

The stations occupied during the test are listed in Table 5.1. Table 5.1 gives the coordinates of these stations as determined by a combination of conventional and Transit measurements by the Surveys and Mapping Branch of EMR. The latitudes and longitudes are with respect to the WGS-72, NWL-10F ellipsoid. The x, y, z values are geocentric coordinates obtained from combining the geodetic coordinates of Table 5.1 with the geoidal undulations of Table 5.2. These coordinates represent the so-called "ground truth." A total of 30 observing sessions were conducted in as many days. The first two comprised three, one-hour observation periods on two short baselines on the National Geodetic Base Line: one of 30 m between stations 6A and 7, and one of 2230 m between stations 6A and 51. The remaining 28 sessions were of longer duration (24 sessions of 5 hours, four sessions of 3 hours) and on longer baselines (13 km to 66 km in length--see Table 5.3). These longer baselines are illustrated in Figure 5.3.

Each observing session contains 60 equally spaced observation epochs where at each epoch up to six satellites were observed simultaneously. Not all observing sessions yielded scientifically useful data. The observation schedule for those sessions producing useful data is given in Table 5.4.

We duplicated the processing of the data by the PRMAC3 and PRMNET programs using DIPOP. As with the previous processing, no orbital or tropospheric biases were estimated; only station coordinates and clock parameters were estimated. No ionospheric modelling was attempted either.

Using DIPOP with the same a priori coordinates and weighting as used with the PRMAC3 and PRMNET programs, we obtained the same final coordinates to within about 1 mm. Using DIPOP with the new GSC a priori coordinates and more realistic weighting of the data and the a priori coordinates, we obtained slightly different results. These results are summarized in the printouts from the postprocessor shown in Tables 5.5 through 5.11. These printouts were designed to be self-explanatory and to follow the format

TABLE 5.1

Coordinates of stations of the Ottawa Test Network
from adjustment of terrestrial observations.
(March 1985 set)

Station	Latitude x(m)	Longitude y(m)	Orthometric height z(m)
NGBL 6A	45 23 55.819611	-75 55 20.635365	77.085
	1091195.86214	-4351431.80995	4518606.95909
NGBL 7	45 23 55.154969	-75 55 21.671856	76.629
	1091177.47094	-4351451.15091	4518592.22376
NGBL 51	45 23 07.188485	-75 56 36.445901	70.190
	1089854.88983	-4352864.72356	451747.72102
Metcalfe	45 14 34.026118	-75 27 30.618371	102.730
	1129491.99048	-4354409.54603	4506430.68909
Panmure	45 20 18.847700	-76 11 03.815900	153.946
	1072438.02803	-4361057.15082	4513955.49291
Morris	45 26 34.326429	-76 15 18.048791	89.605
	1065090.41019	-4354315.52972	4522050.20232

TABLE 5.2

Deflection components and geoidal undulations of the stations of the Ottawa Test Network.

Station	Deflection components ξ (lat)	η (long)	Elevation/ ellipsoid	Observed undulation
NGBL 6A 833001	-0.30"	1.69"	77.085 m 37.13 m	-39.96 m
NGBL 7 833002	-0.30	1.69	76.629 36.67	-39.96
NGBL 51 833012	-0.30	1.69	70.190 30.23	-39.96
Metcalfe 693053	-1.33	2.12	102.730 63.39	-39.34
Panmure 773030	2.33	2.72	153.946 113.65	-40.30
Morris 773027	0.21	2.51	89.605 49.11	-40.50

TABLE 5.3

Chord lengths between stations.

Station 1	Station 2	Chord length
NGBL 6A	NGBL 7	30.487
NGBL 6A	NGBL 51	2230.120
NGBL 6A	Panmure	21590.268
NGBL 6A	Morris	26488.986
NGBL 6A	Metcalfe	40295.433
Panmure	Morris	12843.725
Panmure	Metcalfe	57930.717
Morris	Metcalfe	66268.707

FIGURE 5.3

Sketch of the Ottawa test network.

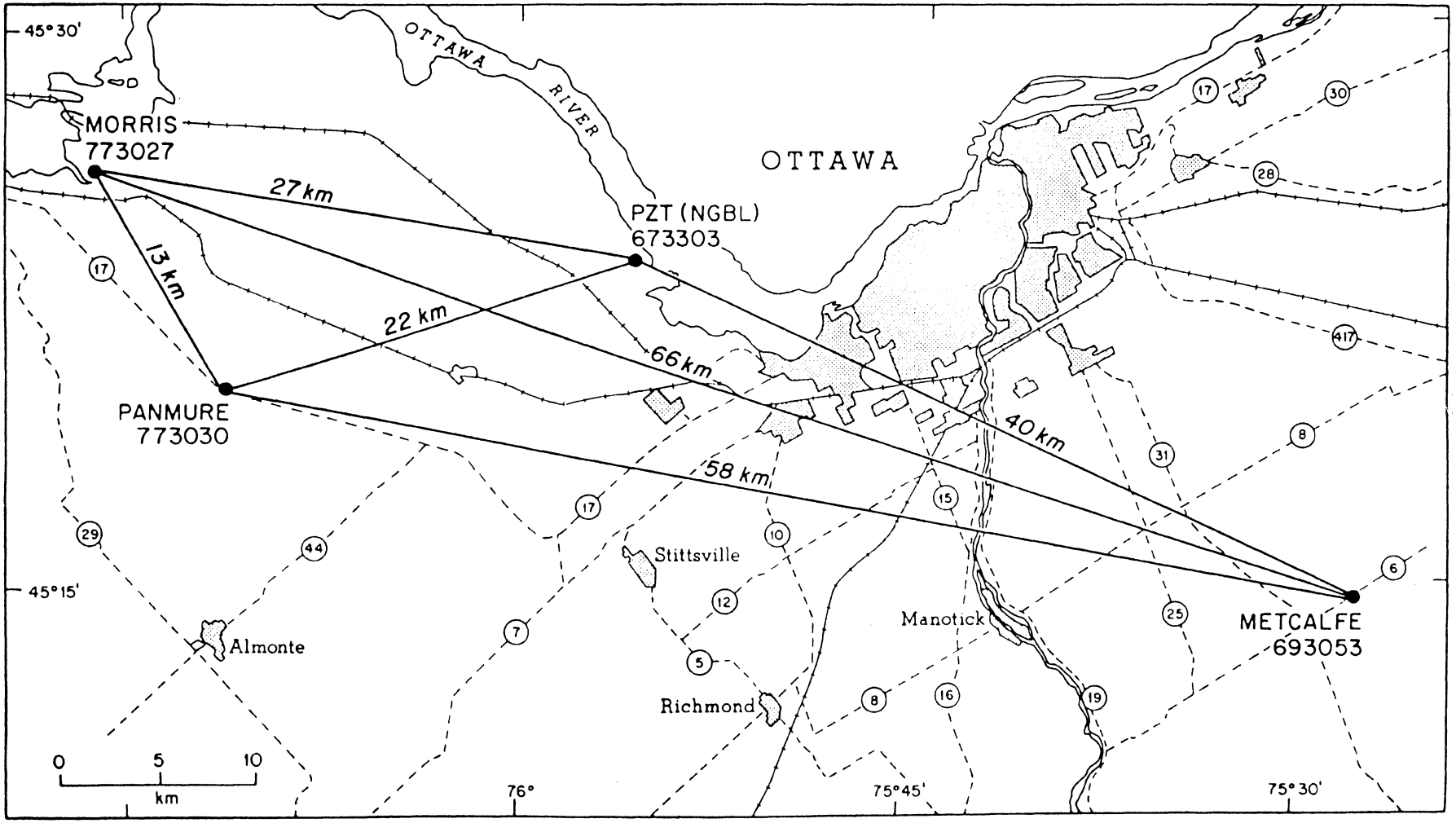

REPRINTED FROM VALLIANT [1984] WITH PERMISSION

TABLE 5.4

Summary of observations.

No.	Baseline	N_s	d	$N_{s/s}$	$N_{o/s}$	N_{obs}
1	6A - 7	3	1/1/1	4/5/3	132/204/110	446
2	6A - 51	3	1/1/1	4/5/3	147/163/103	413
3	Pa - Mo	4	5/5/5/5	5/5	108/113	264
4	Pa - 6A	4	5/5/5/5	5/5/6/5	114/107/149/47	417
5	Mo - 6A	4	5/5/5/5	5/5/6/6	102/106/149/178	535
6	Me - 6A	4	5/5/5/5	5/5/6/6	124/91/163/86	464
7	Me - Pa	4	5/5/3/3	6/6/6/6	118/129/158/182	587
8	Me - Mo	3	5/5/5	5/6/6	117/151/145	413

N_s : Total number of observation sessions per baseline.

d : Duration of session (hours).

$N_{s/s}$: Number of satellites observed per session.

$N_{o/s}$: Number of (double difference) observations per baseline and per session.

N_{obs} : Number of (double difference) observations per baseline.

Mo : Morris

Pa : Panmure

Me : Metcalfe

BASELINE : STATION : 6A & STATION : MO

STATION NAME : 6A

A-PRIORI ELLIPSOIDAL COORDINATES

LATITUDE	: 45 23 55.81961	+/-	
LONGITUDE	: - 75 55 20.63537	+/-	
HEIGHT	: 37.1300	+/-	

A POSTERIORI ELLIPSOIDAL COORDINATES

LATITUDE	: 45 23 55.81638	+/-	518 MM
LONGITUDE	: - 75 55 20.66542	+/-	507 MM
HEIGHT	: 38.0658	+/-	515 MM

CROSS-CORRELATION BETWEEN COORDINATES

A POSTERIORI CARTESIAN COORDINATES

X :	1091195.4052 M	+/-	512 MM
Y :	-4351432.6752 M	+/-	511 MM
Z :	4518607.5553 M	+/-	517 MM

CROSS-CORRELATION BETWEEN COORDINATES

STATION NAME : MO

A-PRIORI ELLIPSOIDAL COORDINATES

LATITUDE	: 45 26 34.32643	+/-	
LONGITUDE	: - 76 15 18.04879	+/-	
HEIGHT	: 49.1100	+/-	

A POSTERIORI ELLIPSOIDAL COORDINATES

LATITUDE	: 45 26 34.31758	+/-	517 MM
LONGITUDE	: - 76 15 18.08106	+/-	507 MM
HEIGHT	: 50.2160	+/-	515 MM

CROSS-CORRELATION BETWEEN COORDINATES

A POSTERIORI CARTESIAN COORDINATES

X :	1065089.9596 M	+/-	512 MM
Y :	-4354316.6392 M	+/-	511 MM
Z :	4522050.7988 M	+/-	517 MM

TABLE 5.5
Results for baseline 6A-Morris.

```
 CROSS-CORRELATION BETWEEN COORDINATES


 BASELINE :    6A   M0
 ---------------------

 A-PRIORI      ELLIPSOID BASELINE COMPONENTS
DELTA  LATITUDE :       0  2 38.50682          +/-
DELTA LONGITUDE : -     0 19 57.41342          +/-
DELTA     HEIGHT :   11.9800                   +/-

 A POSTERIORI ELLIPSOID BASELINE COMPONENTS
DELTA  LATITUDE :       0  2 38.50120          +/-          4 MM
DELTA LONGITUDE : -     0 19 57.41564          +/-          8 MM
DELTA     HEIGHT :   12.1502                   +/-          5 MM

 CROSS-CORRELATION BETWEEN BASELINE COMPONENTS
BASELINE COMPONENT L  AND BASELINE COMPONENT P  CROSS-CORRELATION = /  -.72/ GREATER THAN    .10
BASELINE COMPONENT H  AND BASELINE COMPONENT P  CROSS-CORRELATION = /  -.42/ GREATER THAN    .10
BASELINE COMPONENT H  AND BASELINE COMPONENT L  CROSS-CORRELATION = /   .14/ GREATER THAN    .10

 A POSTERIORI CARTESIAN BASELINE COMPONENTS
DELTA X :        -26105.4456 M  +/-          7 MM
DELTA Y :         -2883.9640 M  +/-          3 MM
DELTA Z :          3443.2434 M  +/-          4 MM

 CROSS-CORRELATION BETWEEN BASELINE COMPONENTS
BASELINE COMPONENT Y  AND BASELINE COMPONENT X  CROSS-CORRELATION = /  -.49/ GREATER THAN    .10
BASELINE COMPONENT Z  AND BASELINE COMPONENT X  CROSS-CORRELATION = /  -.40/ GREATER THAN    .10
BASELINE COMPONENT Z  AND BASELINE COMPONENT Y  CROSS-CORRELATION = /  -.40/ GREATER THAN    .10

BASELINE LENGTH =     26489.0064 M  +/-          7 MM
AZIMUTH =  , -79 DEGREES
```

TABLE 5.5 *continued*

```
 BASELINE :      STATION : 6A & STATION : PA
 ===========================================

 STATION NAME : 6A
 -----------------

 A-PRIORI ELLIPSOIDAL COORDINATES
LATITUDE  :     45 23 55.81961          +/-
LONGITUDE : -   75 55 20.63537          +/-
HEIGHT    :   37.1300                   +/-

 A POSTERIORI ELLIPSOIDAL COORDINATES
LATITUDE  :     45 23 55.81638          +/-         518 MM
LONGITUDE : -   75 55 20.66542          +/-         507 MM
HEIGHT    :   38.0658                   +/-         515 MM

 CROSS-CORRELATION BETWEEN COORDINATES

 A POSTERIORI CARTESIAN   COORDINATES
X :       1091195.4052 M    +/-         512 MM
Y :      -4351432.6752 M    +/-         511 MM
Z :       4518607.5553 M    +/-         517 MM

 CROSS-CORRELATION BETWEEN COORDINATES

 STATION NAME : PA
 -----------------

 A-PRIORI ELLIPSOIDAL COORDINATES
LATITUDE  :     45 20 18.84770          +/-
LONGITUDE : -   76 11  3.81590          +/-
HEIGHT    :  113.6500                   +/-

 A POSTERIORI ELLIPSOIDAL COORDINATES
LATITUDE  :     45 20 18.83931          +/-         517 MM
LONGITUDE : -   76 11  3.84180          +/-         507 MM
HEIGHT    :  114.6410                   +/-         515 MM

 CROSS-CORRELATION BETWEEN COORDINATES

 A POSTERIORI CARTESIAN   COORDINATES
X :       1072437.6907 M    +/-         512 MM
Y :      -4361058.1407 M    +/-         511 MM
Z :       4513956.0157 M    +/-         517 MM
```

TABLE 5.6
Results for baseline 6A-Panmure.

```
 CROSS-CORRELATION BETWEEN COORDINATES

 BASELINE :    6A  PA
 ---------------------

 A-PRIORI      ELLIPSOID BASELINE COMPONENTS
DELTA  LATITUDE : -    0  3 36.97191          +/-
DELTA LONGITUDE : -    0 15 43.18053          +/-
DELTA     HEIGHT :   76.5200                  +/-

 A POSTERIORI ELLIPSOID BASELINE COMPONENTS
DELTA  LATITUDE : -    0  3 36.97707          +/-          5 MM
DELTA LONGITUDE : -    0 15 43.17638          +/-          8 MM
DELTA     HEIGHT :   76.5752                  +/-          5 MM

 CROSS-CORRELATION BETWEEN BASELINE COMPONENTS
BASELINE COMPONENT L  AND BASELINE COMPONENT P  CROSS-CORRELATION = /  -.75/ GREATER THAN    .10
BASELINE COMPONENT H  AND BASELINE COMPONENT P  CROSS-CORRELATION = /  -.36/ GREATER THAN    .10
BASELINE COMPONENT H  AND BASELINE COMPONENT L  CROSS-CORRELATION = /   .21/ GREATER THAN    .10

 A POSTERIORI CARTESIAN BASELINE COMPONENTS
DELTA X :       -18757.7145 M  +/-          8 MM
DELTA Y :        -9625.4656 M  +/-          4 MM
DELTA Z :        -4651.5396 M  +/-          4 MM

 CROSS-CORRELATION BETWEEN BASELINE COMPONENTS
BASELINE COMPONENT Y  AND BASELINE COMPONENT X  CROSS-CORRELATION = /  -.48/ GREATER THAN    .10
BASELINE COMPONENT Z  AND BASELINE COMPONENT X  CROSS-CORRELATION = /  -.44/ GREATER THAN    .10
BASELINE COMPONENT Z  AND BASELINE COMPONENT Y  CROSS-CORRELATION = /  -.37/ GREATER THAN    .10

BASELINE LENGTH =    21590.2353 M  +/-          6 MM
AZIMUTH =  -108 DEGREES
```


TABLE 5.6 *continued*

BASELINE : STATION : 6A & STATION : ME

STATION NAME : 6A

A-PRIORI ELLIPSOIDAL COORDINATES

LATITUDE	: 45 23 55.81961	+/-	
LONGITUDE	: - 75 55 20.63537	+/-	
HEIGHT	: 37.1300	+/-	

A POSTERIORI ELLIPSOIDAL COORDINATES

LATITUDE	: 45 23 55.81638	+/-	518 MM
LONGITUDE	: - 75 55 20.66542	+/-	507 MM
HEIGHT	: 38.0658	+/-	515 MM

CROSS-CORRELATION BETWEEN COORDINATES

A POSTERIORI CARTESIAN COORDINATES

X :	1091195.4052 M	+/-	512 MM
Y :	-4351432.6752 M	+/-	511 MM
Z :	4518607.5553 M	+/-	517 MM

CROSS-CORRELATION BETWEEN COORDINATES

STATION NAME : ME

A-PRIORI ELLIPSOIDAL COORDINATES

LATITUDE	: 45 14 34.02612	+/-	
LONGITUDE	: - 75 27 30.61837	+/-	
HEIGHT	: 63.3900	+/-	

A POSTERIORI ELLIPSOIDAL COORDINATES

LATITUDE	: 45 14 34.03163	+/-	518 MM
LONGITUDE	: - 75 27 30.64175	+/-	507 MM
HEIGHT	: 64.3550	+/-	516 MM

CROSS-CORRELATION BETWEEN COORDINATES

A POSTERIORI CARTESIAN COORDINATES

X :	1129491.6372 M	+/-	512 MM
Y :	-4354410.2148 M	+/-	511 MM
Z :	4506431.4942 M	+/-	518 MM

TABLE 5.7
Results for baseline 6A-Metcalfe.

```
 CROSS-CORRELATION BETWEEN COORDINATES

 BASELINE :   6A  ME
 ____________________

 A-PRIORI      ELLIPSOID BASELINE COMPONENTS
DELTA  LATITUDE : -    0  9 21.79349          +/-
DELTA LONGITUDE :      0 27 50.01700          +/-
DELTA     HEIGHT :  26.2600                   +/-

 A POSTERIORI ELLIPSOID BASELINE COMPONENTS
DELTA  LATITUDE : -    0  9 21.78475          +/-          5 MM
DELTA LONGITUDE :      0 27 50.02367          +/-          8 MM
DELTA     HEIGHT :  26.2892                   +/-          6 MM

 CROSS-CORRELATION BETWEEN BASELINE COMPONENTS
BASELINE COMPONENT L  AND BASELINE COMPONENT P  CROSS-CORRELATION = /  -.65/ GREATER THAN    .10
BASELINE COMPONENT H  AND BASELINE COMPONENT P  CROSS-CORRELATION = /  -.49/ GREATER THAN    .10

 A POSTERIORI CARTESIAN BASELINE COMPONENTS
DELTA X :        38296.2320 M  +/-          7 MM
DELTA Y :        -2977.5396 M  +/-          4 MM
DELTA Z :       -12176.0612 M  +/-          4 MM

 CROSS-CORRELATION BETWEEN BASELINE COMPONENTS
BASELINE COMPONENT Y  AND BASELINE COMPONENT X  CROSS-CORRELATION = /  -.47/ GREATER THAN    .10
BASELINE COMPONENT Z  AND BASELINE COMPONENT X  CROSS-CORRELATION = /  -.41/ GREATER THAN    .10
BASELINE COMPONENT Z  AND BASELINE COMPONENT Y  CROSS-CORRELATION = /  -.40/ GREATER THAN    .10

BASELINE LENGTH =    40295.4537 M  +/-          8 MM
AZIMUTH =   115 DEGREES
```

TABLE 5.7 *continued*

BASELINE : STATION : MO & STATION : PA

STATION NAME : MO

A-PRIORI ELLIPSOIDAL COORDINATES

LATITUDE	: 45 26 34.32643	+/-	
LONGITUDE	: - 76 15 18.04879	+/-	
HEIGHT	: 49.1100	+/-	

A POSTERIORI ELLIPSOIDAL COORDINATES

LATITUDE	: 45 26 34.31758	+/-	517 MM
LONGITUDE	: - 76 15 18.08106	+/-	507 MM
HEIGHT	: 50.2160	+/-	515 MM

CROSS-CORRELATION BETWEEN COORDINATES

A POSTERIORI CARTESIAN COORDINATES

X :	1065089.9596 M	+/-	512 MM
Y :	-4354316.6392 M	+/-	511 MM
Z :	4522050.7988 M	+/-	517 MM

CROSS-CORRELATION BETWEEN COORDINATES

STATION NAME : PA

A-PRIORI ELLIPSOIDAL COORDINATES

LATITUDE	: 45 20 18.84770	+/-	
LONGITUDE	: - 76 11 3.81590	+/-	
HEIGHT	: 113.6500	+/-	

A POSTERIORI ELLIPSOIDAL COORDINATES

LATITUDE	: 45 20 18.83931	+/-	517 MM
LONGITUDE	: - 76 11 3.84180	+/-	507 MM
HEIGHT	: 114.6410	+/-	515 MM

CROSS-CORRELATION BETWEEN COORDINATES

A POSTERIORI CARTESIAN COORDINATES

X :	1072437.6907 M	+/-	512 MM
Y :	-4361058.1407 M	+/-	511 MM
Z :	4513956.0157 M	+/-	517 MM

TABLE 5.8
Results for baseline Morris-Panmure.

```
CROSS-CORRELATION BETWEEN COORDINATES

 BASELINE :    MO   PA
 ---------------------

 A-PRIORI      ELLIPSOID BASELINE COMPONENTS
DELTA  LATITUDE : -    0   6 15.47873          +/-
DELTA LONGITUDE :      0   4 14.23289          +/-
DELTA     HEIGHT :   64.5400                   +/-

 A POSTERIORI ELLIPSOID BASELINE COMPONENTS
DELTA  LATITUDE : -    0   6 15.47827          +/-          5 MM
DELTA LONGITUDE :      0   4 14.23926          +/-          8 MM
DELTA     HEIGHT :   64.4249                   +/-          5 MM

 CROSS-CORRELATION BETWEEN BASELINE COMPONENTS
BASELINE COMPONENT L  AND BASELINE COMPONENT P  CROSS-CORRELATION = /  -.88/ GREATER THAN    .10
BASELINE COMPONENT H  AND BASELINE COMPONENT P  CROSS-CORRELATION = /  -.21/ GREATER THAN    .10
BASELINE COMPONENT H  AND BASELINE COMPONENT L  CROSS-CORRELATION = /   .18/ GREATER THAN    .10

 A POSTERIORI CARTESIAN BASELINE COMPONENTS
DELTA X :          7347.7311 M  +/-          9 MM
DELTA Y :         -6741.5015 M  +/-          4 MM
DELTA Z :         -8094.7830 M  +/-          4 MM

 CROSS-CORRELATION BETWEEN BASELINE COMPONENTS
BASELINE COMPONENT Y  AND BASELINE COMPONENT X  CROSS-CORRELATION = /  -.48/ GREATER THAN    .10
BASELINE COMPONENT Z  AND BASELINE COMPONENT X  CROSS-CORRELATION = /  -.45/ GREATER THAN    .10
BASELINE COMPONENT Z  AND BASELINE COMPONENT Y  CROSS-CORRELATION = /  -.37/ GREATER THAN    .10

BASELINE LENGTH =     12843.7731 M  +/-          7 MM
AZIMUTH =    154 DEGREES
```

TABLE 5.8 *continued*

BASELINE : STATION : MO & STATION : ME

STATION NAME : MO

A-PRIORI ELLIPSOIDAL COORDINATES

LATITUDE	: 45 26 34.32643	+/-	
LONGITUDE	: - 76 15 18.04879	+/-	
HEIGHT	: 49.1100	+/-	

A POSTERIORI ELLIPSOIDAL COORDINATES

LATITUDE	: 45 26 34.31758	+/-	517 MM
LONGITUDE	: - 76 15 18.08106	+/-	507 MM
HEIGHT	: 50.2160	+/-	515 MM

CROSS-CORRELATION BETWEEN COORDINATES

A POSTERIORI CARTESIAN COORDINATES

X :	1065089.9596 M	+/-	512 MM
Y :	-4354316.6392 M	+/-	511 MM
Z :	4522050.7988 M	+/-	517 MM

CROSS-CORRELATION BETWEEN COORDINATES

STATION NAME : ME

A-PRIORI ELLIPSOIDAL COORDINATES

LATITUDE	: 45 14 34.02612	+/-	
LONGITUDE	: - 75 27 30.61837	+/-	
HEIGHT	: 63.3900	+/-	

A POSTERIORI ELLIPSOIDAL COORDINATES

LATITUDE	: 45 14 34.03163	+/-	518 MM
LONGITUDE	: - 75 27 30.64175	+/-	507 MM
HEIGHT	: 64.3550	+/-	516 MM

CROSS-CORRELATION BETWEEN COORDINATES

A POSTERIORI CARTESIAN COORDINATES

X :	1129491.6372 M	+/-	512 MM
Y :	-4354410.2148 M	+/-	511 MM
Z :	4506431.4942 M	+/-	518 MM

TABLE 5.9
Results for baseline Morris-Metcalfe.

```
 CROSS-CORRELATION BETWEEN COORDINATES

 BASELINE :    MO   ME
 ----------------------

 A-PRIORI      ELLIPSOID BASELINE COMPONENTS
DELTA  LATITUDE : -    0 12    .30031          +/-
DELTA LONGITUDE :      0 47 47.43042          +/-
DELTA     HEIGHT :   14.2800                  +/-

 A POSTERIORI ELLIPSOID BASELINE COMPONENTS
DELTA  LATITUDE : -    0 12    .28595          +/-          7 MM
DELTA LONGITUDE :      0 47 47.43931          +/-         10 MM
DELTA     HEIGHT :   14.1390                  +/-          8 MM

 CROSS-CORRELATION BETWEEN BASELINE COMPONENTS
BASELINE COMPONENT L  AND BASELINE COMPONENT P  CROSS-CORRELATION = /  -.47/ GREATER THAN    .10
BASELINE COMPONENT H  AND BASELINE COMPONENT P  CROSS-CORRELATION = /  -.67/ GREATER THAN    .10

 A POSTERIORI CARTESIAN BASELINE COMPONENTS
DELTA X :         64401.6776 M  +/-          8 MM
DELTA Y :           -93.5756 M  +/-          4 MM
DELTA Z :        -15619.3046 M  +/-          4 MM

 CROSS-CORRELATION BETWEEN BASELINE COMPONENTS
BASELINE COMPONENT Y  AND BASELINE COMPONENT X  CROSS-CORRELATION = /  -.48/ GREATER THAN    .10
BASELINE COMPONENT Z  AND BASELINE COMPONENT X  CROSS-CORRELATION = /  -.40/ GREATER THAN    .10
BASELINE COMPONENT Z  AND BASELINE COMPONENT Y  CROSS-CORRELATION = /  -.41/ GREATER THAN    .10

BASELINE LENGTH =     66268.7521 M  +/-          8 MM
AZIMUTH =    109 DEGREES
```

TABLE 5.9 *continued*

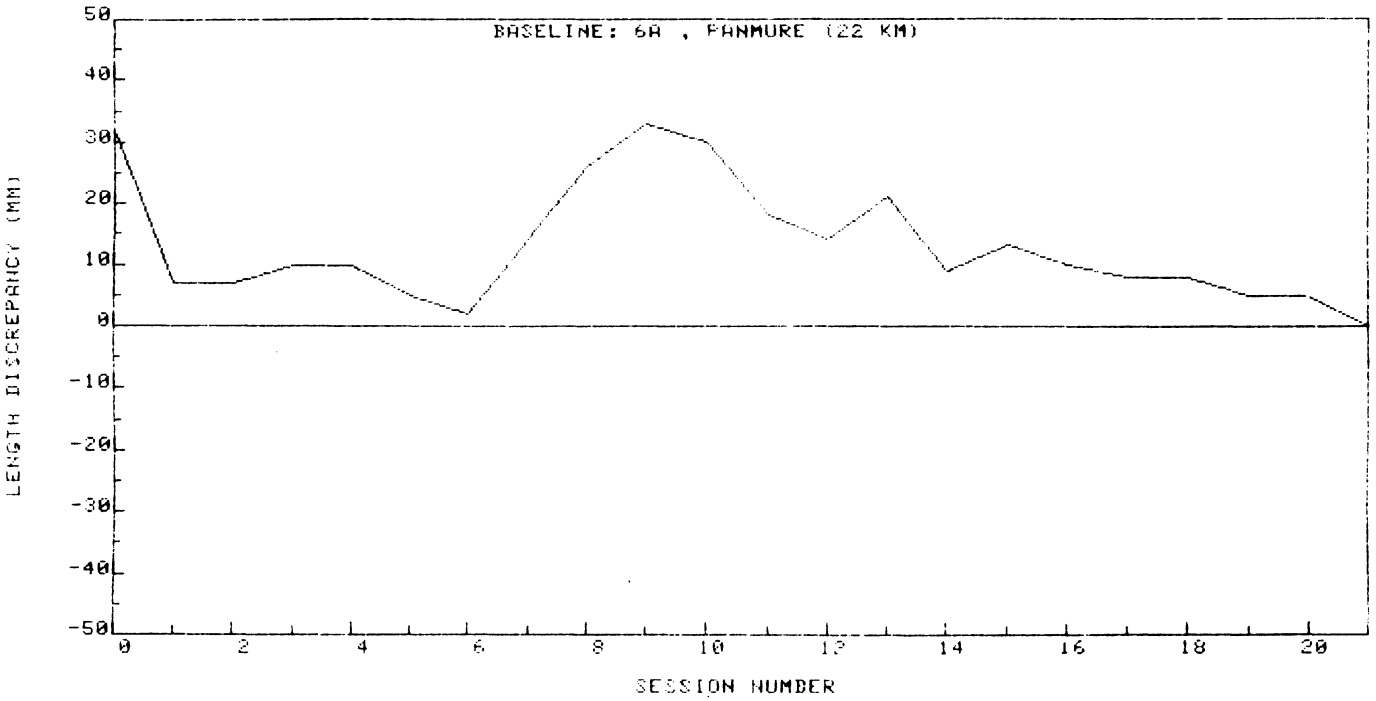

FIGURE 5.5b

Convergence of baseline length solution for the baseline:
6A-Panmure with respect to the final length.

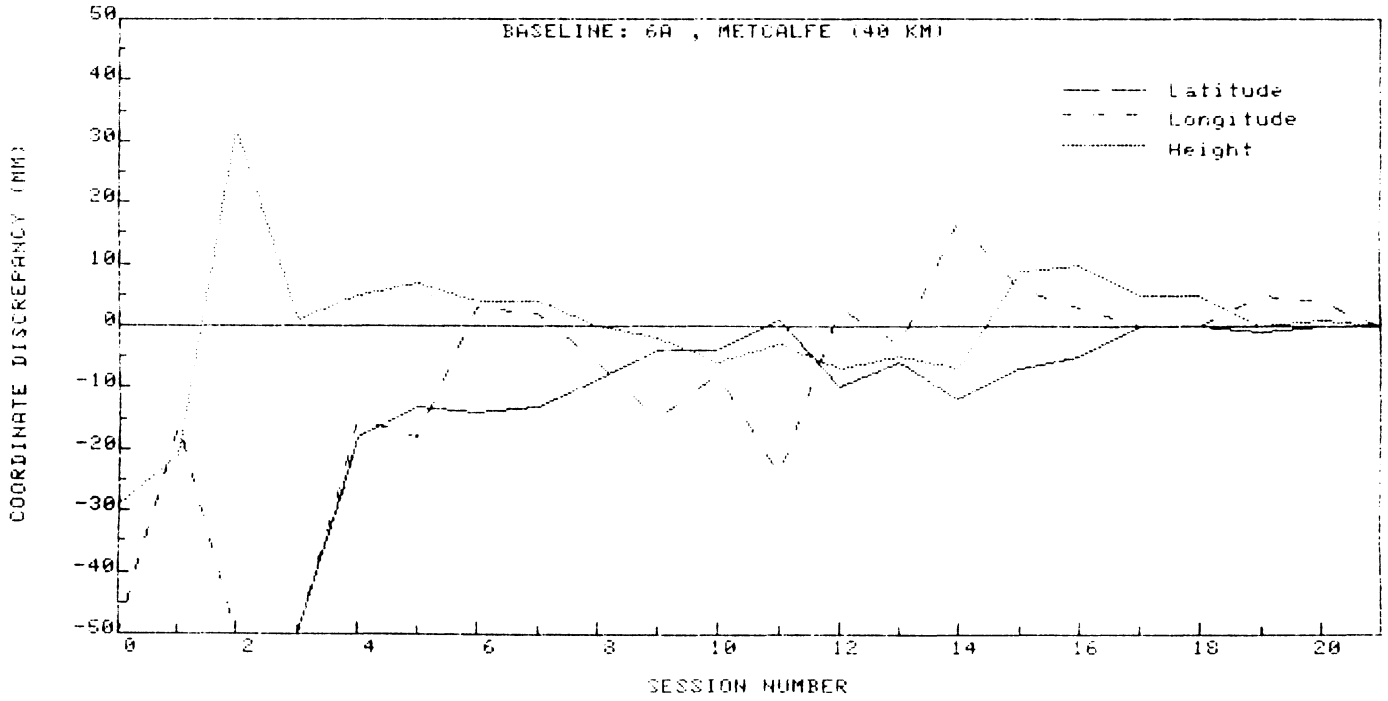

FIGURE 5.6a

Convergence of latitude, longitude and height solutions for the baseline: 6A-Metcalfe with respect to the final coordinates.

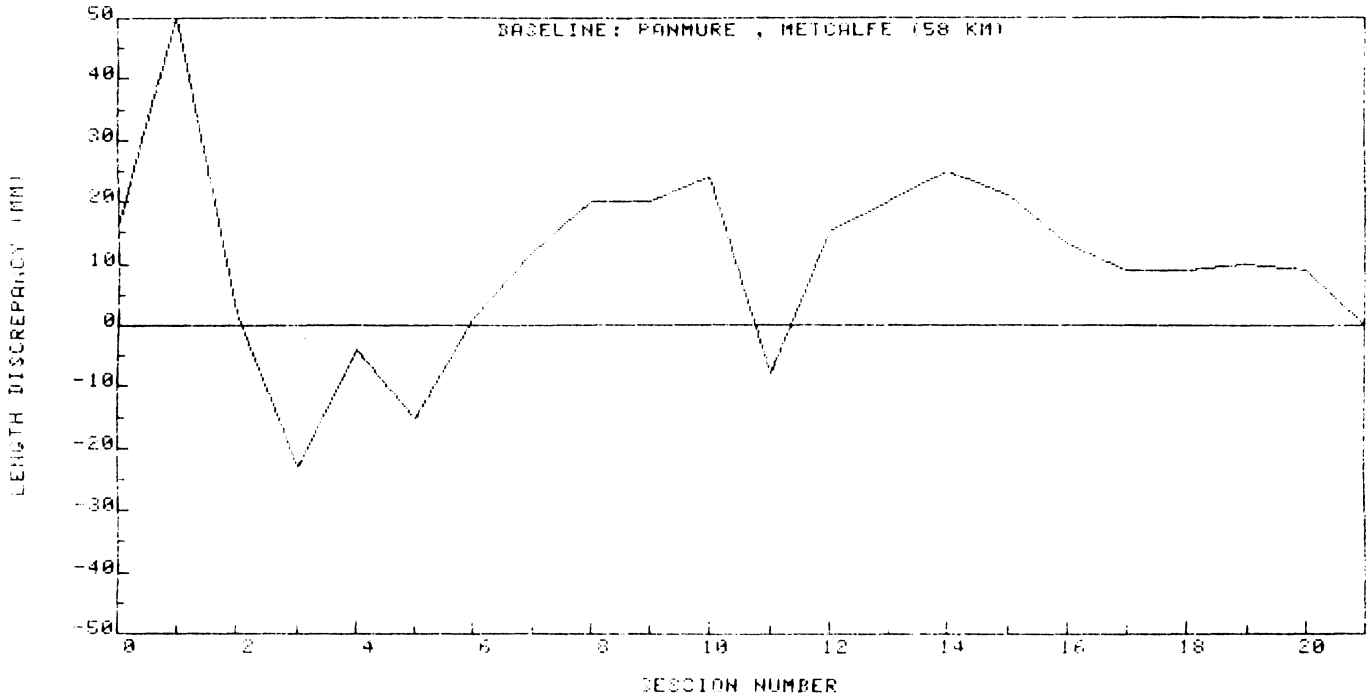

FIGURE 5.9b

Convergence of baseline length solution for the baseline: Panmure-Metcalfe with respect to the final length.

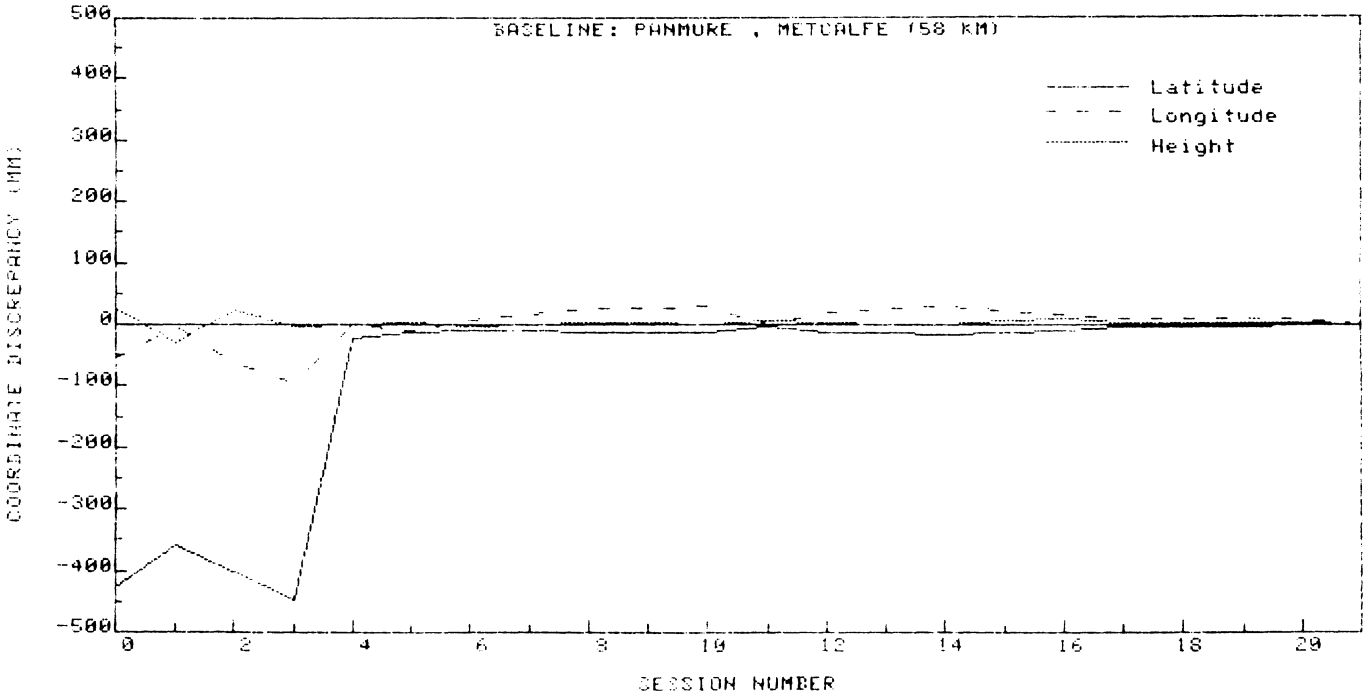

FIGURE 5.10

As for FIGURE 5.9a but with contracted ordinate scale.

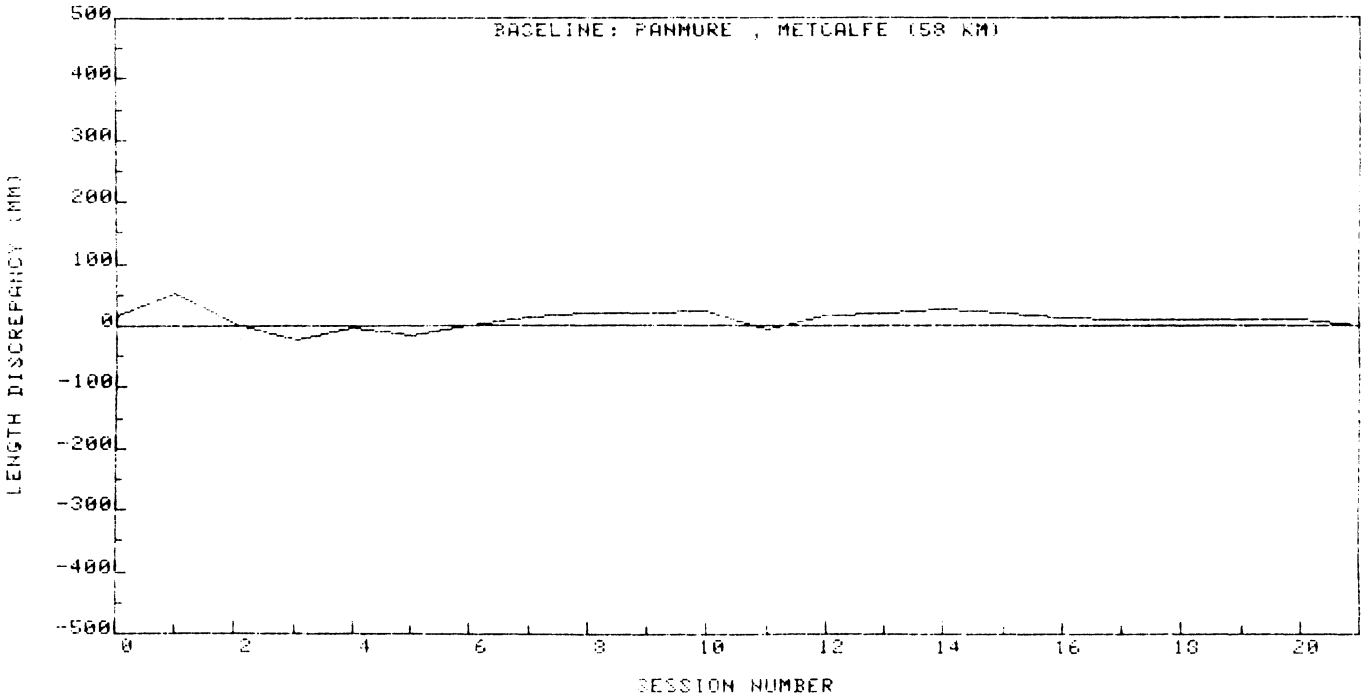

FIGURE 5.11

As for FIGURE 5.9a but with contracted ordinate scale.

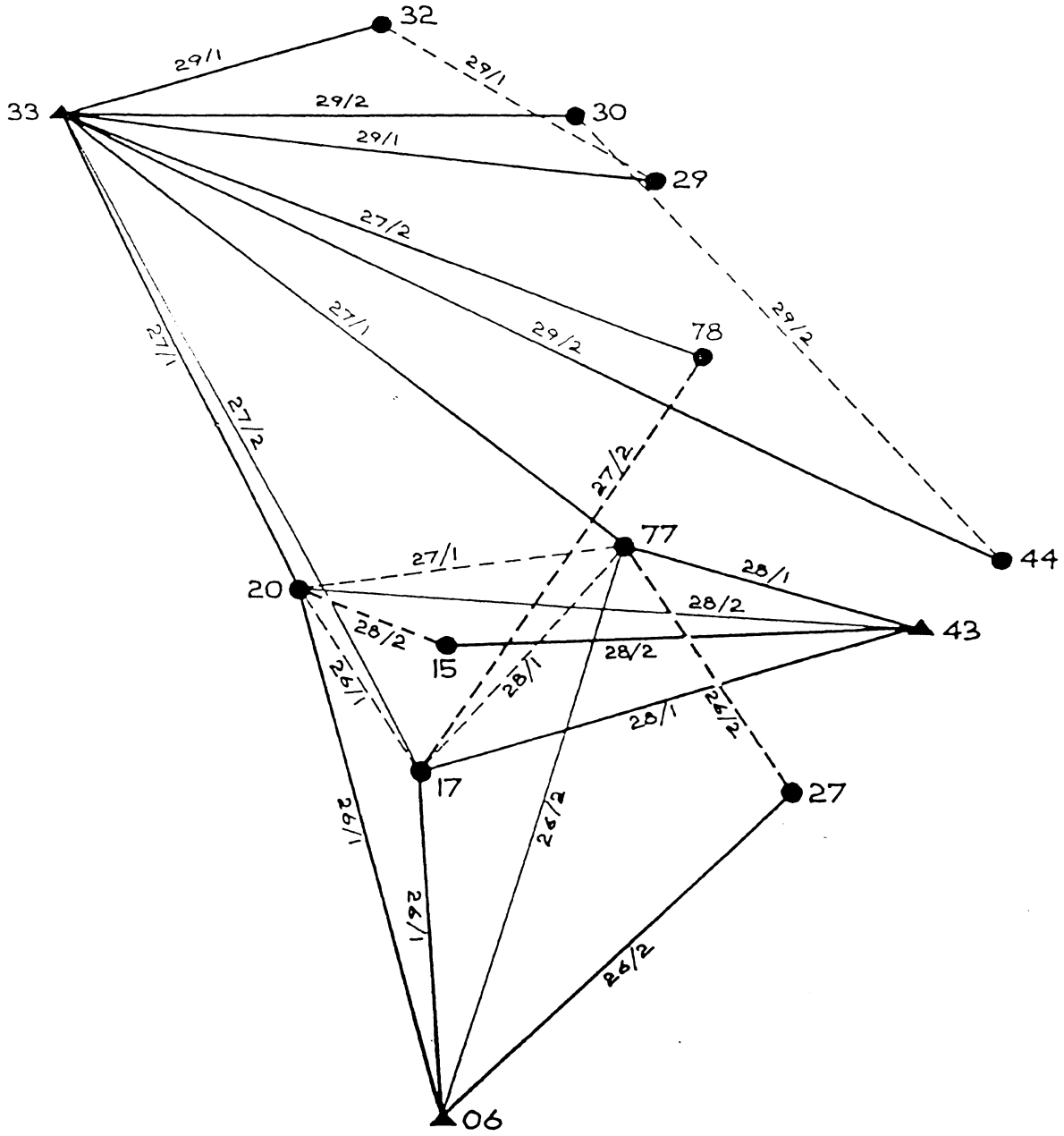

FIGURE 5.12

Ste-Foy Network.

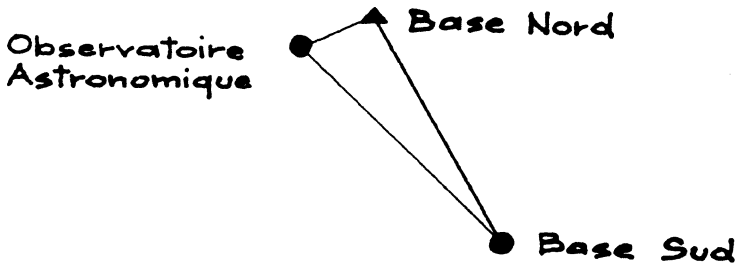

FIGURE 5.13
Université Laval network.

conventional terrestrial means (invar tape).

The Macrometer™ observations were processed by Geo/Hydro Inc. using Macrometrics' software. In the subsequent sections we describe the results of an independent analysis made by a team from the Universities of Bern (Switzerland), Laval (Québec) and New Brunswick (UNB) at UNB in Fredericton.

5.2.2.1 UNB software

The Macrometer™ data were processed at UNB using an interactive data editor and programs PRMAC3 and PRMNET [Beutler, 1984; Beutler et al., 1984]. The programs PRMAC3 and PRMNET work with the so-called "double differences" obtained by differencing the singly-differenced phase observations produced by Macrometrics' program INTRFT. These single differences are simply the differences of the phases recorded by the individual receivers. An interactive editor is used to preprocess the data to identify cycle slips and other problems with the data. PRMAC3 handles data from one or more observing sessions on a single baseline, whereas PRMNET can process data from many baselines simultaneously. The programs were written in FORTRAN and run on an IBM 3081 computer. Both programs estimate receiver coordinates, the relative behaviour of the receiver clocks and the phase ambiguities.

The ambiguities are estimated in two steps. In the first step the ambiguities are estimated as real numbers along with the station coordinates and clock parameters. The ambiguities should be close to integers. In the second step the ambiguities are fixed by rounding them to the nearest integers and then the station coordinates and clock parameters are re-estimated. On the very short baselines of the Ste-Foy network, unambiguously identifying the integer ambiguities was very easy. We have found, from experience, that we can fix the ambiguities on baselines up to about 20 km in length.

The satellite ephemerides we used to process the data were those provided by Macrometrics in the so-called T-files. We used the same coordinates of the earth's rotation pole and departures of UT1 from UTC as those used by Macrometrics with one exception (see below).

5.2.2.2 Baseline solutions

We initially processed the data session by session, which is to say, baseline by baseline, as none of the baselines in the Ste-Foy test was measured more than once. We did not use data from any of the redundant baselines, shown as dashed lines in Figure 5.12.

In Table 5.12 we list the differences in latitude, longitude, and height of the baseline solutions using our software and those obtained by Geo/Hydro Inc. The agreement in latitude and longitude is typically better than 1 mm; the agreement in height is generally 2 mm or better. In view of the fact that our data editing differed slightly from that used by Geo/Hydro (compare numbers n_1, n_2 of observations per session used by Geo/Hydro and ourselves in Table 5.12) the agreement is good. That the differences in height are somewhat larger than those in latitude and longitude may be due to the fact that we used a different procedure for determining the effect of the troposphere on the observations.

For two baselines, 06-27 and 33-29 (see Figure 5.12), the differences between the two solutions are larger than the rest. In the first case (baseline 06-27), we know the differences are caused by a difference in data editing. Geo/Hydro used four observations from the NAVSTAR 3 satellite, whereas we decided that even these four observations were of dubious worth and deleted all the observations of this satellite on this baseline. In the second case (baseline 33-29), the large difference is explained by Geo/Hydro having set UT1 equal to UTC; we set UT1 - UTC = 0.342 sec.

5.2.2.3 Misclosures of looped baselines

It is usually a good check for the single baseline solutions to compute "misclosures" by summing up the interstation vectors resulting from the single baseline estimations along closed loops in the network.

Many different misclosures might be formed in the Ste-Foy network. However, we should ignore the triangles formed by the three stations at which observations were carried out simultaneously. If the same sets of observations are used in forming the single differences for the three baselines, only two of the baselines are independent and the misclosure vector, apart from rounding errors, will be zero. We have chosen two non-trivial loops for misclosure study. The first loop is formed by

TABLE 5.12

COMPARISON OF UNB AND GEO-HYDRO ADJUTMENT

(UNB MINUS GEO-HYDRO)

STE-FOY AND U.LAVAL BASELINES

BASE-LINE	N1	N2	DELTA LAT. (MM)	DELTA LON. (MM)	DELTA ALT. (MM)	DELTA LENGTH (MM)	(PPM)
06,17	104	106	-0.6	0.4	-2	-0.5	0.7
06,20	103	105	-0.3	0.4	-1	-0.4	0.3
06,77	112	124	-0.6	0.6	0	-0.4	0.3
* 06,27	105	95	3.6	-0.6	-5	3.2	3.2
33,20	96	96	0.6	0.4	1	-0.6	0.5
33,77	106	112	0.9	-0.8	1	-1.4	1.0
33,17	126	130	0.3	-0.6	0	-1.0	0.6
33,78	121	135	0.9	-0.2	-2	-1.2	1.0
43,77	115	118	0.3	0.4	0	0.0	0.0
43,17	118	120	0.6	-1.0	2	0.3	0.3
43,20	132	141	-0.9	0.2	2	0.2	0.2
43,15	127	139	-1.2	0.0	2	0.1	0.1
33,32	116	120	-1.2	0.6	-2	0.3	0.5
+ 33,29	115	118	-16.2	2.2	20	0.1	0.1
33,30	116	120	-1.2	1.0	1	0.9	1.2
33,44	125	135	-0.3	0.4	0	0.1	0.1
NO,SU	150	149	-1.2	0.4	0	0.6	1.1
NO,OA	149	147	-0.3	0.2	0	-0.1	0.4
SU,OA	152	152	0.3	-0.2	0	0.7	1.2

N1: NUMBER OF OBSERVATIONS USED BY GEO-HYDRO
N2: NUMBER OF OBSERVATIONS USED BY UNB

* ESSENTIAL DIFFERENCE IN EDITING: UNB SOLUTION USED 4 CHANNELS, GEO-HYDRO USED 5 CHANNELS

+ GEO-HYDRO PROCESSED THIS BASELINE WITH UT1-UTC=0 , INSTEAD OF USING UT1-UTC=0.342 s

stations 43, 77, 33, 20, 06, and 17 and is shown in Figure 5.14. This loop is equivalent to the triangle formed by stations 77, 20, and 17, since the triplets of stations 43, 77, and 17; 33, 20, and 77; and 6, 17, and 20 form triangles which close trivially. The second loop is formed by the same six stations as the first but taken in a different order so as not to reduce the length of the loop by trivial closures. This loop is illustrated in Figure 5.15. The computed misclosures for both loops are shown in Table 5.13.

We note that the misclosures obtained with UNB's and Macrometrics' software are very similar, which is not surprising in view of the good agreement reported in Table 5.12. The results of both analyses indicate a large misclosure in height in the first loop. If we assign this misclosure to the triangle 17-77-20, which we are entitled to do, we get a misclosure of 13.1 ppm using the UNB results. This misclosure is one order of magnitude larger than what one would expect from Macrometer™ results.

The Macrometer™ observations refer to the phase centres of the pair of antennas forming a baseline. The phase centre to phase centre baselines must be corrected for the heights of the phase centres above their respective survey markers. We suspect that the height of one of the antennas was incorrectly measured. That this actually is the case may be proved by the following line of argument:

(a) The points 43, 33, and 06 served as master stations during the first three days of observations (the observations of the last two days are of no importance here). This means that all measurements made at those three points were made with one and the same antenna set-up. It is possible that errors in the heights of the antennas at the three points 43, 33, and 06 occurred, but we would not be able to detect them through misclosures, because such errors would appear twice with opposite signs when the misclosure vector is formed and as such would cancel out.

(b) The points 20, 77, and 17 were all observed three times (once on each of the first three days). Therefore three different antenna set-ups are involved at each of the three sites.

(c) Two different antenna set-ups per site are involved when computing one of the possible misclosures including all three points 20, 17, and 77.

(d) In the first of the two misclosures, antennas belonging to receivers

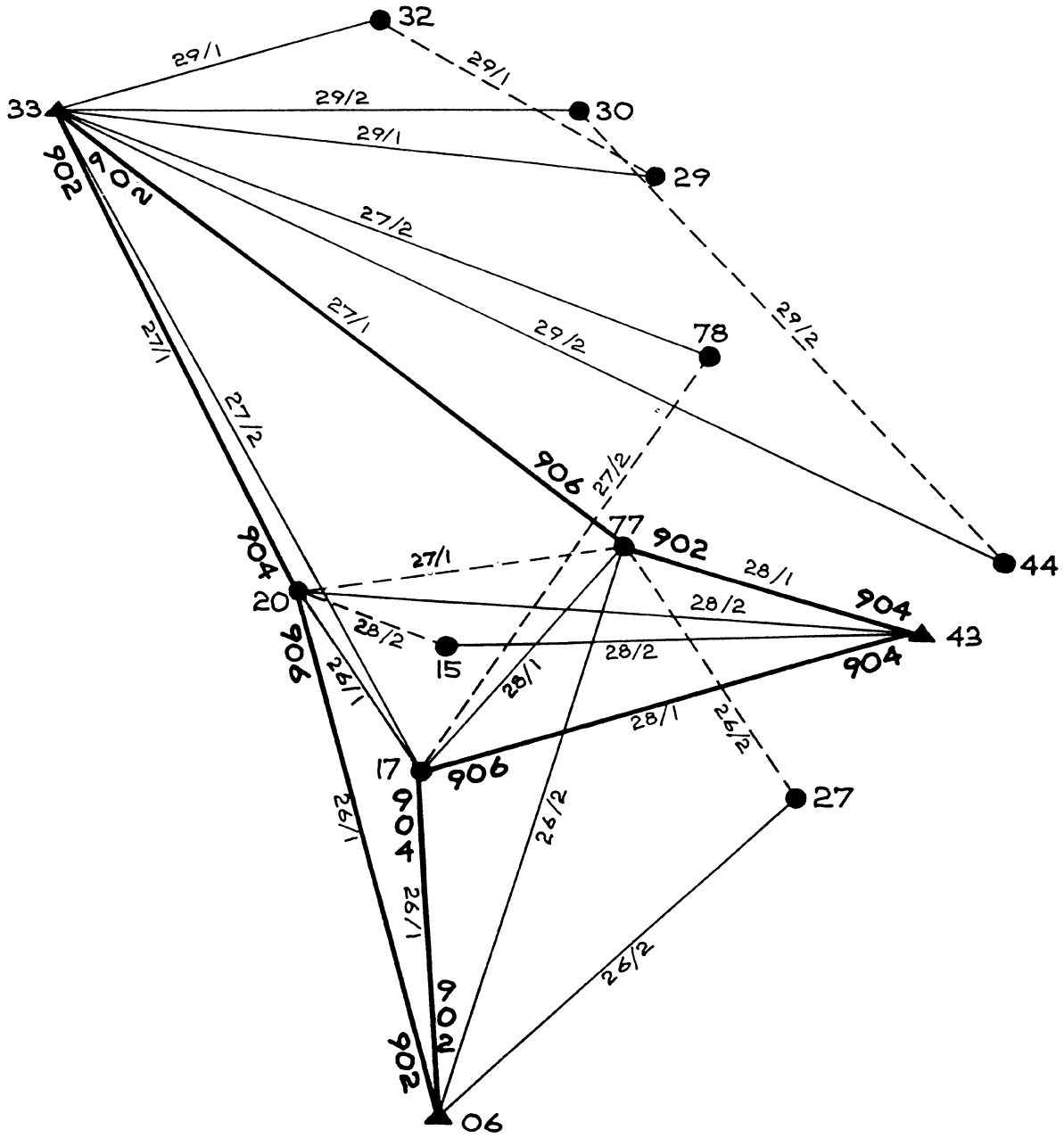

FIGURE 5.14

First baseline loop used for misclosure study.

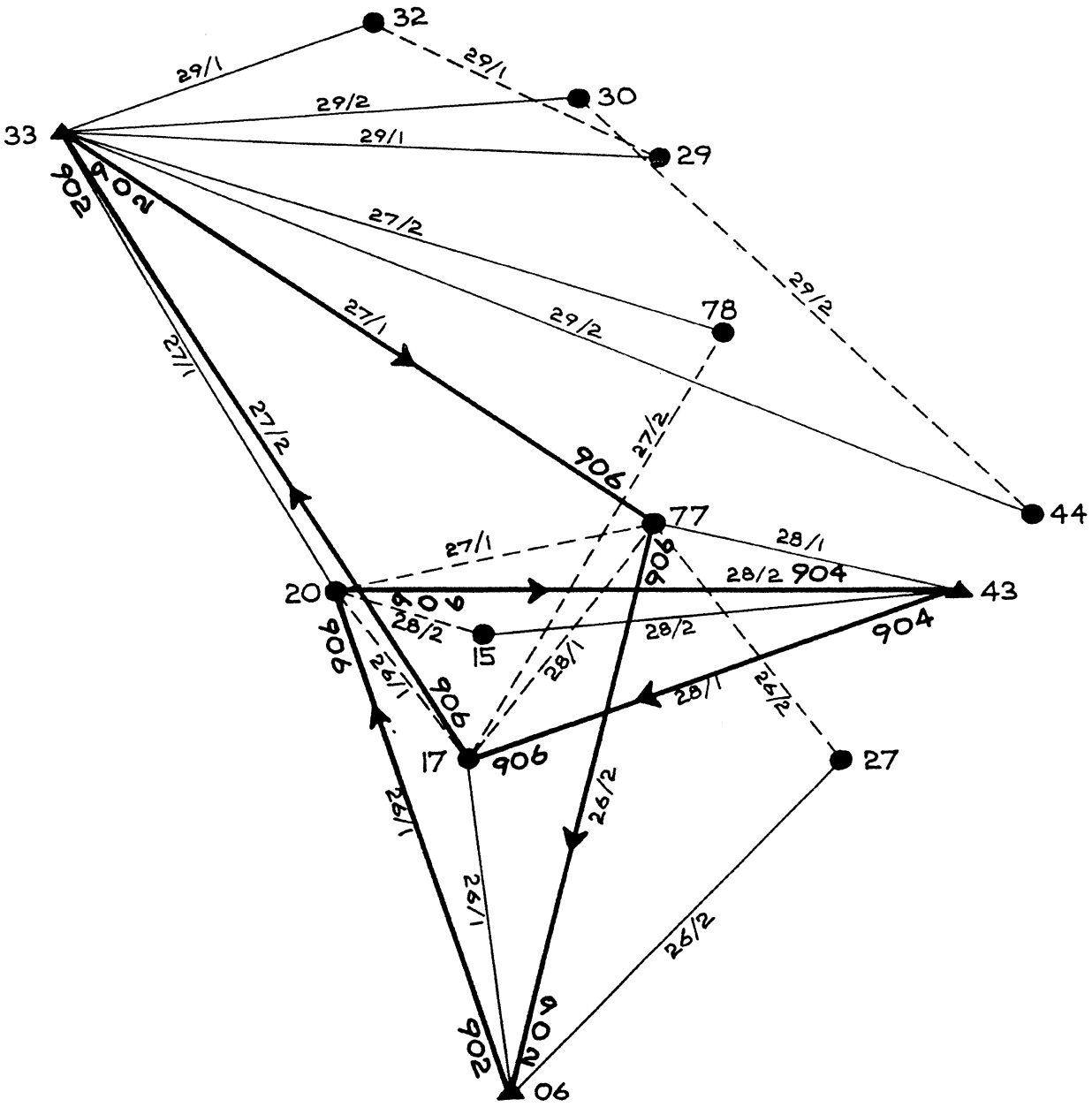

FIGURE 5.15

Second baseline loop used for misclosure study.

TABLE 5.13

Loop Misclosures.

Loop	Circumference (m)	Macrometrics Δφ (mm)	Macrometrics Δλ (mm)	Macrometrics Δh (mm)	UNB Δφ (mm)	UNB Δλ (mm)	UNB Δh (mm)
(1) 43-77-33-20--06-17-43	6057	+1	-4	-21	-2	-2	-23
or 77-20-17-77	or 1773						
(2) 43-17-33-77--06-20-43	7743	12	-1	- 2	12	-1	-1

with serial numbers 902 and 906 at point 77; and 904 and 906 at points 20 and 17 are involved.

(e) In the second misclosure, only the antenna belonging to receiver 906 is involved.

(f) As the misclosure for the loop illustrated in Figure 5.15, when only one antenna (that belonging to receiver 906) is involved, is much better in height (and as the length of the misclosure vector is only 1.6 ppm), this strongly suggests that there exists a non-modelled, antenna-specific error.

The source of the error has not yet been found.

5.2.2.4 Université Laval baselines

In Table 5.14, we give the results of the GPS solution using PRMAC3 for the positions of the two points "Base Sud" and "Observatoire Astronomique" and, for comparison, the positions determined using conventional terrestrial techniques. The conventional coordinates for point "Base Nord" were adopted for the GPS solution. Also shown in Table 5.14 are the differences between the GPS and conventional coordinates.

Of interest is the length comparison of the baseline "Base Nord-Base Sud," as this length was measured most accurately with invar tape. It is clear that the two lengths do not differ significantly considering that standard deviations of 0.5 mm was computed for the terrestrial length measurement and 0.6 mm for the length of the baseline from the GPS solution.

5.2.2.5 Network Solution

We reprocessed all data from the 13 stations of the main network (Figure 5.12) simultaneously using program PRMNET. Our results are shown in Table 5.17. Also shown is the uncertainty (one sigma) in 10^{-5} arc seconds in latitude and longitude and mm for height. We have compared our results with a conventional fourth-order adjustment solution based on direction observations using a Wild T-2 theodolite and distance observations using an optical EDM [Moreau, 1984]. The differences are presented in Table 5.15.

In the network processing, we must fix the coordinates of one of the stations. We fixed the coordinates of station 77, which is near the

TABLE 5.14

TERRESTRIAL COORDINATES

UNIVERSITE LAVAL

NO.	STATION NAME	LATITUDE (GEO.) DEG MIN SEC	LONGITUDE (GEO.) DEG MIN SEC	HEIGHT ORTHO.(M)
NO	BASE NORD	46 45 54.98800	-71 16 41.27990	89.009
SU	BASE SUD	46 46 41.24262	-71 16 24.89808	91.383
OA	OBSERV. ASTRO.	46 46 49.69553	-71 16 48.76694	113.354

GPS COORDINATES (UNB SOFTWARE)

UNIVERSITE LAVAL

NO.	STATION NAME	LATITUDE (GEO.) DEG MIN SEC	LONGITUDE (GEO.) DEG MIN SEC	HEIGHT ORTHO.(M)
NO	BASE NORD	46 45 54.98800 F	-71 16 41.27990 F	89.009 F
SU	BASE SUD	46 46 41.24287 +- 2	-71 16 24.89766 +- 2	91.380 +- 1
OA	OBSERV. ASTRO.	46 46 49.69530 +- 2	-71 16 48.76653 +- 3	113.337 +- 1

TABLE 5.14 (CONTINUED)

COMPARISON OF GPS AND TERRESTRIAL COORDINATES

("GROUND TRUTH" MINUS GPS)

UNIVERSITE LAVAL

NO.	STATION NAME	DELTA LAT. (MM)	DELTA LON. (MM)	DELTA HEIGHT (MM)
NO	BASE NORD	F	F	F
SU	BASE SUD	- 8	- 8	3
OA	OBSERV. ASTRO.	7	- 8	17

DISTANCE : BASE NORD , BASE SUD

TERRESTRIAL TECHNIQUE : 548.5834 M +-.5MM
(INVAR TAPE)

MACROMETER OBSERVATION: 548.5830 M +-.6MM

Table 5.15

COMPARISON OF GPS AND TERRESTRIAL ADJUSTMENT

("GROUND TRUTH" MINUS UNB SOLUTION)

STE-FOY NETWORK

NO.	STATION NAME	DELTA LAT. (MM)	DELTA LON. (MM)	DELTA ALT. (MM)	DELTA LENGTH (MM)	DELTA LENGTH (PPM) *
06	83SF006	-29	2	20	29	21
15	83SF015	-13	- 1	- 9	5	11
17	83SF017	-22	2	7	20	29
20	83SF020	-22	1	0	4	7
27	82SF027	-15	- 6	31	11	18
29	83SF029	15	5	-27	16	18
30	83SF030	- 4	- 4	-15	- 3	3
32	83SF032	- 2	- 5	-14	0	0
33	83SF033	-17	- 4	-20	-10	7
43	82SF043	- 6	2	8	5	9
44	82SF044	17	1	9	2	3
77	83SF077	F	F	F	F	F
78	83SF078	- 1	- 7	- 6	- 4	8

* DIFFERENCE IN LENGTH OF THE BASELINE ENDING AT STATION 77

centroid of the network, at the terrestrially determined values. A total of 1914 double-difference observations were processed by PRMNET.

The agreement in latitude and longitude between the GPS solution and the "ground truth" may be considered satisfactory in view of the errors estimated for the fourth-order terrestrial network.

The agreement in longitude is much better than that in either latitude or height. There is a predominance of negative differences in latitude; only stations 29 and 44 show positive differences. There is also a predominance of positive differences in the length of the baselines formed with station 77. Only stations 30, 33, and 78 show negative differences. This may indicate distortion of the terrestrial coordinates that might be removed by a relative three-dimensional adjustment (see below).

Table 5.16 is presented to illustrate the superiority of the network solution compared to single baseline solutions. Whereas it is very difficult to prove this superiority by analysing the coordinates obtained (as we suffer from a lack of "truth", "ground" or other), we see a substantial improvement in the fractional part of non-integer estimates of the (integer) ambiguity parameters in the network solution with respect to the baseline solution. In the baseline solution the largest deviation from an integer number is 0.43, which is reduced to 0.12 for the network solution. The overall improvement may be measured by the ratio of the sum of the absolute values of the fractional parts of the baseline ambiguity estimates to those of the network estimates. This ratio is 2.5.

It may be expected that the superiority of the network approach would be even more pronounced, if a larger network (but not as large as to be affected by ionospheric modelling problems) is analysed.

5.2.2.6 Three-dimensional adjustment

At the University of Bern, we have carried out a three-dimensional transformation of the UNB GPS results in an attempt to get better agreement with the ground truth values. We minimized the differences between the GPS and terrestrial coordinates by rotating the GPS coordinates with respect to the terrestrial coordinates and by adjusting the scale of the GPS coordinates. The rotations are about orthogonal axes centred on the centroid of the set of the GPS coordinates with the x-axis pointing east, the y-axis pointing north, and the z-axis pointing vertically upwards. The

TABLE 5.16

FRACTIONAL PART OF NON-INTEGER AMBIGUITY ESTIMATES
IN BASELINE AND NETWORK MODES

STE-FOY OBSERVATIONS

BASE-LINE	PROCESSING MODE	
	BASELINE	NETWORK
06,17	.03 -.03 -.01	.03 -.02 .00
06,20	.04 -.01 .01	.03 .00 .01
06,77	-.15 .17 .27 -.05	.03 .00 .07 -.02
33,20	.08 -.08 -.02	.06 -.07 -.02
33,77	-.01 -.01 -.02	-.03 -.03 -.02
33,17	.11 .22 .01	.02 .08 .00
43,77	-.02 .05 .03	-.04 .06 .03
43,17	-.03 .08 .04	-.02 .08 .04
43,20	.43 -.34 -.34 -.10	.12 -.03 -.05 -.01

MEAN ABSOLUTE VALUE FOR BASELINE MODE = 0.10
MEAN ABSOLUTE VALUE FOR NETWORK MODE = 0.04

TABLE 5.17

GPS COORDINATE RESULTS

QUEBEC MACROMETER CAMPAIGN , JANUARY 1984

STE-FOY NETWORK

NO.	STATION NAME	LATITUDE (GEO.) DEG MIN SEC	LONGITUDE (GEO.) DEG MIN SEC	HEIGHT ORTHO.(M)
06	83SF006	46 45 29.19464 +- 2	-71 19 04.10540 +- 2	82.509 +- 1
15	83SF015	46 46 09.35663 +- 4	-71 19 12.38637 +- 6	77.431 +- 2
17	83SF017	46 45 53.36717 +- 2	-71 19 06.89660 +- 5	79.438 +- 2
20	83SF020	46 46 09.75163 +- 2	-71 19 16.58543 +- 5	76.014 +- 2
27	82SF027	46 45 56.03920 +- 6	-71 18 37.77057 +- 4	89.021 +- 2
29	83SF029	46 46 41.60330 +- 3	-71 18 52.01462 +-10	59.576 +- 3
30	83SF030	46 46 47.29628 +- 4	-71 19 00.03896 +- 6	48.521 +- 2
32	83SF032	46 46 53.96072 +- 3	-71 19 10.41875 +- 9	33.717 +- 3
33	83SF033	46 46 46.25009 +- 2	-71 19 35.56252 +- 5	36.590 +- 1
43	82SF043	46 46 08.41252 +- 2	-71 18 28.57980 +- 5	100.926 +- 1
44	82SF044	46 46 13.72296 +- 4	-71 18 21.94128 +- 6	105.543 +- 2
77	83SF077	46 46 13.30185 F	-71 18 51.92205 F	88.677 F
78	83SF078	46 46 29.44455 +- 4	-71 18 44.36656 +- 6	87.916 +- 2

N. B. : STATION 77 FIXED , PRMNET PROGRAM

estimated rotations and their one sigma uncertainties are θ_x = 2".3 ± 1".2, θ_y = 3".4 ± 0".7, and θ_z = 1".2 ± 0".6. The scale adjustment is 8.1 ± 2.7 ppm. The transformation parameters appear to be significant, particularly the rotation about the y-axis and the scale parameter.

The difference between the ground truth values and the transformed GPS coordinates are shown in Table 5.17A. They are given in the sense "ground truth minus GPS."

TABLE 5.17A

Comparison of Transformed GPS and Terrestrial Coordinates ("Ground Truth Minus GPS").

No.	Station Name	Delta Lat. (mm)	Delta Lon. (mm)	Delta Hgt. (mm)
06	83SF006	- 8	+ 4	- 2
15	83SF015	- 2	- 1	- 9
17	83SF017	- 7	0	- 2
20	83SF020	-11	- 4	+ 2
27	82SF027	- 5	+13	+17
29	83SF029	+17	-10	-15
30	83SF030	- 3	- 2	+ 2
32	83SF032	0	- 4	+ 9
33	83SF033	-12	- 9	+ 5
43	82SF043	0	+ 3	- 2
44	82SF044	+21	+ 4	0
77	83SF077	+ 8	0	- 2
78	83SF078	+ 2	+ 7	- 2

The r.m.s. of the differences in Table 5.17A is about 8 millimetres. This compares with 13 mm for the r.m.s. of the differences between the untransformed GPS coordinates and the ground truth values.

The transformation has served to reduce considerably the magnitudes of the differences between the GPS and terrestrial coordinates. Differences approaching 2 cm still remain, however. It is tempting to ascribe the differences to the lower order terrestrial measurements. However, another candidate for the source of the differences is motion of the geodetic markers due to frost heave between the epochs of the terrestrial and GPS measurements. Further terrestrial measurements may indicate the source or sources of the discrepancies.

5.3 TI-4100 - The Ottawa Experiment

During May 1984, the Ottawa Test Network was observed with a pair of TI-4100 receivers owned by Nortech Surveys (Canada) Inc. The campaign included observations on stations 6A, Panmure, Morris, and Metcalfe, which were also used as part of the Macrometer™ campaign in the previous year (see section 5.2.1). The observation sessions were scheduled according to Table 5.18.

TABLE 5.18

The Ottawa TI-4100 Campaign.

Date	Stations involved
May 16	Panmure, 6A
17	Panmure, Morris
18	Metcalfe, 6A
19	Panmure, Morris
20	Morris, 6A
21	Metcalfe, Morris
22	Morris, 6A
23	Metcalfe, Panmure
24	Morris, Panmure

The duration of the observation sessions was about five to six hours in the first half of the night. The satellites visible at this time are shown in Figure 5.16.

Because of the unexplained breaks in the observation records on 18 May 1984, the data for that particular day were excluded from the processing.

During the development of DIPOP, a preliminary program for processing TI-4100 carrier phase data only was used to obtain initial results for the Ottawa TI-4100 campaign. This software included a manual and rather time-comsuming preprocessor to detect cycle slips. Results of this processing were presented at the AGU 1984 Fall Meeting [Kleusberg et al., 1984] and are shown in Table 5.19 and Figure 5.17 in comparison with the Macrometer™ results and the "ground truth" values available at that time. All computations are done in the NAD27 coordinate system, fixing station 6A at its NAD27 "ground truth" coordinates.

Table 5.19 shows excellent agreement in baseline length for the three

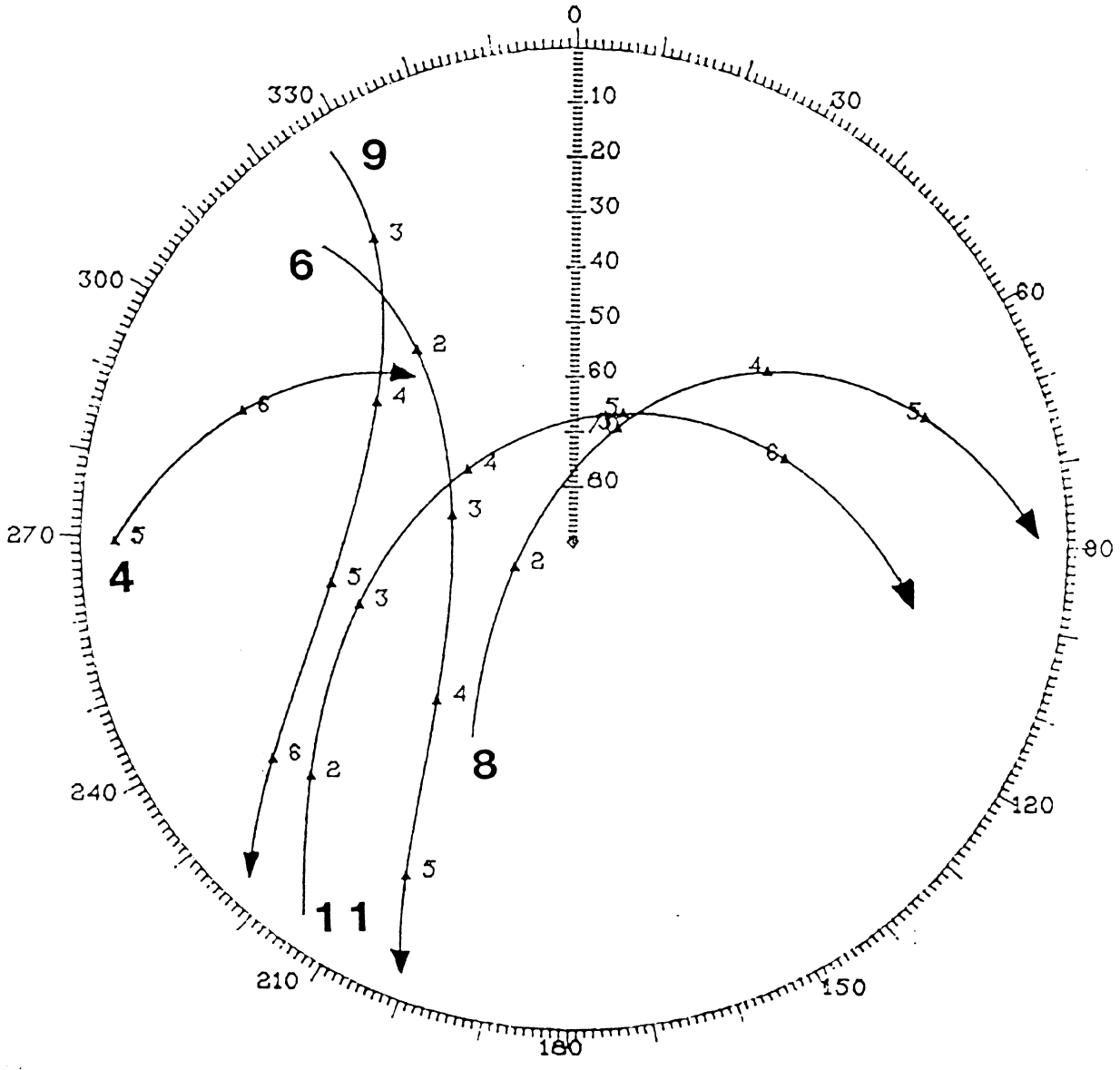

FIGURE 5.16

Visibility of GPS satellites during the Ottawa TI-4100 campaign.

	TERR.	MACROM.	TI4100	MACROM. - TERR.		TI4100 - TERR.		MACROM. -TI4100	
				MM	PPM	MM	PPM	MM	PPM
PN-6A	21590.306	21590.242	21590.226	-64	3.0	-80	3.8	16	0.7
MO-6A	26489.044	26489.013	26489.005	-31	1.2	-39	1.5	8	0.3
MO-PN	12843.738	12843.772	12843.751	34	2.7	13	1.0	21	1.6
MO-ME	66268.767	66268.749	66268.778	-18	0.3	11	0.2	-29	0.4
PN-ME	57930.749	57930.700	57930.733	-49	0.8	-16	0.3	-33	0.6
6A-ME	40295.489	40295.444	40295.474	-45	1.1	-15	0.4	-30	0.7

TABLE 5.19

Comparison of baseline chord lengths;
station 6A fixed to "ground truth" NAD27 coordinates.

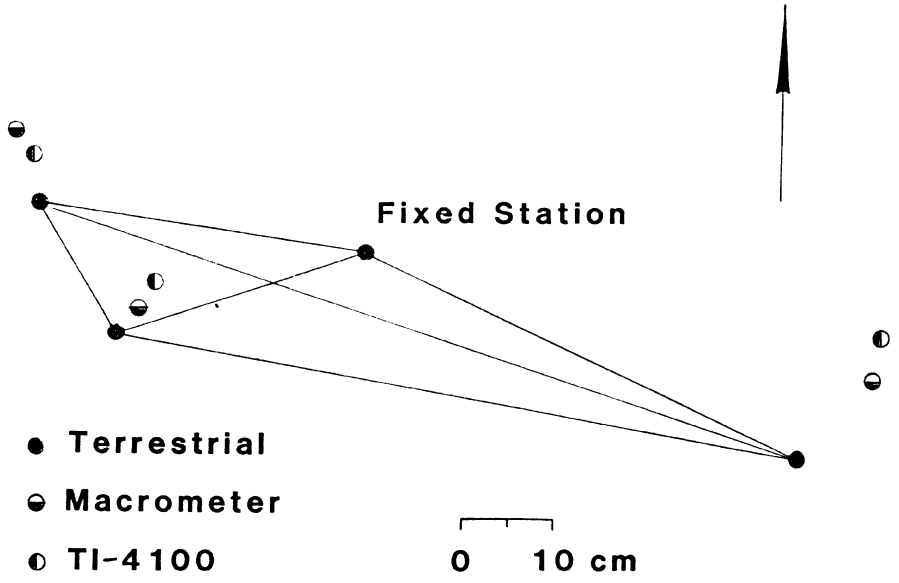

FIGURE 5.17

Comparison of horizontal coordinates
in NAD27, 6A fixed.

long baselines whereas the relative discrepancies are slightly larger for the three short baselines. The agreement between the Macrometer™ and TI-4100 baseline lengths is better than 1 ppm for all but the shortest baseline.

The plot of the discrepancies in the horizontal plane (Figure 5.17) shows again a good agreement between the TI-4100 and the Macrometer™ solution, whereas both GPS solutions have some common displacements with respect to "ground truth." Maximum horizontal discrepancy between the two GPS solutions is 5 cm and the maximum offset with respect to "ground truth" is about 16 cm.

For the processing of the TI-4100 observations by the DIPOP software package, a priori station coordinates (and their weights), as described in the previous section, have been used. Previous experience suggested an a priori standard deviation for the combined L1 and L2 carrier phase double difference observation of 2.5 cm. The results are presented in Tables 5.20 through 5.26.

A second adjustment was performed with the same initial conditions but using the L1 carrier phase observations only. The results are shown in Tables 5.27 through 5.33. These L1 only results disagree with the combined L1 and L2 solutions on the 1 ppm level for several of the baselines. Comparison shows (see Table 5.34 and section 5.4) that the combined L1/L2 result for baseline length agree slightly better with the Macrometer™ solutions and the "ground truth" than the L1 solution.

```
 BASELINE :      STATION : A6 & STATION : MO
 ===========================================

 STATION NAME : A6
 -----------------

 A-PRIORI ELLIPSOIDAL COORDINATES
LATITUDE  :     45 23 55.81961          +/-
LONGITUDE : -   75 55 20.63537          +/-
HEIGHT    :   37.1300                   +/-

 A POSTERIORI ELLIPSOIDAL COORDINATES
LATITUDE  :     45 23 55.79290          +/-         508 MM
LONGITUDE : -   75 55 20.78519          +/-         467 MM
HEIGHT    :   37.4873                   +/-         508 MM

 CROSS-CORRELATION BETWEEN COORDINATES
COORDINATE L    AND COORDINATE P  CROSS-CORRELATION = /  -.10/ GREATER THAN     .10

 A POSTERIORI CARTESIAN   COORDINATES
X :       1091192.9053 M    +/-         480 MM
Y :      -4351433.4153 M    +/-         498 MM
Z :       4518606.6346 M    +/-         506 MM

 CROSS-CORRELATION BETWEEN COORDINATES
COORDINATE Y    AND COORDINATE X  CROSS-CORRELATION = /  -.12/ GREATER THAN     .10

 STATION NAME : MO
 -----------------

 A-PRIORI ELLIPSOIDAL COORDINATES
LATITUDE  :     45 26 34.32643          +/-
LONGITUDE : -   76 15 18.04879          +/-
HEIGHT    :   49.1100                   +/-

 A POSTERIORI ELLIPSOIDAL COORDINATES
LATITUDE  :     45 26 34.29189          +/-         508 MM
LONGITUDE : -   76 15 18.19765          +/-         468 MM
HEIGHT    :   49.6239                   +/-         508 MM

 CROSS-CORRELATION BETWEEN COORDINATES
COORDINATE L    AND COORDINATE P  CROSS-CORRELATION = /  -.10/ GREATER THAN     .10

 A POSTERIORI CARTESIAN   COORDINATES
X :       1065087.5340 M    +/-         480 MM
```

TABLE 5.20

Results for baseline 6A-Morris (combined L1 and L2).

```
Y :      -4354317.3867 M    +/-        497 MM
Z :       4522049.8203 M    +/-        506 MM

 CROSS-CORRELATION BETWEEN COORDINATES
COORDINATE Y   AND COORDINATE X  CROSS-CORRELATION = /  -.11/ GREATER THAN     .10


 BASELINE :   A6  M0
 -------------------

 A-PRIORI     ELLIPSOID BASELINE COMPONENTS
DELTA  LATITUDE :      0  2 38.50682         +/-
DELTA LONGITUDE : -    0 19 57.41342         +/-
DELTA    HEIGHT :   11.9800                  +/-

 A POSTERIORI ELLIPSOID BASELINE COMPONENTS
DELTA  LATITUDE :      0  2 38.49898         +/-          3 MM
DELTA LONGITUDE : -    0 19 57.41246         +/-          6 MM
DELTA    HEIGHT :   12.1365                  +/-          4 MM

 CROSS-CORRELATION BETWEEN BASELINE COMPONENTS
BASELINE COMPONENT L  AND BASELINE COMPONENT P  CROSS-CORRELATION = /  -.59/ GREATER THAN     .10
BASELINE COMPONENT H  AND BASELINE COMPONENT P  CROSS-CORRELATION = /  -.63/ GREATER THAN     .10
BASELINE COMPONENT H  AND BASELINE COMPONENT L  CROSS-CORRELATION = /   .23/ GREATER THAN     .10

 A POSTERIORI CARTESIAN BASELINE COMPONENTS
DELTA X :       -26105.3713 M  +/-          6 MM
DELTA Y :        -2883.9714 M  +/-          3 MM
DELTA Z :         3443.1857 M  +/-          2 MM

 CROSS-CORRELATION BETWEEN BASELINE COMPONENTS
BASELINE COMPONENT Y  AND BASELINE COMPONENT X  CROSS-CORRELATION = /  -.69/ GREATER THAN     .10
BASELINE COMPONENT Z  AND BASELINE COMPONENT X  CROSS-CORRELATION = /  -.26/ GREATER THAN     .10
BASELINE COMPONENT Z  AND BASELINE COMPONENT Y  CROSS-CORRELATION = /  -.24/ GREATER THAN     .10

BASELINE LENGTH =    26488.9265 M  +/-          5 MM
AZIMUTH =   -79 DEGREES
```

TABLE 5.20 *continued*

```
 BASELINE :      STATION : A6 & STATION : PA
 ===========================================

 STATION NAME : A6
 -----------------

 A-PRIORI ELLIPSOIDAL COORDINATES
LATITUDE  :     45 23 55.81961          +/-
LONGITUDE : -   75 55 20.63537          +/-
HEIGHT    :   37.1300                   +/-

 A POSTERIORI ELLIPSOIDAL COORDINATES
LATITUDE  :     45 23 55.79290          +/-         508 MM
LONGITUDE : -   75 55 20.78519          +/-         467 MM
HEIGHT    :   37.4873                   +/-         508 MM

 CROSS-CORRELATION BETWEEN COORDINATES
COORDINATE L    AND COORDINATE P  CROSS-CORRELATION = /  -.10/ GREATER THAN     .10

 A POSTERIORI CARTESIAN   COORDINATES
X :       1091192.9053 M   +/-         480 MM
Y :      -4351433.4153 M   +/-         498 MM
Z :       4518606.6346 M   +/-         506 MM

 CROSS-CORRELATION BETWEEN COORDINATES
COORDINATE Y    AND COORDINATE X  CROSS-CORRELATION = /  -.12/ GREATER THAN     .10

 STATION NAME : PA
 -----------------

 A-PRIORI ELLIPSOIDAL COORDINATES
LATITUDE  :     45 20 18.84770          +/-
LONGITUDE : -   76 11  3.81590          +/-
HEIGHT    :  113.6500                   +/-

 A POSTERIORI ELLIPSOIDAL COORDINATES
LATITUDE  :     45 20 18.81335          +/-         508 MM
LONGITUDE : -   76 11  3.95911          +/-         468 MM
HEIGHT    :  114.0791                   +/-         508 MM

 CROSS-CORRELATION BETWEEN COORDINATES
COORDINATE L    AND COORDINATE P  CROSS-CORRELATION = /  -.10/ GREATER THAN     .10

 A POSTERIORI CARTESIAN   COORDINATES
X :       1072435.2523 M   +/-         480 MM
```

TABLE 5.21

Results for baseline 6A-Panmure (combined L1 and L2).

```
Y :      -4361058.9208 M    +/-        498 MM
Z :       4513955.0527 M    +/-        506 MM

 CROSS-CORRELATION BETWEEN COORDINATES
COORDINATE Y    AND COORDINATE X  CROSS-CORRELATION = /  -.12/ GREATER THAN     .10


 BASELINE :    A6  PA
 -------------------

 A-PRIORI      ELLIPSOID BASELINE COMPONENTS
DELTA  LATITUDE : -    0  3 36.97191          +/-
DELTA LONGITUDE : -    0 15 43.18053          +/-
DELTA     HEIGHT :  76.5200                   +/-

 A POSTERIORI ELLIPSOID BASELINE COMPONENTS
DELTA  LATITUDE : -    0  3 36.97955          +/-          4 MM
DELTA LONGITUDE : -    0 15 43.17392          +/-          7 MM
DELTA     HEIGHT :  76.5917                   +/-          4 MM

 CROSS-CORRELATION BETWEEN BASELINE COMPONENTS
BASELINE COMPONENT L  AND BASELINE COMPONENT P  CROSS-CORRELATION = /  -.71/ GREATER THAN     .10
BASELINE COMPONENT H  AND BASELINE COMPONENT P  CROSS-CORRELATION = /  -.59/ GREATER THAN     .10
BASELINE COMPONENT H  AND BASELINE COMPONENT L  CROSS-CORRELATION = /   .49/ GREATER THAN     .10

 A POSTERIORI CARTESIAN BASELINE COMPONENTS
DELTA X :       -18757.6530 M  +/-          7 MM
DELTA Y :        -9625.5054 M  +/-          4 MM
DELTA Z :        -4651.5819 M  +/-          3 MM

 CROSS-CORRELATION BETWEEN BASELINE COMPONENTS
BASELINE COMPONENT Y  AND BASELINE COMPONENT X  CROSS-CORRELATION = /  -.76/ GREATER THAN     .10
BASELINE COMPONENT Z  AND BASELINE COMPONENT X  CROSS-CORRELATION = /  -.33/ GREATER THAN     .10

BASELINE LENGTH =    21590.2088 M  +/-          5 MM
AZIMUTH =  -108 DEGREES
```

TABLE 5.21 *continued*

```
 BASELINE :      STATION : A6 & STATION : ME
 ========================================

 STATION NAME : A6
 -----------------

 A-PRIORI ELLIPSOIDAL COORDINATES
LATITUDE  :     45 23 55.81961          +/-
LONGITUDE : -   75 55 20.63537          +/-
HEIGHT    :   37.1300                   +/-

 A POSTERIORI ELLIPSOIDAL COORDINATES
LATITUDE  :     45 23 55.79290          +/-         508 MM
LONGITUDE : -   75 55 20.78519          +/-         467 MM
HEIGHT    :   37.4873                   +/-         508 MM

 CROSS-CORRELATION BETWEEN COORDINATES
COORDINATE L    AND COORDINATE P  CROSS-CORRELATION = /  -.10/ GREATER THAN     .10

 A POSTERIORI CARTESIAN   COORDINATES
X :       1091192.9053 M    +/-         480 MM
Y :      -4351433.4153 M    +/-         498 MM
Z :       4518606.6346 M    +/-         506 MM

 CROSS-CORRELATION BETWEEN COORDINATES
COORDINATE Y    AND COORDINATE X  CROSS-CORRELATION = /  -.12/ GREATER THAN     .10

 STATION NAME : ME
 -----------------

 A-PRIORI ELLIPSOIDAL COORDINATES
LATITUDE  :     45 14 34.02612          +/-
LONGITUDE : -   75 27 30.61837          +/-
HEIGHT    :   63.3900                   +/-

 A POSTERIORI ELLIPSOIDAL COORDINATES
LATITUDE  :     45 14 34.00912          +/-         509 MM
LONGITUDE : -   75 27 30.75768          +/-         466 MM
HEIGHT    :   63.8063                   +/-         508 MM

 CROSS-CORRELATION BETWEEN COORDINATES
COORDINATE L    AND COORDINATE P  CROSS-CORRELATION = /  -.10/ GREATER THAN     .10

 A POSTERIORI CARTESIAN   COORDINATES
X :       1129489.2167 M    +/-         479 MM
```

TABLE 5.22

Results for baseline 6A-Metcalfe (combined L1 and L2).

```
Y :      -4354410.9532 M    +/-        498 MM
Z :       4506430.6152 M    +/-        507 MM

 CROSS-CORRELATION BETWEEN COORDINATES
COORDINATE Y   AND COORDINATE X  CROSS-CORRELATION = /  -.12/ GREATER THAN     .10


 BASELINE :   A6  ME
 -------------------

 A-PRIORI     ELLIPSOID BASELINE COMPONENTS
DELTA  LATITUDE : -    0  9 21.79349         +/-
DELTA LONGITUDE :      0 27 50.01700         +/-
DELTA    HEIGHT :  26.2600                   +/-

 A POSTERIORI ELLIPSOID BASELINE COMPONENTS
DELTA  LATITUDE : -    0  9 21.78378         +/-          5 MM
DELTA LONGITUDE :      0 27 50.02750         +/-          7 MM
DELTA    HEIGHT :  26.3189                   +/-          5 MM

 CROSS-CORRELATION BETWEEN BASELINE COMPONENTS
BASELINE COMPONENT L  AND BASELINE COMPONENT P  CROSS-CORRELATION = /  -.59/ GREATER THAN     .10
BASELINE COMPONENT H  AND BASELINE COMPONENT P  CROSS-CORRELATION = /  -.62/ GREATER THAN     .10

 A POSTERIORI CARTESIAN BASELINE COMPONENTS
DELTA X :        38296.3114 M  +/-          7 MM
DELTA Y :        -2977.5379 M  +/-          3 MM
DELTA Z :       -12176.0193 M  +/-          3 MM

 CROSS-CORRELATION BETWEEN BASELINE COMPONENTS
BASELINE COMPONENT Y  AND BASELINE COMPONENT X  CROSS-CORRELATION = /  -.69/ GREATER THAN     .10
BASELINE COMPONENT Z  AND BASELINE COMPONENT X  CROSS-CORRELATION = /  -.27/ GREATER THAN     .10
BASELINE COMPONENT Z  AND BASELINE COMPONENT Y  CROSS-CORRELATION = /  -.25/ GREATER THAN     .10

BASELINE LENGTH =    40295.5164 M  +/-          7 MM
AZIMUTH =    115 DEGREES
```

TABLE 5.22 *continued*

```
 BASELINE :     STATION : MO & STATION : PA
 ==========================================

 STATION NAME : MO
 -----------------

 A-PRIORI ELLIPSOIDAL COORDINATES
LATITUDE  :     45 26 34.32643          +/-
LONGITUDE : -   76 15 18.04879          +/-
HEIGHT    :   49.1100                   +/-

 A POSTERIORI ELLIPSOIDAL COORDINATES
LATITUDE  :     45 26 34.29189          +/-        508 MM
LONGITUDE : -   76 15 18.19765          +/-        468 MM
HEIGHT    :   49.6239                   +/-        508 MM

 CROSS-CORRELATION BETWEEN COORDINATES
COORDINATE L    AND COORDINATE P  CROSS-CORRELATION = /  -.10/ GREATER THAN     .10

 A POSTERIORI CARTESIAN   COORDINATES
X :       1065087.5340 M    +/-        480 MM
Y :      -4354317.3867 M    +/-        497 MM
Z :       4522049.8203 M    +/-        506 MM

 CROSS-CORRELATION BETWEEN COORDINATES
COORDINATE Y    AND COORDINATE X  CROSS-CORRELATION = /  -.11/ GREATER THAN     .10

 STATION NAME : PA
 -----------------

 A-PRIORI ELLIPSOIDAL COORDINATES
LATITUDE  :     45 20 18.84770          +/-
LONGITUDE : -   76 11  3.81590          +/-
HEIGHT    :  113.6500                   +/-

 A POSTERIORI ELLIPSOIDAL COORDINATES
LATITUDE  :     45 20 18.81335          +/-        508 MM
LONGITUDE : -   76 11  3.95911          +/-        468 MM
HEIGHT    :  114.0791                   +/-        508 MM

 CROSS-CORRELATION BETWEEN COORDINATES
COORDINATE L    AND COORDINATE P  CROSS-CORRELATION = /  -.10/ GREATER THAN     .10

 A POSTERIORI CARTESIAN   COORDINATES
X :       1072435.2523 M    +/-        480 MM
```

TABLE 5.23

Results for baseline Morris-Panmure (combined L1 and L2).

```
Y :      -4361058.9208 M    +/-        498 MM
Z :       4513955.0527 M    +/-        506 MM

 CROSS-CORRELATION BETWEEN COORDINATES
COORDINATE Y   AND COORDINATE X  CROSS-CORRELATION = /  -.12/ GREATER THAN     .10


 BASELINE :   MO  PA
 ------------------

 A-PRIORI     ELLIPSOID BASELINE COMPONENTS
DELTA  LATITUDE : -    0  6 15.47873         +/-
DELTA LONGITUDE :      0  4 14.23289         +/-
DELTA    HEIGHT :  64.5400                   +/-

 A POSTERIORI ELLIPSOID BASELINE COMPONENTS
DELTA  LATITUDE : -    0  6 15.47854         +/-          4 MM
DELTA LONGITUDE :      0  4 14.23854         +/-          6 MM
DELTA    HEIGHT :  64.4552                   +/-          4 MM

 CROSS-CORRELATION BETWEEN BASELINE COMPONENTS
BASELINE COMPONENT L  AND BASELINE COMPONENT P  CROSS-CORRELATION = /  -.80/ GREATER THAN     .10
BASELINE COMPONENT H  AND BASELINE COMPONENT P  CROSS-CORRELATION = /  -.53/ GREATER THAN     .10
BASELINE COMPONENT H  AND BASELINE COMPONENT L  CROSS-CORRELATION = /   .51/ GREATER THAN     .10

 A POSTERIORI CARTESIAN BASELINE COMPONENTS
DELTA X :         7347.7183 M  +/-          7 MM
DELTA Y :        -6741.5340 M  +/-          4 MM
DELTA Z :        -8094.7676 M  +/-          3 MM

 CROSS-CORRELATION BETWEEN BASELINE COMPONENTS
BASELINE COMPONENT Y  AND BASELINE COMPONENT X  CROSS-CORRELATION = /  -.77/ GREATER THAN     .10
BASELINE COMPONENT Z  AND BASELINE COMPONENT X  CROSS-CORRELATION = /  -.39/ GREATER THAN     .10

BASELINE LENGTH =    12843.7731 M  +/-          6 MM
AZIMUTH =   154 DEGREES
```

TABLE 5.23 *continued*

```
 BASELINE :      STATION : MO & STATION : ME
 ========================================

 STATION NAME : MO
 -----------------

 A-PRIORI ELLIPSOIDAL COORDINATES
LATITUDE  :     45 26 34.32643          +/-
LONGITUDE : -   76 15 18.04879          +/-
HEIGHT    :   49.1100                   +/-

 A POSTERIORI ELLIPSOIDAL COORDINATES
LATITUDE  :     45 26 34.29189          +/-         508 MM
LONGITUDE : -   76 15 18.19765          +/-         468 MM
HEIGHT    :   49.6239                   +/-         508 MM

 CROSS-CORRELATION BETWEEN COORDINATES
COORDINATE L    AND COORDINATE P  CROSS-CORRELATION = /  -.10/ GREATER THAN     .10

 A POSTERIORI CARTESIAN   COORDINATES
X :       1065087.5340 M    +/-         480 MM
Y :      -4354317.3867 M    +/-         497 MM
Z :       4522049.8203 M    +/-         506 MM

 CROSS-CORRELATION BETWEEN COORDINATES
COORDINATE Y    AND COORDINATE X  CROSS-CORRELATION = /  -.11/ GREATER THAN     .10

 STATION NAME : ME
 -----------------

 A-PRIORI ELLIPSOIDAL COORDINATES
LATITUDE  :     45 14 34.02612          +/-
LONGITUDE : -   75 27 30.61837          +/-
HEIGHT    :   63.3900                   +/-

 A POSTERIORI ELLIPSOIDAL COORDINATES
LATITUDE  :     45 14 34.00912          +/-         509 MM
LONGITUDE : -   75 27 30.75768          +/-         466 MM
HEIGHT    :   63.8063                   +/-         508 MM

 CROSS-CORRELATION BETWEEN COORDINATES
COORDINATE L    AND COORDINATE P  CROSS-CORRELATION = /  -.10/ GREATER THAN     .10

 A POSTERIORI CARTESIAN   COORDINATES
X :       1129489.2167 M    +/-         479 MM
```

TABLE 5.24

Results for baseline Morris-Metcalfe (combined L1 and L2).

```
Y :      -4354410.9532 M   +/-        498 MM
Z :       4506430.6152 M   +/-        507 MM

 CROSS-CORRELATION BETWEEN COORDINATES
COORDINATE Y   AND COORDINATE X  CROSS-CORRELATION = /  -.12/ GREATER THAN     .10


 BASELINE :   MO  ME
 -------------------

 A-PRIORI     ELLIPSOID BASELINE COMPONENTS
DELTA  LATITUDE : -    0 12    .30031        +/-
DELTA LONGITUDE :      0 47 47.43042        +/-
DELTA    HEIGHT :  14.2800                  +/-

 A POSTERIORI ELLIPSOID BASELINE COMPONENTS
DELTA  LATITUDE : -    0 12    .28276        +/-          6 MM
DELTA LONGITUDE :      0 47 47.43997        +/-         10 MM
DELTA    HEIGHT :  14.1824                  +/-          7 MM

 CROSS-CORRELATION BETWEEN BASELINE COMPONENTS
BASELINE COMPONENT L  AND BASELINE COMPONENT P  CROSS-CORRELATION = /  -.39/ GREATER THAN     .10
BASELINE COMPONENT H  AND BASELINE COMPONENT P  CROSS-CORRELATION = /  -.74/ GREATER THAN     .10

 A POSTERIORI CARTESIAN BASELINE COMPONENTS
DELTA X :        64401.6827 M  +/-          8 MM
DELTA Y :          -93.5665 M  +/-          4 MM
DELTA Z :       -15619.2050 M  +/-          3 MM

 CROSS-CORRELATION BETWEEN BASELINE COMPONENTS
BASELINE COMPONENT Y  AND BASELINE COMPONENT X  CROSS-CORRELATION = /  -.69/ GREATER THAN     .10
BASELINE COMPONENT Z  AND BASELINE COMPONENT X  CROSS-CORRELATION = /  -.35/ GREATER THAN     .10
BASELINE COMPONENT Z  AND BASELINE COMPONENT Y  CROSS-CORRELATION = /  -.15/ GREATER THAN     .10

BASELINE LENGTH =    66268.7336 M  +/-          8 MM
AZIMUTH =   109 DEGREES
```

TABLE 5.24 *continued*

```
 BASELINE :     STATION : PA & STATION : ME
 ========================================

 STATION NAME : PA
 -----------------

 A-PRIORI ELLIPSOIDAL COORDINATES
LATITUDE  :     45 20 18.84770         +/-
LONGITUDE : -   76 11  3.81590         +/-
HEIGHT    : 113.6500                   +/-

 A POSTERIORI ELLIPSOIDAL COORDINATES
LATITUDE  :     45 20 18.81335         +/-        508 MM
LONGITUDE : -   76 11  3.95911         +/-        468 MM
HEIGHT    : 114.0791                   +/-        508 MM

 CROSS-CORRELATION BETWEEN COORDINATES
COORDINATE L   AND COORDINATE P  CROSS-CORRELATION = /  -.10/ GREATER THAN    .10

 A POSTERIORI CARTESIAN   COORDINATES
X :       1072435.2523 M   +/-        480 MM
Y :      -4361058.9208 M   +/-        498 MM
Z :       4513955.0527 M   +/-        506 MM

 CROSS-CORRELATION BETWEEN COORDINATES
COORDINATE Y   AND COORDINATE X  CROSS-CORRELATION = /  -.12/ GREATER THAN    .10

 STATION NAME : ME
 -----------------

 A-PRIORI ELLIPSOIDAL COORDINATES
LATITUDE  :     45 14 34.02612         +/-
LONGITUDE : -   75 27 30.61837         +/-
HEIGHT    :   63.3900                  +/-

 A POSTERIORI ELLIPSOIDAL COORDINATES
LATITUDE  :     45 14 34.00912         +/-        509 MM
LONGITUDE : -   75 27 30.75768         +/-        466 MM
HEIGHT    :   63.8063                  +/-        508 MM

 CROSS-CORRELATION BETWEEN COORDINATES
COORDINATE L   AND COORDINATE P  CROSS-CORRELATION = /  -.10/ GREATER THAN    .10

 A POSTERIORI CARTESIAN   COORDINATES
X :       1129489.2167 M   +/-        479 MM
```

TABLE 5.25

Results for baseline Panmure-Metcalfe (combined L1 and L2).

```
Y :      -4354410.9532 M    +/-        498 MM
Z :       4506430.6152 M    +/-        507 MM

 CROSS-CORRELATION BETWEEN COORDINATES
COORDINATE Y   AND COORDINATE X  CROSS-CORRELATION = /  -.12/ GREATER THAN     .10


 BASELINE :   PA  ME
 -------------------

 A-PRIORI     ELLIPSOID BASELINE COMPONENTS
DELTA  LATITUDE : -    0  5 44.82158         +/-
DELTA LONGITUDE :      0 43 33.19753         +/-
DELTA    HEIGHT : -50.2600                   +/-

 A POSTERIORI ELLIPSOID BASELINE COMPONENTS
DELTA  LATITUDE : -    0  5 44.80423         +/-          6 MM
DELTA LONGITUDE :      0 43 33.20143         +/-          9 MM
DELTA    HEIGHT : -50.2728                   +/-          6 MM

 CROSS-CORRELATION BETWEEN BASELINE COMPONENTS
BASELINE COMPONENT L  AND BASELINE COMPONENT P  CROSS-CORRELATION = /  -.39/ GREATER THAN     .10
BASELINE COMPONENT H  AND BASELINE COMPONENT P  CROSS-CORRELATION = /  -.77/ GREATER THAN     .10

 A POSTERIORI CARTESIAN BASELINE COMPONENTS
DELTA X :        57053.9644 M  +/-          8 MM
DELTA Y :         6647.9675 M  +/-          4 MM
DELTA Z :        -7524.4374 M  +/-          3 MM

 CROSS-CORRELATION BETWEEN BASELINE COMPONENTS
BASELINE COMPONENT Y  AND BASELINE COMPONENT X  CROSS-CORRELATION = /  -.73/ GREATER THAN     .10
BASELINE COMPONENT Z  AND BASELINE COMPONENT X  CROSS-CORRELATION = /  -.33/ GREATER THAN     .10
BASELINE COMPONENT Z  AND BASELINE COMPONENT Y  CROSS-CORRELATION = /  -.13/ GREATER THAN     .10

BASELINE LENGTH =    57930.7128 M  +/-          7 MM
AZIMUTH =    100 DEGREES
```

TABLE 5.25 *continued*

```
 RELATIVE COVARIANCE MATRIX WRT STATION (CARTESIAN)
  .204
-.245E-01   .220
-.122E-01  -.302E-02   .228
  .204      -.245E-01  -.120E-01   .205
-.244E-01   .220       -.302E-02  -.244E-01   .220
-.124E-01  -.307E-02   .227       -.122E-01  -.307E-02   .227
  .204      -.246E-01  -.123E-01   .205       -.245E-01  -.124E-01   .205
-.245E-01   .220       -.288E-02  -.244E-01   .220       -.293E-02  -.245E-01   .220
-.123E-01  -.314E-02   .227       -.122E-01  -.315E-02   .227       -.124E-01  -.300E-02   .227
  .204      -.247E-01  -.126E-01   .204       -.246E-01  -.127E-01   .204       -.246E-01  -.127E-01   .204
-.247E-01   .220       -.291E-02  -.246E-01   .220       -.296E-02  -.247E-01   .220       -.304E-02  -.248E-01
-.120E-01  -.302E-02   .228       -.119E-01  -.303E-02   .228       -.121E-01  -.289E-02   .228       -.124E-01  -

 RELATIVE COVARIANCE MATRIX WRT STATION (ELLIPSOID)
  .229
-.217E-01   .194
-.143E-02   .367E-02   .229
  .229      -.209E-01  -.159E-02   .229
-.225E-01   .194       .474E-02  -.218E-01   .194
-.113E-02   .274E-02   .229       -.130E-02   .381E-02   .229
  .229      -.211E-01  -.107E-02   .229       -.219E-01  -.787E-03   .229
-.224E-01   .194       .445E-02  -.217E-01   .194       .352E-02   -.219E-01   .194
-.174E-02   .296E-02   .229       -.190E-02   .403E-02   .229       -.140E-02   .374E-02   .229
  .229      -.227E-01  -.723E-03   .229       -.235E-01  -.426E-03   .229       -.235E-01  -.103E-02   .230
-.206E-01   .193       .214E-02  -.198E-01   .193       .121E-02   -.200E-01   .193       .143E-02  -.216E-01
-.232E-02   .499E-02   .229       -.247E-02   .606E-02   .229       -.196E-02   .577E-02   .229       -.163E-02

 DISCREPENCIES ARE STORED IN FILE                    :JUNK1::SF
FINAL XSTAT , PNX , S02 , C ,CE STORED IN FILE :JUNK2::SF
```

TABLE 5.26

Covariance matrices (combined L1 and L2).

```
REFERENCE ELLIPSOID
AE =  6378135.0 ,F-1 =    298.2600 ,XE =       0.000 ,YE =       0.000 ,ZE =       0.000

A POSTERIORI VARIANCE FACTOR :      1.1270

 CROSS-CORRELATION BETWEEN STATION
STATION: MO COORD.: P  AND STATION: A6 COORD.: P  CROSS CORRELATION = /  1.00/ GREATER THAN    .10
STATION: MO COORD.: L  AND STATION: A6 COORD.: P  CROSS CORRELATION = /  -.11/ GREATER THAN    .10
STATION: MO COORD.: L  AND STATION: A6 COORD.: L  CROSS CORRELATION = /  1.00/ GREATER THAN    .10
STATION: MO COORD.: H  AND STATION: A6 COORD.: H  CROSS CORRELATION = /  1.00/ GREATER THAN    .10
STATION: PA COORD.: P  AND STATION: A6 COORD.: P  CROSS CORRELATION = /  1.00/ GREATER THAN    .10
STATION: PA COORD.: P  AND STATION: A6 COORD.: L  CROSS CORRELATION = /  -.10/ GREATER THAN    .10
STATION: PA COORD.: P  AND STATION: MO COORD.: P  CROSS CORRELATION = /  1.00/ GREATER THAN    .10
STATION: PA COORD.: P  AND STATION: MO COORD.: L  CROSS CORRELATION = /  -.10/ GREATER THAN    .10
STATION: PA COORD.: L  AND STATION: A6 COORD.: P  CROSS CORRELATION = /  -.11/ GREATER THAN    .10
STATION: PA COORD.: L  AND STATION: A6 COORD.: L  CROSS CORRELATION = /  1.00/ GREATER THAN    .10
STATION: PA COORD.: L  AND STATION: MO COORD.: P  CROSS CORRELATION = /  -.10/ GREATER THAN    .10
STATION: PA COORD.: L  AND STATION: MO COORD.: L  CROSS CORRELATION = /  1.00/ GREATER THAN    .10
STATION: PA COORD.: H  AND STATION: A6 COORD.: H  CROSS CORRELATION = /  1.00/ GREATER THAN    .10
STATION: PA COORD.: H  AND STATION: MO COORD.: H  CROSS CORRELATION = /  1.00/ GREATER THAN    .10
STATION: ME COORD.: P  AND STATION: A6 COORD.: P  CROSS CORRELATION = /  1.00/ GREATER THAN    .10
STATION: ME COORD.: P  AND STATION: A6 COORD.: L  CROSS CORRELATION = /  -.11/ GREATER THAN    .10
STATION: ME COORD.: P  AND STATION: MO COORD.: P  CROSS CORRELATION = /  1.00/ GREATER THAN    .10
STATION: ME COORD.: P  AND STATION: MO COORD.: L  CROSS CORRELATION = /  -.11/ GREATER THAN    .10
STATION: ME COORD.: P  AND STATION: PA COORD.: P  CROSS CORRELATION = /  1.00/ GREATER THAN    .10
STATION: ME COORD.: P  AND STATION: PA COORD.: L  CROSS CORRELATION = /  -.11/ GREATER THAN    .10
STATION: ME COORD.: L  AND STATION: A6 COORD.: L  CROSS CORRELATION = /  1.00/ GREATER THAN    .10
STATION: ME COORD.: L  AND STATION: MO COORD.: L  CROSS CORRELATION = /  1.00/ GREATER THAN    .10
STATION: ME COORD.: L  AND STATION: PA COORD.: L  CROSS CORRELATION = /  1.00/ GREATER THAN    .10
STATION: ME COORD.: H  AND STATION: A6 COORD.: H  CROSS CORRELATION = /  1.00/ GREATER THAN    .10
STATION: ME COORD.: H  AND STATION: MO COORD.: H  CROSS CORRELATION = /  1.00/ GREATER THAN    .10
STATION: ME COORD.: H  AND STATION: PA COORD.: H  CROSS CORRELATION = /  1.00/ GREATER THAN    .10
```

TABLE 5.26 *continued*

```
 BASELINE :      STATION : A6 & STATION : MO
 ===========================================

 STATION NAME : A6
 -----------------

 A-PRIORI ELLIPSOIDAL COORDINATES
LATITUDE  :     45 23 55.81961          +/-
LONGITUDE : -   75 55 20.63537          +/-
HEIGHT    :   37.1300                   +/-

 A POSTERIORI ELLIPSOIDAL COORDINATES
LATITUDE  :     45 23 55.79565          +/-         794 MM
LONGITUDE : -   75 55 20.78810          +/-         730 MM
HEIGHT    :   40.3775                   +/-         794 MM

 CROSS-CORRELATION BETWEEN COORDINATES
COORDINATE L    AND COORDINATE P  CROSS-CORRELATION = /  -.10/ GREATER THAN     .10

 A POSTERIORI CARTESIAN   COORDINATES
X :       1091193.3229 M   +/-         750 MM
Y :      -4351435.3407 M   +/-         778 MM
Z :       4518608.7518 M   +/-         791 MM

 CROSS-CORRELATION BETWEEN COORDINATES
COORDINATE Y    AND COORDINATE X  CROSS-CORRELATION = /  -.12/ GREATER THAN     .10

 STATION NAME : MO
 -----------------

 A-PRIORI ELLIPSOIDAL COORDINATES
LATITUDE  :     45 26 34.32643          +/-
LONGITUDE : -   76 15 18.04879          +/-
HEIGHT    :   49.1100                   +/-

 A POSTERIORI ELLIPSOIDAL COORDINATES
LATITUDE  :     45 26 34.29410          +/-         793 MM
LONGITUDE : -   76 15 18.19768          +/-         731 MM
HEIGHT    :   52.5531                   +/-         793 MM

 CROSS-CORRELATION BETWEEN COORDINATES
COORDINATE L    AND COORDINATE P  CROSS-CORRELATION = /  -.10/ GREATER THAN     .10

 A POSTERIORI CARTESIAN   COORDINATES
X :       1065088.0099 M   +/-         751 MM
```

TABLE 5.27

Results for baseline 6A-Morris (L1).

```
Y :      -4354319.3358 M    +/-        777 MM
Z :       4522051.9555 M    +/-        791 MM

 CROSS-CORRELATION BETWEEN COORDINATES
COORDINATE Y   AND COORDINATE X  CROSS-CORRELATION = /  -.11/ GREATER THAN     .10


 BASELINE :   A6  M0
 ___________________

 A-PRIORI     ELLIPSOID BASELINE COMPONENTS
DELTA  LATITUDE :      0  2 38.50682          +/-
DELTA LONGITUDE : -    0 19 57.41342          +/-
DELTA    HEIGHT :   11.9800                   +/-

 A POSTERIORI ELLIPSOID BASELINE COMPONENTS
DELTA  LATITUDE :      0  2 38.49846          +/-          5 MM
DELTA LONGITUDE : -    0 19 57.40959          +/-          9 MM
DELTA    HEIGHT :   12.1756                   +/-          6 MM

 CROSS-CORRELATION BETWEEN BASELINE COMPONENTS
BASELINE COMPONENT L  AND BASELINE COMPONENT P  CROSS-CORRELATION = /  -.59/ GREATER THAN     .10
BASELINE COMPONENT H  AND BASELINE COMPONENT P  CROSS-CORRELATION = /  -.63/ GREATER THAN     .10
BASELINE COMPONENT H  AND BASELINE COMPONENT L  CROSS-CORRELATION = /   .23/ GREATER THAN     .10

 A POSTERIORI CARTESIAN BASELINE COMPONENTS
DELTA X :       -26105.3129 M  +/-          9 MM
DELTA Y :        -2883.9951 M  +/-          4 MM
DELTA Z :         3443.2037 M  +/-          3 MM

 CROSS-CORRELATION BETWEEN BASELINE COMPONENTS
BASELINE COMPONENT Y  AND BASELINE COMPONENT X  CROSS-CORRELATION = /  -.69/ GREATER THAN     .10
BASELINE COMPONENT Z  AND BASELINE COMPONENT X  CROSS-CORRELATION = /  -.26/ GREATER THAN     .10
BASELINE COMPONENT Z  AND BASELINE COMPONENT Y  CROSS-CORRELATION = /  -.24/ GREATER THAN     .10

BASELINE LENGTH =    26488.8739 M  +/-          8 MM
AZIMUTH =   -79 DEGREES
```

TABLE 5.27 *continued*

```
 BASELINE :      STATION : A6 & STATION : PA
 ===========================================

 STATION NAME : A6
 -----------------

 A-PRIORI ELLIPSOIDAL COORDINATES
LATITUDE  :     45 23 55.81961          +/-
LONGITUDE : -   75 55 20.63537          +/-
HEIGHT    :   37.1300                   +/-

 A POSTERIORI ELLIPSOIDAL COORDINATES
LATITUDE  :     45 23 55.79565          +/-         794 MM
LONGITUDE : -   75 55 20.78810          +/-         730 MM
HEIGHT    :   40.3775                   +/-         794 MM

 CROSS-CORRELATION BETWEEN COORDINATES
COORDINATE L   AND COORDINATE P  CROSS-CORRELATION = /  -.10/ GREATER THAN     .10

 A POSTERIORI CARTESIAN  COORDINATES
X :       1091193.3229 M   +/-        750 MM
Y :      -4351435.3407 M   +/-        778 MM
Z :       4518608.7518 M   +/-        791 MM

 CROSS-CORRELATION BETWEEN COORDINATES
COORDINATE Y   AND COORDINATE X  CROSS-CORRELATION = /  -.12/ GREATER THAN     .10

 STATION NAME : PA
 -----------------

 A-PRIORI ELLIPSOIDAL COORDINATES
LATITUDE  :     45 20 18.84770          +/-
LONGITUDE : -   76 11  3.81590          +/-
HEIGHT    :  113.6500                   +/-

 A POSTERIORI ELLIPSOIDAL COORDINATES
LATITUDE  :     45 20 18.81561          +/-         794 MM
LONGITUDE : -   76 11  3.96064          +/-         731 MM
HEIGHT    :  117.0397                   +/-         793 MM

 CROSS-CORRELATION BETWEEN COORDINATES
COORDINATE L   AND COORDINATE P  CROSS-CORRELATION = /  -.10/ GREATER THAN     .10

 A POSTERIORI CARTESIAN  COORDINATES
X :       1072435.7051 M   +/-        750 MM
```

TABLE 5.28

Results for baseline 6A-Panmure (L1).

```
Y :      -4361060.9014 M    +/-        778 MM
Z :       4513957.2076 M    +/-        791 MM

 CROSS-CORRELATION BETWEEN COORDINATES
COORDINATE Y    AND COORDINATE X  CROSS-CORRELATION = /  -.12/ GREATER THAN     .10


 BASELINE :    A6  PA
 -------------------

 A-PRIORI      ELLIPSOID BASELINE COMPONENTS
DELTA  LATITUDE : -    0  3 36.97191          +/-
DELTA LONGITUDE : -    0 15 43.18053          +/-
DELTA     HEIGHT :   76.5200                  +/-

 A POSTERIORI ELLIPSOID BASELINE COMPONENTS
DELTA  LATITUDE : -    0  3 36.98003          +/-          7 MM
DELTA LONGITUDE : -    0 15 43.17254          +/-         10 MM
DELTA     HEIGHT :   76.6623                  +/-          7 MM

 CROSS-CORRELATION BETWEEN BASELINE COMPONENTS
BASELINE COMPONENT L  AND BASELINE COMPONENT P  CROSS-CORRELATION = /  -.71/ GREATER THAN     .10
BASELINE COMPONENT H  AND BASELINE COMPONENT P  CROSS-CORRELATION = /  -.59/ GREATER THAN     .10
BASELINE COMPONENT H  AND BASELINE COMPONENT L  CROSS-CORRELATION = /   .49/ GREATER THAN     .10

 A POSTERIORI CARTESIAN BASELINE COMPONENTS
DELTA X :       -18757.6178 M  +/-         11 MM
DELTA Y :        -9625.5607 M  +/-          6 MM
DELTA Z :        -4651.5442 M  +/-          4 MM

 CROSS-CORRELATION BETWEEN BASELINE COMPONENTS
BASELINE COMPONENT Y  AND BASELINE COMPONENT X  CROSS-CORRELATION = /  -.76/ GREATER THAN     .10
BASELINE COMPONENT Z  AND BASELINE COMPONENT X  CROSS-CORRELATION = /  -.33/ GREATER THAN     .10

BASELINE LENGTH =    21590.1947 M  +/-          7 MM
AZIMUTH =  -108 DEGREES
```

TABLE 5.28 *continued*

```
 BASELINE :      STATION : A6 & STATION : ME
 ========================================

 STATION NAME : A6
 -----------------

 A-PRIORI ELLIPSOIDAL COORDINATES
LATITUDE  :     45 23 55.81961          +/-
LONGITUDE : -   75 55 20.63537          +/-
HEIGHT    :   37.1300                   +/-

 A POSTERIORI ELLIPSOIDAL COORDINATES
LATITUDE  :     45 23 55.79565          +/-         794 MM
LONGITUDE : -   75 55 20.78810          +/-         730 MM
HEIGHT    :   40.3775                   +/-         794 MM

 CROSS-CORRELATION BETWEEN COORDINATES
COORDINATE L   AND COORDINATE P  CROSS-CORRELATION = /  -.10/ GREATER THAN     .10

 A POSTERIORI CARTESIAN   COORDINATES
X :       1091193.3229 M   +/-         750 MM
Y :      -4351435.3407 M   +/-         778 MM
Z :       4518608.7518 M   +/-         791 MM

 CROSS-CORRELATION BETWEEN COORDINATES
COORDINATE Y   AND COORDINATE X  CROSS-CORRELATION = /  -.12/ GREATER THAN     .10

 STATION NAME : ME
 -----------------

 A-PRIORI ELLIPSOIDAL COORDINATES
LATITUDE  :     45 14 34.02612          +/-
LONGITUDE : -   75 27 30.61837          +/-
HEIGHT    :   63.3900                   +/-

 A POSTERIORI ELLIPSOIDAL COORDINATES
LATITUDE  :     45 14 34.01034          +/-         795 MM
LONGITUDE : -   75 27 30.76095          +/-         728 MM
HEIGHT    :   66.7749                   +/-         794 MM

 CROSS-CORRELATION BETWEEN COORDINATES
COORDINATE L   AND COORDINATE P  CROSS-CORRELATION = /  -.10/ GREATER THAN     .10

 A POSTERIORI CARTESIAN   COORDINATES
X :       1129489.6658 M   +/-         749 MM
```

TABLE 5.29

Results for baseline 6A-Metcalfe (Ll).

```
Y :      -4354412.9686 M    +/-        778 MM
Z :       4506432.7497 M    +/-        792 MM

 CROSS-CORRELATION BETWEEN COORDINATES
COORDINATE Y   AND COORDINATE X  CROSS-CORRELATION = /  -.12/ GREATER THAN     .10


 BASELINE :   A6  ME
 -------------------

 A-PRIORI     ELLIPSOID BASELINE COMPONENTS
DELTA  LATITUDE : -    0  9 21.79349         +/-
DELTA LONGITUDE :      0 27 50.01700         +/-
DELTA    HEIGHT :  26.2600                   +/-

 A POSTERIORI ELLIPSOID BASELINE COMPONENTS
DELTA  LATITUDE : -    0  9 21.78531         +/-          7 MM
DELTA LONGITUDE :      0 27 50.02715         +/-         11 MM
DELTA    HEIGHT :  26.3974                   +/-          8 MM

 CROSS-CORRELATION BETWEEN BASELINE COMPONENTS
BASELINE COMPONENT L  AND BASELINE COMPONENT P  CROSS-CORRELATION = /  -.59/ GREATER THAN     .10
BASELINE COMPONENT H  AND BASELINE COMPONENT P  CROSS-CORRELATION = /  -.62/ GREATER THAN     .10

 A POSTERIORI CARTESIAN BASELINE COMPONENTS
DELTA X :        38296.3430 M  +/-         11 MM
DELTA Y :        -2977.6279 M  +/-          5 MM
DELTA Z :       -12176.0021 M  +/-          4 MM

 CROSS-CORRELATION BETWEEN BASELINE COMPONENTS
BASELINE COMPONENT Y  AND BASELINE COMPONENT X  CROSS-CORRELATION = /  -.69/ GREATER THAN     .10
BASELINE COMPONENT Z  AND BASELINE COMPONENT X  CROSS-CORRELATION = /  -.27/ GREATER THAN     .10
BASELINE COMPONENT Z  AND BASELINE COMPONENT Y  CROSS-CORRELATION = /  -.25/ GREATER THAN     .10

BASELINE LENGTH =    40295.5479 M  +/-         11 MM
AZIMUTH =   115 DEGREES
```

TABLE 5.29 *continued*

```
 BASELINE :     STATION : MO & STATION : PA
 ===========================================

 STATION NAME : MO
 -----------------

 A-PRIORI ELLIPSOIDAL COORDINATES
LATITUDE  :     45 26 34.32643          +/-
LONGITUDE : -   76 15 18.04879          +/-
HEIGHT    :   49.1100                   +/-

 A POSTERIORI ELLIPSOIDAL COORDINATES
LATITUDE  :     45 26 34.29410          +/-        793 MM
LONGITUDE : -   76 15 18.19768          +/-        731 MM
HEIGHT    :   52.5531                   +/-        793 MM

 CROSS-CORRELATION BETWEEN COORDINATES
COORDINATE L   AND COORDINATE P  CROSS-CORRELATION = /  -.10/ GREATER THAN     .10

 A POSTERIORI CARTESIAN   COORDINATES
X :       1065088.0099 M   +/-        751 MM
Y :      -4354319.3358 M   +/-        777 MM
Z :       4522051.9555 M   +/-        791 MM

 CROSS-CORRELATION BETWEEN COORDINATES
COORDINATE Y   AND COORDINATE X  CROSS-CORRELATION = /  -.11/ GREATER THAN     .10

 STATION NAME : PA
 -----------------

 A-PRIORI ELLIPSOIDAL COORDINATES
LATITUDE  :     45 20 18.84770          +/-
LONGITUDE : -   76 11  3.81590          +/-
HEIGHT    : 113.6500                    +/-

 A POSTERIORI ELLIPSOIDAL COORDINATES
LATITUDE  :     45 20 18.81561          +/-        794 MM
LONGITUDE : -   76 11  3.96064          +/-        731 MM
HEIGHT    : 117.0397                    +/-        793 MM

 CROSS-CORRELATION BETWEEN COORDINATES
COORDINATE L   AND COORDINATE P  CROSS-CORRELATION = /  -.10/ GREATER THAN     .10

 A POSTERIORI CARTESIAN   COORDINATES
X :       1072435.7051 M   +/-        750 MM
```

TABLE 5.30

Results for baseline Morris-Panmure (L1).

```
Y :      -4361060.9014 M    +/-        778 MM
Z :       4513957.2076 M    +/-        791 MM

 CROSS-CORRELATION BETWEEN COORDINATES
COORDINATE Y    AND COORDINATE X  CROSS-CORRELATION = /  -.12/ GREATER THAN     .10


 BASELINE :    MO  PA
 -------------------

 A-PRIORI      ELLIPSOID BASELINE COMPONENTS
DELTA  LATITUDE : -    0  6 15.47873         +/-
DELTA LONGITUDE :      0  4 14.23289         +/-
DELTA     HEIGHT :  64.5400                  +/-

 A POSTERIORI ELLIPSOID BASELINE COMPONENTS
DELTA  LATITUDE : -    0  6 15.47849         +/-          7 MM
DELTA LONGITUDE :      0  4 14.23705         +/-          9 MM
DELTA     HEIGHT :  64.4866                  +/-          6 MM

 CROSS-CORRELATION BETWEEN BASELINE COMPONENTS
BASELINE COMPONENT L  AND BASELINE COMPONENT P  CROSS-CORRELATION = /  -.88/ GREATER THAN     .10
BASELINE COMPONENT H  AND BASELINE COMPONENT P  CROSS-CORRELATION = /  -.53/ GREATER THAN     .10
BASELINE COMPONENT H  AND BASELINE COMPONENT L  CROSS-CORRELATION = /   .51/ GREATER THAN     .10

 A POSTERIORI CARTESIAN BASELINE COMPONENTS
DELTA X :         7347.6951 M  +/-         11 MM
DELTA Y :        -6741.5655 M  +/-          6 MM
DELTA Z :        -8094.7479 M  +/-          4 MM

 CROSS-CORRELATION BETWEEN BASELINE COMPONENTS
BASELINE COMPONENT Y  AND BASELINE COMPONENT X  CROSS-CORRELATION = /  -.77/ GREATER THAN     .10
BASELINE COMPONENT Z  AND BASELINE COMPONENT X  CROSS-CORRELATION = /  -.39/ GREATER THAN     .10

BASELINE LENGTH =    12843.7640 M  +/-         10 MM
AZIMUTH =   154 DEGREES
```

TABLE 5.30 *continued*

```
 BASELINE :      STATION : MO & STATION : ME
 ===========================================

 STATION NAME : MO
 -----------------

 A-PRIORI ELLIPSOIDAL COORDINATES
LATITUDE  :     45 26 34.32643          +/-
LONGITUDE : -   76 15 18.04879          +/-
HEIGHT    :   49.1100                   +/-

 A POSTERIORI ELLIPSOIDAL COORDINATES
LATITUDE  :     45 26 34.29410          +/-         793 MM
LONGITUDE : -   76 15 18.19768          +/-         731 MM
HEIGHT    :   52.5531                   +/-         793 MM

 CROSS-CORRELATION BETWEEN COORDINATES
COORDINATE L   AND COORDINATE P  CROSS-CORRELATION = /  -.10/ GREATER THAN     .10

 A POSTERIORI CARTESIAN   COORDINATES
X :       1065088.0099 M   +/-         751 MM
Y :      -4354319.3358 M   +/-         777 MM
Z :       4522051.9555 M   +/-         791 MM

 CROSS-CORRELATION BETWEEN COORDINATES
COORDINATE Y   AND COORDINATE X  CROSS-CORRELATION = /  -.11/ GREATER THAN     .10

 STATION NAME : ME
 -----------------

 A-PRIORI ELLIPSOIDAL COORDINATES
LATITUDE  :     45 14 34.02612          +/-
LONGITUDE : -   75 27 30.61837          +/-
HEIGHT    :   63.3900                   +/-

 A POSTERIORI ELLIPSOIDAL COORDINATES
LATITUDE  :     45 14 34.01034          +/-         795 MM
LONGITUDE : -   75 27 30.76095          +/-         728 MM
HEIGHT    :   66.7749                   +/-         794 MM

 CROSS-CORRELATION BETWEEN COORDINATES
COORDINATE L   AND COORDINATE P  CROSS-CORRELATION = /  -.10/ GREATER THAN     .10

 A POSTERIORI CARTESIAN   COORDINATES
X :       1129489.6658 M   +/-         749 MM
```

TABLE 5.31

Results for baseline Morris-Metcalfe (L1).

```
Y :      -4354412.9686 M    +/-        778 MM
Z :       4506432.7497 M    +/-        792 MM

 CROSS-CORRELATION BETWEEN COORDINATES
COORDINATE Y   AND COORDINATE X  CROSS-CORRELATION = /  -.12/ GREATER THAN     .10


 BASELINE :   MO  ME
 ------------------

 A-PRIORI     ELLIPSOID BASELINE COMPONENTS
DELTA  LATITUDE : -   0 12   .30031         +/-
DELTA LONGITUDE :     0 47 47.43042         +/-
DELTA    HEIGHT :  14.2800                  +/-

 A POSTERIORI ELLIPSOID BASELINE COMPONENTS
DELTA  LATITUDE : -   0 12   .28377         +/-         10 MM
DELTA LONGITUDE :     0 47 47.43674         +/-         15 MM
DELTA    HEIGHT :  14.2218                  +/-         11 MM

 CROSS-CORRELATION BETWEEN BASELINE COMPONENTS
BASELINE COMPONENT L  AND BASELINE COMPONENT P  CROSS-CORRELATION = /  -.39/ GREATER THAN     .10
BASELINE COMPONENT H  AND BASELINE COMPONENT P  CROSS-CORRELATION = /  -.74/ GREATER THAN     .10

 A POSTERIORI CARTESIAN BASELINE COMPONENTS
DELTA X :        64401.6559 M  +/-        12 MM
DELTA Y :          -93.6327 M  +/-         6 MM
DELTA Z :       -15619.2058 M  +/-         4 MM

 CROSS-CORRELATION BETWEEN BASELINE COMPONENTS
BASELINE COMPONENT Y  AND BASELINE COMPONENT X  CROSS-CORRELATION = /  -.69/ GREATER THAN     .10
BASELINE COMPONENT Z  AND BASELINE COMPONENT X  CROSS-CORRELATION = /  -.35/ GREATER THAN     .10
BASELINE COMPONENT Z  AND BASELINE COMPONENT Y  CROSS-CORRELATION = /  -.15/ GREATER THAN     .10

BASELINE LENGTH =    66268.7078 M  +/-        12 MM
AZIMUTH =   109 DEGREES
```

TABLE 5.31 *continued*

```
 BASELINE :     STATION : PA & STATION : ME
 ==========================================

 STATION NAME : PA
 -----------------

 A-PRIORI ELLIPSOIDAL COORDINATES
LATITUDE  :     45 20 18.84770          +/-
LONGITUDE : -   76 11  3.81590          +/-
HEIGHT    : 113.6500                    +/-

 A POSTERIORI ELLIPSOIDAL COORDINATES
LATITUDE  :     45 20 18.81561          +/-        794 MM
LONGITUDE : -   76 11  3.96064          +/-        731 MM
HEIGHT    : 117.0397                    +/-        793 MM

 CROSS-CORRELATION BETWEEN COORDINATES
COORDINATE L   AND COORDINATE P  CROSS-CORRELATION = /  -.10/ GREATER THAN    .10

 A POSTERIORI CARTESIAN   COORDINATES
X :       1072435.7051 M   +/-        750 MM
Y :      -4361060.9014 M   +/-        778 MM
Z :       4513957.2076 M   +/-        791 MM

 CROSS-CORRELATION BETWEEN COORDINATES
COORDINATE Y   AND COORDINATE X  CROSS-CORRELATION = /  -.12/ GREATER THAN    .10

 STATION NAME : ME
 -----------------

 A-PRIORI ELLIPSOIDAL COORDINATES
LATITUDE  :     45 14 34.02612          +/-
LONGITUDE : -   75 27 30.61837          +/-
HEIGHT    :   63.3900                   +/-

 A POSTERIORI ELLIPSOIDAL COORDINATES
LATITUDE  :     45 14 34.01034          +/-        795 MM
LONGITUDE : -   75 27 30.76095          +/-        728 MM
HEIGHT    :   66.7749                   +/-        794 MM

 CROSS-CORRELATION BETWEEN COORDINATES
COORDINATE L   AND COORDINATE P  CROSS-CORRELATION = /  -.10/ GREATER THAN    .10

 A POSTERIORI CARTESIAN   COORDINATES
X :       1129489.6658 M   +/-        749 MM
```

TABLE 5.32

Results for baseline Panmure-Metcalfe (L1).

```
Y :      -4354412.9686 M    +/-        778 MM
Z :       4506432.7497 M    +/-        792 MM

 CROSS-CORRELATION BETWEEN COORDINATES
COORDINATE Y    AND COORDINATE X  CROSS-CORRELATION = /  -.12/ GREATER THAN     .10


 BASELINE :    PA  ME
 --------------------

 A-PRIORI      ELLIPSOID BASELINE COMPONENTS
DELTA  LATITUDE : -    0  5 44.82158         +/-
DELTA LONGITUDE :      0 43 33.19753         +/-
DELTA     HEIGHT : -50.2600                  +/-

 A POSTERIORI ELLIPSOID BASELINE COMPONENTS
DELTA  LATITUDE : -    0  5 44.80527         +/-          9 MM
DELTA LONGITUDE :      0 43 33.19969         +/-         15 MM
DELTA     HEIGHT : -50.2649                  +/-         10 MM

 CROSS-CORRELATION BETWEEN BASELINE COMPONENTS
BASELINE COMPONENT L.  AND BASELINE COMPONENT P  CROSS-CORRELATION = /  -.39/ GREATER THAN     .10
BASELINE COMPONENT H   AND BASELINE COMPONENT P  CROSS-CORRELATION = /  -.77/ GREATER THAN     .10

 A POSTERIORI CARTESIAN BASELINE COMPONENTS
DELTA X :         57053.9607 M  +/-         12 MM
DELTA Y :          6647.9328 M  +/-          6 MM
DELTA Z :         -7524.4579 M  +/-          4 MM

 CROSS-CORRELATION BETWEEN BASELINE COMPONENTS
BASELINE COMPONENT Y  AND BASELINE COMPONENT X  CROSS-CORRELATION = /  -.73/ GREATER THAN     .10
BASELINE COMPONENT Z  AND BASELINE COMPONENT X  CROSS-CORRELATION = /  -.33/ GREATER THAN     .10
BASELINE COMPONENT Z  AND BASELINE COMPONENT Y  CROSS-CORRELATION = /  -.13/ GREATER THAN     .10

BASELINE LENGTH =     57930.7079 M  +/-         12 MM
AZIMUTH =    100 DEGREES
```

TABLE 5.32 *continued*

```
 RELATIVE COVARIANCE MATRIX WRT STATION (CARTESIAN)
  .204
-.245E-01   .220
-.122E-01  -.302E-02   .228
  .204      -.245E-01  -.120E-01   .205
-.244E-01   .220       -.302E-02  -.244E-01   .220
-.124E-01  -.307E-02   .227       -.122E-01  -.307E-02   .227
  .204      -.246E-01  -.123E-01   .205       -.245E-01  -.124E-01   .205
-.245E-01   .220       -.288E-02  -.244E-01   .220       -.293E-02  -.245E-01   .220
-.123E-01  -.314E-02   .227       -.122E-01  -.315E-02   .227       -.124E-01  -.300E-02   .227
  .204      -.247E-01  -.126E-01   .204       -.246E-01  -.127E-01   .204       -.246E-01  -.127E-01   .204
-.247E-01   .220       -.291E-02  -.246E-01   .220       -.296E-02  -.247E-01   .220       -.304E-02  -.248E-01   .22
-.120E-01  -.302E-02   .228       -.119E-01  -.303E-02   .228       -.121E-01  -.289E-02   .228       -.124E-01  -.29

 RELATIVE COVARIANCE MATRIX WRT STATION (ELLIPSOID)
  .229
-.217E-01   .194
-.143E-02   .367E-02   .229
  .229      -.209E-01  -.159E-02   .229
-.225E-01   .194       .474E-02  -.218E-01   .194
-.113E-02   .274E-02   .229       -.130E-02   .381E-02   .229
  .229      -.211E-01  -.107E-02   .229       -.219E-01  -.787E-03   .229
-.224E-01   .194       .445E-02  -.217E-01   .194       .352E-02  -.219E-01   .194
-.174E-02   .296E-02   .229       -.190E-02   .403E-02   .229       -.140E-02   .374E-02   .229
  .229      -.227E-01  -.723E-03   .229       -.235E-01  -.426E-03   .229       -.235E-01  -.103E-02   .230
-.206E-01   .193       .214E-02  -.198E-01   .193       .121E-02  -.200E-01   .193       .143E-02  -.216E-01   .19
-.232E-02   .499E-02   .229       -.247E-02   .606E-02   .229       -.196E-02   .577E-02   .229       -.163E-02   .34

 DISCREPENCIES ARE STORED IN FILE                    :JUNK1::SF
FINAL XSTAT , PNX , S02 , C ,CE STORED IN FILE :JUNK2::SF
```

TABLE 5.33

Covariance matrices (L1).

```
 REFERENCE ELLIPSOID
 AE =  6378135.0 ,F-1 =   298.2600 ,XE =       0.000 ,YE =       0.000 ,ZE =       0.000

 A POSTERIORI VARIANCE FACTOR :     2.7529

 CROSS-CORRELATION BETWEEN STATION
STATION: MO COORD.: P  AND STATION: A6 COORD.: P  CROSS CORRELATION = /  1.00/ GREATER THAN    .10
STATION: MO COORD.: L  AND STATION: A6 COORD.: P  CROSS CORRELATION = /  -.11/ GREATER THAN    .10
STATION: MO COORD.: L  AND STATION: A6 COORD.: L  CROSS CORRELATION = /  1.00/ GREATER THAN    .10
STATION: MO COORD.: H  AND STATION: A6 COORD.: H  CROSS CORRELATION = /  1.00/ GREATER THAN    .10
STATION: PA COORD.: P  AND STATION: A6 COORD.: P  CROSS CORRELATION = /  1.00/ GREATER THAN    .10
STATION: PA COORD.: P  AND STATION: A6 COORD.: L  CROSS CORRELATION = /  -.10/ GREATER THAN    .10
STATION: PA COORD.: P  AND STATION: MO COORD.: P  CROSS CORRELATION = /  1.00/ GREATER THAN    .10
STATION: PA COORD.: P  AND STATION: MO COORD.: L  CROSS CORRELATION = /  -.10/ GREATER THAN    .10
STATION: PA COORD.: L  AND STATION: A6 COORD.: P  CROSS CORRELATION = /  -.11/ GREATER THAN    .10
STATION: PA COORD.: L  AND STATION: A6 COORD.: L  CROSS CORRELATION = /  1.00/ GREATER THAN    .10
STATION: PA COORD.: L  AND STATION: MO COORD.: P  CROSS CORRELATION = /  -.10/ GREATER THAN    .10
STATION: PA COORD.: L  AND STATION: MO COORD.: L  CROSS CORRELATION = /  1.00/ GREATER THAN    .10
STATION: PA COORD.: H  AND STATION: A6 COORD.: H  CROSS CORRELATION = /  1.00/ GREATER THAN    .10
STATION: PA COORD.: H  AND STATION: MO COORD.: H  CROSS CORRELATION = /  1.00/ GREATER THAN    .10
STATION: ME COORD.: P  AND STATION: A6 COORD.: P  CROSS CORRELATION = /  1.00/ GREATER THAN    .10
STATION: ME COORD.: P  AND STATION: A6 COORD.: L  CROSS CORRELATION = /  -.11/ GREATER THAN    .10
STATION: ME COORD.: P  AND STATION: MO COORD.: P  CROSS CORRELATION = /  1.00/ GREATER THAN    .10
STATION: ME COORD.: P  AND STATION: MO COORD.: L  CROSS CORRELATION = /  -.11/ GREATER THAN    .10
STATION: ME COORD.: P  AND STATION: PA COORD.: P  CROSS CORRELATION = /  1.00/ GREATER THAN    .10
STATION: ME COORD.: P  AND STATION: PA COORD.: L  CROSS CORRELATION = /  -.11/ GREATER THAN    .10
STATION: ME COORD.: L  AND STATION: A6 COORD.: L  CROSS CORRELATION = /  1.00/ GREATER THAN    .10
STATION: ME COORD.: L  AND STATION: MO COORD.: L  CROSS CORRELATION = /  1.00/ GREATER THAN    .10
STATION: ME COORD.: L  AND STATION: PA COORD.: L  CROSS CORRELATION = /  1.00/ GREATER THAN    .10
STATION: ME COORD.: H  AND STATION: A6 COORD.: H  CROSS CORRELATION = /  1.00/ GREATER THAN    .10
STATION: ME COORD.: H  AND STATION: MO COORD.: H  CROSS CORRELATION = /  1.00/ GREATER THAN    .10
STATION: ME COORD.: H  AND STATION: PA COORD.: H  CROSS CORRELATION = /  1.00/ GREATER THAN    .10
```

TABLE 5.33 *continued*

TABLE 5.34

Comparison of baseline lengths from the L1, L2 combination, and the L1 only.

Baseline	Length using combined L1 and L2 (m)	Length using L1 only (m)	Difference (ppm)
6A - Mo	26 488.926	26 488.874	+ 2.0
6A - Pa	21 590.209	21 590.195	+ 0.6
6A - Me	40 295.516	40 295.548	- 0.8
Mo - Pa	12 843.773	12 843.764	+ 0.7
Mo - Me	66 268.734	66 268.708	+ 0.4
Pa - Me	57 930.713	57 930.708	+ 0.1

The differences between the combined L1, L2 solution and the L1 only solution for the baseline lengths are at the ppm level. As can be seen from Table 5.35, the combined solution agrees better with the Macrometer V-1000 solution

5.4 Comparisons

This section compares the results of the Macrometer™ V-1000 and the Texas Instruments TI-4100 Ottawa campaigns with the "ground truth" provided by the Geodetic Survey of Canada (see section 5.2). The discrepancies in height differences and lengths between these "ground truth" values and the estimated values for all six baselines are listed in Table 5.35.

All baselines connected to station Morris show height discrepancies of some 150 mm between "ground truth" and the GPS solutions. It seems remarkable that the baseline height differences between the Macrometer™ and TI-4100 solutions agree on the 5 cm level (see also Figures 5.18 through 5.20).

The baseline lengths agree best between the Macrometer™ solutions and "ground truth." With the exception of the 12 km baseline, Panmure-Morris, the discrepancies are on the 1 ppm level. The disagreement between the TI-4100 solution and "ground truth" seems to be slightly worse. The agreement between the TI-4100 solution and the V-1000 solution is at the 1 ppm level with the exception of the 26 km baseline 6A-Morris. For further comparisons of the DIPOP results, see Kleusberg et al. [1985].

The discrepancies in horizontal and vertical coordinates are shown in Figures 5.18 through 5.20. For a general explanation of the figures, see section 5.1.

TABLE 5.35

Baseline discrepancies between "ground truth," V-1000 results and TI-4100 results.

		6A-Mo	6A-Pa	6A-Me	Mo-Pa	Mo-Me	Pa-Me
"Ground truth" - TI-4100	Δh(mm)	-157	-72	- 59	+ 85	+ 98	-13
	Δℓ(mm)	+ 59	+59	- 83	- 48	- 27	+ 4
	Δℓ(ppm)	+ 2.2	+ 2.7	- 2.1	- 3.8	- 0.4	+ 0.1
"Ground truth" - V-1000	Δh(mm)	-170	-55	- 29	+115	+141	-26
	Δℓ(mm)	- 20	+33	- 21	- 48	- 45	+16
	Δℓ(ppm)	- 0.8	+ 1.5	- 0.5	- 3.8	- 0.7	+ 0.3
V-1000 - TI-4100	Δh(mm)	+ 13	-17	- 30	- 30	- 43	+13
	Δℓ(mm)	+ 79	+26	- 62	0	+ 18	-12
	Δℓ(ppm)	+ 3.0	+ 1.2	- 1.5	0.0	+ 0.3	- 0.2
V-1000 - TI-4100 (L1)	Δh(mm)	- 25	-93	-108	- 62	- 83	+21
	Δℓ(mm)	+132	+40	- 94	+ 9	+ 44	- 7
	Δℓ(ppm)	+ 5.0	+ 1.9	- 2.3	+ 0.8	+ 0.7	- 0.1

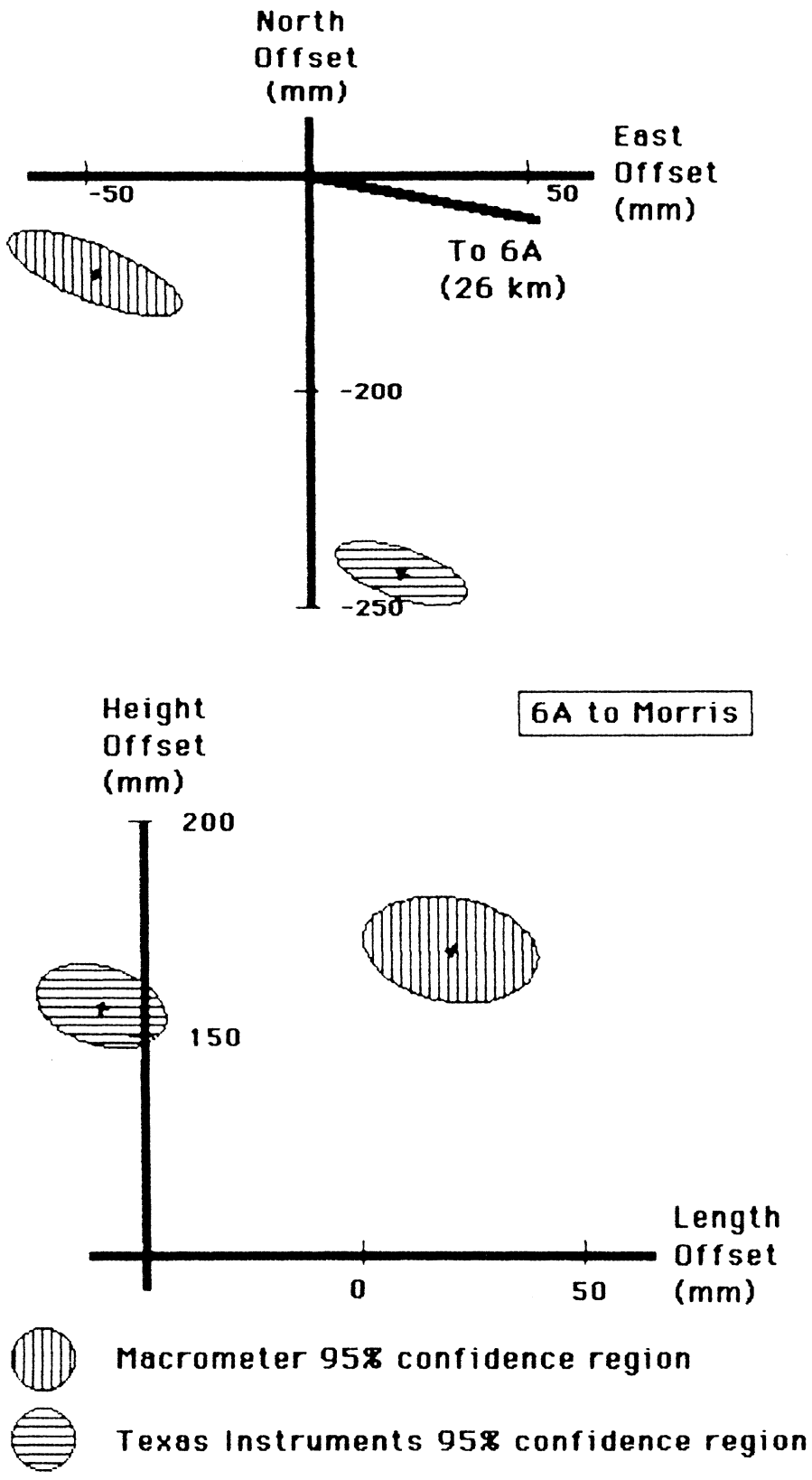

FIGURE 5.18

Intercomparison of Macrometer™, TI-4100, and "ground truth" by baselines: 6A to Morris.

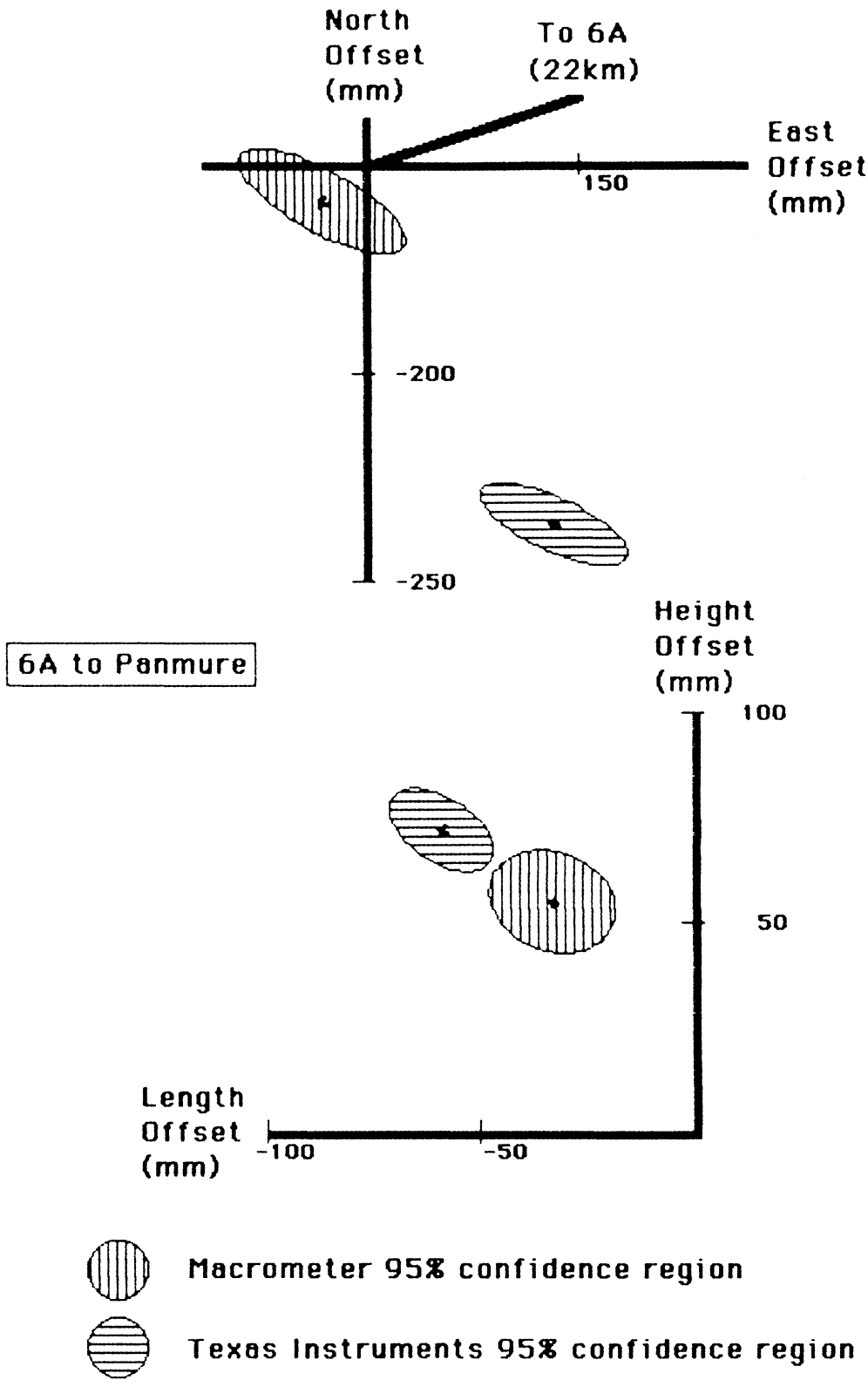

FIGURE 5.19

Intercomparison of Macrometer™, TI-4100, and "ground truth" by baselines: 6A to Panmure.

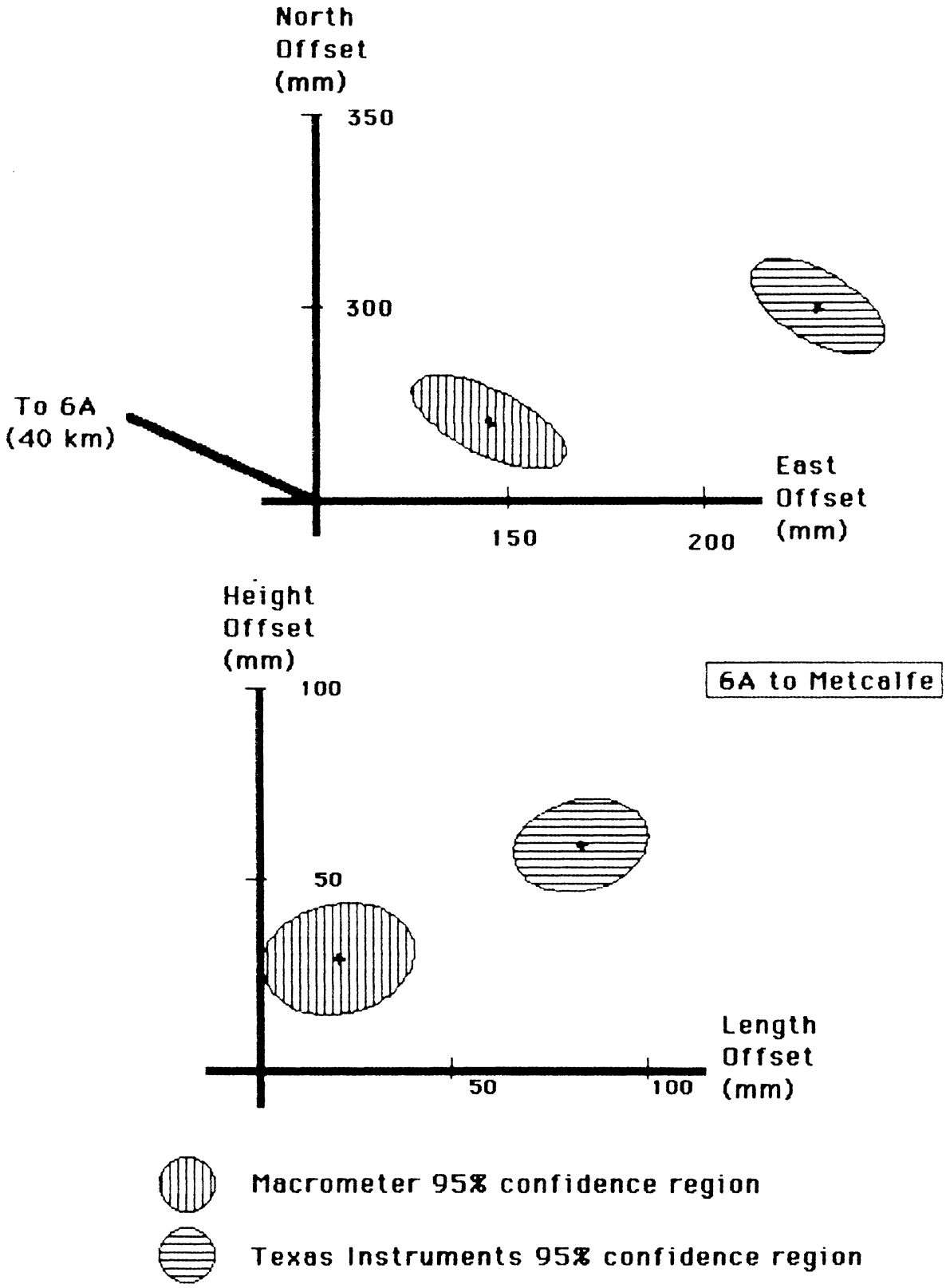

FIGURE 5.20

Intercomparison of Macrometer™, TI-4100, and "ground truth" by baselines: 6A to Metcalfe.

6. CONCLUSIONS AND RECOMMENDATIONS

In this report we have documented the development of a new interactive software package DIPOP for processing GPS differential observations. A very flexible program architecture was adopted in order that the software could be used with different types of data from different types of receivers. The software has been tested on double differences from Macrometer™ V-1000 and TI-4100 receivers. Other observables from the same or different types of receivers can be added. The point positions and specified nuisance parameters are estimated in a phased adjustment that takes into account a priori weights. This package has been tested with data from one Macrometer™ V-1000 campaign and one TI-4100 campaign. DIPOP yields baseline vectors identical (differences of less than 1 mm) to those obtained using the programs PRMAC3 and PRMNET dedicated to the Macrometer™ when the same a priori coordinates and a priori weights were used.

We compared our GPS results with the "ground truth" values of the baseline components and we have inter-compared the results from processing Macrometer™ and TI data obtained for the same network. We conclude, once more, that the GPS results agree with the "ground truth" values to about 1 or 2 ppm, and that the two types of receivers yield results that also agree with each other at about the 1 or 2 ppm level.

In association with the development of the new software, we have undertaken some studies concerning the temporal and spatial correlations in the observations, the degree of completeness of the satellite force model required to achieve a certain accuracy in the baseline vector, and the problem of ambiguities inherent in GPS carrier phase measurements.

We feel we have come up with a solution for the orbit modelling satisfactory for baselines up to about 100 km. Orbit improvement for long baselines by means of bias elimination has not yet been tested due to constraints of our present HP 1000 operating system. We will implement the orbit determination component of DIPOP when the RTE-VI operating system is installed. This installation is imminent. Modelling of physical correlations between observations also remains a problem. However, we have taken the first step towards the solution by having formulated a strategy which now remains to be tried on actual observations. We have implemented

an algorithm for ambiguity determination (and elimination) which seems to perform well. It now has to be tested against the other possible approaches.

The software we have developed, although intended for future production work in processing GPS data, is an ideal tool for further investigating many different aspects of GPS positioning. We forsee the possibility of using DIPOP to conduct:

(i) a study of the optimum length of observation series and the optimum data sampling rate;

(ii) a study of the correlations and cross-correlations between GPS observation series with the aim of constructing an appropriate covariance model and an analytical expression for evaluating the weight matrix of the observables;

(iii) a study to determine how often should nuisance parameters be updated during the data processing;

(iv) a comparison of the efficiency and accuracy of actual singly, doubly, and triply differenced phase observations;

(v) an estimation of satellite orbit biases from long baseline observations;

(vi) a study of positioning accuracy at latitudes above 55° where there are no overhead passes.

There is also more work that could be done on the DIPOP program itself. Besides the implementation of the orbital bias elimination mentioned in section 3.4.2, and the completion of the postprocessor (cf. section 3.5), we think that at least the following two features should be considered for realization:

(i) implementation of the Choleski root algorithm in the nuisance parameter elimination;

(ii) development of microcomputer software for the program front-end control, postprocessing and, perhaps, even for some field preprocessing of observations.

An additional item that should be given serious attention is the optimum observing strategy (cf. section 2.2 and Appendix A).

7. REFERENCES

Abdullah, K.A. (1984). "Ionospheric correction of single frequency GPS data using electron content derived from simultaneous Transit observations." M.Eng. Report, Department of Surveying Engineering, University of New Brunswick, Fredericton, N.B.

Anderle, R.J. (1984). "Prospects for Global Positioning System." Paper presented at the AGU Spring Meeting, Cincinnati, OH, May.

Bauersima, I. (1983). "NAVSTAR/Global Positioning System (GPS) III." Mitteilungen der Satelliten-beobachtungstation Zimmerwals, Nr. 12, Universitaet Bern, Switzerland.

Bendat, J.S. and A.G. Piersol (1971). Random Data: Analysis and Measurement Procedures. Wiley Interscience.

Beutler, G. (1982). "Loesung von Parameterbestimmungsproblemen in Himmelsmechanik und Satellitengeodaesie mit modernen Hilfsmittilm." Astronomisch geodaetische Arbeiten in der Schweiz, Schweizerische geodatische Kommission, ETH Honggerberg, CH-8093, Zurich.

Beutler, G. (1984). "GPS carrier phase difference observation software." Department of Surveying Engineering Technical Memorandum #TM-2, University of New Brunswick, Fredericton, N.B.

Beutler, G., D.A. Davidson, R.B. Langley, R. Santerre, P. Vaníček and D.E. Wells (1984). "Some theoretical and practical aspects of geodetic positioning using carrier phase difference observations of GPS satellites." Department of Surveyeing Engineering Technical Report 109, University of New Brunswick, Fredericton, N.B., July.

Bock, Y., R.I. Abbot, C.C. Counselman III, S.A. Gourevitch and R.W. King (1984). "Establishment of three-dimensional geodetic control by interferometry with the Global Positioning System." Submitted to the Journal of Geophysical Research.

Godin, G. (1972). The Analysis of Tides. University of Toronto Press.

Hopfield, H. (1971). "Tropospheric effect on electromagnetically measured range: Prediction from surface weather data." Radio Science, 6, pp. 357-367.

King, R.W., R.I. Abbot, C.C. Counselman, S.A. Gourevitch, B.J. Rosen and Y. Bock (1984). "Interferometric determination of GPS satellite orbits." Paper presented at the AGU Fall Meeting, San Francisco, CA, December.

Kleusberg, A., G. Beutler, D. Delkiaraoglou, R. Langley, R. Santerre, R. Steeves, H. Valliant, P. Vaníček, D. Wells (1984). "Comparison of Macrometer™ V-1000 and Texas Instruments TI-4100 GPS survey results." Paper presented at the AGU Fall Meeting, San Francisco, CA, December.

Kleusberg, A., G. Beutler, R. Langley, R. Santerre, P. Vaníček and D. Wells (1985). "Comparison of survey results from different types of GPS receivers." Proceedings of the First International Symposium on Precise Positioning with the Global Positioning System, Rockville, MD, 15-19 April.

Kouba, J. (1985). Personal communication.

Langley, R.B., G. Beutler, D. Delikaraoglou, B.G. Nickerson, R. Santerre, P. Vaníček and D.E. Wells (1984). "Studies in the application of the Global Positioning System to differential positioning." Department of Surveying Engineering Technical Report No. 108, University of New Brunswick, Fredericton, N.B.

Lerch, F.J., S.M. Klosko, R.E. Laubscher and C.A. Wagner (1979). "Gravity model improvement using GEOS-3 (GEM9 and 10)." J. Geophys. Res. 84, pp. 3897-3916.

Moreau, R. (1984). Personal communication. October.

Moreau, R., G. Beutler, J.G. Leclerc, B. Labrecque, R. Santerre and R.B. Langley (1985). "The Quebec 1984 Macrometer test." To be presented at the GPS Symposium, Washington, D.C., April.

Santerre, R., A. Kleusberg and G. Beutler (1985). "The DIPOP software documentation." Department of Surveying Engineering Technical Memorandum TM 6, University of New Brunswick, Fredericton, N.B.

Snay, R.A. (1985). "Network design strategies applicable to GPS surveys with three receivers." Submitted to Bulletin Geodesique.

Texas Instruments (1982). TI4100 NAVSTAR Navigator Owner's Manual. Texas Instruments Inc., Lewisville, TX.

Texas Instruments (1984). TI4100 NAVSTAR Navigator Instrumentation Port. Revision 1.1, Texas Instruments Inc., Lewisville, TX.

Valliant, H.D., D.E. Wells and D. McArthur (1985). "A Canadian evaluation of the Macrometer interferometric surveyor." In preparation.

van Dierendonck, A.J., S.S. Russell, E.R. Kopitze and M. Birnbaum (1980). "The GPS navigation message." Navigation, Journal of The Institute of Navigation (U.S.), 25(2), pp. 147-165.

Vaníček, P. and E.J. Krakiwsky (1982). Geodesy: The Concepts. North Holland, Amsterdam.

Vaníček, P., R.B. Langley, D.E. Wells and D. Delikaraoglou (1984). "Geometrical aspects of differential GPS positioning." Bulletin Géodésique, 58, pp. 37-52.

Vaníček, P., A. Kleusberg, R. Langley, R. Santerre and D. Wells (1985). "On the elimination of bias in processing differential GPS observations." Proceedings of the First International Symposium on Precise Positioning with the Global Positioning System, Rockville, MD, 15-19 April.

Wells, D., A. Kleusberg and S.H. Quek (1985). "Precise ship's velocity from GPS: Some test results." Proceedings of the First International Symposium on Precise Positioning with the Global Positioning System, Rockville, MD, 15-19 April.

Wells, D.E., P. Vaníček and D. Delikaraoglou (1981). "Application of NAVSTAR/GPS to geodesy in Canada: Pilot study." Department of Surveying Engineering Technical Report No. 76, University of New Brunswick, Fredericton, N.B.

APPENDIX A

Idealized Rolling Balloon Geometry

Assume a network of stations at the vertices of a hexagonal lattice of equilateral triangles (see Figure A.1). Let L be the (homogeneous) station spacing (lengths of sides of the equilateral triangles). Consider a hexagonal subnet of radius r station spacings. Then the number of stations m in this subnet is:

$$m = 1 + 3r(r + 1). \tag{A.1}$$

Inverting this, the diameter 2r of a subnet of m stations is:

$$2r = [(4m - 1)/3]^{1/2} - 1. \tag{A.2}$$

The number of triangles t in the subnet is:

$$t = 6r^2. \tag{A.3}$$

The area of one triangle is $(L/2)^2\sqrt{3}$. Hence the area of the subnet is:

$$A = (1.5\sqrt{3})(rL)^2. \tag{A.4}$$

The diameter D of a circle having the same area as the subnet is found from $\pi D^2/4 = A$. Solving for D as a function of L and m,

$$D = [1.5\sqrt{3}/\pi]^{1/2}\ 2r\ L = 0.9L\{[(4m - 1)/3]^{1/2} - 1\}. \tag{A.5}$$

A reasonable approximation is:

$$D = L\sqrt{m}. \tag{A.6}$$

Both the full expression and the approximation for D/L are plotted in Figure A.2.

Assume that receivers must operate on a station for T_o minutes to acquire sufficient GPS data, and that it takes a total of T_s minutes to set up and tear down the equipment. The total occupation time then is $T_o + T_s$. To transport a receiver across a subnet of diameter D kilometres, at an average speed of v kilometres per minute will require $T_t = D/v$ minutes. Then if we want to maintain m receivers in operation at all times, we will require a total of n receivers, where:

$$n = m[T_o + T_s + T_t]/T_o\ , \tag{A.7}$$

or, substituting for T_t, and for D

$$n = m[T_o + T_s + L\sqrt{m}/v]/T_o. \tag{A.8}$$

Inverting the question (and eqn. (A.8)); given a supply of n receivers, the number m of these which will be in operation (in the steady state approximation) at any one time is found by iteratively solving (for

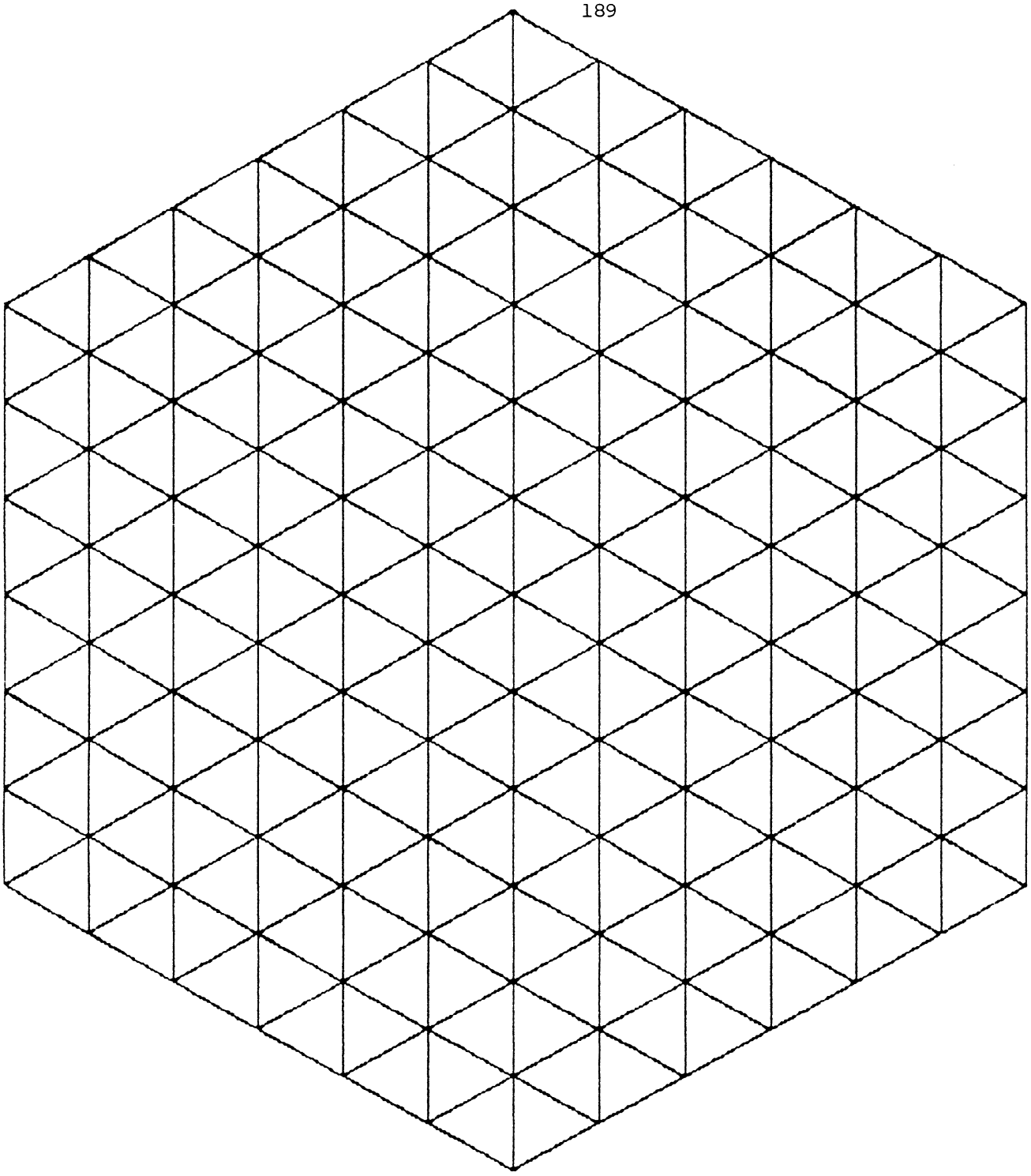

FIGURE A.1 HEXAGONAL NETWORK OF STATIONS

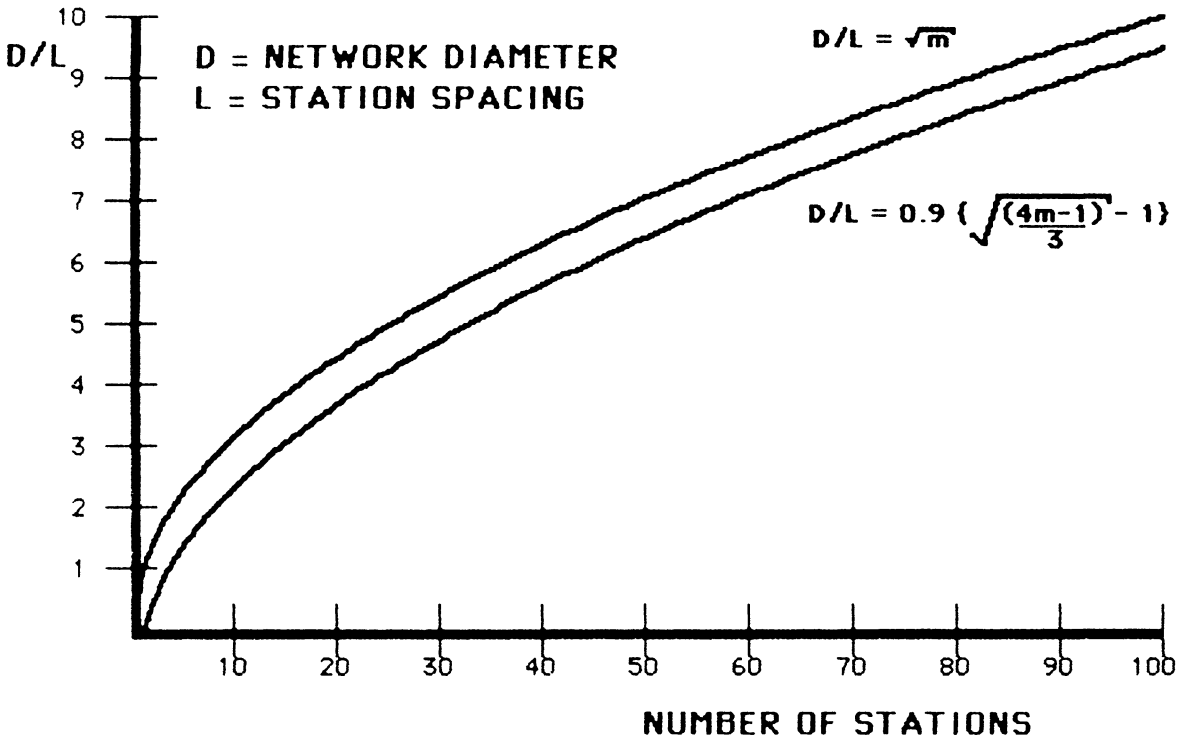

FIGURE A.2 NETWORK SIZE AS A FUNCTION OF NUMBER OF STATIONS

i=1,2,...)

$$m_i = nT_o/(T_o + T_s + L\sqrt{m_{i-1}}/v) \quad , \tag{A.9}$$

where $m_o = n$ is usually a reasonable first approximation.

Assigning typical values to T_o = 60 min, T_s = 30 min, v = 1 km/min for surface transportation, and v = 5 km/min for helicopter transportation, we have from eqn. (A.8):

	Station Spacing L(km)	Number of Active Receivers m	Network Diameter D(km)	Total numbers of receivers required n(surface)	n(air)
Urban	1	10	3	15	15
	1	100	10	167	153
Rural	10	10	32	20	16
	10	100	100	316	183
Mapping	100	10	316	67	25
	100	100	1000	1816	483

Expressing the same results according to eqn. (A.9), the percentages (m/n)*100 of receivers in operation, for a given number n of available receivers, are shown in Figures A.3, A.4, and A.5. It is clear that use of a large number of receivers (say more than 20) is very inefficient for 100-kilometre station spacing. This is only marginally improved (see Figure A.6) if we assume that the total set-up and tear-down delay is reduced (through intelligent equipment design) to 10 minutes. On the other hand, if the observing time can be reduced from 60 to 15 minutes, the efficiency is seriously worsened (see Figure A.7). For a fixed number (n=20) of available receivers, and with the station spacing L as the independent variable, we obtain the results in Figures A.8 to A.10. With N=50, we obtain Figure A.11.

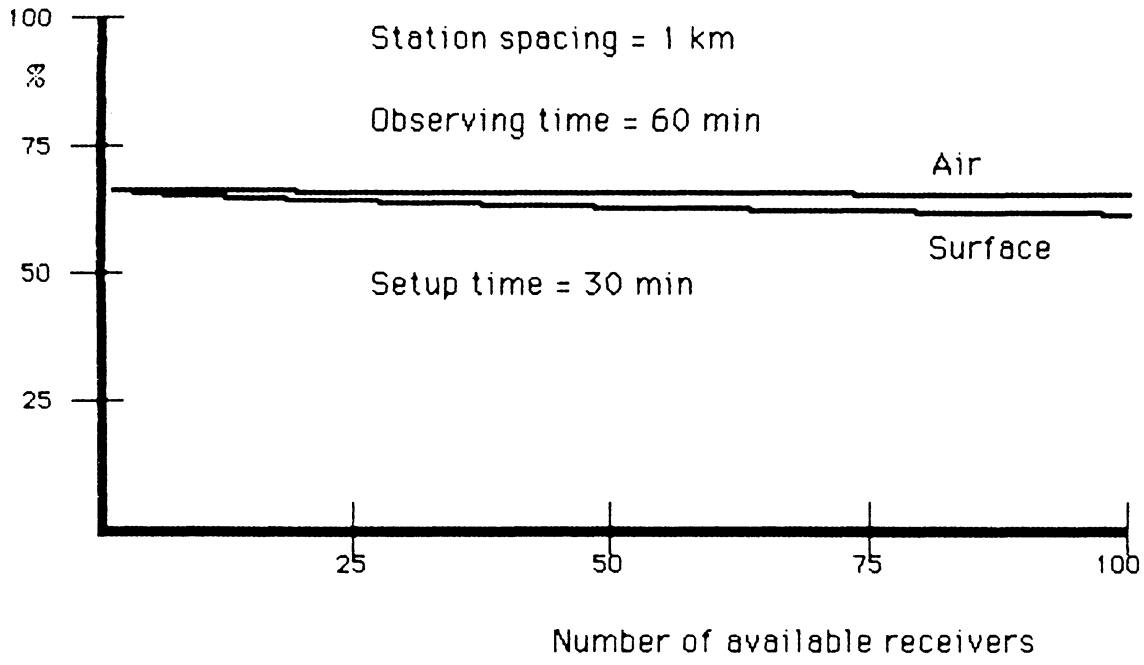

FIGURE A.3 PERCENTAGE OF AVAILABLE RECEIVERS IN OPERATION (URBAN SCENARIO)

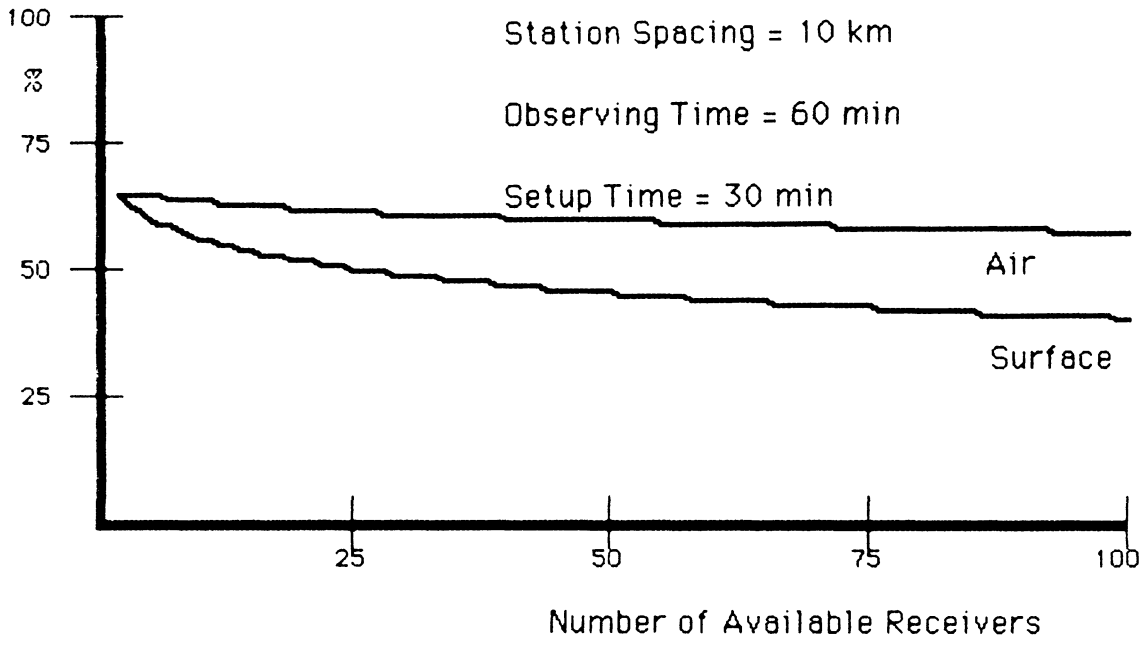

FIGURE A.4 PERCENTAGE OF AVAILABLE RECEIVERS IN OPERATION (RURAL SCENARIO)

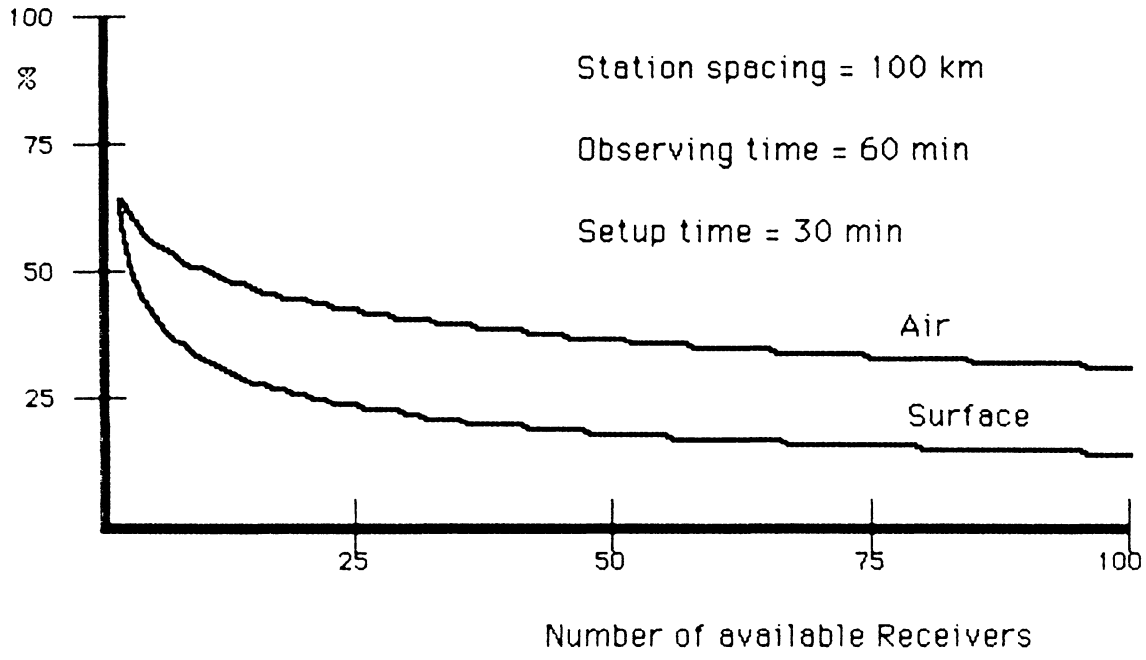

FIGURE A.5 PERCENTAGE OF AVAILABLE RECEIVERS IN OPERATION (MAPPING SCENARIO)

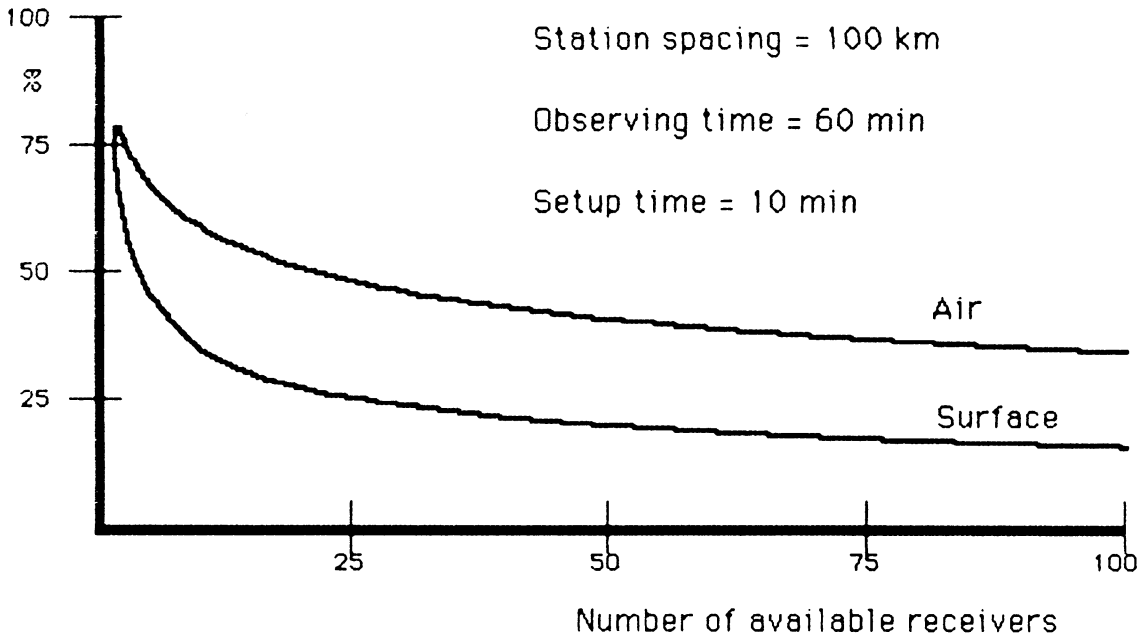

FIGURE A.6 PERCENTAGE OF AVAILABLE RECEIVERS IN OPERATION (MAPPING WITH FAST SETUP)

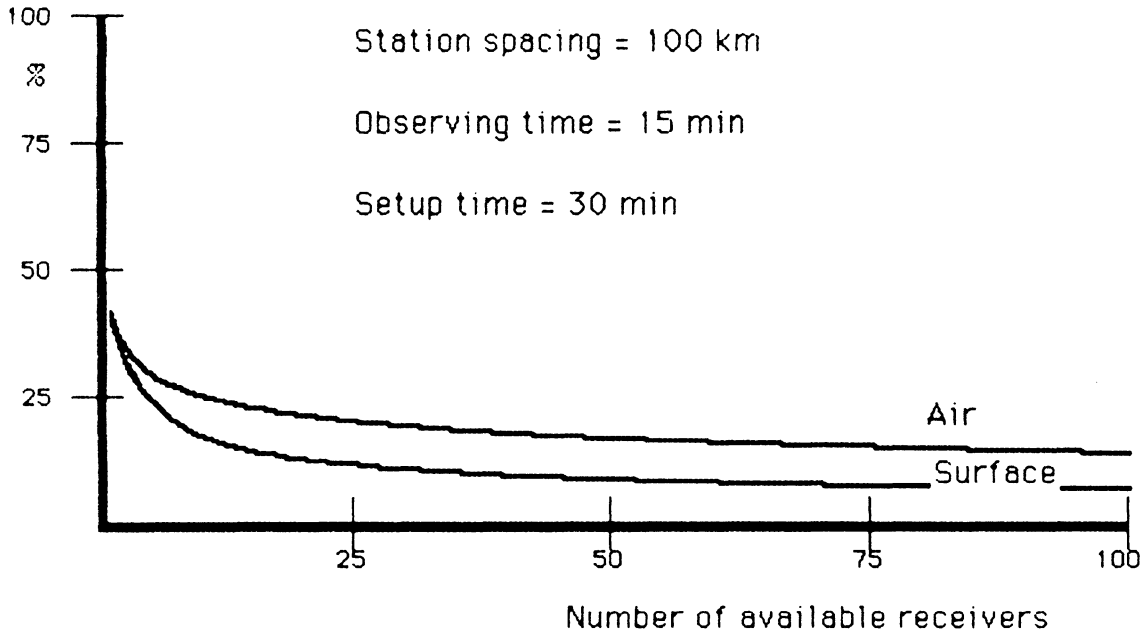

FIGURE A.7 PERCENTAGE OF AVAILABLE RECEIVERS IN OPERATION (MAPPING WITH FAST OBSERVING)

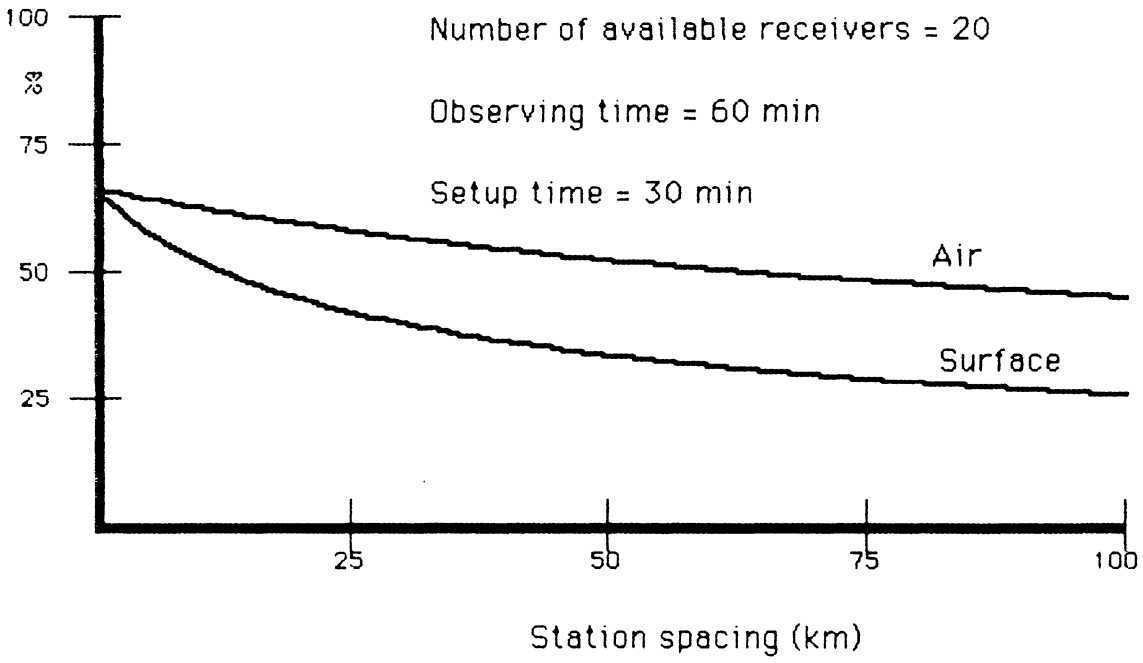

FIGURE A.8 PERCENTAGE OF AVAILABLE RECEIVERS IN OPERATION (vs. STATION SPACING)

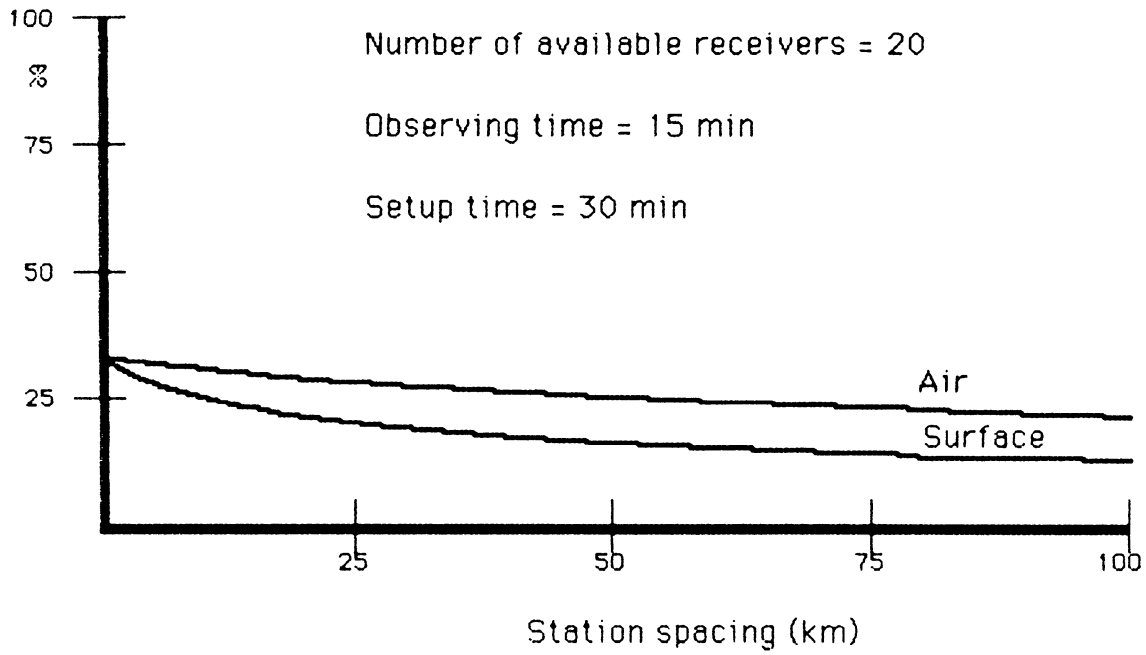

FIGURE A.9 PERCENTAGE OF AVAILABLE RECEIVERS IN OPERATION (vs. STATION SPACING WITH FAST OBSERVING)

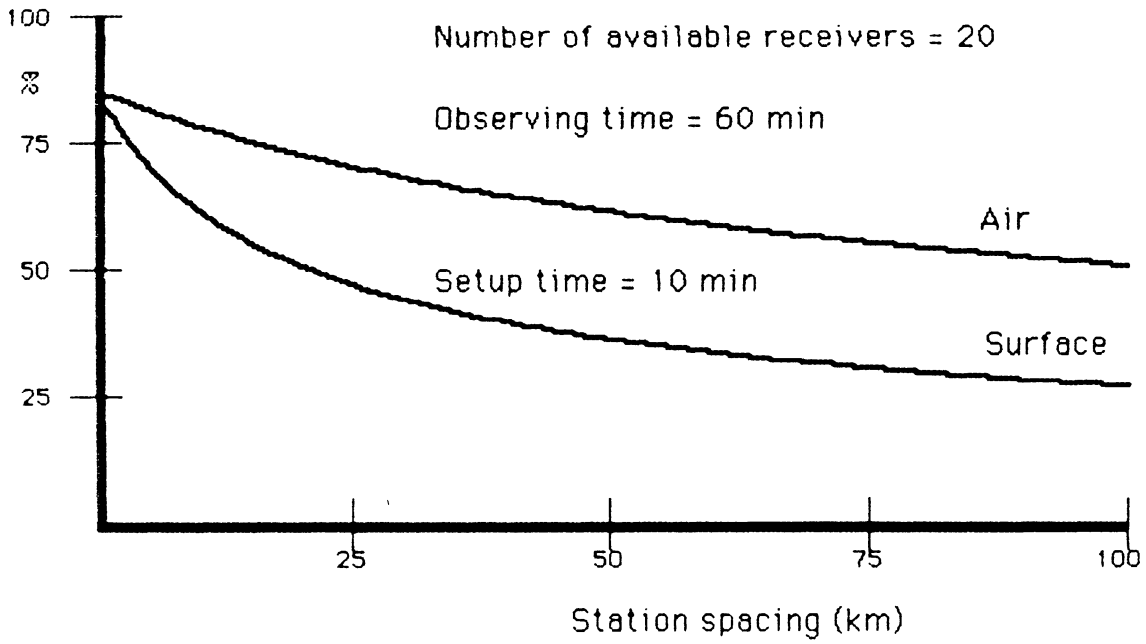

FIGURE A.10 PERCENTAGE OF AVAILABLE RECEIVERS IN OPERATION (vs STATION SPACING WITH FAST SETUP)

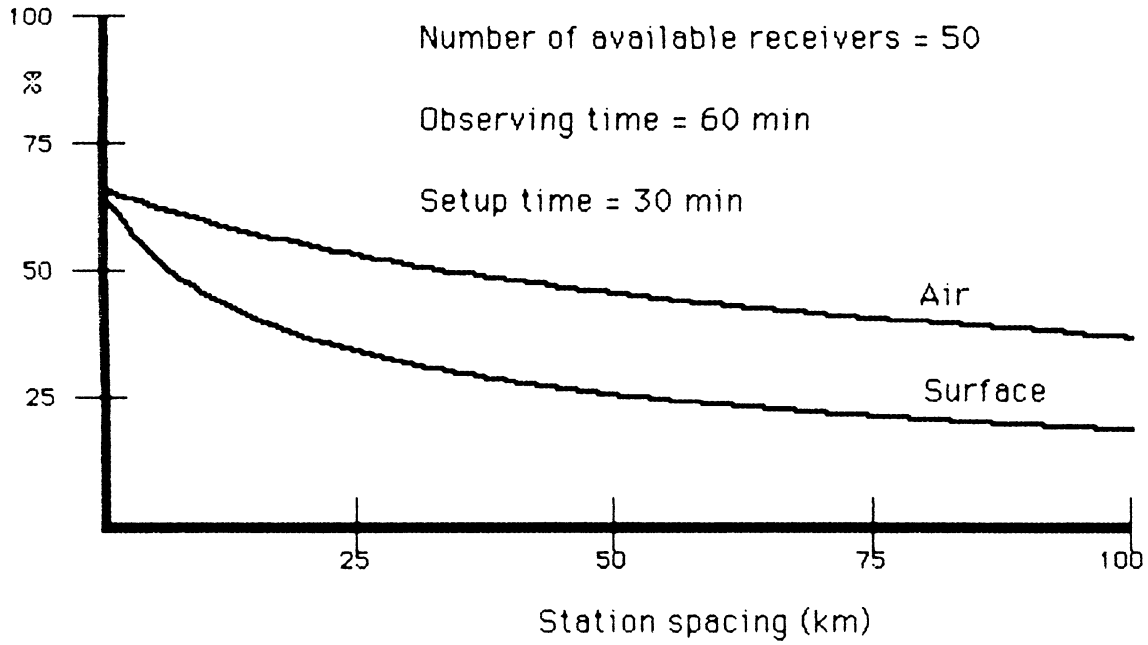

FIGURE A.11 PERCENTAGE OF AVAILABLE RECEIVERS IN OPERATION (vs STATION SPACING WITH 50 RECEIVERS AVAILABLE)

APPENDIX B

UNB PAPERS PRESENTED AT THE FIRST INTERNATIONAL SYMPOSIUM ON PRECISE POSITIONING WITH THE GLOBAL POSITIONING SYSTEM

Rockville, Maryland
15-19 April 1985

(i) Beutler, G., W. Gurtner, I. Bauersima and R. Langley. Modelling and Estimating the Orbits of GPS Satellites.

(ii) Vaníček, P., A. Kleusberg, R.B. Langley, R. Santerre and D.E. Wells. On the Elimination of Biases in Processing Differential GPS Observations.

(iii) Moreau, R., J.G. Leclerc, B. Labrecque, G. Beutler, R.B. Langley and R. Santerre. The Quebec 1984 Macrometer™ Test.

(iv) Kleusberg, A., R.B. Langley, R. Santerre, P. Vaníček, D.E. Wells and G. Beutler. Comparison of Survey Results from Different Types of GPS Receivers.

(v) Wells, D.E. Recommended GPS Terminology.

MODELLING AND ESTIMATING THE ORBITS OF GPS SATELLITES

G. Beutler (1)
W. Gurtner (1)
I. Bauersima (1)
R. Langley (2)

(1) Astronomical Institute
University of Berne
Sidlerstrasse 5
3012 - Berne
Switzerland

(2) Department of Surveying Engineering
University of New Brunswick
P.O. Box 4400
Fredericton, N.B.
Canada
E3B 5A3

ABSTRACT. The exploitation of the Global Positioning System (GPS) for high precision geodetic surveys requires precise knowledge of the observed GPS orbits. Differential positioning with an accuracy of 0.1 ppm presupposes overall orbital accuracies of 2.5 meters or better. In the present paper we first give a general description of our orbit modelling and orbit estimation techniques. We then discuss the problem of adequately modelling the force field acting on the satellites as a function of the lengths of the arcs. Finally we investigate the problem of estimating orbital biases along with the parameters of geodetic interest. We illustrate this technique by processing phase observations of networks using a priori orbits of very different qualities.

1. INTRODUCTION

When we process carrier phase difference observations, the accuracy of GPS orbits needed to obtain baselines of a certain accuracy depends on the baseline length (Bauersima 1983, eqn. 84):

$$\frac{db}{b} = \frac{dr}{\rho} \qquad (1.1)$$

Where b is the baseline length
ρ is the range receiver to satellite
dr is the orbit error
db is the resulting baseline error.

We use eqn. (1.1) to compute the relative baseline error db/b expressed in parts per million (ppm) for a number of orbit errors dr. The results are compiled in table 1.1, where a mean value of ρ = 25000 km is assumed for GPS satellites.

Table 1.1
Relative Baseline Error db/b for a Certain Orbit Accuracy dr

dr(m)	db/b (ppm)
125.0	5
25.0	1
12.5	0.5
2.5	0.1

Until quite recently mainly short baselines of the order of some kilometers were measured with high precision equipment. There a 1 ppm accuracy corresponds to absolute coordinate errors of a few millimeters which was sufficient for most applications. If we want to measure a 1000 km baseline with a 5 cm accuracy (0.05 ppm) we have to know the orbits with an accuracy of roughly one meter. Orbits of that quality (worldwide!) are not openly available at present. Therefore the scientist using GPS for large scale high precision surveys may have to estimate so called orbital biases along with the parameters in which he is actually interested, i.e., the coordinates of the satellite receivers.

In this paper we are dealing with some aspects of estimating orbital biases: In section 2 we give a brief review of our orbit-modelling and -estimating algorithms and we discuss the application to the orbits of GPS satellites. Section 3 is reserved to questions of modelling the forces acting on GPS satellites as a function of the lengths of the orbital arcs. In section 4 we present some practical examples for estimating orbital biases using so called double difference phase observations.

2. PRINCIPLES OF ORBIT DETERMINATION AND APPLICATION TO THE ORBITS OF GPS SATELLITES

2.1 Principles of Orbit Determination

Methods to estimate orbital biases have been developed and widely used in the processing of Transit Doppler data. With the exception of some of the so called short arc procedures, these algorithms do not describe the orbits by physical parameters. Our orbit modelling and orbit determination procedure on the other hand is purely physical:

The orbit of every satellite is a particular solution of the equations of motion:

$$\vec{r}^{(2)} = \vec{f}(t;\vec{r},\vec{r}^{(1)},s_1,s_2,\ldots,s_n) \qquad (2.1)$$

where $\vec{r} = \vec{r}(t)$ is the geocentric position of the satellite.

$\vec{r}^{(i)}$, i=1,2 is the i-th time derivative of $\vec{r}(t)$.

s_i, i=1,2,...,n are parameters defining (some of) the forces acting on the satellite.

To define an orbit uniquely, additional information has to be supplied. We use a special set of osculating orbital elements pertaining to one initial epoch t_0 (Langley et al. 1984, chapter 4). These elements in turn uniquely define the initial values at time t_0:

$$\vec{r}(t_0) = \vec{r}_0(t_0;a,e,i,\Omega,\omega,T_0)$$
$$\vec{r}^{(1)}(t_0) = \vec{r}_0^{(1)}(t_0;a,e,i,\Omega,\omega,T_0) \qquad (2.2)$$

Orbit determination in its usual, restricted, sense is the problem of estimating six parameters. In the subsequent discussion we will exclusively use the above mentioned set of osculating elements.

Orbit determination in a more general sense is the problem of estimating six orbital elements and some of the dynamical parameters s_i, i=1,2,...,n. (See section 3 for an example).

To solve an orbit determination problem, at some point one needs observations. Essentially an observation is a function of one or more satellite positions, ground positions and nuisance parameters like offsets and drifts of receiver- and satellite-clocks. In the subsequent analysis we will deal with two types of observations:

(a) Geocentric positions $\vec{r}(t_j)$; j=1,2,...,n_o as fictitious observations to discuss modelling questions (section 3).

(b) Double difference carrier phase observations for the processing of real observations (section 4).

What follows is a standard procedure in celestial mechanics and in geodesy. For a more complete discussion see (Beutler et al. 1984):

(1) We form the observation equations for either of the two mentioned observation types.

(2) The observation equations are rigorously linearized in the unknown parameters.

(3) The process of linearization implies that the orbit determination process becomes an orbit improvement process.

(4) In each iteration step of this process one initial value problem as defined by eqns. (2.1) and (2.2) (with known values for the parameters) has to be solved. Moreover the so called variational equations (Beutler et al. 1984, eqn. (3.7)) have to be solved to get the partials of the observables with respect to the unknown parameters.

2.2 Application to the Orbits of GPS Satellites

Every research group developing a program system for the estimation of orbits of GPS satellites has to take some important decisions. We present here our considerations:

(a) We decided to accomodate a relatively sophisticated model for the force field in our program system in order to avoid a priori limitations in the length of the satellite arcs:
   (1) The earth's gravity field is expressed by spherical harmonics, where we may select the coefficients of either the GEM-10 model (Lerch et al. 1979) or the GRIM-3L1 model (Reigber et al. 1984). (The GEM-10 coefficients are complete up to degree and order 22, those of the GRIM-3L1 model up to degree and order 36).

(2) Point mass attractions from sun and moon.

(3) A very simple radiation pressure model to start with (vector of constant length parallel to the line sun-satellite). An update of this model is possible without problems. Radiation pressure parameters are the only dynamical parameters which may be estimated by our orbit determination procedures.

(b) The initial value problem defined by eqns. (2.1), (2.2) is solved by a special numerical integration technique giving not some kind of tabular ephemerides but the coefficients of the approximating polynomials as the result (Beutler et al. 1984, Beutler 1982). This characteristic allows us to separate the integration process from the parameter estimation process(es). A block diagram showing the interactions between the orbital part and the other parts of the Bernese program system are given in (Gurtner et al. 1985).

(c) The variational equations are solved approximately by taking the partials not of the orbit defined by eqns. (2.1), (2.2) but of the elliptic orbit defined by the osculating elements at time t_0. Our experience shows that this simple approximation is good enough, even for arcs of one week length. Explicit formulae for the partials with respect to the osculating elements are given in (Langley et al. 1984). For the computation of the partials with respect to radiation pressure parameters we use a very simple integration technique (to be presented in a subsequent report).

(d) A priori orbits may be defined in different ways: (1) Sets of osculating elements, (2) tabular ephemerides, (3) sets of broadcast ephemerides. In order to define an orbit determination process that really makes sense these different orbit representations have to be transformed into standard orbits that actually are solutions of exactly one initial value problem of the type represented by eqns. (2.1), (2.2). This is a straight forward procedure for orbits defined in the way (1). For orbits defined in the way (2) we interpret the tabular positions as fictitious observations. Our standard orbit actually is the result of an orbit determination process in this case. Type (3) of a priori orbit definition is reduced to type (2) by first producing tabular ephemerides.

(e) When processing real observations we may estimate any combination of osculating elements per arc (the number varying between 0 and 6). Moreover we may assign a priori variances to each element. Our program system therefore may be used for pure orbit determination or we may implement very simple models for estimating orbital biases (e.g. estimation of only one along track error per arc).

3. MODELLING THE ORBITS OF GPS SATELLITES

The complexity of the model of the force field acting on a GPS satellite necessary to obtain satellite arcs of a certain quality depends mainly on the length of the satellite arcs. In (Beutler et al. 1984) we showed that for relatively short arcs (about 12 hours or one revolution) a very simple model (J_2, J_3 and J_4 terms of the earth's gravity field and a simple model for luni-solar gravitation included) may be used to generate orbits of roughly 20 meters accuracy.
In this section we use tabular satellite positions of various sources - namely Macrometrics' T-Files (Counselman 1983) in figures 3.1a,b and 3.2a and positions

Figure 3.1a

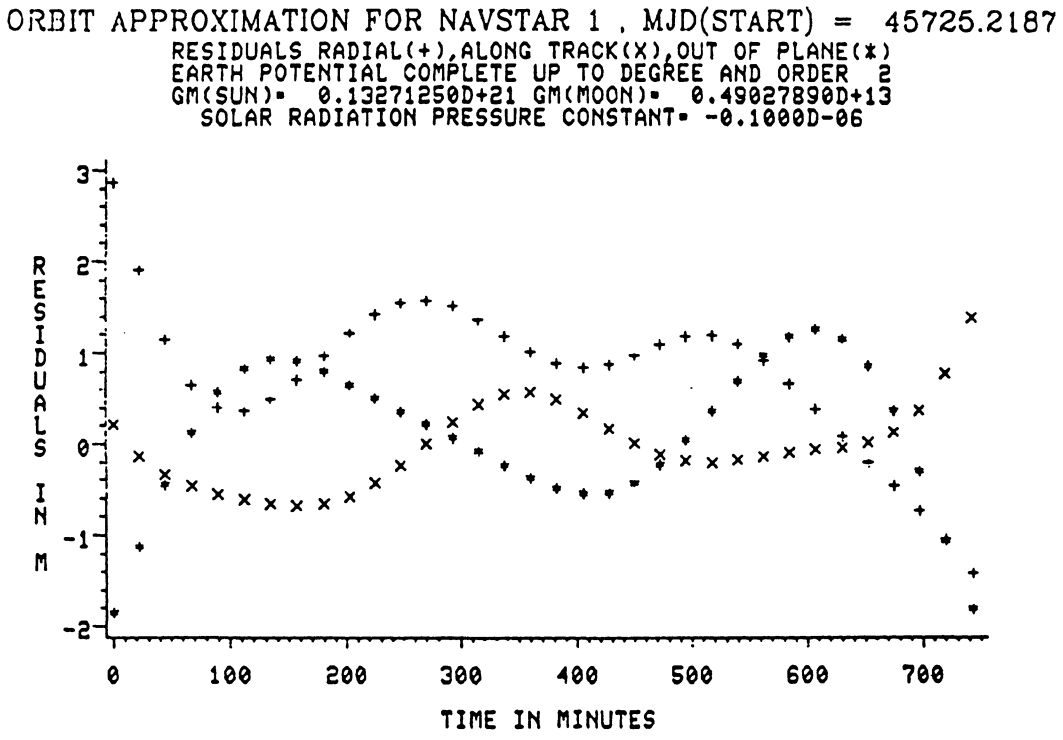

Figure 3.1b

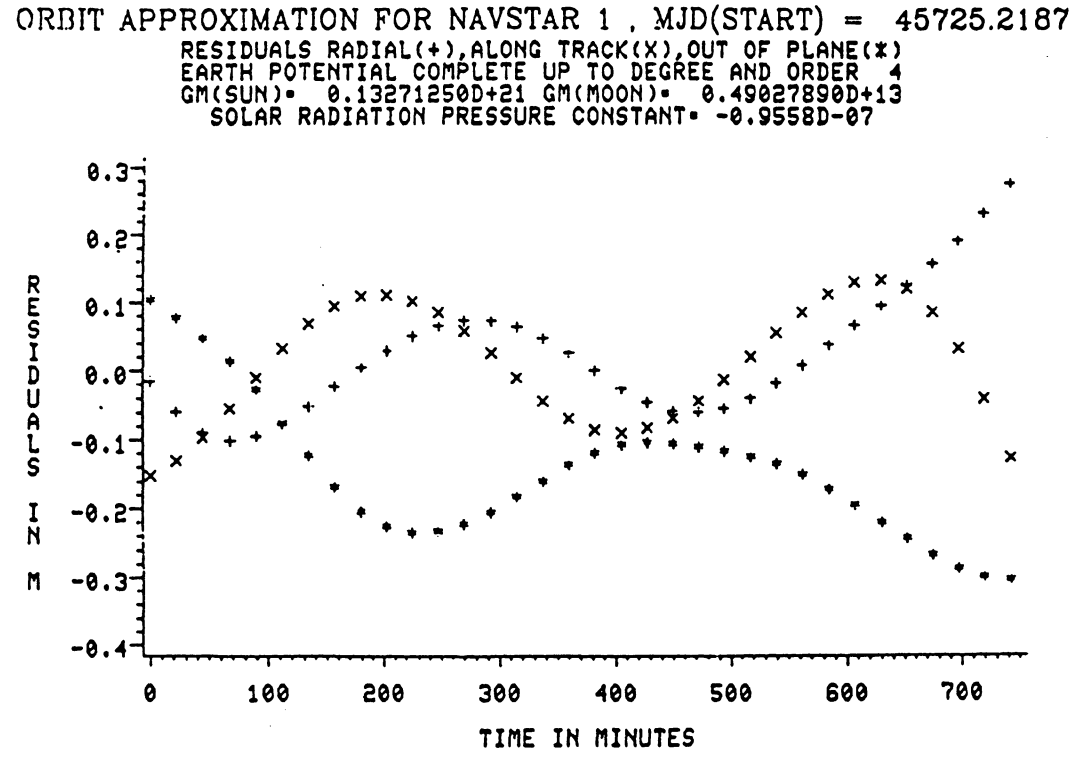

Figure 3.2a

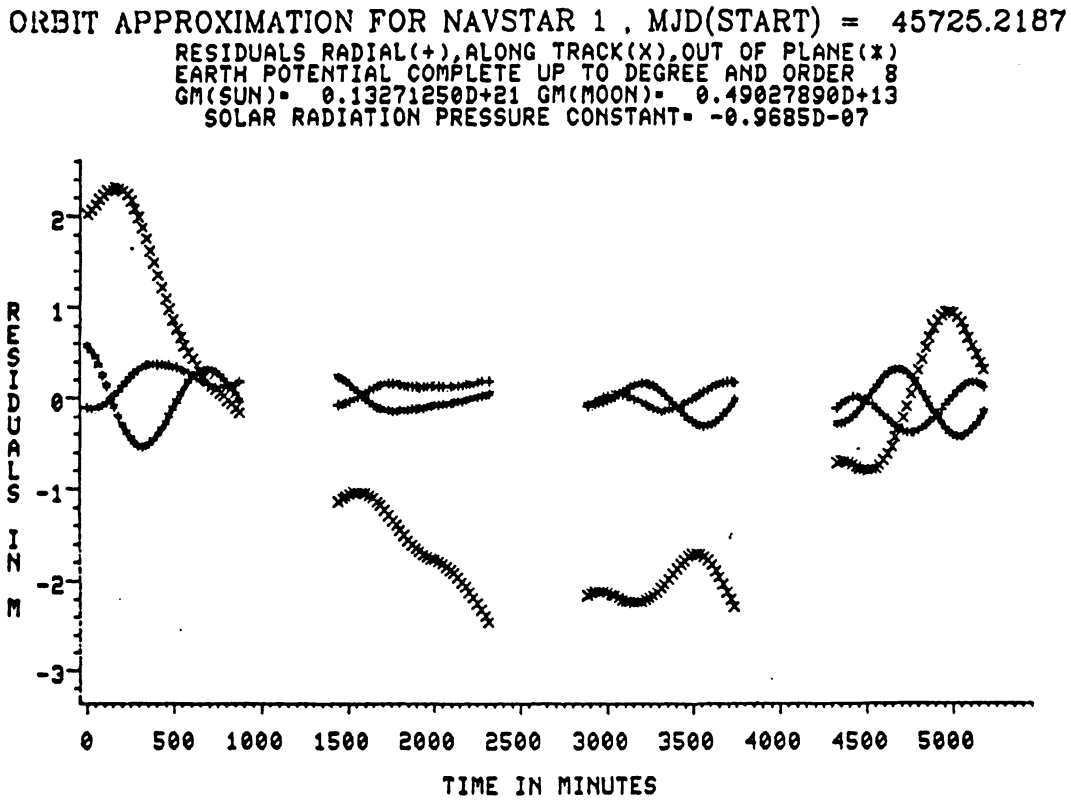

Figure 3.2b

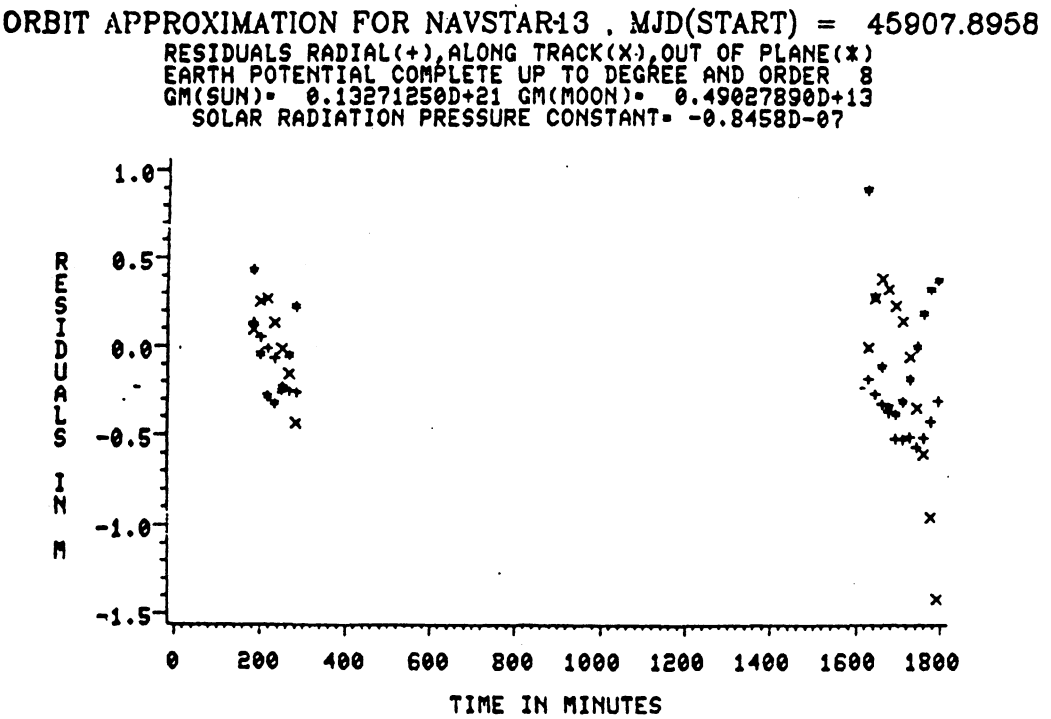

computed with broadcast elements in figure 3.2b - as input into orbit determination processes using different force field models.

In figure 3.1a we see that the orbit accuracy is improved roughly by a factor of 10 with respect to the above mentioned model, if we implement a radiation pressure pointing in the direction sun - satellite using a constant acceleration of .0000001 m/s^2 (as published in (van Dierendonck et al. 1980, table 2)). Figure 3.1b shows that the orbit representation is again improved by an order of magnitude if we estimate the radiation pressure constant and if we use earth potential coefficients up to degree and order 4. In table 3.1 we summarize the orbit accuracies obtained with our orbit determination procedures as a function of the force model and the number of parameters estimated. In order to save space we just give the results for 12 hour arcs.

Table 3.1
Orbit Accuracies as a Function of the Force Model and the Number of Estimated Orbital Parameters

Force Model	# of parameters	Mean errors	Maximum errors
G M	6	800 m	3300 m
plus potential up to degree and order 2.	6	20 m	100 m
plus sun, moon	6	6 m	24 m
plus nominal radiation pressure of .0000001 m/s	6	1 m	3 m
earth potential up to degree and order 4, plus sun and moon	7 *)	.1 m	.3 m

*) six osculating elements and one radiation pressure parameter estimated.

That we are able to generate longer arc (of the order of one week) of a similar quality is indicated by the next two figures. In figure 3.2a the positions of four T-Files (Counselman 1983) of four consecutive days (1984 January 26 to 29) were used as artificial observations in an orbit determination process with seven parameters (6 osculating elements and one radiation pressure parameter). If we use GRIM-3L1 coefficients up to degree and order 8 we obtain residuals smaller than 1m in the radial and out of plane directions. The residuals are somewhat larger along track, but still the agreement is excellent for two totally independent integration procedures (different sets of potential coefficients, different algorithms to compute positions of sun and moon).

A more realistic test of the orbit quality we may expect with our simple model for radiation pressure could be obtained using the precise ephemerides (produced by the NSWC) as artificial observations. Such material was not available to us so far. Instead we used tabular positions computed with broadcast ephemerides of two consecutive days as input into our orbit determination process. In figure 3.2b we see that the agreement is of the order of 1 m.

These tests indicate that we will be able to model GPS arcs of at about one week length with an accuracy of about one meter with very few unknown parameters (7 to 10 per arc). The most important impliciation of this result is the fact that we ar able to model the orbits of entire campaigns by one set of elements per orbit.

4. ESTIMATING ORBITAL BIASES WHEN PROCESSING GEODETIC NETWORKS OBSERVED WITH GPS

Here we present two typical examples for estimating orbit parameters simultaneously with receiver coordinates and carrier cycle ambiguities using so called double difference phase observations. The first example stems from a typical small scale network where only the L_1 carrier phase was observed, the second from the 1984 Alaska GPS observation campaign, where relatively long baselines (of the order of 1000 km) were measured with dual frequency instruments.

4.1 CERN LEP Campaign

In December 1984 seven points of the local geodetic network for the alignment of the new CERN elementary particle accelerator (Large Electron Positron ring (LEP)) were observed with differential GPS. Six independent baselines were measured twice on three consecutive days using three Macrometer V-1000 surveyor instruments.

These observations were processed with our second generation software (Gurtner et al. 1985). In a first phase we only had 30 days old sets of osculating elements of bad quality at our disposal. With these elements we produced ephemerides for the CERN campaign using our numerical integration program. Next we made a (very pessimistic) guess for the quality of the osculating elements for the observation times (see table 4.1, set A).

Table 4.1
Estimated Quality of Osculating Orbital Elements.

Set A : 30 days extrapolated orbit starting from low quality elements Set B : 7 days extrapolated orbit starting from high quality elements		
Element	Estimated quality of orbital elements Set A	Set B
semimajor axis a	100 m	5 m
eccentriciy e	.0000100	.0000003
inclination i	1.0 "	0.1 "
ascending node	1.0 "	0.1 "
perigee	1.0 "	0.1 "
perigee passing time T0	10.0 sec	0.025 sec

The entire preprocessing, namely the repair of cycle slips was performed without problems with the 30 days extrapolated orbit. Moreover we produced a first solution estimating six osculating elements per observed satellite (for the entire campaign). The results of this solution are given in the following two tables.

Table 4.2
Orbital Elements Used and Estimated in the CERN - LEP Campaign
Osculation Epoch : 1984 December 11.106927

Element Set A : Elements extrapolated from old osculating elements (age 30 days) of bad quality using an accurate Numerical integration procedure
Set B : Elements estimated with Bernese Second Generation Software using element sets A from table 4.1 as a priori orbits
Set C : Elements derived from Macrometrics' T-files

Nav	Set	a	e	i	Node	Perigee	M0+Per.
1	A	26561907.0	.00573149	63.30704	151.15509	195.83123	353.86275
1	B	26561875.5	.00573167	63.30699	151.15508	195.83123	353.90277
1	C	26561877.4	.00573237	63.30701	151.15528	195.82792	353.90272
3	A	26561722.5	.00331861	64.08394	29.20742	121.41305	163.15516
3	B	26561740.0	.00331872	64.08400	29.20742	121.41305	163.12927
3	C	26561736.9	.00332082	64.08395	29.20759	121.39389	163.13019
6	A	26559372.2	.01038612	63.88852	29.24443	71.15182	121.31892
6	B	26559404.7	.01038790	63.88854	29.24449	71.15181	121.28378
6	C	26559394.6	.01038830	63.88851	29.24460	71.15965	121.28492
8	A	26559186.6	.01045499	62.91741	150.41509	196.89326	69.81548
8	B	26559187.2	.01045560	62.91750	150.41523	196.89425	69.80746
8	C	26559202.3	.01045272	62.91738	150.41523	196.89466	69.80615
9	A	26561558.2	.00580695	62.63154	150.16833	352.44204	16.43141
9	B	26561540.6	.00580605	62.63150	150.16842	352.44204	16.42607
9	C	26561554.8	.00580855	62.63151	150.16850	352.43791	16.42574

In table 4.2 we give - for one osculation epoch at the start of the campaign - three sets of elements per observed satellite. Sets A are the 30 days extrapolated orbits, sets B are the elements estimated by our program system when using the orbit quality (set A, table 4.1) as a priori estimates for the mean errors of the elements, sets C are elements deduced from Macrometrics' T-Files which we obtained later on. Two facts are worth being mentioned: (a) The principal errors of the extrapolated orbits are the along track errors (differences of the order of 20 km, see column "mean anomaly + perigee" in table 4.2). (b) Our program actually improved the orbits essentially where again the main improvement is along track (the errors are reduced from 20 km in sets A to at about 150 m, which according to table 1.1 should be good enough to give coordinates on the 5 ppm level.

That this is actually true may be seen in table 4.3, solution A. (The distances between the points of the network vary between 5 and 13 km).

In table 4.3 we also include the result of a network solution when we use element sets C (table 4.2) as a priori orbits and sets B (table 4.1) as a priori variances for the orbit elements. We estimate that this configuration corresponds to one week extrapolated orbits. The results are very promising: 75 % of the ambiguities could be resolved, the RMS errors clearly are below one centimeter. We should mention that an ambiguity resolution was not possible for solution A.

In addition to solutions A and B we include solution X in table 4.3 where we use element sets A without orbit improvement.

That the relative geometry of our network solutions of table 4.3 are even better than indicated by this table, follows if we perform a Helmert (similarity) transformation between the satellite solutions and the terrestrial solution (three rotations and one scale factor are estimated), see table 4.4.

Table 4.3
Network Solutions without and with orbit improvement compared with "Ground Truth"

Solution X : Element Set A (Table 4.2) used as a priori orbits, no orbit improvement
Solution A : Element Set A (Table 4.2) used as a priori orbits, Set A,Table 4.1 used as a priori variances for elements.
Solution B : Element Set C (Table 4.2) used as a priori orbits, Set B,Table 4.1 used as a priori variances for elements.

Point	solution	Estimated-Ground Truth x(m)	y(m)	z(m)	RMS x(m)	y(m)	z(m)
P 226	X	-2.776	-3.378	-1.056	.323	.125	.092
P 230	X	-.698	1.154	1.512	.255	.127	.079
P 232	X	-.108	-.718	-2.170	.025	.019	.023
P 233	X	2.477	1.824	-.122	.223	.127	.068
P 234	X	-.914	-4.731	-4.100	.232	.119	.069
P 236	X	-2.705	-.385	1.313	.286	.141	.091
P 226	A	.030	.103	-.004	.057	.072	.026
P 230	A	.027	.011	-.060	.017	.015	.016
P 232	A	-.006	-.047	.053	.025	.019	.023
P 233	A	-.062	-.163	.023	.043	.068	.019
P 234	A	.002	.019	.095	.065	.036	.045
P 236	A	-.011	.088	-.054	.028	.060	.021
P 226	B	-.026	.006	-.017	.005	.004	.003
P 230	B	-.005	.002	-.026	.003	.003	.002
P 232	B	-.004	.003	.010	.002	.002	.002
P 233	B	.021	-.027	.010	.003	.003	.002
P 234	B	-.024	-.020	.025	.005	.004	.003
P 236	B	-.025	.014	-.019	.003	.003	.003

Table 4.4
Residuals of a Helmert Transformation between Satellite Solutions A respectively B and the Terrestrial Solution

Point	Solution	Terrestrial minus satellite Latitude(m)	Longitude(m)	Height(m)
P 226	A	.031	.009	.002
P 230	A	.006	.018	-.015
P 232	A	.018	-.020	-.003
P 233	A	-.049	-.039	.012
P 234	A	.038	-.017	.001
P 236	A	-.037	.028	.015
P 231	A	-.006	.021	-.012
		rms of transformation = .021 m		
P 226	B	.007	-.005	.001
P 230	B	.007	-.001	.006
P 232	B	.002	.017	.002
P 233	B	-.001	-.004	.000
P 234	B	-.010	-.010	.000
P 236	B	-.005	-.001	-.003
P 231	B	.000	.004	-.005
		rms of transformation = .007 m		

4.2 Some Remarks concerning the 1984 GPS Observation Campaign in Alaska and Canada

In July and August 1984 the National Geodetic Survey of the United States organized a GPS survey in Alaska. Simultaneously the Canadian Federal Department of Energy, Mines and Resources observed several points in the Northern Territories of Canada. A large portion of this observation material was made available to the Astronomical Institute of the University of Berne. So far we processed the observations of the Anchorage test (Gurtner et al. 1985) and the first two days of the "real" campaign held on long baselines. Here we make some remarks concerning the evaluation of the latter experiment using broadcast ephemerides without presenting complete results (these will be presented in a subsequent report).

On July 26 and 27 five TI-4100 dual frequency receivers were operated in Fairbanks, Nome, Cape Yakataga, Sourdough (all Alaska) and in Whitehorse (Canada). Six satellites were observed on both days (space vehicles 6, 8, 9, 11 from 21 to 24 UT, space vehicles 4, 9, 11, 13 during the next hour). In addition to that the satellite passes twelve hours earlier were observed on both days, but these data proved to be rather poor and we decided not to evaluate them.

Our data processing consisted in the following steps:

(1) We used the broadcast ephemerides to compute tabular ephemerides.
(2) These tabular positions were used as artificial observations in an orbit determination process with seven unknown parameters. (GRIM-3L1 earth potential coefficients up to degree and order 8 and luni-solar gravitation were implemented as a priori information, one radiation pressure parameter was estimated). The result of this process was used as a priori orbits.
(3) The L_1 and the L_2 observations were combined to form the "ionosphere-free linear combination".
(4) The observations of the two days were processed in one program run using the following options:
    (a) The coordinates of all stations were treated as unknown.
    (b) The coordinates of one station (Nome) were constrained to the Doppler position with a priori variances of 1 m^2 per coordinate.
    (c) Six osculating elements were estimated per orbit using the quality estimates in table 4.5 to compute the a priori variances for the osculating elements.

Table 4.5
Estimated Quality of Osculating Orbital Elements derived from broadcast elements

Element	Estimated Quality of Orbital Elements
semimajor axis a	2 m
eccentricity e	.000001
inclination i	0.1 "
ascending node	0.1 "
perigee	0.1 "
perigee passing time T0	0.025 sec

In table 4.6 we present the estimated slope distances between the stations together with the corresponding rms errors. These values are of the order of 0.25 ppm. The rms-errors for the coordinate differences (not included in this report) are of the same order of magnitude.

Table 4.6
Alaska Experiment: Estimated Slope Distances and their rms Errors in Meters.

Station 1 : Fairbanks 2 : Nome 3 : Sourdough		Station 4 : Yakataga 5 : Whitehorse			
Nr		2	3	4	5
1	d	848395.60	276325.13	602983.86	788752.52
	RMS	.22	.05	.10	.16
2	d		1003586.24	1276159.51	1591078.80
	RMS		.24	.27	.39
3	d			329299.25	591315.92
	RMS			.05	.15
4	d				414189.02
	RMS				.12

5. CONCLUSIONS

We developed algorithms for representing and estimating the orbits of GPS satellites. These algorithms have been implemented into the Bernese second generation software. The main characteristics are:
- The orbits are modelled as solutions of the equations of motion. The gravity fields of earth, sun and moon are assumed to be known. A simple model for radiation pressure was implemented.
- Six osculating elements and one radiation pressure parameter may be estimated.
- The equations of motion are solved with numerical integration giving the approximating functions as result.
- The partials of the orbit with respect to the parameters are computed approximately (see section 3).

In section 3 we showed that we are able to model GPS orbits of several days with an accuracy of a few meters.

In section 4 we applied our orbit improvement techniques to typical GPS carrier phase observation campaigns. In section 4.1 we showed that it is possible to compute small scale networks (diameters typically 10 to 20 km) with an accuracy of a few ppm (typically 5 ppm) even if the a priori orbital information is very poor (four weeks extrapolated starting from poor initial values). The relative geometry is even better defined than that, as indicated by table 4.4.

Results of the order of 1 ppm may be expected, if one week extrapolated orbits (starting from good initial values) are available.

In section 4.2 we gave an example for a larger network observed with dual frequency receivers. First results indicate that we will be able to produce results on the .25 ppm level using the broadcast ephemerides as a priori orbits.

6. ACKNOWLEDGMENT

We would like to express our thanks to Larry D. Hothem (NGS) and Jim Collins (Geo/Hydro Inc.) who provided us with the observation material necessary to perform the presented investigations and to test our software. We also thank Jean Gervaise and Michel Mayoud (CERN) who entrusted us with the network solution of the CERN GPS campaign.

References

Bauersima, I. (1983). "NAVSTAR/Global Positioning System (GPS III)." Mitteilungen der Satellitenbeobachtungsstation Zimmerwald, No. 10, Astronomical Institute, University of Berne, Switzerland.

Beutler, G. (1982). "Lösung von Parameterbestimmungsproblemen in Himmelsmechanik und Satellitengeodäsie mit modernen Hilfsmitteln." Astronomisch-geodätische Arbeiten in der Schweiz, Band 34, Schweizerische geodätische Kommission, ETH-Hönggerberg, CH-8093 Zürich, Switzerland.

Beutler, G., D.A. Davidson, R.B. Langley, R. Santerre, P. Vanicek, D.E. Wells (1984). "Some Theoretical and Practical Aspects of Geodetic Positioning Using Carrier Phase Difference Observations of GPS Satellites." Mitteilungen der Satellitenbeobachtungsstation Zimmerwald, No. 14, Astronomical Institute, University of Berne, Switzerland and Department of Surveying Engineering Technical Report No. 109, University of New Brunswick, Canada.

Counselman, C.C. III (1983). "Data processing with INTERF V01.02A1 and LSQ V01.04A1." Macrometrics Inc., Woburn, MA.

Gurtner, W., G. Beutler, I. Bauersima, T. Schildknecht (1985). "Evaluation of GPS Carrier Phase Difference Observations: The Bernese Second Generation Software Package." Paper presented at the First International Symposium on Precise Positioning with the Global Positioning System "POSITIONING WITH GPS - 1985", Rockville.

Langley, R.B., G. Beutler, D. Delikaraoglou, B. Nickerson, R. Santerre, P. Vanicek, D. Wells (1984). "Studies in the Application of the Global Positioning System for Differential Positioning." Department of Surveying Engineering Technical Report No. 108, University of New Brunswick, Canada.

Lerch, F.J., S.M. Klosko, R.E. Laubscher, C.A. Wagner (1979). "Gravity Model Improvement Using GEOS 3 (GEM 9 and 10)." Journal of Geophysical Research, Vol. 84, p. 3897.

Reigber, Ch., H. Müller, W. Bosch, G. Balmino, B. Moynot (1984). "GRIM Gravity Model Improvement Using Lageos (GRIM3-L1)." Submitted for publication in Journal of Geophysical Research.

van Dierendonck, A.J., S.S. Russell, E.R. Kopitze, M. Birnbaum (1980). "The GPS Navigation Message." Navigation, Journal of The Institute of Navigation (U.S.), Vol. 25, No. 2, pp. 147-165.

ON THE ELIMINATION OF BIASES IN PROCESSING DIFFERENTIAL GPS OBSERVATIONS

P. Vaníček
A. Kleusberg
R.B. Langley
R. Santerre
D.E. Wells
Department of Surveying Engineering
University of New Brunswick
P.O. Box 4400
Fredericton, New Brunswick, Canada
E3B 5A3

ABSTRACT

An ideal processor of GPS differential observations should have the capability to eliminate as much as possible the effect on estimated positions of different biases--e.g., those originating in orbital ephemerides, clocks, and atmospheric delays--and of phase ambiguities. These effects can be eliminated either implicitly (as was implemented, for instance, in the GEODOP Transit data processing program) or explicitly, after the biases themselves have been estimated. In this paper, we show the relative merits of both these approaches and experimental results using different update intervals. Other attributes of an ideal processor of GPS differential observations are also discussed.

INTRODUCTION

The Department of Surveying Engineering at the University of New Brunswick (UNB) has been involved in designing GPS positioning software for the past five years. During this time, our thinking has evolved resulting in the differential positioning software package presented here. This latest version of our software was implimented on an HP 1000 minicomputer.

This paper focusses on the bias modelling aspects of our software. Other aspects of our experience are described in other papers appearing in these Proceedings [Kleusberg et al., 1985; Wells et al., 1985; Beutler et al., 1985; Moreau et al., 1985]. However, to put the bias modelling in perspective, we also outline what we think an ideal software package should do and what it is that our software does at present.

We have also decided to concentrate on the explanation of the problems and concepts involved as well as presentations of numerical results rather than the mathematical formulation. We have discussed the mathematical and physical basis of our software elsewhere [Vaníček et al., 1985].

THE IDEAL PROCESSOR

The basic GPS observations, be they code pseudoranges or carrier phase, are biased ranges. The challenge in processing GPS data is in how best to handle the biases in order to extract the true ranges. The biases originate from a small number of sources:

- imperfect clocks in both satellites and receivers;
- ionospheric and tropospheric delays;
- cycle ambiguities, in the case of carrier phase observations;
- orbit errors.

We introduce the concept of observing "session": it is the time span over which GPS signals are received continuously and simultaneously by both receivers. It is also that part of an observing campaign characterized by a unique set of biases.

Several approaches can be taken to deal with these biases. If a bias has a stable, well understood structure, it can be estimated together with the station coordinates as nuisance parameters (cycle ambiguities, tropospheric delay scaling, orbit biases). In some cases, additional observations can be used, either to directly measure the bias (ionospheric delay), or to derive a model for the bias (tropospheric delay). Finally, if a bias is perfectly linearly correlated across different data sets, it can be eliminated by differencing the data sets (clock biases).

This last approach warrants further discussion. The double differencing technique (differencing across satellites, to eliminate receiver clock biases, and across receivers, to eliminate satellite clock biases) works well. However, it introduces some mathematical correlations in the data.

If r receivers continuously and simultaneously track s satellites, then there are $r(r-1)\cdot s(s-1)/4$ possible double difference data series which can be formed, only $(r-1)\cdot(s-1)$ of which will be independent. Even with the present baseline-by-baseline observing techniques, it is not always simple to decide how best to form the double differences. It is worth while considering whether alternatives to double differencing can be devised, which will be as effective in handling clock biases. In particular, can the nuisance parameter approach be taken? If we have phase measurements from s satellites at r receivers (i.e., r·s time series $\phi(t)$), to form the "traditional" single differences we subtract the time series between pairs of stations (eliminating the influence of satellite clock errors). This reduces the number of time series from r·s to (r-1)s.

If, instead, we were to introduce as nuisance parameters s time series of satellite clock bias parameters, one such time series for each satellite clock, the effect should be similar. More specifically, consider the (simplified) observation equation:

$$\rho_i^j(t_k) = |\vec{r}^j(t_k) - \vec{R}_i| + c\Delta t^j(t_k) + c\Delta T_i(t_k) \ ,$$

where $\rho_i^j(t_k)$ is the observed range from receiver i at $\vec{R}_i$ to satellite j at $\vec{r}^j$ at time t_k; c is the speed of light, and where Δt^j represents the satellite clock error, and ΔT_i the receiver clock error. In the differencing approach, we difference two such equations from different stations i, in which case the $\Delta t^j(t_k)$ term (which is independent of i) disappears. In the nuisance parameter estimation approach, we solve for independent values of $\Delta t^j(t_k)$ for each t_k, using observations from all stations i. (Note, if we were to explicitly eliminate the nuisance parameters from the normal equations, we would, in effect, return to the differencing approach.) The advantage of the nuisance parameter approach is that we can then work with "raw" phase

measurements, and not have the complicated bookkeeping and correlation problems involved in processing differenced observations.

Similarly for double differences--instead of differencing between satellites, and (in the "traditonal" method) reducing the number of observational time series from (r-1)s to (r-1)(s-1) (eliminating the influence of the receiver pair differential clock errors)--we could introduce instead r time series of receiver clock bias parameters.

We lose nothing from the degrees of freedom point of view. In the differencing approach we reduce the same number of observation time series as we add in the nuisance parameter estimation. And our flexibility is vastly improved. For example, merely by fiddling with the a priori weights on these nuisance parameter time series we can enforce the equivalent of single difference or double difference (and "partial" differencing) very easily. Also, by introducing some kind of serial correlation function (i.e., smoothing the nuisance parameter time series), we can effectively vary our model for these clocks from something that is considered completely uncorrelated (an independent nuisance parameter for each satellite and each receiver at each time epoch) to something having strong serial correlation over lengthy periods (equivalent to using a model with only a few nuisance parameters such as a truncated power series in time).

This would mean that one algorithm, with options on the nuisance parameter weighting and serial correlation, would effectively duplicate the phase, single, and double difference algorithms.

This approach would make it imperative to process all the observations from one epoch in one step. It would, however, place no limitations on which of the many possible observing strategies was used, the selection of which could then be made on other grounds (logistics, cost, time, etc.).

DIPOP PHILOSOPHY

Our present program package, the DIfferential POsitioning Program (DIPOP) package is the result of several years of development. It stems from the following basic ideas:

(i) It should be capable of processing data collected by any GPS receiver through a system of tailored preprocesors. (So far only Macrometer™ V-1000 and TI 4100 preprocessors exist in the DIPOP.)

(ii) Observations (carrier phase time series) could be processed in any desired mode: biased ranges, single differences, double differences, triple differences.

(iii) Cleaning up of observations (pre-estimation of range biases--ambiguities, elimination of cycle slips, elimination of bad observations, reduction of number of observations if necessary), preparation of pseudo-observations (various differences) and evaluation of satellite positions (see, e.g., Beutler et al.[1984]) should be done within the preprocessors.

(iv) The main processor should process pseudo-observations in a sequential manner within each session [Langley et al., 1984] as well as session by session. At present, the step of the sequential process is variable from one epoch up.

(v) Positioning, rather than position differences, must be estimated. This is made possible by employing the weight matrix of the initial estimates of positions, called P_x-matrix (see, e.g., Vaníček and Krakiwsky [1982]). Proper employment of a P_x-matrix can also take care of the crudest form of orbital biases, the common translational bias of all orbits with respect to the coordinate system in which the initial positions of unknown stations are given.

(vi) The main processor must be designed to estimate (and eliminate the effect of) the whole family of biases: the ambiguities, clock biases, orbital biases, tropospheric and ionospheric delay biases. (At the moment only ambiguity and clock bias estimation have been fully implemented.) Biases can be estimated at any step of the sequential filter. The most up-to-date estimates of biases are used continuously to eliminate the effects on observations. Biases are estimated only within individual sessions [Vaníček et al., 1985].

(vii) Full variance-covariance information about the estimated positions and biases must be available.

(viii) A comprehensive output, including optional plots of position determination histories, residuals and biases, should be available. (At present this is the role of the postprocessing program.)

COMPARISON OF BIAS ELIMINATION MODES

It is clear that the biases can be evaluated/updated either at each epoch, at desired intermittent times, or only at the end of each observing session. For the time the biases have been updated, it is immaterial what mode has been used up until that instant; the results are--at that instant--identical.

One strategy--elimination for each satellite pass--is similar to the strategy used in the Doppler observation processing program GEODOP [Kouba and Boal, 1976]. The other extreme strategy--elimination at the completion of processing of unknowns--is equivalent to a batch mode adjustment. The most compelling argument for the bias to be evaluated as often as possible is to keep the resulting positions determined by the sequential filter as accurate as possible at all times.

The most compelling argument for the bias to be evaluated as seldom as possible is to keep the computer time (consumption) low. To illustrate this point, let us quote a study done by our undergraduate students in SE4231 (Special Studies in Adjustment): For a configuration consisting of 3 satellite receivers and 4 satellites, 1 hour session sampling at a rate of 1 observation per minute (resulting in 720 "observed" double differences), the following statistics hold. The bias elimination and bias evaluation/elimination approaches require about 3.4×10^6 operations each. Evaluation at every second epoch results in a reduction of 41% in the number of operations, every fifth epoch gives a reduction of 65%, and every tenth epoch a reduction of 74%.

Clearly, if the study of evolution in time of position parameters is of interest, we may wish to either evaluate the biases at each epoch or go for some intermittent solution, as we have done in the cases discussed in the next section.

EXPERIMENTAL RESULTS

In this section, we describe some results obtained by range bias and clock bias modelling using data (carrier phase series) collected by Macrometer™ and TI 4100 instruments in two different locations in Canada (Ottawa and Quebec City) for short (550 m) and long (66 km) baselines processed in a "baseline mode." The "network mode" results require more extensive analysis which would be inappropriate for a paper of this length.

On Figure 1 we show changes in the length of a 548.58 m long baseline observed during the Quebec City Macrometer™ 1984 campaign [Moreau et al., 1985]. Double differences of carrier phase recorded by the V-1000 receivers during one 3-hour 20-minute long session were processed in a baseline processing mode using three different approaches to range bias (ambiguity) elimination.

In the first approach, the range biases were solved for in the preprocessing stage, using the values obtained from an earlier processing run rounded off to the nearest integers and all double differences corrected accordingly. No further estimation for these biases was carried out during the main processing.

The second approach consisted of solving for range biases during the main processing at every 10th epoch. So estimated values we rounded off to nearest integers and held fixed for the next 9 epochs. It can be seen from the plots that the final solutions from both these approaches are identical (548.5845 m) and depart from the invar-taped "ground truth" (548.5834 m) by 1.1 mm, i.e., by 2 ppm. Clearly these two approaches give identical position results every 10th epoch. The Macrometer™ results presented here do not take into account the mathematical correlations between the double difference observations and therefore differ from the values presented in the paper by Moreau et al [1985].

In the third approach, we solved for range biases during the main processing at every epoch. These estimates, however, were not rounded off; they were used as real values in correcting "observed" double differences. The final solution for the baseline length (548.5815 m) departs from the ground truth by -1.9 mm, i.e., by -3.5 ppm, and from the two integer-bias-solutions by -3.0 mm, i.e., by -5.5 ppm. It is interesting to note, however, that during the course of measurements, the difference between this and the integer-bias approaches reaches up to 12.5 mm (epoch 41), i.e., to 22.8 ppm, clearly an unacceptable difference.

In Figure 2 we have displayed results from another experiment. This time we have taken the longest baseline (66,268.70 m) observed during the 1983 Ottawa Macrometer™ campaign [Beutler et al., 1984]. The recorded double differences from three 5-hour long sessions were processed again in the baseline mode using three different techniques. For the sake of simplicity, results are displayed again in terms of baseline length variations.

The first technique solves for ambiguity and clock biases at every 20th observing epoch as well as every time a new satellite rises above local horizon and uses these biases to evaluate baseline coordinate differences for all the intermediate epochs. We arbitrarily perturbed the "ground truth" coordinates of both points by about 3 metres and specified again the P_x matrix for both points accordingly. This we call the "floating points solution."

Significant perturbations of the order of 10 ppm occur at the very beginning of the plot (around epochs 20 and 40). At epochs 60 and 160 perturbations of the order of 1 ppm perturb an otherwise relatively smooth curve. These glitches are associated with some changes in the satellite configuration as shown on the plot.

The second technique seeks the solution by eliminating both ambiguity and clock biases at each epoch. The final solution as well as all the interim solutions at 20th epochs are identical, with the final length being 66,268.827 m. The result differs from the fixed point solution presented by Kleusberg et al. [1985]. Between the evaluation epochs the two solutions vary but no more than expected from the character of the curve as discussed above in the context of the first technique.

The third technique was essentially the same as the first except that clock bias was not sought. The character of the curve is similar to the first curve except that the departures from the mean are less pronounced. The final line length is 35 mm shorter (corresponding to a difference of -0.5 ppm) compared to the first two techniques, the latter being closer to the ground truth. None of the three techniques shows any discontinuity between sessions.

Figure 3 shows the last experiment we wish to report on here. The experiment focusses on the question of what effect does weighting of initial positions have on relative positioning. We have taken again the longest (66 km) baseline of the Ottawa network and double differences collected by a couple of TI 4100 receivers [Kleusberg et al., 1985]. Then we have estimated the baseline components ($\Delta\phi$, $\Delta\lambda$, Δh) using two different solutions: first we specified the initial coordinates of both points to have the values obtained from GSC adjustment of terrestrial and Doppler data [McArthur, 1985]. We then declared the position of the first point to be known exactly rendering the diagonal elements of that part of P_x matrix which belongs to the first point very large. The part corresponding to the second point was chosen so that it represented one sigma uncertainties in coordinates of the second point equal to 1 m. This is what we call "fixed point solution."

The second approach solves for the relative positions assuming both points to be equally badly known (the floating point solution). Again we perturbed the "ground truth" coordinates at both points by about 3 metres and specified again the P_x matrix for both points accordingly. In this case, both points are forced to wander away from their initial positions to a certain degree to assume positions that are the most compatible with the observations. One may think of this solution as acknowledging that there may be a several metre translative bias in the given ground coordinates compared to the coordinate system in which the GPS satellite positions are given. This is probably a realistic assumption. However, other sources of error may contribute to the observed translation.

The comparison of the two sets of results is interesting. There seems to be a definite bias involved in the comparison of the two coordinate systems used. The differences "floating points minus fixed point solutions" given in local geodetic coordinate systems of the end point are $\delta\phi$ = -85 mm, $\delta\lambda$ = -58 mm, Δh = +105 mm, ranging between 1 and 2 ppm. The difference in the implied length of the baseline is $\Delta\ell$ = +36 mm, corresponding to about +0.5 ppm. The floating points solution (66,268.698 m) is only 9 mm shorter than the ground truth and

closer to the Macrometer™ determined value (66,268.752 for network mode) than the fixed point solution. The length of the baseline ground truth being likely to be more accurate than any of the three baseline components, we may claim that the floating points solution has in this case, been more successful than the fixed point solution. This is, of course, what one would expect theoretically.

CONCLUSIONS

The first experiment described above confirms the known fact that if the range ambiguity is resolvable to an integer number of carrier wavelengths it is a must to treat it as an integer number. This situation occurs when we deal with shorter baselines, and under these circumstances we get significantly degraded results if we do not force the ambiguities to be integer numbers. On the other hand, it is not necessary to solve for ambiguities at each observation epoch.

The second experiment, which involved a two orders of magnitude longer baseline, has confirmed the finding that it is not necessary to solve for biases (ambiguities and others) at each observation epoch. Moreover, if a solution for biases is sought only every nth epoch, the impact of changing satellite geometry may be more clearly visible if the evaluation of position differences is displayed. As expected, the choice of kinds of biases to be modelled affects the results but only slightly significantly.

The third experiment shows that even the crude modelling of orbital biases, by allowing a baseline to shift in a direction preferred by "observed" double differences, may have an appreciable effect on computed position differences. Clearly, the approach where both ends of the baseline are left free to find their optimal positions would be favoured by us.

ACKNOWLEDGEMENTS

Parts of the work reported herein were funded by the Natural Sciences and Engineering Research Council of Canada. The Geodetic Survey of Canada contributed to this research in the form of a Department of Supplies and Services contract. Support under the New Technology Employment program of Employment and Immigration Canada also contributed to this work.

We wish to acknowledge gratefully the diverse forms of assistance we have received from Dr. D. Delikaraoglou. The Earth Physics Branch of Energy, Mines and Resources Canada kindly supplied the Ottawa Macrometer™ data; the Geodetic Survey of Canada supplied the Ottawa TI 4100 data. Mr. R. Moreau, Récherche Territoriale, Ministère de l'Energie et des Ressources, Québec, was instrumental in arranging for us to have access to the data from the Québec experiment. We also wish to thank Ms. W. Wells for her, as usual, flawless word processing.

REFERENCES

Beutler, G., D. Davidson, R. Langley, R. Santerre, P. Vaníček and D. Wells (1984). "Some theoretical and practical aspects of geodetic positioning using carrier phase difference observations of GPS satellites." Department of Surveying Engineering Technical Report 109, University of New Brunswick, Fredericton, N.B., Canada.

Beutler, G., W. Gurtner, I. Bauersima and R. Langley (1985). "Modeling and estimating the orbits of GPS satellites." Paper presented at the First International Symposium on Precise Positioning with the Global Positioning System, Rockville, MD, 15-19 April.

Kleusberg, A., R. Langley, R. Santerre, P. Vaníček and D. Wells (1985). "Comparison of survey results from different GPS receiver types." Paper presented at the First International Symposium on Precise Positioning with the Global Positioning System, Rockville, MD, 15-19 April.

Kouba, J. and J.D. Boal (1976). "Program GEODOP." Surveys and Mapping Branch, Energy, Mines and Resources Canada, Ottawa, Ontario, Canada.

Langley, R.B., G. Beutler, D. Delikaraoglou, B.G. Nickerson, R. Santerre, P. Vaníček and D.E. Wells (1984). "Studies in the application of the Global Positioning System to differential positioning." Department of Surveying Engineering Technical Report No. 108, University of New Brunswick, Fredericton, N.B., Canada.

McArthur, D. (1985). Personal communication. Geodetic Survey of Canada, Ottawa.

Moreau, R., G. Beutler, J.G. Leclerc, B. Labrecque, R. Santerre and R.B. Langley (1985). "The Quebec 1984 Macrometer™ test: Comparison of phase-difference processing and network solution methods." Paper presented at the First International Symposium on Precise Positioning with the Global Positioning System, Rockville, MD, 15-19 April.

Vaníček, P. and E.J. Krakiwsky (1982). Geodesy: The Concepts. North-Holland, Amsterdam.

Vaníček, P., G. Beutler, A. Kleusberg, R.B. Langley, R. Santerre and D.E. Wells (1985). "DIPOP: Differential positioning program package for the Global Positioning System." Final contract report for the Geodetic Survey of Canada, Energy, Mines and Resources Canada, Ottawa, Ontario, Canada.

Wells, D., A. Kleusberg, S.H. Quek, J. McCullough and J. Hagglund (1985). "Precise ship's velocity from GPS: Some test results." Paper presented at the First International Symposium on Precise Positioning with the Global Positioning System, Rockville, MD, 15-19 April.

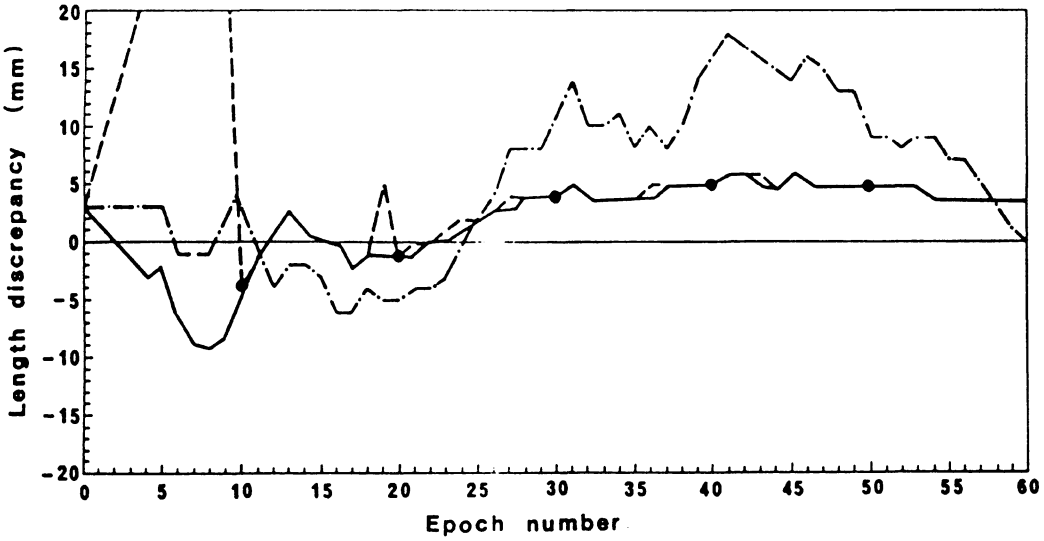

FIGURE 1. Change in the length of a 550 m long baseline implied by partial solutions. (1) —— integer range biases solved for during preprocessing. (2) ---- integer range biases solved for at each 10th epoch. (3) -·-· real valued range biases solved for at each epoch. • epoch of bias update. Discrepancies are with respect to the final length obtained from solution (3).

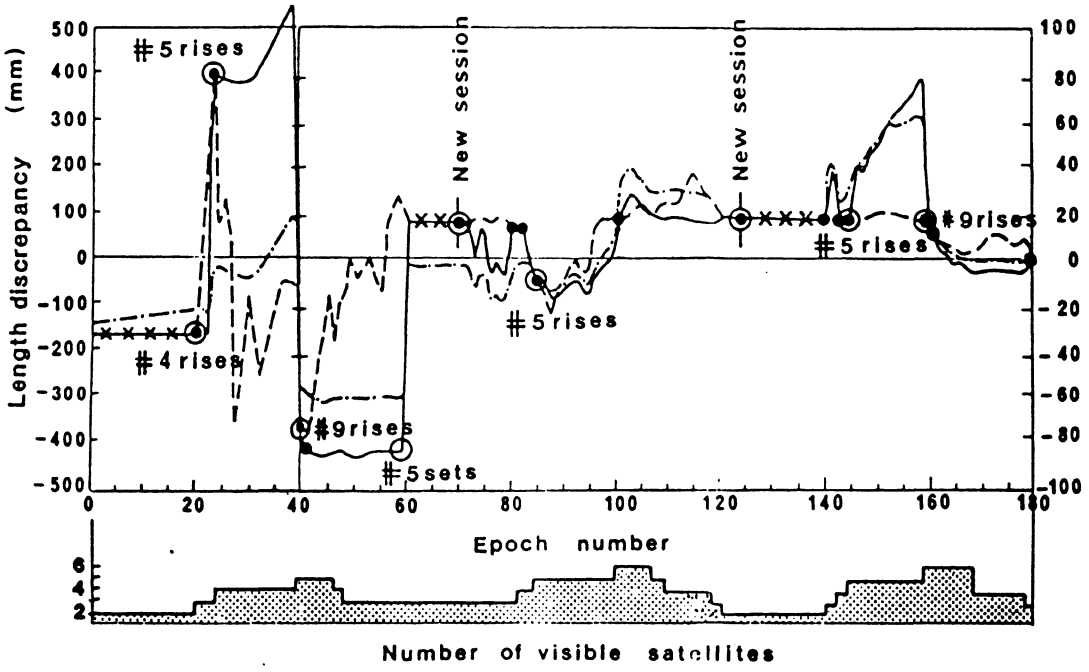

FIGURE 2. Change in the length of a 66 km long baseline implied by partial solutions. (1) —— solution for clock and range biases determined at every 20th epoch. (2) ---- solution for clock and range biases determined at each epoch. (3) -·-· solution without clock biases. • epoch of bias update for solution (1). 0 special event. xxxx no solution in this interval due to lack of observations. Note change of scale at epoch 40. Discrepancies are, for each solution, with respect to the final length of the solution.

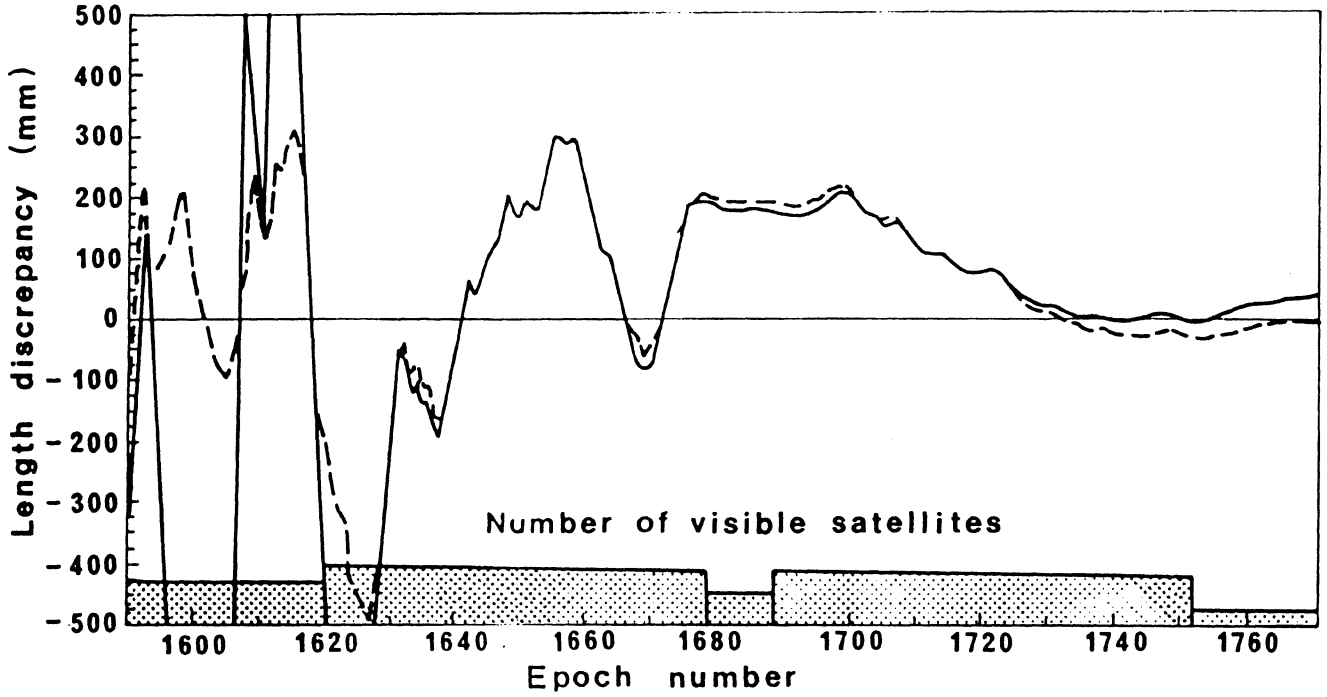

- - - One point fixed.

——— Both points floating.

FIGURE 3. Change in the length of a 66 km baseline implied by partial solutions. Discrepancies are with respect to the final length obtained from the "one point fixed" solution.

THE QUEBEC 1984 MACROMETER ™ TEST

Comparison of phase-difference processing and network solution methods

R. Moreau
Ministère de l'Energie et des Ressources (MER)
1995 ouest, boul. Charest (1.01 B)
Sainte-Foy, Québec
Canada G1N 4H9

G. Beutler
University of Bern (UB)
Astronomical Institute
Sidlerstrasse 5, CH-3012
Bern, Switzerland

J.G. Leclerc, B. Labrecque
Université Laval (UL)
Sciences géodésiques (Pavillon Casault)
Sainte-Foy, Québec
Canada G1K 7P4

R. B. Langley and R. Santerre
University of New Brunswick (UNB)
Dept. of Surveying Engineering
Fredericton P.O.B. 4400
Canada E3B 5A3

ABSTRACT. This paper describes a 5-day test (January 1984) of three MACROMETER™ V-1000 GPS receivers, conducted by MER in Sainte-Foy, Quebec. The initial purpose was to: 1) ascertain conformity of phase-difference results with Quebec requirements for urban/suburban control densification ($\leqslant$20 mm sd relative to peripheral networks); 2) verify instrumental behaviour in adverse conditions such as very low temperatures and an environment favouring multi-path signal reception. The test base comprised 16 ground points, with spacings 200 to 2000 metres: especially meticulous terrestrial methods provided the classical geodetic parameter values for purposes of comparison. Eighteen independent lines were measured by GPS. Phase difference processing results obtained by INTRFT/LSQT and PRMAC-3 are compared and found almost identical. In the comparison between GPS coordinates and terrestrial values, it is found that, after removal of inter-system distortion and terrestrial random error, estimated GPS densification accuracies are better than 5 mm rms in each coordinate. It is shown also that rigorous network processing by PRMNET yields better formal accuracy estimates than standard geodetic computations applied to single-line GPS results. It is concluded that despite adverse observation conditions, much better accuracy than initial requirements has been achieved, and that many applications more stringent than urban/suburban densification may also benefit from GPS.

INTRODUCTION

Early information, eg (FGCC 1983) encouraged MER to investigate further on the capabilities of the MACROMETER. A test was designed in the fall of 1983 in order to verify three-dimensional accuracies obtainable on short lines ranging from 200 to 2000 metres, for purposes of control densification in urban/suburban areas (present Quebec specifications require a sd of + 20 mm or less on lines in such networks). Existing points determined by conventional methods were chosen as two test bases: a 13-point configuration in the Sainte-Foy network and a 3-point configuration on Université Laval campus. Field preparation and general coordination of the MACROMETER experiment were contracted to Michel Perron et Associés (MPA) of Ville St-Laurent, Quebec; measurements and computations were subcontracted by MPA to Geohydro (GH) of Maryland. The measurements took place during the last week of January, 1984. Thus the test was conducted in a difficult environment (multi-path reception due to the variety of flat surfaces found in urban areas) and under adverse climatic conditions. The GPS results of the 18 independent lines were furnished by MPA/GH in March 1984 (processing by programs INTRFT/LSQT). Terrestrial coordinates for the test bases were provided by Service de la géodésie du Québec and UL.

In the following sections, comparisons will be made between LSQT results and those obtained by PRMAC-3 (UB/UNB with collaboration of UL), internal and external consistencies of GPS results will be shown, and network solutions will be discussed, in particular program PRMNET (UB/UNB). The paper will be concluded by practical and technical considerations from MER and UL.

TEST BASES

The high-quality terrestrial measurements of the 70-point Sainte-Foy network were processed by standard least-squares programs TOGAS and ASTRAL for horizontal and vertical adjustments respectively. Figure 1 shows the 13-point configuration chosen from the said network for the purpose of GPS testing. Though of somewhat better quality than usual urban networks, the Ste-Foy test base cannot be regarded as "absolute truth": some distortion is to be expected from various causes such as constraint to so-called "higher-order" points, measurement and centering uncertainties amounting to several mm and also possibility of slight movement of the points themselves between the terrestrial and GPS measurements. Coordinates and formal accuracy estimates may be found in (Champagne 1984). The Université Laval points however, can be considered of ultra-high stability; also the length and levelling measurements were very precise; they are indicated in (Jobin 1984).

MACROMETER MEASUREMENTS

Simultaneous phase-variation measurements were obtained by means of three MACROMETER V-1000 GPS receivers. The 5-to-6 hour "visibility periods" of the NAVSTAR system were divided in two for the Sainte-Foy configuration, resulting in 4 independant lines being measured per day; the full period was exploited for the 2 UL lines. In all, 5 days were spent on the test (Jan 26 to 30 incl.) as initially scheduled, no time having been lost. The day by day production of GPS lines is symbolized in Figure 1. The coordinate differences, relative to the indicated "base" points, and resulting from the INTRFT/LSQT processing are listed in (Perron 1984).

SINGLE-LINE SOLUTIONS

The line-by-line computations of the GPS coordinate differences were obtained at UNB using program PRMAC-3 (Beutler 1984). Comparisons between these results and those from INTRFT/LSQT are shown in Table 1 (Beutler et al 1985) for all except two of the lines. The results on these were not comparable for reasons of data editing (06-27) and of a mistake in the UT1-UTC correction in the LSQT processing (33-29). For both programs, much the same observations were input (see n_1 and n_2). Also coordinates of the pole, universal time parameters, as well as satellite ephemerides (Macrometrics T-files), were identical in both cases. As can be concluded from Table 1, agreement is excellent between the two programs: rms differences being less than 1 mm in latitude and longitude and little more than 1 mm in height.

SIMPLIFIED NETWORK SOLUTIONS

Under this heading are summarized the detailed initial analyses and comparisons from (MOREAU 1984). The GPS coordinate-difference values are those computed by INTRFT/LSQT programs. The network solutions are termed "simplified" in that they treat the GPS single-line results as any other geodetic measurement.

Planimetry (internal consistency)

When considering only the independent lines in the Sainte-Foy network, there is little redundancy. To obtain as detailed a view as possible of the internal consistency of the GPS measurements, a traverse approach was initially used, in opposition to simultaneous least squares processing which in certain cases might "spread about" local inconsistencies. Using as origins two points (30 and 32) which had also been held fixed in the conventional adjustment of the terrestrial values, GPS coordinate differences (Perron 1984) were cumulated, yielding 2 values for 33, one each for 17, 20 and 77, and 3 each for 06 and 43. Discrepancies with respect to the means at 33,06 and 43 are shown in Table 2. Values of "n" indicate discrepancies due to one line (point 33) or to two lines (other two points). In this manner single-line rms dispersion is found to be 3.4 and 2.7 mm in North and East respectively.

A classical simultaneous least-squares adjustment was also exercised on the same portion of the GPS network ("free" adjustment except for translation constraint at 30 and 32). Each independent GPS line was expressed in azimuth and length weighted identically. Error ellipse information indicated practically identical standard deviations for each line: approximately 2.5 mm in each of N and E. Thus the least-squares solution gives a slightly more optimistic view of the internal consistency within the redundant part of the GPS network. It was noted that independently of the method used, the "free GPS" coordinates obtained for the extreme points 06 and 43 were identical.

Heights (internal consistency)

In similar fashion, GPS height differences were accumulated from point 33 out to points 06 and 43. In this case six discrepancies are available, as shown in Table 2. The rms result is for a single line (initial result divided by $\sqrt{2}$): $\pm$ 5.1 mm.

The corresponding least-squares free adjustment yielded a slightly better estimate of GPS height-difference internal consistency: standard deviation ± 4.1 mm. As with planimetry, the "free GPS" heights obtained for 06 and 43 were identical between the traverse and least squares solutions.

Planimetry (external consistency)

The method adopted for comparing GPS with terrestrial values is the same as that recommended for doppler densification (Moreau 1981). A minimum of three base points is required, and their official (terrestrial) values are assumed correct. In this case, the mid-point between 30 and 32 serves as the base point (p = 30/32) of zero correction, since the official terrestrial values were there assigned to the GPS network. The discrepancies noted at points 06 and 43 are then used to establish corrective terms by bilinear interpolation for all the GPS values. This is meant to remove not only scale and orientation differences but also local distortion between the two systems. In the particular case of the Sainte-Foy network, the corrections at the bases were found to be: $CN_{30/32} = 0$; $CN_{06} = -21$ mm; $CE_{06} = +8$ mm; $CN_{43} = +1$ mm, and $CE_{43} = +7$mm (N and E stand for North and East, C stands for correction to the GPS value to convert it to the terrestrial value). For the general point "p", corrections are

$$CNp = FN' \times \Delta Np + FE' \times \Delta Ep \quad (1)$$
$$CEp = FN'' \times \Delta Np + FE'' \times \Delta Ep \quad (2)$$

Where ΔN and ΔE are plane coordinate differences between 30/32 and p, and FN and FE are the conversion factors computed after solving equations 1 and 2 using above numerical values for the C's at 06 and 43. Values of CN and CE are applied to the initial discrepacies DN and DE to give final discrepancies δN and δE. These are now assumed corrected for the systematic part of the TERR (terrestrial) system error: however they still contain the random TERR uncertainties. According to (Champagne 1984) the standard deviation of a coordinate difference is ± 7 mm: this must be subtracted quadratically from the global "σ" to obtain an estimation of σ_{GPS}. Numerical values observed and computed are shown in Table 3. Thus, after removal of inter-system distortion and the estimated random part of the terrestrial coordinate errors, it is found that GPS discrepancies are approximately 4 mm rms in each axis for two-hour observations and about 1 mm for 5-hour observations, on lines within 200 to 2 000 metres.

Heights (external consistency)

As in the preceding section a zero-point was chosen, in this instance no 33: $CH_{33} = 0$. Numerical values $CH_{06} = +43$ mm and $CH_{43} = +29$ mm resulted from the traverse and free adjustment computations previously mentionned. The equation for the correction at point "p", with Δ's counted from 33, was found to be:

$$CHp = -0.01613 \times \Delta Np + 0.00705 \times \Delta Ep \quad (3)$$

where CH is in mm and ΔN, ΔE in metres. It is to be noted here that the conversion factors represent the tangents ($\times 10^3$) of the components of the deviation of the vertical, since GPS values are deemed relative to the spheroid whereas MSL (terrestrial) values are considered relative to the geoid. Table 4 shows the detailed discrepancy values; for the final evaluation of σ_H for GPS alone, the formal estimations (Champagne 1984) of the MSL height difference

uncertainties are subtracted quadratically from the global rms values of δ H. Thus, after removal of the apparent geoidal slope effect and the estimated terrestrial random error, the estimated GPS uncertainty for one line (elevation difference) is nearly 5 mm rms for 2-hour observations and around 3 mm for 5-hour observations, on lines 200-2000 metres long. As mentioned in (Beutler et al 1985), loop misclosure analysis has pointed to the strong possibility of a blunder in antenna-height measurement on one of the lines in the redundant part of the Ste-Foy network: the dilution of this error throughout the network could well account for a slightly larger sd in heights than in planimetry.

RIGOROUS NETWORK SOLUTION

In this section information contained in (Beutler et al 1985) is summarized. The network solution developped by UB/UNB is embodied in program PRMNET which uses as input the GPS single-difference phase outputs produced by Macrometrics' program INTRFT. PRMNET derives the so-called "double-differences", simultaneously optimizes the ambiguity parameters and performs a three-dimensional least-squares solution (Beutler et al 1984). The Sainte-Foy observations were used in a free adjustment centered on point 77. The formal sd values obtained for coordinate differences in the redundant part ot the network were $\sigma_N \approx 1$ mm, $\sigma_E \approx 1.5$ mm and $\sigma_H \approx 2$ mm, which values are 50% smaller than the formal sd's of the classical least-squares solutions exercised individually in planimetry and heights. Also, in comparison with the independent single-line solutions, PRMNET introduced a substantial improvement (ratio 2.5 to 1) in the fractional part of the non-integer estimates of the ambiguity parameters. For comparing with the terrestrial coordinates, a Helmert tranformation centered on the centroid of all 13 points was performed. Resulting differences (GPS minus TERR) were 9.4, 6.1 and 7.5 mm rms in N, E and H respectively. The fact that such a transformation does not account for distortion as does the bilinear one, explains the larger horizontal discrepancies. However in the vertical, where the inter-system difference is essentially due to geoid slope, and both the Helmert and bilinear methods are essentially equivalent, it is noted that PRMNET is superior.

It is therefore expected that the best manner of computing GPS data for densification comprises an initial free adjustment using a rigorous approach such as with PRMNET, completed by constraint to the three official peripheral base points by means of the bilinear interpolation method. In cases where a group of GPS points could be tied to more than three official geodetic base points, it is suggested that a transformation lending itself to taking distortion into account, such as an affine transformation, be used following PRMNET.

CONCLUSIONS

To a high degree of certainty it is concluded that:

1. GPS phase-variation measuments easily meet accuracy criteria for Quebec urban/suburban densification, even in the presence of adverse observational conditions.
2. Other more stringent applications such as for earth works deformations and geodynamics measurements, are feasible.
3. Macrometrics' as well as the independently-developped software at UB/UNB correctly process the GPS phase-variation data for the short lines of the test.

Further investigation is in progress at UL since a preliminary study in 1983/84 (Leclerc 1984). Particular attention is being given to predicting behaviour of signals on longer lines, especially in the matters of refraction and of the effect of earth rotation between the times of arrival at the various receivers.

On the question of cost-effectiveness, it was pointed out in (Moreau 1984) that there is a high probability of GPS costs for urban/suburban densification becoming lower than those of actual methods when the full NAVSTAR constellation becomes operational. However immediate cost-effective applications can be found in engineering and geodynamics especially in cases where line-of-sight methods are difficult, such as when suitably stable reference points are relatively far from the points to be monitored, and standard methods require many costly intermediate points.

REFERENCES

Beutler, G., 1984: GPS carrier-phase difference observation software, University of New Brunswick, Fredericton, N.B.

Beutler, G., Davidson, D.A., Langley, R.B., Santerre, R., Vanicek, P., Wells, D.E., 1984: Some theoretical and practical aspects of geodetic positionning using carrier-phase difference observations of GPS satellites, University of New Brunswick, Fredericton, N.B.

Beutler, G., Langley, R.B., Santerre, R., 1985: UNB contribution to the Quebec 1984 Macrometer test, University of New Brunswick, Fredericton, N.B.

Champagne, M., 1984: Coordonnées terrestres du réseau de Sainte-Foy, Service de la Géodésie du Québec, Sainte-Foy, Québec.

Federal Geodetic Control Commitee (FGCC), 1983: Report on test and demonstration of MACROMETER V-1000, report FGCC-IS-83-2, Rockville, Maryland.

Jobin, J., 1984: Coordonnées terrestres du réseau de l'Université Laval, Département des sciences géodésiques et de télédétection, Université Laval, Sainte-Foy, Québec.

Leclerc, J.G., 1984: Etude préliminaire du récepteur Macrometer, Département des sciences géodésiques et de télédétection, Université Laval, Sainte-Foy, Québec.

Moreau, R., 1981: Integrated densification by doppler, ACSM technical papers, 1981 Fall Meetings, San Francisco, CA.

Moreau R., 1984: Projet GPS 1983/84, Domaine territorial/recherche-développement, Sainte-Foy, Québec.

Perron, M., 1984: Positionnement GPS à l'aide de l'équipement Macrometer, Michel Perron et Associés, Ville St-Laurent, Québec.

FIGURE 1

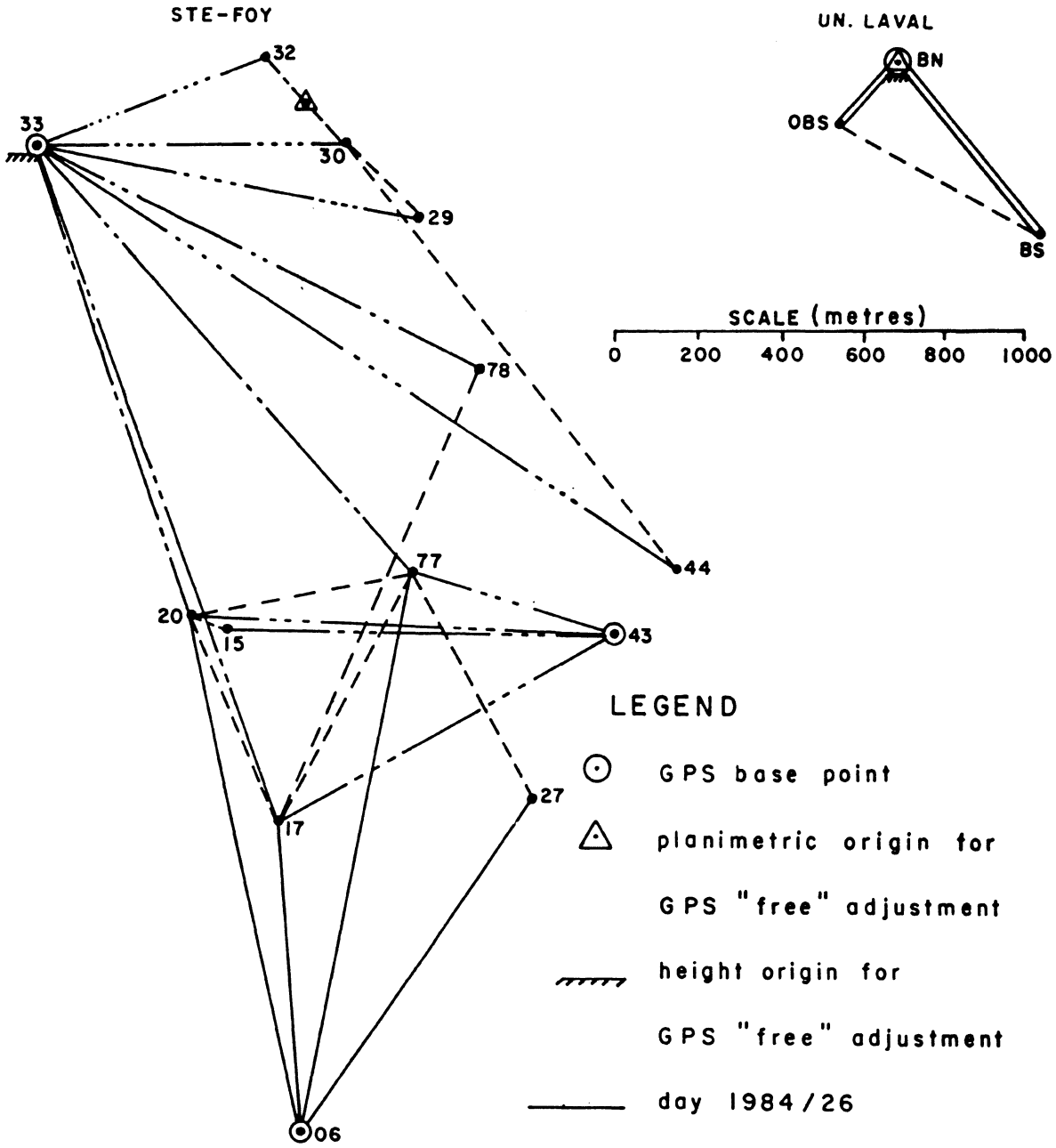
STE-FOY
32
33
30
29
78
44
77
20
15
43
27
17
06
UN. LAVAL
BN
OBS
BS
SCALE (metres)
0 200 400 600 800 1000
LEGEND
GPS base point
planimetric origin for GPS "free" adjustment
height origin for GPS "free" adjustment
day 1984/26
day 1984/27
day 1984/28
day 1984/29
day 1984/30
dependent lines

TABLE 1

COMPARISON OF SINGLE-LINE PROCESSING METHODS
(PRMAC-3 MINUS INTRFT/LSQT)

LINE	N1	N2	DELTA LAT. (MM)	DELTA LONG. (MM)	DELTA HGT. (MM)	DELTA LENGTH (MM)	DELTA LENGTH (PPM)
06,17	104	106	-0.6	0.4	-2	-0.5	0.7
06,20	103	105	-0.3	0.4	-1	-0.4	0.3
06,77	112	124	-0.6	0.6	0	-0.4	0.3
33,20	96	96	0.6	0.4	1	-0.6	0.5
33,77	106	112	0.9	-0.8	1	-1.4	1.0
33,17	126	130	0.3	-0.6	0	-1.0	0.6
33,78	121	135	0.9	-0.2	-2	-1.2	1.0
43,77	115	118	0.3	0.4	0	0.0	0.0
43,17	118	120	0.6	-1.0	2	0.3	0.3
43,20	132	141	-0.9	0.2	2	0.2	0.2
43,15	127	139	-1.2	0.0	2	0.1	0.1
33,32	116	120	-1.2	0.6	-2	0.3	0.5
33,30	116	120	-1.2	1.0	1	0.9	1.2
33,44	125	135	-0.3	0.4	0	0.1	0.1
NO.SU	150	149	-1.2	0.4	0	0.6	1.1
NO.OA	149	147	-0.3	0.2	0	-0.1	0.4
SU.OA	152	152	0.3	-0.2	0	0.7	1.2
			rms: ±0.8	±0.6	±1.3		

N1: NUMBER OF OBSERVATIONS USED IN INTRFT/LSQT
N2: NUMBER OF OBSERVATIONS USED IN PRMAC-3

TABLE 2

TRAVERSE SOLUTIONS-INTERNAL GPS CONSISTENCY

Point no.	DETERMINATION	δN(mm)	n	δE(mm)	n	δH(mm)	n
33	1	+2	1	+1	1		
33	2	-2	1	-1	1		
06	1	-8	2	+6	2	+5	2
06	2	+1	2	-5	2	-9	2
06	3	+7	2	-1	2	+4	2
43	1	-5	2	+5	2	+4	2
43	2	+1	2	-2	2	-11	2
43	3	+4	2	-3	2	+7	2
rms values for single line:		±3.4 mm		±2.7 mm		±5.1 mm	

TABLE 3 - PLANIMETRY

COMPARISON BETWEEN GPS AND "TERRESTRIAL" COORDINATES

DETERMINATION FROM	TO	DN(GPS-TERR) mm	CN mm	δN mm	DE(GPS-TERR) mm	CE mm	δE mm
Sainte-Foy							
30	33	+19	-11	+08	-06	+01	-05
32	33	+15	-11	+04	-07	+01	-06
33	17	+09	-15	-06	+08	-06	+02
33	20	+19	-15	+04	-04	-03	-07
33	77	-03	-05	-08	+04	-05	-01
17	06	+13	-21	-08	+14	-08	+06
20	06	+22	-21	+01	+03	-08	-05
77	06	+28	-21	+07	+07	-08	-01
17	43	-06	+01	-05	+12	-07	+05
20	43	00	+01	+01	+05	-07	-02
77	43	+03	+01	+04	+04	-07	-03
43	15	+11	-13	-02	+03	-05	-02
06	27	+05	-06	-01	+17	-07	+10
33	29	-16	+02	-14	-05	-02	-07
33	78	-09	+01	-08	+13	-04	+09
33	44	-20	+05	-15	+07	-07	00
			rms:	$\pm$7.2			$\pm$5.3

global rms (GPS + TERR): $\sqrt{7.2^2 + 5.3^2}$ = 9 mm
sd of TERR alone = 7 mm
estimated sd of GPS line $\sqrt{9^2 - 7^2}$ = 5.7 mm
estimated sd of GPS: $\sigma_N \approx \sigma_E \approx$ 4 mm

Université Laval

BN	BS	length difference (GPS-TERR)	= -1.2 mm
BN	OBS	length difference (GPS-TERR)	= -0.6 mm

TABLE 4 - HEIGHTS

COMPARISON BETWEEN GPS AND MSL HEIGHTS

DETERMINATION FROM	TO	DH(GPS-MSL) mm	CH mm	δH mm
Sainte-Foy				
33	17	-25	+31	+06
33	20	-27	+20	-07
33	77	-17	+23	+06
33	78	-17	+16	-01
33	29	+06	+08	+14
33	30	-09	+05	-04
33	32	-02	00	-02
33	44	-29	+27	-02
17	06	-38	+43	+05
20	06	-52	+43	-09
77	06	-39	+43	+04
17	43	-25	+29	+04
20	43	-40	+29	-11
77	43	-22	+29	+07
06	27	-50	+34	-16
43	15	-09	+21	+12
			rms:	$\pm$ 8.1
			s.d. of MSL alone:	$\pm$ 6.5
			estimated s.d. of GPS: $\sqrt{8.1^2 - 6.5^2}$	$\pm$ 4.8 mm
Université Laval				
BN	BS	-02	+07	+5
BN	OBS	-01	+02	+1

COMPARISON OF SURVEY RESULTS FROM DIFFERENT TYPES OF GPS RECEIVERS

Alfred Kleusberg
Richard B. Langley
Rock Santerre
Petr Vaníček
David E. Wells
Department of Surveying Engineering
University of New Brunswick
Fredericton, N.B.
Canada E3B 5A3

Gerhard Beutler
Astronomical Institute
University of Bern
CH-3012 Bern
Switzerland

ABSTRACT. Observation equations for single and dual frequency GPS carrier phase measurements and their single and double differences are derived. The effects of dispersive refraction on the observables and on derived relative position vectors are discussed. Results from processing single frequency MACROMETER™ V-1000 and dual frequency Texas Instruments TI 4100 observations on the Ottawa test network both in 'baseline mode' and in 'network mode' are presented.

INTRODUCTION

Simultaneous GPS carrier phase observations have become one of most precise methods for relative geodetic positioning. Several instruments based on different hardware philosophies have been developed and their usefulness for establishing geodetic control is presently being investigated. The analysis of observations from different types of receivers and the comparison of the relative positioning results is the primary goal of this paper. Accordingly we will derive the observation equations for GPS carrier phase measurements and show the necessary modifications for 'squaring type' receivers and dual frequency observations. These equations are the basis for the differential positioning software DIPOP developed at the University of New Brunswick (Vanicek et al, 1985). This software has been applied to the reduction of observations using MACROMETER V-1000 and Texas Instruments TI 4100 receivers on the Ottawa Geodetic Test Network shown in figure 1.

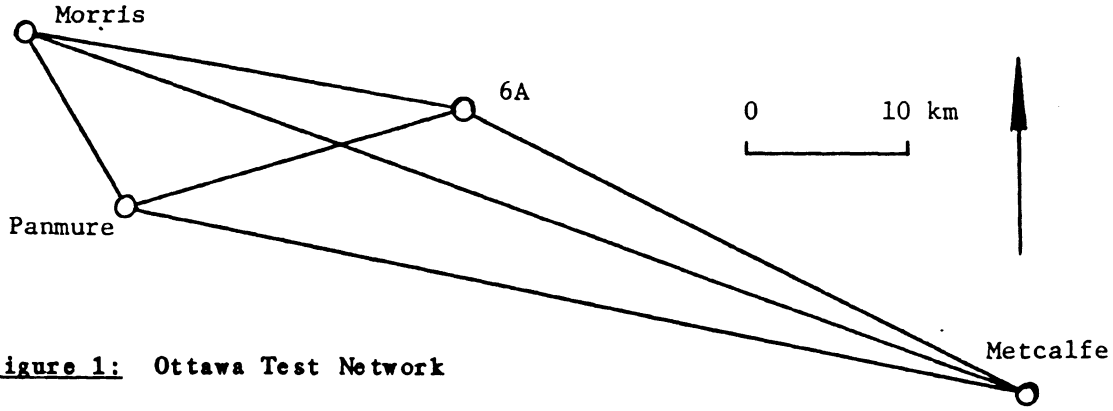

Figure 1: Ottawa Test Network

During the summer of 1983, the Earth Physics Branch of Energy, Mines and Resources Canada through a contract with GEO/HYDRO of Rockville, MD conducted Macrometer V-1000 GPS carrier phase observations on the network. The observation schedule is given in Table 1. In the spring of 1984, the network was reobserved by Nortech Surveys (Canada) Inc. of Calgary for the Geodetic Survey of Canada using Texas Instruments TI 4100 GPS receivers. The observation sessions are listed in Table 2. Further details concerning the Macrometer observations have been given by Valliant (1984). The TI 4100 observations have been discussed by McArthur (1984) and Vanicek et al. (1985).

Table 1: Macrometer V-1000 observations

Baseline	Number of Sessions	Observation time per Session [h]	Approximate length [m]
Panmure - Morris	2	5/5	12844
Panmure - 6A	4	5/5/5/5	21590
Morris - 6A	4	5/5/5/5	26489
Metcalfe - 6A	4	5/5/5/5	40295
Metcalfe - Panmure	4	5/5/3/3	57931
Metcalfe - Morris	3	5/5/5	66269

Table 2: Texas Instruments TI 4100 observations

Baseline	Number of Sessions	Observation time per Session [h]	Approximate length [m]
Panmure - Morris	2	5/5	12844
Panmure - 6A	2	5/5	21590
Morris - 6A	2	5/5	26489
Metcalfe - 6A	1	5	40295
Metcalfe - Panmure	1	5	57931
Metcalfe - Morris	1	5	66269

CARRIER PHASE OBSERVATION EQUATION

The basic GPS carrier phase observable is the phase P_i^k of the intermediate frequency signal (IF signal), corrupted by an unknown integer number of cycles (e.g. Bauersima, 1983):

$$P_i^k(t_{i\beta}) = P_r^k(t_{i\beta}) - P_i(t_{i\beta}) + N_i^k \qquad (1)$$

where

$t_{i\beta}$ is the observation epoch β on the time scale t_i of receiver i

$P_r^k(t_{i\beta})$ stands for phase of received signal transmitted by satellite k

$P_i(t_{i\beta})$ is the Phase of oscillator of receiver i at signal reception time

N_i^k denotes the Phase ambiguity of observation P_i^k (integer number of cycles

The phase of the received signal at reception time is equal to the phase P^k of the transmitted signal at transmission time. Thus we obtain from eqn.(1)

$$P_i^k(t_{i\beta}) = P^k(t^k(t_{i\beta})-\Delta t_i^k) - P_i(t_{i\beta}) + N_i^k \tag{2}$$

where

$t^k(t_{i\beta})$ denotes the time of satellite k at signal reception time, $t_{i\beta}$

Δt_i^k is the signal propagation delay between satellite k and receiver i

At observation epoch β, the receiver time t_i and satellite time t^k are assumed to be closely aligned to some independent time t (e.g. GPS time or UTC) according to the following expressions:

$$\begin{aligned} t^k(t_\beta) &= t_\beta^k + dt_\beta^k \\ t_i(t_\beta) &= t_{i\beta} + dt_{i\beta} \\ t^k(t_{i\beta}) &= t_\beta^k + dt_\beta^k - dt_{i\beta} \end{aligned} \tag{3}$$

with small time offsets dt_β^k and $dt_{i\beta}$. This leads to

$$\begin{aligned} P^k(t^k(t_{i\beta})-\Delta t_i^k) &= P^k(t_\beta^k+dt_\beta^k-dt_{i\beta}-\Delta t_i^k) \\ &= f \cdot (t_\beta^k+dt_\beta^k-dt_{i\beta}-\Delta t_i^k) + A^k, \end{aligned} \tag{4}$$

where we have denoted the nominal frequency of the satellite oscillator by f and its initial phase by A^k. Similarly, we replace the receiver oscillator phase by

$$P_i(t_{i\beta}) = f_R \cdot t_{i\beta} + A_i \tag{5}$$

with nominal receiver frequency f_R and initial phase A_i. The nominal receiver oscillator frequency f_R may be offset from the nominal satellite oscillator frequency by

$$df = f - f_R. \tag{6}$$

Using further the frequency–time relation

$$f \cdot t_\beta^k = f \cdot t_{i\beta} \tag{7}$$

and equations (4) through (6), we obtain from eqn.(2)

$$P_i^k(t_{i\beta}) = f \cdot (dt_\beta^k-dt_{i\beta}-\Delta t_i^k) + df \cdot t_{i\beta} + N_i^k + A^k - A_i. \tag{8}$$

The signal propagation delay is modelled by

$$\Delta t_i^k = (\rho_i^k + dI_i^k + dT_i^k) / c \qquad (9)$$

where

ρ_i^k is the geometric signal path length between satellite and receiver

dI_i^k is the signal path lengthening due to ionospheric refraction

dT_i^k is the signal path lengthening due to tropospheric refraction

and c the vacuum speed of light. Inserting eqn.(9) in eqn.(8) and replacing c/f by the carrier wavelength λ, we obtain finally:

$$\lambda \cdot P_i^k(t_{i\beta}) = c \cdot (dt_\beta^k - dt_{i\beta}) - \rho_i^k - dI_i^k - dT_i^k + \lambda \cdot (df \cdot t_{i\beta} + N_i^k + A^k - A_i) \qquad (10)$$

CARRIER PHASE DIFFERENCES

Two receivers at the i-th and j-th station may observe carrier phases of a signal transmitted by satellite k. Taking the difference between carrier phases observed at the same nominal time, we obtain the so called 'carrier phase single difference' (Davidson et al., 1983):

$$\begin{aligned} \lambda \cdot P_{ij}^k(t_{i\beta}, t_{j\beta}) &= \lambda \cdot (P_j^k(t_{j\beta}) - P_i^k(t_{i\beta})) \\ &= -c \cdot dt_{ij\beta} - \rho_{ij}^k - dI_{ij}^k - dT_{ij}^k + \lambda \cdot (N_{ij}^k + A_{ij}) \end{aligned} \qquad (11)$$

where we have abbreviated

$$(\cdot)_j - (\cdot)_i = (\cdot)_{ij}.$$

In taking the observation difference, the initial phase of the satellite oscillator and the offset of the satellite clock are removed from the observation equation.

Subtracting the single difference observed on the signal transmitted by satellite k from that observed at the same nominal time on the signal transmitted by satellite n leads to the 'carrier phase double difference':

$$\begin{aligned} \lambda \cdot P_{ij}^{kn}(t_{i\beta}, t_{j\beta}) &= \lambda \cdot (P_{ij}^n(t_{i\beta}, t_{j\beta}) - P_{ij}^k(t_{i\beta}, t_{j\beta})) \\ &= -\rho_{ij}^{kn} - dI_{ij}^{kn} - dT_{ij}^{kn} + \lambda \cdot N_{ij}^{kn}. \end{aligned} \qquad (12)$$

In taking the observation double difference, the initial phase of the receiver oscillator and the receiver clock offset are removed from the observation equation. The first term on the right hand side of eqn.(12) represents the double difference of geometric distances according to Figure 2. The distances from the i-th receiver to the satellites are referred to satellite positions slightly different from those

from the j-th receiver to the satellites. This effect is due to different signal propagation delays and errors in the synchronization of the two receiver clocks and has to be taken into account when linearizing eqn.(12) for the purpose of a least squares adjustment.

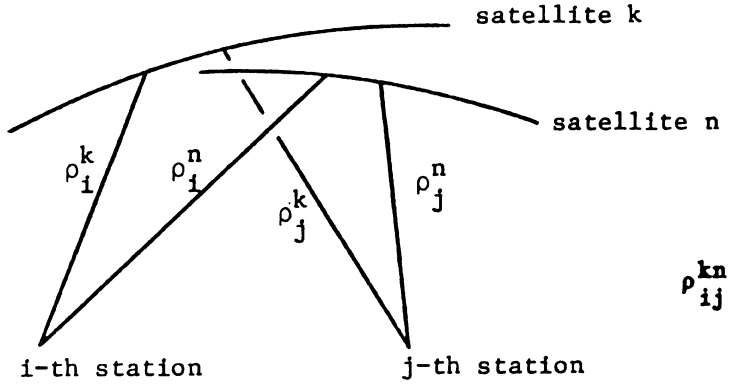

$$\rho_{ij}^{kn} = \rho_j^n - \rho_j^k - \rho_i^n + \rho_i^k$$

Figure 2: Double difference geometry

Equation (12) is the basis for the reduction of carrier phase observations by DIPOP. Two modifications are introduced to account for the specifications of the Macrometer V-1000 and the Texas Instruments TI 4100 observations. The V-1000 is a squaring type receiver and the effective wavelength in the observation equation is half the carrier wavelength (Beutler et al., 1984):

$$\lambda/2 \cdot P_{ij}^{kn}(t_{i\beta},t_{j\beta}) = -\rho_{ij}^{kn} - dI_{ij}^{kn} - dT_{ij}^{kn} + \lambda/2 \cdot N_{ij}^{kn}. \qquad (13)$$

The TI 4100 provides phase observations on both GPS carriers L1 and L2. Denoting the carrier by the subscript q we write

$$\lambda_q \cdot P_{ijq}^{kn}(t_{i\beta},t_{j\beta}) = -\rho_{ij}^{kn} - dI_{ijq}^{kn} - dT_{ij}^{kn} + \lambda_q \cdot N_{ijq}^{kn}, \quad q = 1,2 \qquad (14)$$

and using a first order approximation for the dispersive ionospheric delay

$$dI_{ij1}^{kn} = f_2^2/(f_2^2-f_1^2) \cdot (dI_{ij1}^{kn} - dI_{ij2}^{kn}), \qquad (15)$$

we obtain a linear combination of the L1 and L2 observations free of first order dispersive refraction:

$$C \cdot (P_{ij1}^{kn}/\lambda_1 - P_{ij2}^{kn}/\lambda_2) = -\rho_{ij}^{kn} - dT_{ij}^{kn} + C \cdot (N_{ij1}^{kn}/\lambda_1 - N_{ij2}^{kn}/\lambda_2) \qquad (16)$$

with

$$C = c^2 / (f_2^2 - f_1^2). \qquad (17)$$

The differential tropospheric delay dT in eqns.(13), (14) and (16) can be modelled with the well known Hopfield model (Hopfield, 1969) and standard atmospheric parameters. The use of actual temperature, air pressure and humidity seems not to be necessary for the present level of accuracy, at least on baselines with lengths shorter than about 65 km (Valliant, 1984). Due to the lack of a reasonably accurate model for the ionospheric delay, we have neglected the ionospheric refraction effect dI in the analysis of single frequency carrier phase double differences.

It has been shown by several authors (e.g. Bauersima, 1983, Davidson et al., 1983), that for baselines shorter than about 100 km the double difference observable depends only weakly on the absolute position of the receivers and the satellites. On the other hand, it is strongly dependent on the relative position of the observing stations. Therefore, if reasonably accurate orbital information is available (satellite position uncertainty less than about 50 m), no estimation of orbital parameters is performed to obtain baseline uncertainties approaching one part per million.

Thus the remaining unknowns in equations (13), (14) and (16) are the relative station coordinates and the carrier phase ambiguities.

EFFECT OF DIFFERENTIAL DISPERSIVE DELAY

To examine the effect of neglecting the differential ionospheric delay in the adjustment of single frequency carrier phase measurements, several TI 4100 dual frequency observation records have been reduced in three different ways. Firstly, we used only the L1 observations in eqn.(14), secondly, we used only the L2 observations in eqn.(14) and thirdly, we combined L1 and L2 observations for the use of eqn.(16). Before looking at the results, we note:

1) In combining L1 and L2 observations we amplify the measurement noise. Assuming some noise σ_s in the single frequency observations, uncorrelated between L1 and L2, the law of error propagation gives for the linear combination of eqn.(16)

$$\sigma_d \sim 4.1\ \sigma_s. \qquad (18)$$

Hence, if the differential dispersive delay dI is negligibly small (or constant in time, see below), the only result of combining L1 and L2 observations is an increase in the measurement noise level.

2) Any differential ionospher c delay dI, constant in time, distorts only the estimation of the carrier phase ambiguity N and does not affect the estimation of relative coordinates (c.f. equation (14)). As long as the ambiguity estimate is not forced to be an integer number, the constant part of the neglected differential dispersive delay will not show up in the residuals of a least squares adjustment.

However, if the differential ionospheric delay is not constant during the observation time span, its neglect in the modelling of the observation may cause a distortion in the estimation of the relative coordinates and will increase the estimated a posteriori variance factor of the adjustment. A typical example for this case is depicted in Figure 3. which shows the least sqares residuals of carrier phase double differences observed on the 40 km baseline Metcalfe – 6A of the Ottawa Test Network during the single TI 4100 observing session. The adjustment included

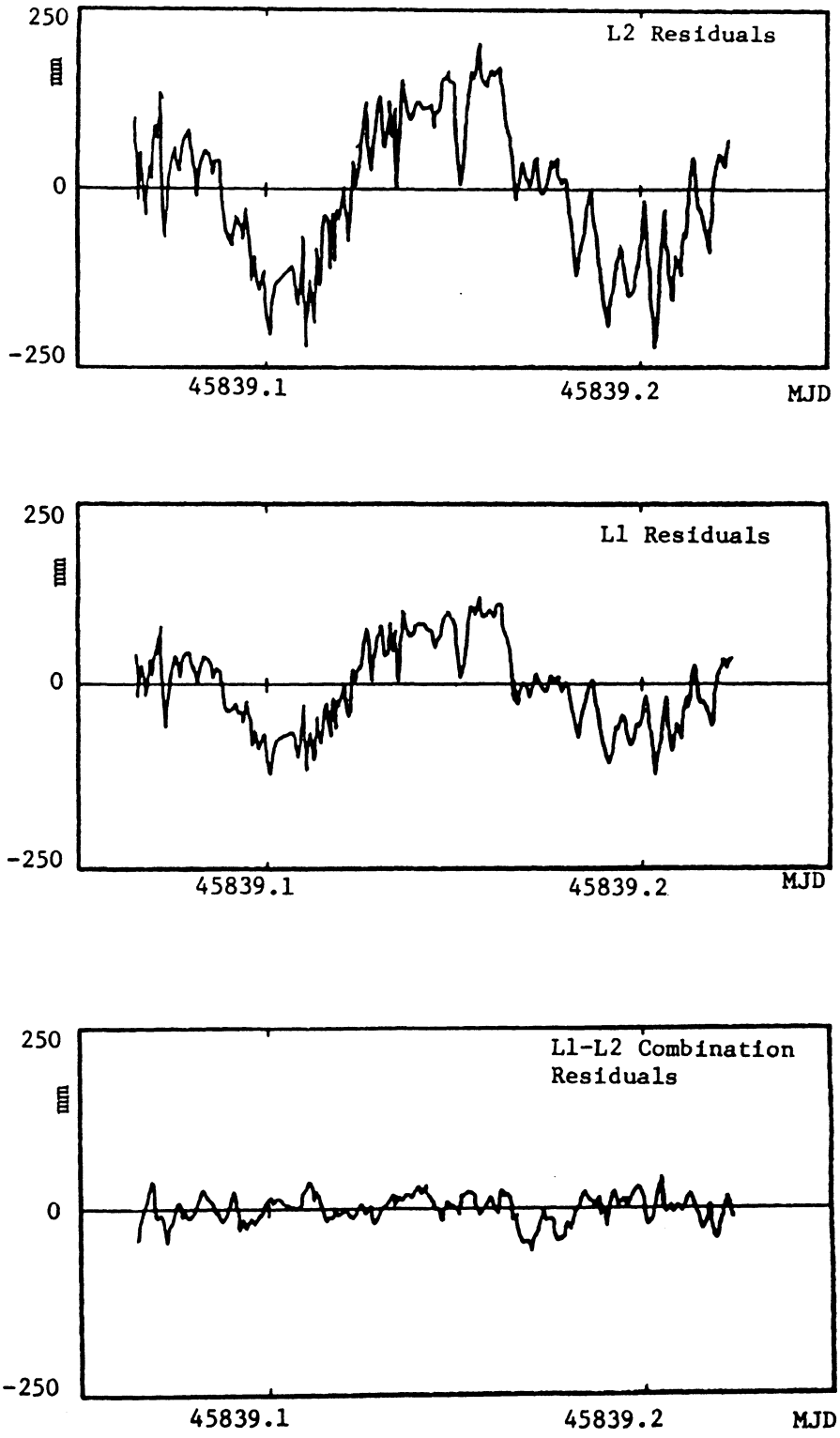

Figure 3: Single and dual frequency carrier phase double difference residuals

five hours of observations to five different GPS satellites. For the sake of clarity, only the residuals of carrier phase double differences between satellites 6 and 8 (PRN identification) are shown. A comparison of the first two plots demonstrates the dispersive character of the residuals quite clearly. The rather large systematic variations in the residuals disappear when combined observations according to eqn.(16) are used in the adjustment. The estimated precision of the carrier phase double difference observation for L2, L1 and L1-L2 combination based on the r.m.s. of the residuals was 88 mm, 55 mm and 22 mm respectively.

Table 3 gives the baseline component numerical results for the three separate adjustments. Also included are the corresponding 'ground truth' values from terrestrial measurements .

Table 3: Results for baseline Metcalfe - 6A using different carriers (Station 6A held fixed)

	Lat.Diff.	Long.Diff.	Hgt.Diff.	Length
L2 only	9'21.7883''	27'50.0261''	26.472 m	40295.542 m +/- 28 mm
L1 only	9'21.7868''	27'50.0261''	26.411 m	40295.522 m +/- 18 mm
L1-L2 comb.	9'21.7844''	27'50.0261''	26.316 m	40295.491 m +/- 7 mm
terrestrial	9'21.7935''	27'50.0170''	26.260 m	40295.429 m

The terrestrial values were obtained from the Geodetic Survey of Canada (McArthur, 1985). It can be seen, that in this particular sample only a relatively small difference exists between the baseline lengths derived from L1 only and the L1-L2 combination. The situation is quite different for the baseline components, especially the height coordinate. The height difference from the L1-L2 combination agrees with the terrestrial value reasonably well whereas the L1 solution is off by some 15 cm.

For the shorter baseline Morris - Panmure (13 km), no dispersive character such as that shown in Figure 3 was found in the residuals. The precision of a carrier phase double difference observation on this baseline was estimated as 19 mm, 12 mm and 22 mm for the L2, the L1 and the L1-L2 combined solution. The previously described increase in noise level in the combined solution compared with the L1 solution is obvious. Numerical results for the corresponding estimations of baseline components are given in Table 4.

Table 4: Results for baseline Morris-Panmure using different carriers (Station Morris held fixed)

	Lat.Diff.	Long.Diff.	Hgt.Diff.	Length
L2 only	6'15.4780''	4'14.2375''	64.432 m	12843.746 m +/- 13 mm
L1 only	6'15.4783''	4'14.2381''	64.447 m	12843.760 m +/- 8 mm
L1-L2 comb.	6'15.4788''	4'14.2389''	64.471 m	12843.782 m +/- 15 mm
terrestrial	6'15.4787''	4'14.2329''	64.540 m	12843.725 m

COMPARISON OF 'BASELINE' SOLUTIONS WITH 'NETWORK' SOLUTIONS

This section deals with the comparison of solutions for repeated Macrometer V-1000 observations of the same baseline with the solution from a network adjustment. For the three baselines involving station 6A, Table 5 gives the estimate of the station height difference and baseline length for each of the four observing sessions (denoted by day number), for the combined solution for all sessions on a particular baseline and for the network solution involving all observations of the network. Also given are the estimated uncertainties based on the observation residuals. For all 'baseline' solutions, one point of the baseline was held fixed whereas in the 'network' solution all a priori coordinates were given a weight matrix (see next section).

Table 5: Macrometer V-1000 baseline and network solutions

Baseline		Height Difference	Length
6A - Morris	Day 205	12.142 m +/- 11 mm	26488.993 m +/- 22 mm
	Day 211	12.133 m +/- 11 mm	26489.076 m +/- 22 mm
	Day 217	12.132 m +/- 6 mm	26488.955 m +/- 22 mm
	Day 223	12.109 m +/- 6 mm	26488.955 m +/- 22 mm
	All Days	12.127 m +/- 4 mm	26488.984 m +/- 7 mm
	Network	12.150 m +/- 5 mm	26489.007 m +/- 7 mm
6A - Panmure	Day 206	76.584 m +/- 9 mm	21590.242 m +/- 14 mm
	Day 212	76.557 m +/- 7 mm	21590.287 m +/- 12 mm
	Day 218	76.574 m +/- 10 mm	21590.279 m +/- 12 mm
	Day 224	76.551 m +/- 15 mm	21590.255 m +/- 27 mm
	All Days	76.574 m +/- 5 mm	21590.266 m +/- 7 mm
	Network	76.575 m +/- 5 mm	21590.235 m +/- 6 mm
6A - Metcalfe	Day 204	26.294 m +/- 13 mm	40295.442 m +/- 27 mm
	Day 210	26.271 m +/- 12 mm	40295.489 m +/- 24 mm
	Day 216	26.361 m +/- 10 mm	40295.460 m +/- 18 mm
	Day 222	26.372 m +/- 29 mm	40295.466 m +/- 27 mm
	All Days	26.317 m +/- 6 mm	40295.446 m +/- 11 mm
	Network	26.289 m +/- 6 mm	40295.454 m +/- 8 mm

It can be seen from Table 5, that the combined solution for all sessions agrees with the network solution in length at the 1 ppm level. The agreement for the height differences is better than 3 cm. However, the single session solutions disagree with the network solution by up to 3 ppm in length and 8 cm in height differences.

Figure 4 depicts the discrepancies between the single session solutions and and the combined solution for the horizontal baseline components relative to station 6A and their error ellipses (95% confidence level). It can be seen, that the single session solutions and the combined solution for the baselines 6A-Panmure and 6A-Metcalfe agree within their estimated error ellipses whereas for baseline 6A-Morris the result of day 211 is off by about 10 cm.

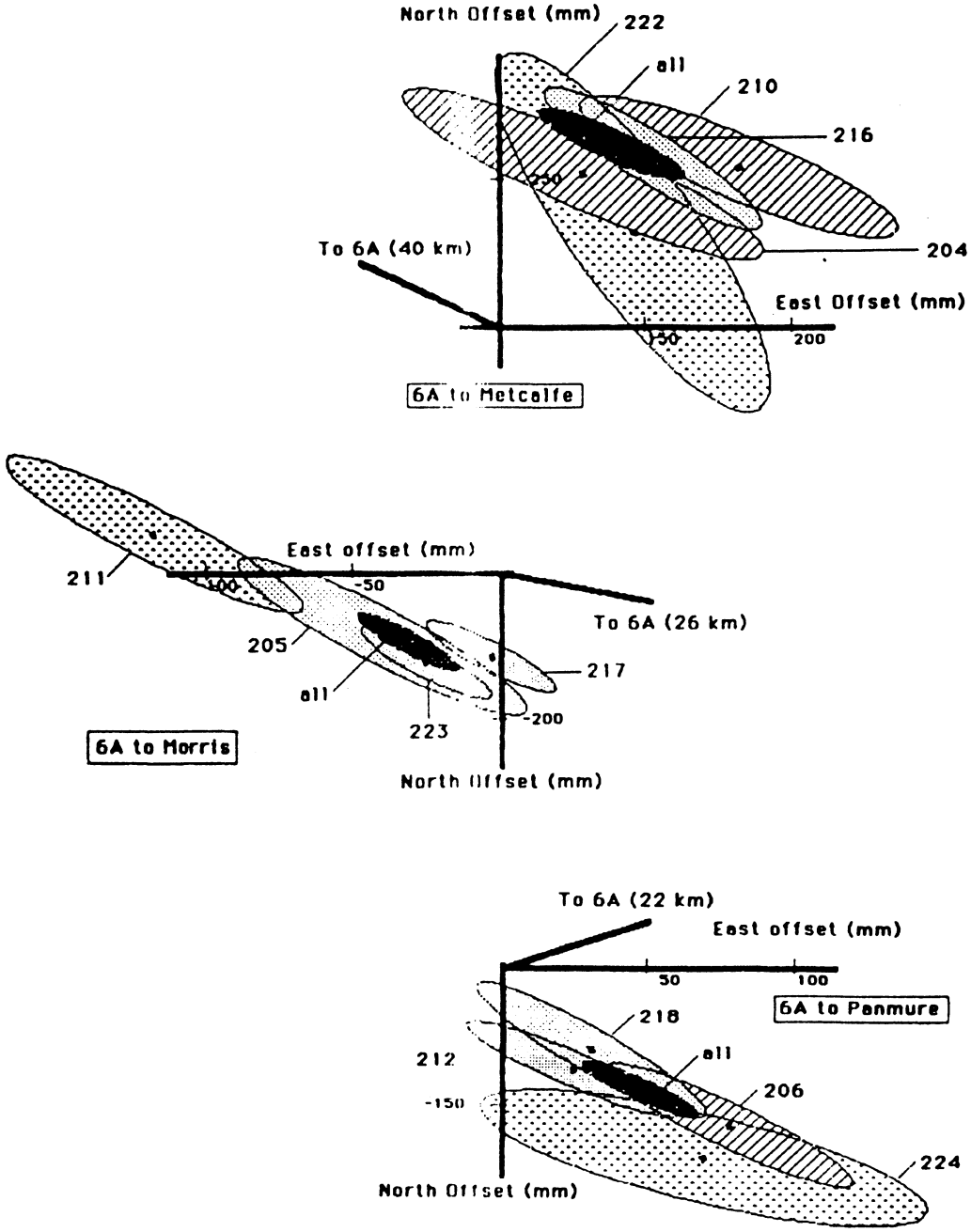

Figure 4 : Comparison of single session solutions with combined solution for all sessions

COMPARISON OF MACROMETER V-1000 AND TEXAS INSTRUMENTS TI 4100 RESULTS

In this section we compare 'network solutions' of DIPOP for the Macrometer V-1000 and Texas Instruments TI 4100 observations on the Ottawa Test Network described in the introduction. The TI 4100 results discussed here are derived from linear combinations of L1 and L2 observations according to eqn.(16). We restrict ourselves to a rather short description, more details can be found in Vanicek et al., (1985a).

The a priori coordinates of the stations were obtained from the Geodetic Survey of Canada (McArthur, 1985). These coordinates were given an a priori weight corresponding to a standard deviation of 1 m. The numerical results for estimated baseline components and baseline lengths are given in Table 6.

Table 6: Comparison of V-1000 and TI 4100 network results

Baseline		Diff. in Latitude	Diff. in Longitude	Diff. in Height	Length
6A - Morris	terr.	2'38.5068''	-19'57.4134''	11.98 m	26488.986 m
	V-1000	2'38.5012''	-19'57.4157'	12.150 m	26489.007 m
	TI 4100	2'38.4990''	-19'57.4125''	12.136 m	26488.926 m
6A - Panmure	terr.	-3'36.9719''	-15'43.1806''	76.52 m	21590.268 m
	V-1000	-3'36.9771''	-15'43.1764''	76.575 m	21590.235 m
	TI 4100	-3'36.9796''	-15'43.1739''	76.592 m	21590.209 m
6A - Metcalfe	terr.	-9'21.7935''	27'50.0170''	26.26 m	40295.433 m
	V-1000	-9'21.7848''	27'50.0238''	26.289 m	40295.454 m
	TI 4100	-9'21.7839''	27'50.0275'	26.319 m	40295.516 m
Morris-Panm.	terr.	-6'15.4787''	4'14.2329''	64.54 m	12843.725 m
	V-1000	-6'15.4783''	4'14.2393''	64.425 m	12843.773 m
	TI 4100	-6'15.4785''	4'14.2385''	64.455 m	12843.773 m
Morris-Metc.	terr.	-12'00.3003''	47'47.4304''	14.28 m	66268.707 m
	V-1000	-12'00.2860''	47'47.4394''	14.138 m	66268.752 m
	TI 4100	-12'00.2828''	47'47.4400''	14.182 m	66268.734 m
Panm.-Metc.	terr.	-5'44.8216''	43'33.1975''	-50.26 m	57930.717 m
	V-1000	-5'44.8077''	43'33.2002''	-50.286 m	57930.702 m
	TI 4100	-5'44.8042''	43'33.2014''	-50.273 m	57930.713 m

The baseline length estimated from V-1000 and TI 4100 observations agree at the ppm level with the exception of baseline 6A-Morris with a length discrepancy of 81 mm or 3 ppm. The height difference agreement is surprisingly good: the largest difference between V-1000 and TI 4100 results is 44 mm for the 66 km baseline Morris-Metcalfe. On the other hand, the GPS solutions disagree with the terrestrial height differences by as much as 17 cm in the baselines involving station Morris.

The differences in horizontal coordinates relative to station 6A between the GPS solutions and the terrestrial values are sketched in Figure 5. These discrepancies are as large as 35 cm, whereas the differences between the two GPS solutions do not exceed 10 cm. The rotation about the vertical axis between the terrestrial

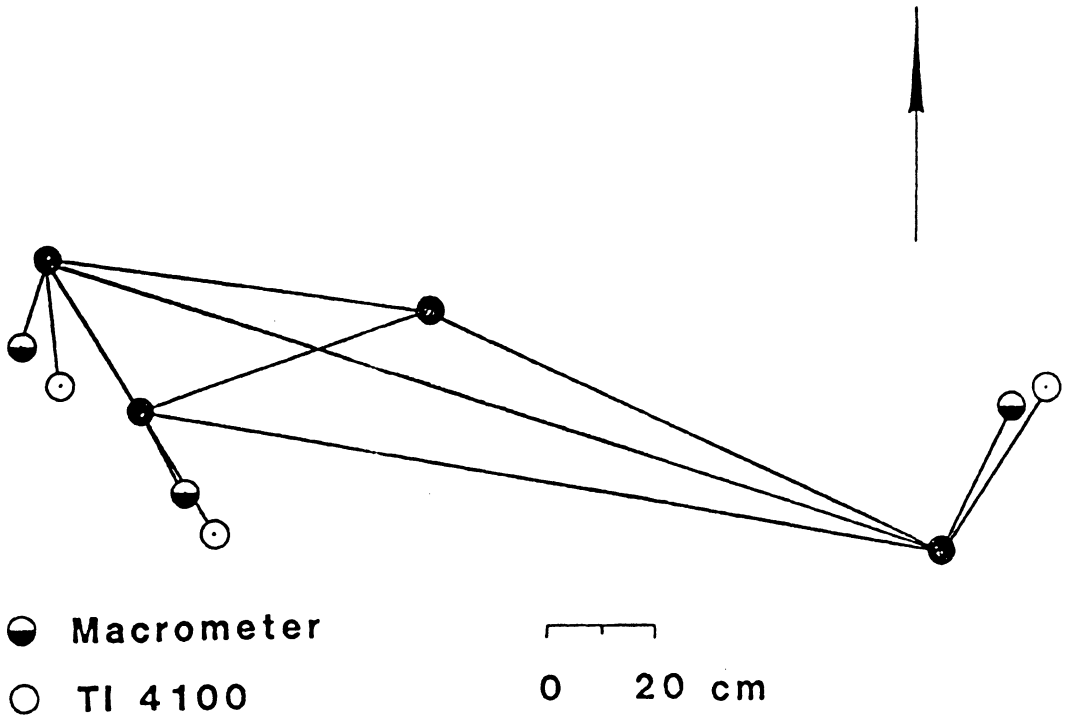

Figure 5: Discrepancies between GPS solution and terrestrial coordinates relative to station 6A

coordinates and the solutions from GPS observations is quite obvious, it amounts to 1.5'' for the Macrometer V-1000 result and 2.0'' for the TI 4100 result. More detailed information on the horizontal discrepancies of Figure 5 and the estimated accuracies of the baseline components can be taken from Figure 6. This Figure shows for each of the three baselines involving station 6A the horizontal offset of the GPS solutions with respect to the terrestrial coordinates for the other involved. Also plotted are the error ellipses (95% confidence level) based on the r.m.s. of the observation residuals.

CONCLUSIONS

We summarize our results obtained with the program DIPOP as follows:

The differential ionospheric delay may introduce errors up to 1 ppm in estimations of baseline lengths of several tens of kilometers.

Differences in baseline length obtained from single session and single baseline solutions and a combination network solution are at the 1 ppm level.

The network solutions for observations from two different receiver types agree on the 1 ppm level.

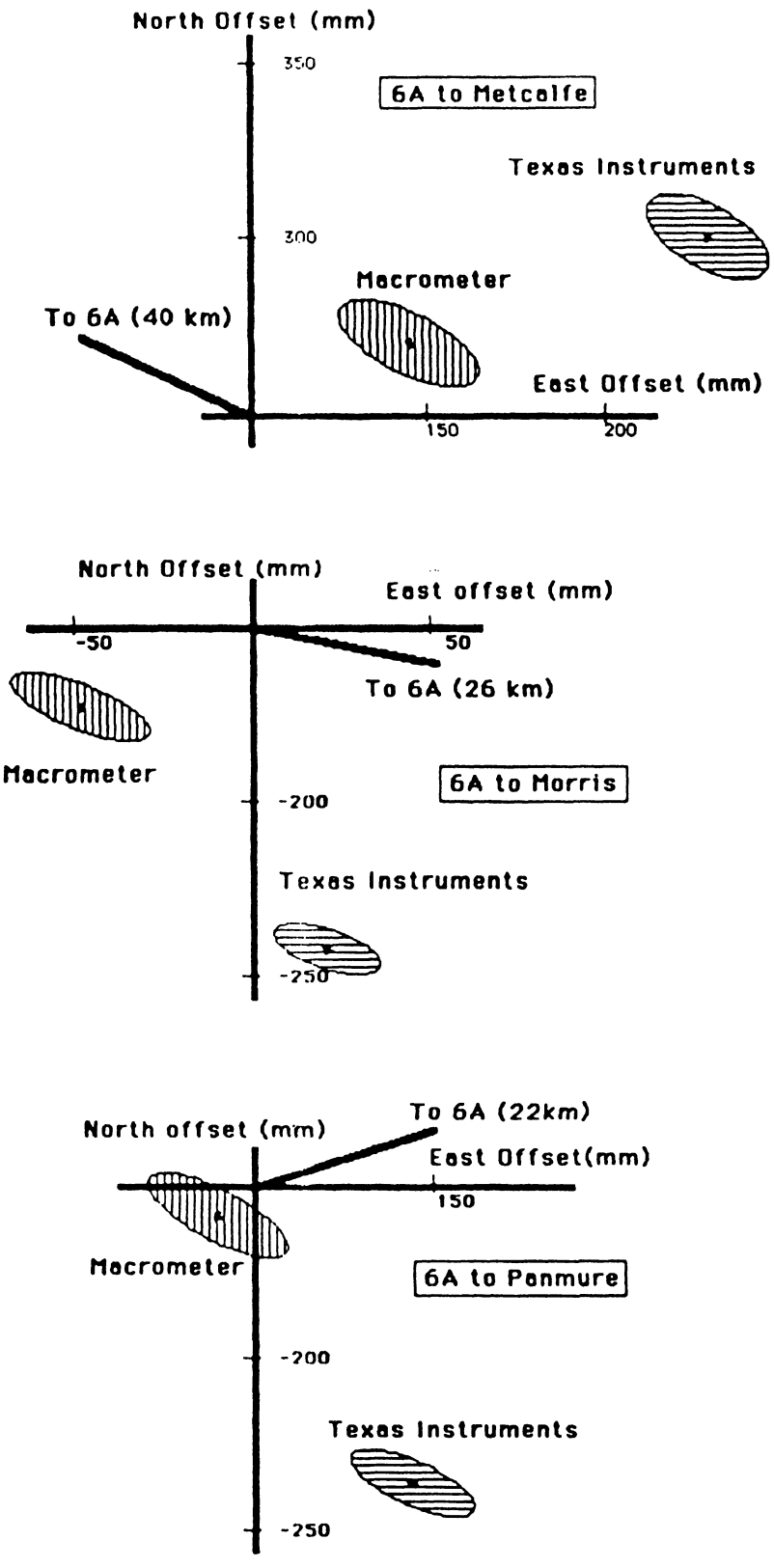

Figure 6: Offset of GPS solutions and their error ellipses with respect to terrestrial coordinates

ACKNOWLEDGEMENTS

Parts of the work reported herein were funded by the Natural Sciences and Engineering Research Council of Canada and a research contract with the Geodetic Survey of Canada. The Earth Physics Branch of Energy, Mines and Resources Canada supplied the Ottawa Macrometer data and the Geodetic Survey of Canada provided the Ottawa TI-4100 data.

REFERENCES

Bauersima, I., 1983: NAVSTAR/Global Positioning System (GPS) III, Mitteilungen der Satelliten-Beobachtungsstation Zimmerwald Nr. 12, Druckerei der Universitaet Bern

Beutler, G., D.Davidson, R.Langley, R.Santerre, P.Vanicek, D.Wells, 1984: Some Theoretical and Practical Aspects of Geodetic Positioning Using Carrier Phase Difference Observations of GPS Satellites, Technical Report No. 109, Dept. of Surveying Engineering, University of New Brunswick

Davidson, D., D.Delikaraoglou, R.Langley, B.Nickerson, P.Vanicek, D.Wells, 1983: Global Positioning System Differential Positioning Simulations, Technical Report No. 90, Dept. of Surveying Engineering, University of New Brunswick

Hopfield, H.S., 1969: Two-quartic Tropospheric Refractivity Profile for Correcting Satellite Data, Journal of Geophysical Research, Vol. 74, 4487-4499

McArthur, D.J., 1984: TI 4100 Observations at the Geodetic Survey of Canada, R+D Section, Geodetic Survey of Canada, Ottawa

McArthur, D.J., 1985: Personal communication, Geodetic Survey of Canada, Ottawa

Valliant, H., 1984: Canadian Evaluation of the Macrometer Interferometric Surveyor, EPB Open File No. 84-4, Earth Physics Branch of Energy, Mines and Resources, Ottawa

Vanicek, P., A.Kleusberg, R.B.Langley, R.Santerre, D.E.Wells, 1985: On the Elimination of Bias in Processing Differential GPS Observations, Paper presented at the First International Symposium on Precise Positioning with the Global Positioning System, Rockville, MD, 15-19 April

Vanicek, P., G.Beutler, A.Kleusberg, R.B.Langley, R.Santerre, D.E.Wells, 1985a: DIPOP: Differential Positioning Program Package for the Global Positioning System, Final Report for DSS Research Contract No. OST83-00353, Dept. of Surveying Engineering, University of New Brunswick

RECOMMENDED GPS TERMINOLOGY

David E. Wells
Department of Surveying Engineering
University of New Brunswick
Fredericton, New Brunswick
Canada E3B 5A3

ABSTRACT. A proposal for standardized GPS terminology is presented. The concepts behind the terms are defined, and the reasons for selecting particular terms are given. A Glossary of terms is appended.

INTRODUCTION

It is probable that the Global Positioning System (GPS), and perhaps other similar systems such as GLONASS, GEOSTAR and NAVSAT (McDonald and Greenspan, 1985), will find wide applications in surveying and geodesy over the next several years. The community of users and variety of equipment are both likely to be very heterogeneous. The establishment of standards is necessary to permit communication and cooperation among these users, who may employ various kinds of equipment and software.

Such communication and cooperation (and hence such standards) should exist on at least three levels. A common understanding of the concepts involved in GPS positioning requires standard terminology. The possibility for exchange of observed data requires standard data structures. The combination of results from various GPS campaigns requires consistency among these results, which would ideally be achieved by use of standard processing algorithms. In this paper an attempt is made to deal with only the first of these, a standard terminology.

Many new concepts and terms have begun to appear in the surveying literature as a result of the complexity and flexibility of GPS. This paper recommends a standard terminology for GPS which is specific enough to describe the complexities, but general enough to accomodate the flexibility of GPS and the possible use of other similar systems. A Glossary of terms, both recommended and otherwise, drawn from the recent GPS literature, appears as an Appendix.

A standard terminology is no more than a set of conventions, assigning specific meanings to a set of terms. We have tried to keep these terms as few and as simple as possible, and have included enough discussion to place them in context, and to give reasons why they are preferred over alternatives. The proposed terms are presented under eight headings: applications, satellites, signal, measurements, receivers, differencing, network solutions, and uncertainties.

As GPS continues to evolve, so will the most appropriate terminology used to describe it. This proposal should be considered as only one step in this evolutionary process. Comments and suggestions for future versions are welcome, and should be sent to the author.

A word of acknowledgement. The original version of this paper was prepared by the author and Demitris Paradissis, and presented by the latter at a meeting in Sopron Hungary in July 1984 of the Subcommission on Standards of the Committee on Space Techniques for Geodynamics. Subsequent comments and corrections were provided by Gerhard Beutler, Nick Christou, Charles Counselman, Mike Eaton, Ron Hatch, Larry Hothem, Patrick Hui, Hal Janes, Alfred Kleusberg, Richard Langley, Richard Moreau, Ben Remondi, Fred Spiess, Rock Santerre, Tom Stansell, Petr Vanicek, Richard Wong, and Larry Young. The present version was compiled from their comments, and further revised with the help of Yehuda Bock, Claude Boucher, Ron Hatch, Hal Janes, Alfred Kleusberg, and Ben Remondi. Without this extensive help, this proposal would not exist. However, errors and misconceptions which remain are the sole responsibility of the author.

APPLICATIONS

KINEMATIC (or DYNAMIC) POSITIONING refers to applications in which a trajectory (of a ship, ice field, tectonic plate, etc.) is determined.

STATIC POSITIONING refers to applications in which the positions of points are determined, without regard for any trajectory they may or may not have.

Consideration was given to basing these definitions on whether there was significant receiver motion or not, or in terms of the required accuracies. However, in the first case, the existance of receiver motion, *per se,* did not seem to introduce a fundamental difference from static applications, so long as the accuracy obtainable for instantaneous positioning is adequate. In the second case, there are examples of kinematic applications (e.g. marine 3D seismic) which may have higher accuracy requirements than some static applications (e.g. small scale mapping control).

Formally, kinematics is that branch of mechanics which treats motion without regard to its cause, which is the case here. Dynamics relates the motion to its cause. However, the term dynamic positioning has become so firmly rooted in common (mis)usage, that it may be unrealistic to expect a switch to the term kinematic positioning.

RELATIVE POSITIONING refers to the determination of relative positions between two or more receivers which are simultaneously tracking the same radiopositioning signals (e.g from GPS).

Alternatives to the term "relative" which were considered were "differential" and "interferometric". While both are valid, "differential" may be misconstrued to imply some infinitesimal process, and "interferometric" has specific, as well as general, connotations (see the discussion on this point in the Receivers section below). As well, "interferometric" emphasizes the measurement technique rather than the relative positioning application.

Real time relative positioning implies that signals (containing sufficient information for relative positioning) from all receivers are somehow broadcast in real time for processing at a central site (which may be at one of the receivers).

Because many GPS errors (clock errors, ephemeris errors, propagation errors) are correlated between observations obtained simultaneously at different sites, the relative positions between these sites can be determined to a higher accuracy than the absolute positions of the sites. In its simplest form, relative positioning involves a pair of receivers. For **kinematic relative positioning**, where the trajectory is of interest, one of these will be a monitor receiver at a known stationary location, and the other will be a mobile receiver tracing out the trajectory of interest. **Static relative positioning** involves determination of the difference in coordinates between pairs of points of a network. In this case, there is no restriction that one receiver remain at the same control point throughout the network survey (although that may be one feasible strategy). Usually at present independent baseline vectors between pairs of these points are computed as an intermediate step. When only two receivers are used for relative positioning (one baseline at a time), baselines can be considered independent. In general, using **n** receivers, the number of combinations of receiver pairs (baselines) is **n (n-1) / 2**. However, only **(n-1)** of these are rigorously independent (see the Network Solutions section below for more on relative static positioning).

SATELLITES

One confusing issue concerning GPS terminology is the numbering or identification of the GPS satellites. Several systems are used: the launch sequence number, an orbit position number, a number identifying which week of the 37-week long P-code has been assigned to the satellite (the PRN number), as well as more conventional NASA and international satellite identification numbers. Table 1 lists all these numbers for the

eleven GPS Block I (prototype) satellites. Since the satellite ephemeris message uses the PRN number to identify satellites, that is the one which has gained widest use.

TABLE 1. GPS SATELLITE IDENTIFICATION

LAUNCH SEQUENCE NUMBER	ORBITAL POSITION NUMBER	ASSIGNED VEHICLE PRN CODE	NASA CATALOGUE NUMBER	INTERNATIONAL DESIGNATION	LAUNCH DATE (YY-MM-DD)	STATUS
1	0	4	10684	1978-020A	78-02-22	crystal clock
2	4	7	10893	1978-047A	78-05-13	not operating
3	6	6	11054	1978-093A	78-10-07	operating
4	3	8	11141	1978-112A	78-12-11	operating
5	1	5	11690	1980-011A	80-02-09	not operating
6	5	9	11783	1980-032A	80-04-26	operating
7					81-12-18	launch failed
8	2	11	14189	1983-072A	83-07-14	operating
9	1	13	15039	1984-059A	84-06-13	operating
10	4	12	15271	1984-097A	84-09-08	operating
11					85-08-??	launch plan

SIGNAL

The GPS signal has a number of components, all based on the fundamental frequency F = 10.23 MHz (see Figure 1). Two carriers are generated at 154 F (called L1), and 120 F (called L2). Pseudorandom noise codes are added to the carriers as binary biphase modulations at F (P-code) and F/10 (S-code, previously called C/A-code). A 1500-bit-long binary message is added to the carriers as binary biphase modulations at 50 bits per second.

PSEUDORANDOM NOISE CODE (PRN code) is any of a group of binary sequences that exhibit noise-like properties, the most important of which is that the sequence has a maximum autocorrelation at zero lag.

BINARY BIPHASE MODULATIONS on a constant frequency carrier are phase changes of either 0° (to represent a binary 0) or 180° (to represent a binary 1). These can be modelled by

$$y = A(t) \cos(\omega t - \phi) \qquad (1)$$

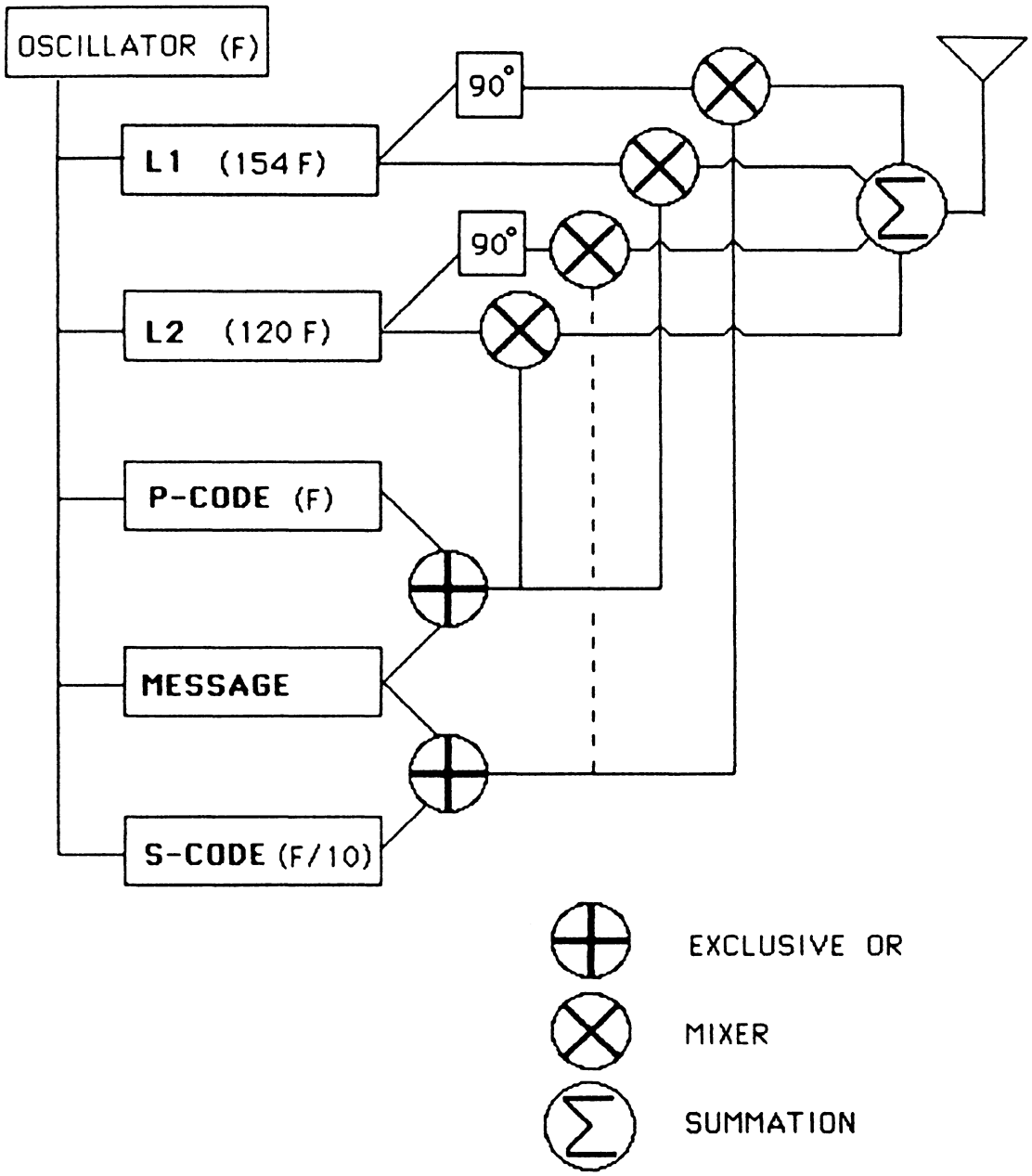

GPS SATELLITE SIGNALS

FIGURE 1

where the amplitude function **A(t)** is a sequence of +1 and -1 values (to represent 0° and 180° phase changes, respectively).

The P-code is a long (about 10^{14} bits) sequence, and the S-code is a short (1023 bit) sequence. The two codes are impressed on separate carriers that are in quadrature (the carriers are 90° apart in phase). For the present prototype (Block I) GPS satellites, and those to be used for the next decade (Block II), the S-code is normally available only on the L1 frequency. It is likely that access of civilian users to the P-code will be restricted, once the present prototype GPS satellites are replaced by production versions. Other similar systems (e.g. GLONASS) will undoubtedly have signal structures different to GPS.

MEASUREMENTS

Either the carrier or the code can be used to obtain GPS observations. In the case of carrier observations, phase is measured. In the case of code observations, usually pseudoranges are measured, but phase of the code can also be measured. Carrier measurements are subject to ionospheric phase advance, and code measurements to ionospheric group delay.

> **CARRIER BEAT PHASE** is the phase of the signal which remains when the incoming Doppler-shifted satellite carrier signal is beat (the difference frequency signal is generated) with the nominally-constant reference frequency generated in the receiver.

This term is preferable to the four alternatives "phase", "carrier phase", "reconstructed carrier phase" and "Doppler phase" for the following reasons. "Phase" does not distinguish between carrier and code measurements, for each of which phase measurements can be made (by very different techniques). "Carrier phase" implies that the phase of the GPS signal carrier itself is observed, which is not the case. "Reconstructed carrier phase" emphasizes the technique by which the signal to be observed is obtained, rather than emphasizing the signal itself. "Doppler phase" implies that the signal to be observed is due solely to the Doppler shift of the satellite carrier signal, which may not be the case (if, for example, the receiver reference frequency is intentionally offset significantly from the unshifted satellite carrier frequency).

Measurements of the carrier beat phase can be either **complete instantaneous phase measurements**, or **fractional instantaneous phase measurements**. The distinction between the two is that the former includes the integer number of cycles of the carrier beat phase since the initial phase measurement, and the latter is a number between zero and one cycles.

CARRIER BEAT PHASE AMBIGUITY is the uncertainty in the initial measurement, which biases all measurements in an unbroken sequence. The ambiguity consists of three components

$$\alpha_i + \beta^j + N_i^j \qquad (2)$$

where

α_i is the fractional initial phase in the receiver,

β^j is the fractional initial phase in the satellite, (both due to various contributions to phase bias, such as unknown clock phase, circuit delays, etc.), and

N_i^j is an integer cycle bias in the initial measurement.

The carrier beat phase can be related to the satellite-to-receiver range, once the phase ambiguity has been determined. A change in the satellite-to-receiver range of one wavelength of the GPS carrier (19 cm for L1) will result in one cycle change in the phase of the carrier. Carrier beat phase measurement resolutions of a few degrees of phase are possible. Hence the measurements are sensitive to sub-centimetre range changes.

The complete instantaneous phase measurement differs from the more familiar continuously integrated Doppler measurement only because the latter does not include this ambiguity (assumes it to be zero).

Depending on receiver design, the phase samples are made at either epochs of the receiver clock, or at epochs of the satellite clock (as transferred through the modulations imbedded in the received satellite signal). I am not aware of a receiver which uses satellite timing, however.

Delta Pseudorange is a commonly used term which incorrectly implies it is somehow associated with code measurements. In fact Delta Pseudorange is the difference between two carrier beat phase measurements, made coincidently with (code) pseudorange epochs.

PSEUDORANGE is the time shift required to align (correlate) a replica of the GPS code generated in the receiver with the incoming GPS code, scaled into distance by the speed of light. This time shift is the difference between the time of signal reception (measured in the receiver time frame) and the time of emission (measured in the satellite time frame).

Pseudoranges change due to variations in the satellite-to-receiver propagation delay, and are biased by the time offset between satellite and receiver clocks. The resolution of pseudorange measurements depends on the accuracy with which the incoming and replicated codes can be aligned. An alignment accuracy of a few nanoseconds is equivalent to metre-level range resolution.

RECEIVERS

GPS receivers have one or more channels. Two kinds of channels are useful for static positioning using carrier phase measurements: squaring type channels, and correlation type channels.

> A **CHANNEL** of a GPS receiver consists of the radiofrequency and digital hardware, and the software, required to track the signal from one GPS satellite at one of the two GPS carrier frequencies.
>
> A **SQUARING-TYPE CHANNEL** multiplies the received signal by itself to obtain a second harmonic of the carrier, which does not contain the code modulation.

The squaring concept is simply shown by squaring equation (1) to obtain

$$y^2 = A^2 \cos^2(\omega t + \phi) = A^2 [1 + \cos(2\omega t + 2\phi)] / 2 \qquad (3)$$

Since $A(t)$ is the sequence of +1 and -1 values representing the code, $A(t)^2 = A^2$ is always equal to +1 and may be dropped from equation (3). The resulting signal y^2 is then pure carrier, but at twice the original frequency. Note that for a simple squaring loop, any noise on the signal is also squared. In practice as shown in Figure 2, the incoming signal is first differenced with a local reference frequency to obtain the carrier beat phase signal, at an intermediate frequency much lower than the original carrier frequency.

This is a simple conceptual description of the squaring process which, in practice, is implemented by one of several proprietary techniques which have been developed. These proprietary techniques often involve some method of narrowing the GPS signal bandwidth from 20 MHz (due to the P-code "spreading"), to a bandwidth the order of several Hertz. Only the carrier is obtained from a squaring-type channel. Pseudoranges and the message cannot be obtained. An example of such a receiver is the Macrometer™ V-1000, a six channel receiver which does not require any knowledge of the code, capable of continuously tracking the L1 carrier beat phase second harmonic, from six satellites.

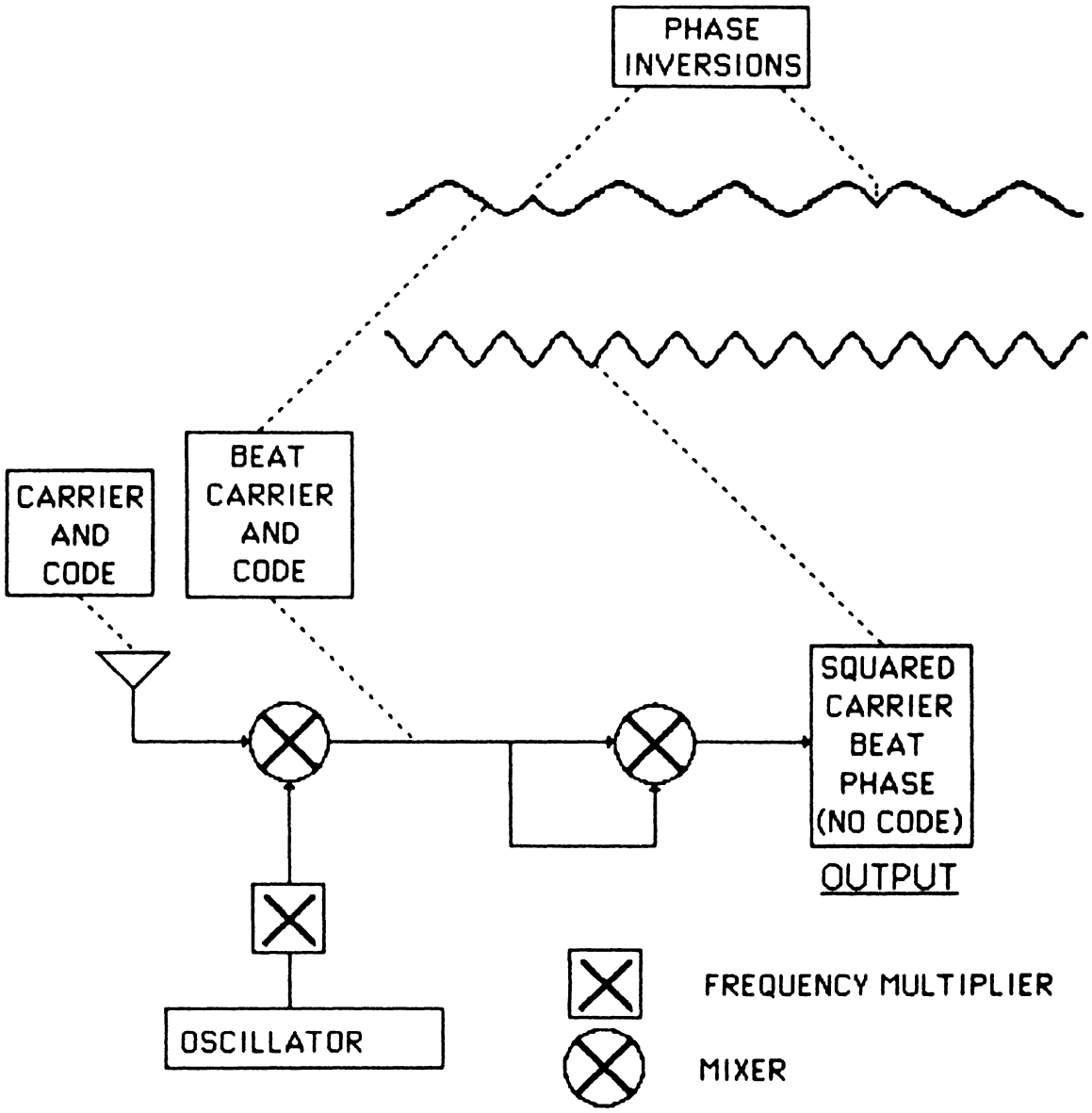

GPS SQUARING-TYPE CHANNEL

FIGURE 2

An alternative to the squaring process, which also does not require detailed knowledge of the code, is the SERIES technique [Buennagel et al., 1984] in which the GPS signal is despread by tracking the Doppler shift of the code modulation transitions, without detailed knowledge or recovery of the actual code sequences or use of the carrier.

> A **CORRELATION-TYPE CHANNEL** uses a delay lock loop to maintain an alignment (correlation peak) between the replica of the GPS code generated in the receiver, and the incoming code.

In simple terms, the code correlation concept involves generating a replica of the code sequence [the sequence of +1 and -1 values represented by **A(t)** in equation (1)] within the receiver, and to align this replica in time (correlate) with the incoming signal. Once aligned, multiplying the two codes together results in only +1 values for the resulting amplitude function. In Figure 3, the incoming signal is first reduced in frequency by differencing with a local carrier (point A). The signal resulting from multiplying this incoming signal by the local code replica (point B) will have the code removed, but only if the two codes are aligned. The correlation peak detector tests for the presence of the code, and corrects the delay (point C) of the locally generated code replica to maintain alignment, completing the delay lock loop. This time delay is the pseudorange measurement (see above). Also, once the receiver code generator is aligned to the incoming code, its output is a reading of the satellite clock at the time of signal transmission. The fourth and final kind of information obtained from a code correlation channel is the 50 bit per second message containing the ephemeris.

This is a simple conceptual description of a correlation-type channel. In practice, details of the correlation process may involve any of a number of advanced techniques (e.g. tau dither, early minus late gating), and may be implemented predominantly in hardware, or predominantly in software, depending on receiver design.

Code correlation channels may be either multiplexing or switching, depending on how the satellite message bits are accumulated.

> A **MULTIPLEXING CHANNEL** is sequenced through a number of satellite signals (each from a specific satellite and at a specific frequency) at a rate which is synchronous with the satellite message bit-rate (50 bits per second, or 20 milliseconds per bit). Thus one complete sequence is completed in a multiple of 20 milliseconds.
>
> A **SWITCHING CHANNEL** is sequenced through a number of satellite signals (each from a specific satellite and at a

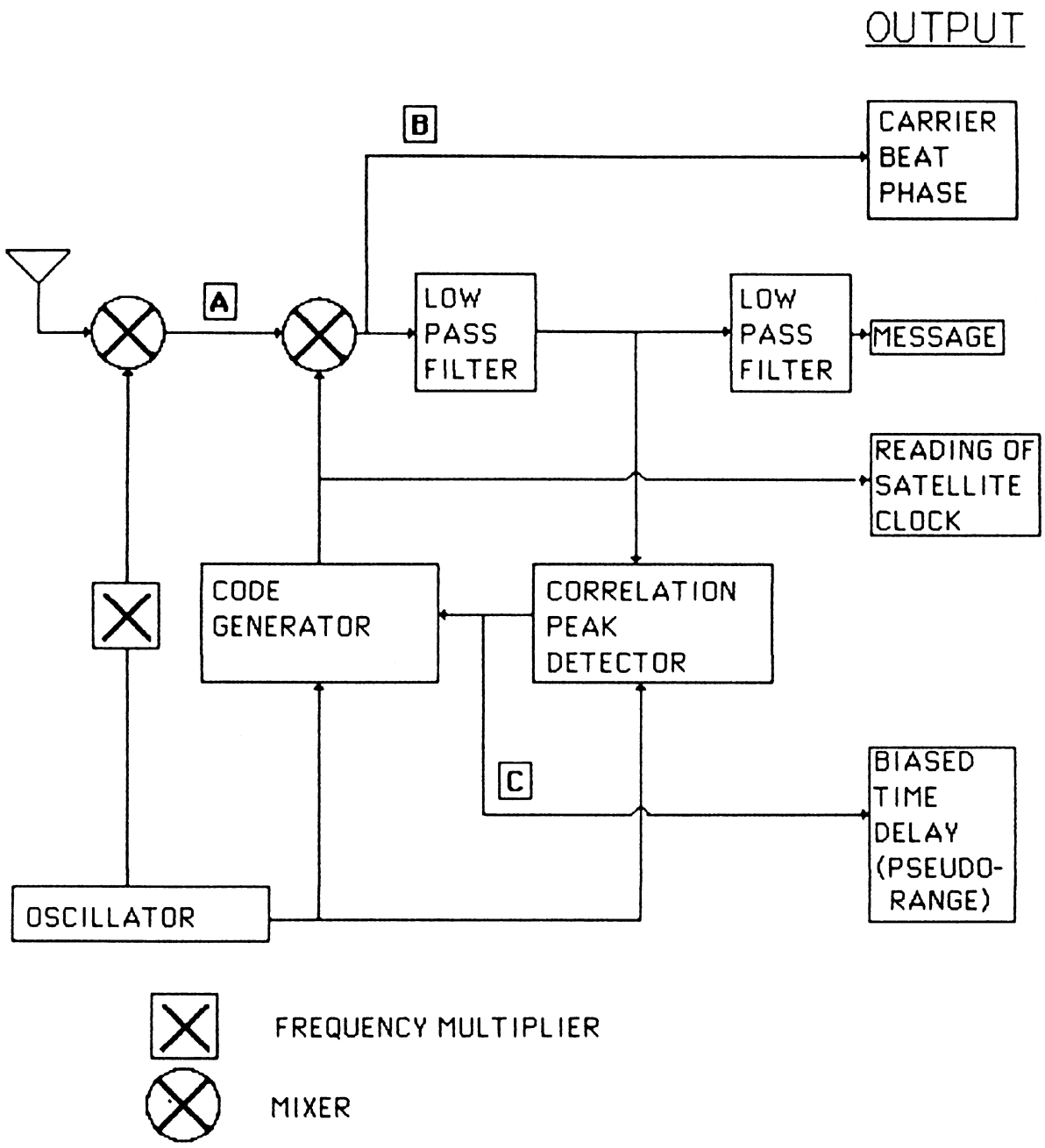

GPS CORRELATION CHANNEL

FIGURE 3

specific frequency) at a rate which is slower than, and asynchronous with, the message data rate.

A multiplexing channel builds up a map of the message from each satellite one bit (for each satellite) per sequence cycle. An example of a multiplexing receiver is the Texas Instruments 4100, which has one multiplexing channel which tracks both L1 and L2 signals from up to four satellites (a total of eight signals), dwelling on each for five milliseconds, hence taking two bit-periods (40 milliseconds) to complete one sequence. Each satellite is visited once per bit period (on alternating frequencies), in order not to lose any message bits. Software in the receiver tracks all signals in such a way that values for all signals, referred to the same epoch, can be obtained.

Switching channels may dwell on each signal for relatively short (less than a second) or relatively long (tens of seconds to hours) periods. If the sequence time is short enough for the channel to recover (through software prediction) the integer part of the carrier beat phase (in practice no more than several seconds), then the channel is a **fast-switching channel**. A switching channel builds up a map of the message from each satellite many bits per signal dwell time. In order that all parts of each satellite message are sampled, the dwell times must progress through the message (that is the sequencing must be asynchronous with the message data rate).

A receiver with many channels is a multichannel receiever. It may be that these channels are of the same type (all code correlation, or all squaring), or of different types. For example, since civil access to the P-code is expected to be restricted in the future, and the S-code is not expected to be available on the L2 carrier, a civilian dual frequency receiver must either have squaring channels for both L1 and L2, or code correlation channels for L1 and squaring channels for L2.

A multichannel switching receiver may have more or less flexibility in how the channels are used. For example, three possible scenarios are

- All channels track the same signal continuously (while the satellite is visible). For highly kinematic applications, where the receiver motion over even a fast-switching sequence period is significant, this may be the only feasible strategy.
- All channels fast-sequence through a subset of the signals to be tracked. This reduces the number of channels required (perhaps to one).
- Some channels track one signal continuously, with other channels switching through the signals (perhaps to collect ephemeris data from all visible satellites).

A very different alternative is to simply record the total GPS received signal as a "noise" signal (although it consists of carriers and codes from all visible satellites) at each station in a network, and then to extract between-receiver differences (see below) by correlating the recorded data station-pair by station-pair, and satellite by satellite. This is the interferometric approach. The receiver in this case would be very simple and inexpensive. The lack of real time quality control, however, makes this an

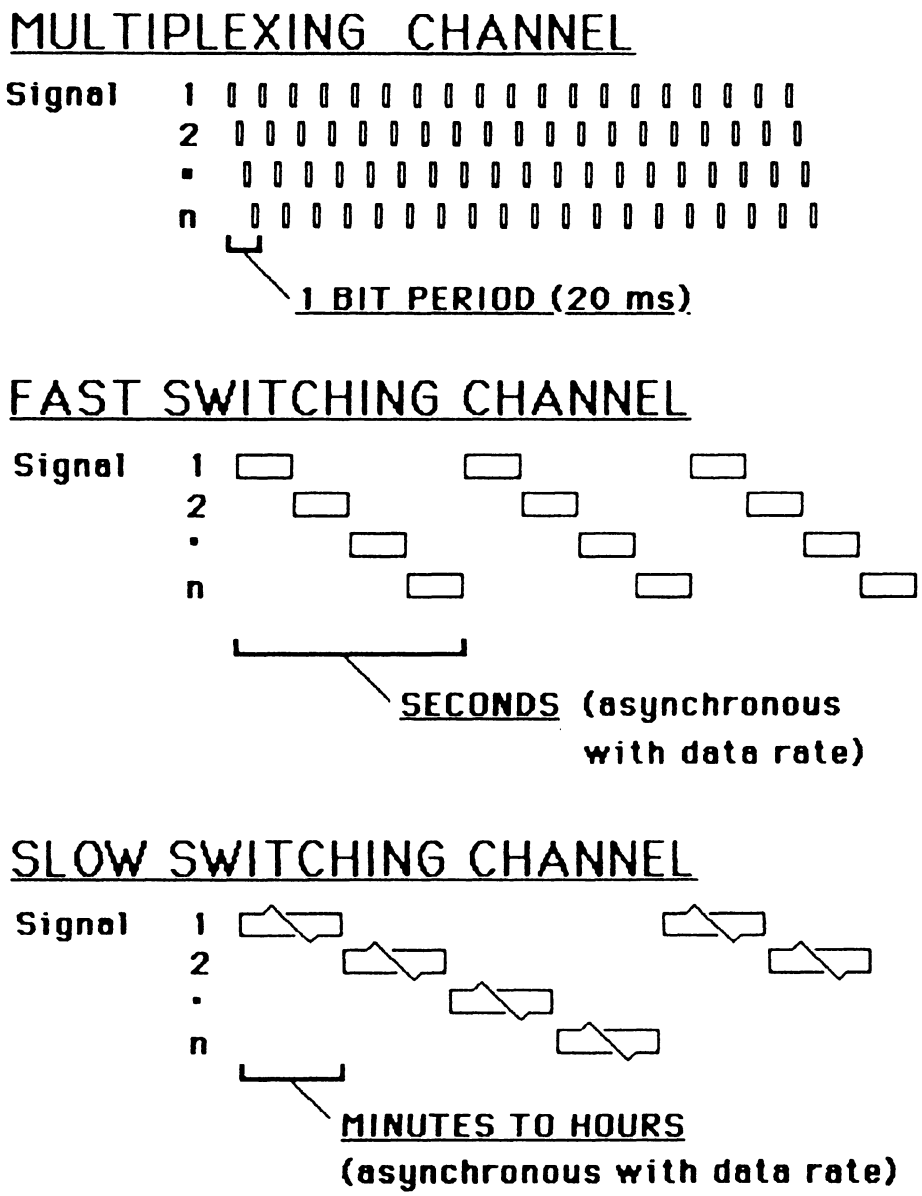

MULTIPLEXING AND SWITCHING CHANNELS

FIGURE 4

impractical option. Note that, in principle, any technique involving comparison of measurements made by two receivers could be called an interferometric technique. We have noted above the preference for using "relative positioning" in place of this more general meaning for interferometry.

DIFFERENCING

For relative static positioning, many of the errors are correlated among the various measurements which are made. One approach is to attempt to model this correlation through bias parameter estimation and correlated weighting of the observations. Another commonly used approach for processing carrier measurements involves taking differences between measurements, since this removes or reduces the effect of errors which are common to the measurements being differenced. GPS measurements can be differenced in several ways: between receivers, between satellites, between time epochs, and between L1 and L2 frequencies. Figure 5 illustrates the first three of these. All but between-epoch differences involve the concept of simultaneity.

> **SIMULTANEOUS MEASUREMENTS** are measurements referred to time frame epochs which are either exactly equal, or else so closely spaced in time that the time misalignment can be accomodated by correction terms in the observation equation, rather than by parameter estimation.
>
> A **BETWEEN-RECEIVER** carrier beat phase difference is the instantaneous difference in the complete carrier beat phase measurement made at two receivers simultaneously observing the same received signal (same satellite, same frequency).
>
> A **BETWEEN-SATELLITE** carrier beat phase difference is the instantaneous difference in the complete carrier beat phase measurement made by the same receiver observing two satellite signals simultaneously (same frequency).
>
> A **BETWEEN-EPOCH** carrier beat phase difference is the difference between two complete carrier beat phase measurements made by the same receiver on the same signal (same satellite, same frequency).
>
> A **BETWEEN-FREQUENCY** carrier beat phase difference is the instantaneous difference between (or, more generally, any other linear combination involving) the complete carrier beat phase measurements made by the same receiver observing signals from the same satellite at two (or more) different frequencies.

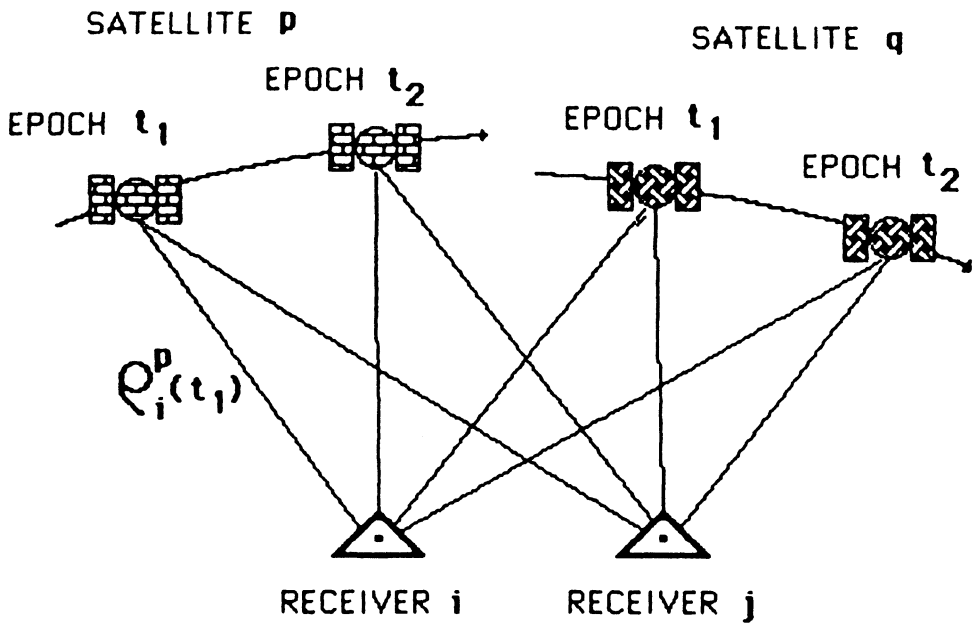

BETWEEN-RECEIVER	BETWEEN-SATELLITE	BETWEEN-EPOCH
$[\rho_i^p(t_1) - \rho_j^p(t_1)]$	$[\rho_i^p(t_1) - \rho_i^q(t_1)]$	$[\rho_i^p(t_2) - \rho_i^p(t_1)]$
$[\rho_i^q(t_1) - \rho_j^q(t_1)]$	$[\rho_i^p(t_1) - \rho_i^q(t_1)]$	$[\rho_j^p(t_2) - \rho_j^p(t_1)]$
$[\rho_i^p(t_2) - \rho_j^p(t_2)]$	$[\rho_i^p(t_2) - \rho_i^q(t_2)]$	$[\rho_i^q(t_2) - \rho_i^q(t_1)]$
$[\rho_i^q(t_2) - \rho_j^q(t_2)]$	$[\rho_j^p(t_2) - \rho_j^p(t_2)]$	$[\rho_j^q(t_2) - \rho_j^q(t_1)]$

GPS PHASE MEASUREMENT DIFFERENCING

FIGURE 5

Between-receiver differences remove or reduce the effect of satellite clock errors (and cancel the β^j term in the ambiguity expression of equation 2, which is common to both measurements). For baselines which are short compared to the 20,000 km GPS satellite height, between-receiver differences also significantly reduce the effect of satellite ephemeris and atmospheric refraction errors. **Between-satellite** differences remove or reduce the effects of receiver clock errors (and cancel the α_i term in the ambiguity expression of equation 2, which is common to both measurements). **Between-epoch** differences are the same as integrated Doppler measurements (and cancel all three terms $\alpha_i + \beta^j + N_i^j$ in the ambiguity expression of equation 2, all of which are common to both measurements). However, clock errors remain in this case. **Between-frequency** differences are not made for the purpose of ionospheric refraction correction, but rather to generate a signal which is a linear combination of L1 and L2, and hence has a coarser (or finer) wavelength (Hatch and Larson, 1985).

Many combinations of these differences are possible. It is important that which differences, and their order, be specified in describing a processing method. For example, **Receiver-Satellite Double Differences** refers to differencing between receivers first and between satellites second; **Receiver-Time Double Differences** refers to differencing between receivers first, then between time epochs; **Receiver-Satellite-Time Triple Differences** refers to differencing between receivers, then satellites, and finally time.

Figure 5 illustrates differences between receivers, satellites and epochs for the simplest possible case (two receivers, two satellites, two epochs, and one frequency). A total of eight carrier beat phase measurements are made. Each of the three possible single differences reduces this to four. Double differencing further reduces this to two measurements. These measurements correspond to only one triple difference measurement. In practice, many more receivers, satellites and epochs are involved. In this case, there are, for example, many ways in which Receiver-Satellite Double Differences can be formed.

NETWORK SOLUTIONS

GPS network processing techniques are still in their infancy, and it is probably too early to fully define the terminology required to describe and distinguish between them. However some of the simple concepts can be stated.

The simplest static relative positioning observation strategy, to survey a network of points, is to use one pair of receivers which occupy, in some sequence, all the baselines desired to determine the network. Most of the work done to date has used this method. In this case, two concepts are well defined:

A **BASELINE** consists of a pair of stations for which simultaneous GPS data has been collected.

A two-receiver **OBSERVING SESSION** is the period of time over which GPS data is collected simultaneously at both ends of one baseline.

When more than two receivers are used simultaneously, the baseline and session concepts must be extended:

A **n**-receiver **OBSERVING SESSION** is the period of time over which GPS data is collected simultaneously at **n** stations.

Two **SESSIONS** are **INDEPENDENT** to the extent that we can ignore any common biases affecting the observations in both cases.

Two **BASELINES** are **INDEPENDENT** if they have been determined from independent sessions.

Once enough GPS satellites are in orbit to provide continuous coverage, the definition of a multi-receiver observing session will become more blurred, since the definite break between sessions now provided by the limited periods of satellite availability will no longer exist.

To obtain a network solution, either the GPS observations can be taken directly into a network adjustment program, or else the baseline solutions can be obtained individually first, and taken as vector pseudo-observations into a simpler three dimensional network adjustment. The advantage of the former approach is that biases and correlations affecting the data can more easily be taken into account. In each case, the network adjustment may use either a batch algorithm (processing the entire set of observations in one run), or a sequential algorithm (in which the data can be processed and results obtained on a session by session, or even observation by observation, basis). The most important practical property of a sequential alogorithm is that the data can be processed in a sequence of computer runs, rather than in one large run. Programs having this property are said to have a "restart" capability.

UNCERTAINTIES

Uncertainties in surveying are conventionally expressed in terms of covariance matrices. The uncertainty in a set observations ℓ is contained in the covariance matrix C_ℓ for those observations. In general this quantity will be the sum of the contributions from many error sources. Each error source will have its own properties, such as

dependence on geometry, correlations in various ways between observations, etc. Accounting for these properties is not a simple task, and to date has not been fully addressed for GPS.

The uncertainty in a solution **X** is contained in the solution covariance matrix $C_x = (P_x + A^T P_\ell A)^{-1}$ where P_x = the *apriori* solution weight matrix, **A** = the design matrix, and $P_\ell = C_\ell^{-1}$.

For planning and preanalysis, it is often convenient to separate the geometric factors affecting the solution (contained in **A**) from the measurement uncertainties (contained in P_ℓ). One scalar measure of these geometrical factors is the dilution of precision

The **DILUTION OF PRECISION (DOP)** is given by

$$DOP = \sqrt{Trace(A^T A)^{-1}} \quad .$$

The smaller the DOP, the stronger the geometry.

In the case of kinematic point positioning, several kinds of DOP exist, depending on the parameters of the solution:

- **GDOP** = geometrical DOP (three position coordinates plus clock offset)
- **PDOP** = position DOP (three coordinates)
- **HDOP** = horizontal DOP (two horizontal coordinates)
- **VDOP** = vertical DOP (height only)
- **TDOP** = time DOP (clock offset only)
- **HTDOP** = horizontal-time DOP (two horizontal coordinates and clock offset).

When the DOP factor exceeds a specified maximum value at some location for some period of time, it indicates that the normal equation matrices in those circumstances have become ill-conditioned to some extent. This is sometimes referred to as an "outage" of the GPS system.

For static positioning applications, what is important are the variations in the geometry of the satellite configuration over the entire time span of the data, and over the network of receivers simultaneously tracking the signals. This may not be adequately represented by the geometrical configuration at one instant at a single location. However, it may be impractical to attempt to evaluate a more rigorous DOP.

Standard methods of expressing kinematic application accuracies recently adopted by NATO [1983] are presented here without recommendation, for comment:

- For one dimensional error, the interval in metres containing 95% of the observations.

- For two or three dimensional radial error, the number which represents the radial distance in metres centred on the mean position of a large number of trials of the actual or desired system, which includes 95% of the observations.
- To express performance independant of geometrical factors, a 95% measure in terms of portions of a cycle or of a second.
- Speed accuracy as a dimensioned number (e.g. cm/sec) including 95% of observations from a large number of trials.

REFERENCES

Bauersima, I. (1983). "NAVSTAR/Global Positioning System (GPS) III: Erdvermessung durch radiointerferometriche satellitenbeobachtungen." Miteilungen der satelliten-beobachtungstation Zimmerwald Nr. 12, Drucherei der Universitat Bern.

Bossler, J.D., C.C. Goad and P.L. Bender (1980). "Using the Global Positioning System (GPS) for geodetic positioning." Bulletin Geodesique, 54, pp. 553-563.

Bowditch, N. (1981). "Useful tables, calculations, glossary of marine navigation." Vol. II of The American Practical Navigator, Publication No. 9, DMAHTC, Washington, D.C.

Buennagal, L.A., P.F. MacDoran, R.E. Neilan, D.J. Spitzmesser and L.E. Young (1984). "Satellite emission range inferred earth survey (SERIES) project: Final report on research and development phase, 1979 to 1983." JPL publication 84-16, March.

Counselman, C. and S. Gourevitch (1981). "Miniature interferometer terminals for earth surveying: Ambiguity and multipath with Global Positioning System." IEEE Transactions on Geoscience and Remote Sensing, Vol. GE-19, No. 4, pp. 244-252.

Davidson, D., D. Delikaraoglou, R. Langley, B. Nickerson, P. Vanicek and D. Wells (1983). "Global Positioning System differential positioning simulations." Department of Surveying Engineering Technical Report 90, University of New Brusnwick, Fredericton.

Dixon, R.C. (1975). Spread Spectrum Systems. John Wiley.

Goad, C.C. and B.W. Remondi (1983). "Initial relative positioning results using the Global Positioning System." Paper presented at the XVIII General Assembly of the IUGG, IAG Symposium D, Hamburg, F.R.G., August.

Hatch, R. and K. Larson (1985). "MAGNET-4100 GPS survey program test results." These proceedings.

Johnson, C.R., P.W. Ward, M.D. Turner and S.D. Roemerman (1981). "Applications of a multiplexed GPS user set." In: Global Positioning System. Papers published in Navigation, reprinted by The (U.S.) Institute of Navigation, Vol. II, pp. 61-77.

Jorgensen, P.S. (1980). "NAVSTAR/Global Positioning System 18-satellite constellations." In: Global Positioning System. Papers published in Navigation, reprinted by The (U.S.) Institute of Navigation, Vol. II, pp. 1-12.

Kalafus, R.M. (1984). "RTCM SC-104 progress on differential GPS standards." Presented at the Annual Meeting of the U.S. Institute of Navigation, Cambridge, MA, June.

Martin, E.H. (1980). "GPS user equipment error models." In: Global Positioning System. Papers published in Navigation, reprinted by The (U.S.) Institute of Navigation, pp. 109-118.

McDonald, K.D. and R. L. Greenspan (1985). "A survey of GPS satellite system alternatives and their potential for precise positioning" These proceedings.

Mertikas, S. (1983). "Differential Global Positioning System navigation: A geometrical analysis." M.Sc. thesis, Department of Surveying Engineering, University of New Brunswick, Fredericton, May.

Milliken, R.J. and C.J. Zoller (1980). "Principle of operation of NAVSTAR and system characteristics." In: Global Positioning System. Papers published in Navigation, reprinted by The (U.S.) Institute of Navigation, pp. 3-14.

NATO (1983). "Method of expressing navigation accuracies." North Atlantic Treaty Organization Standardization Agreement 4278.

Remondi, B.W. (1984). "Using the Global Positioning System (GPS) phase observable for relative geodesy: Modelling, processing, and results." Ph.D. dissertation, The University of Texas at Austin, May.

Scott, V.D. and J.G. Peters (1983). "A standardized exchange format for NAVSTAR GPS geodetic data." Applied Research Laboratories, The University of Texas at Austin, March.

Spilker, J.J. (1980). "GPS signal structure and performance characteristics." In: Global Positioning System. Papers published in Navigation, reprinted by The (U.S.) Institute of Navigation, pp. 29-54.

Stiffler, J.J. (1966). "Telecommunications." Vol. V of Space Technology, NASA.

United States Department of Defense/Department of Transportation (1982). Federal Radionavigation Plan. Vols. I-IV, March.

van Dierendock, A.J., S.S. Russell, E.R. Kopitzke and M. Birnbaum (1980). "The GPS navigation message." In: Global Positioning System. Papers published in Navigation, reprinted by The (U.S.) Institute of Navigation, pp. 55-73.

Ward, P. (1981). "An inside view of pseudorange and delta pseudorange measurements in a digital NAVSTAR GPS receiver." Presented at the ITC/USA/'81 International Telemetering Conference, San Diego, October.

Wells, D. (1974). "Doppler satellite control." Department of Surveying Engineering Technical Report 29, University of New Brunswick, Fredericton, N.B.

Wells, D., P. Vanicek and D. Delikaraoglou (1981). "Application of NAVSTAR/GPS to geodesy in Canada: Pilot study." Department of Surveying Engineering Technical Report 76, University of New Brunswick, Fredericton, N.B.

APPENDIX 1
GLOSSARY OF GPS TERMINOLOGY

Ambiguity

see Carrier Beat Phase Ambiguity

Bandwidth

A measure of the width of the spectrum of a signal (frequency domain representation of a signal) expressed in Hertz (Stiffler, 1966).

Baseline

A baseline consists of a pair of stations for which simultaneous GPS data has been collected.

Beat frequency

Either of the two additional frequencies obtained when signals of two frequencies are mixed, equal to the sum or difference of the original frequencies, respectively. For example, in the identity,

$$\cos A \cos B = (\cos(A+B) + \cos(A-B))/2,$$

the original signals are **A** and **B** and the beat signals are **A+B** and **A-B**. The term Carrier Beat Phase refers only to the difference **A-B**, where **A** is the incoming Doppler-shifted satellite carrier signal, and **B** is the nominally-constant reference frequency generated in the receiver.

Between-epoch difference

The difference between two complete carrier beat phase measurements made by the same receiver on the same signal (same satellite, same frequency), but at different time epochs.

Between-frequency difference

The instantaneous difference between (or, more generally, any other linear combination involving) the complete carrier beat phase measurements made by the same receiver observing signals from the same satellite at two (or more) different frequencies.

Between-receiver difference

The instantaneous difference in the complete carrier beat phase measurement made at two receivers simultaneously observing the same received signal (same satellite, same frequency).

Between satellite difference

The instantaneous difference in the complete carrier beat phase measurement made by the same receiver observing two satellite signals simultaneously (same frequency).

Binary pulse code modulation

Pulse modulation using a string (code) of binary numbers. This coding is usually represented by ones and zeros with definite meanings assigned to them, such as changes in phase or direction of a wave (Dixon, 1975).

Binary biphase modulation

Phase changes on a constant frequency carrier of either 0° or 180° (to represent binary 0 or 1 respectively). These can be modelled by $y = A(t) \cos(\omega t + \phi)$, where the amplitude function $A(t)$ is a sequence of +1 and -1 values (to represent 0° and 180°phase changes respectively) (Dixon, 1975).

Carrier

A radio wave having at least one characteristic (e.g., frequency, amplitude, phase) which may be varied from a known reference value by modulation (Bowditch, 1981, Vol. II).

Carrier frequency

The frequency of the unmodulated fundamental output of a radio transmitter (Bowditch, 1981, Vol. II).

Carrier beat phase

The phase of the signal which remains when the incoming Doppler-shifted satellite carrier signal is beat (the difference frequency signal is generated) with the nominally-constant reference frequency generated in the receiver.

Carrier beat phase ambiguity

The uncertainty in the initial measurement, which biases all measurements in an unbroken sequence. The ambiguity consists of three components

$$\alpha_i + \beta^j + N_1^j$$

where

α_i is the fractional initial phase in the receiver

β^j is the fractional initial phase in the satellite (both due to various contributions to phase bias, such as unknown clock phase, circuit delays, etc.), and

N_1^j is an integer cycle bias in the initial measurement.

Channel

A channel of a GPS receiver consists of the radiofrequency and digital hardware, and the software, required to track the signal from one GPS satellite at one of the two GPS carrier frequencies.

Chip

The minimum time interval of either a zero or a one in a binary pulse code.

C/A-code

see S-code.

Complete instantaneous phase measurement

A measurement of carrier beat phase which includes the integer number of cycles of carrier beat phase since the initial phase measurement. See fractional instantaneous phase measurement.

Correlation-type channel

A GPS receiver channel which uses a delay lock loop to maintain an alignment (correlation peak) between the replica of the GPS code generated in the receiver and the incoming code.

Delay lock

The technique whereby the received code (generated by the satellite clock) is compared with the internal code (generated by the receiver clock) and the latter shifted in time until the two codes match. Delay lock loops can be implemented in several ways, for example, tau dither and early-minus-late gating (Spilker, 1980).

Delta pseudorange

The difference between two carrier beat phase measurements, made coincidentally with (code) pseudorange epochs.

Differenced measurements

see Between-epoch difference; Between-frequency difference; Between-receievr difference; Between-satellite difference.

Many combinations of differences are possible. Which differences, and their order, should be specified in describing a processing method (for example Receiver-Satellite Double Differences).

Differential positioning

see Relative Positioning

Dilution of precision (DOP)

A description of the purely geometrical contribution to the uncertainty in a dynamic position fix, given by the expression

$$DOP = \sqrt{TRACE(A^T A)^{-1}},$$

where **A** is the design matrix for the solution (dependent on satellite/receiver geometry). The DOP factor depends on the parameters of the position fix solution. Standard terms in the case of kinematic GPS are:
GDOP (three position coordinates plus clock offset in the solution)
PDOP (three coordinates)
HDOP (two horizontal coordinates)
VDOP (height only)
TDOP (clock offset only), and
HTDOP (horizontal position and time).

Doppler shift

The apparent change in frequency of a received signal due to the rate of change of the range between the transmitter and receiver. See carrier beat phase.

Dynamic positioning

see Kinematic positioning

Fast switching channel

A switching channel with a sequence time short enough to recover (through software prediction) the integer part of the carrier beat phase.

Fractional instantaneous phase measurement

A measurement of the carrier beat phase which does not include any integer cycle count. It is a value between zero and one cycle. See complete instantaneous phase measurement.

Frequency band

A range of frequencies in a particular region of the electromagnetic spectrum (Wells, 1974).

Frequency spectrum

The distribution of amplitudes as a function of frequency of the constituent waves in a signal (Wells, 1974).

Handover word

The word in the GPS message that contains time synchronization information for the transfer from the S-code to the P-code (Milliken and Zoller, 1980).

Independent baselines

Baselines determined from independent observing sessions.

Independent observing sessions

Sessions for which any common biases affecting the observations can be ignored.

Ionospheric refraction

A signal travelling through the ionosphere (which is a nonhomogeneous and dispersive medium) experiences a propagation time different from that which would occur in a vacuum. Phase advance depends on electron content and affects carrier signals. Group delay depends on dispersion in the ionosphere as well, and affects signal modulation (codes). The phase and group advance are of the same magnitude but opposite sign (Davidson et al., 1983).

Interferometry

see Relative positioning

Kinematic positioning

Kinematic positioning refers to applications in which a trajectory (of a ship, ice field, tectonic plate, etc.) is determined.

Lane

The area (or volume) enclosed by adjacent lines (or surfaces) of zero phase of either the carrier beat phase signal, or of the difference between two carrier beat phase signals. On the earth's surface a line of zero phase is the locus of all points for which the observed value would have a exact integer value for the complete instantaneous phase measurement. In three dimensions, this locus becomes a surface.

L-band

The radio frequency band extending from 390 MHz to (nominally) 1550 MHz (Bowditch 1981, Vol. II).

Multipath error

An error resulting from interference between radiowaves which have travelled between the transmitter and the receiver by two paths of different electrical lengths (Bowditch, 1981, Vol. II).

Multichannel receiver

A receiver containing many channels.

Multiplexing channel

A receiver channel which is sequenced through a number of satellite signals (each from a specific satellite and at a specific frequency) at a rate which is synchronous with the satellite message bit-rate (50 bits per second, or 20 milliseconds per bit). Thus one complete sequence is completed in a multiple of 20 milliseconds.

Observing session

The period of time over which GPS data is collected simultaneously by two or more receivers.

Outage

The occurrence in time and space of a GPS Dilution of Precision value exceeding a specified maximum.

Phase lock

The technique whereby the phase of an oscillator signal is made to become a smoothed replica of the phase of a reference signal by first comparing the phases of the two signals and then using the resulting phase difference signal to adjust the reference oscillator frequency to eliminate phase difference when the two signals are next compared (Bowditch, 1981, Vol. II). The smoothing time span occurs over approximately the inverse of the bandwidth. Thus a 40 hertz loop bandwidth implies an approximately 25 millisecond smoothing time constant.

Phase observable

See carrier beat phase.

P-code

The Precise (or Protected) GPS code--a very long (about 1014 bit) sequence of pseudorandom binary biphase modulations on the GPS carrier at a chip rate of 10.23 MHz which does not repeat itself for about 267 days. Each one-week segment of the P-code is unique to one GPS satellite, and is reset each week.

Precise positioning service (PPS)

The highest level of dynamic positioning accuracy that will be provided by GPS, based on the dual frequency P-code (U.S. DoD/DOT, 1982).

Pseudolite

The ground-based differential GPS station which transmits a signal with a structure similar to that of an actual GPS satellite (Kalafus, 1984).

Pseudorandom noise (PRN) code

Any of a group of binary sequences that exhibit noise-like properties, the most important of which is that the sequence has a maximum autocorrelation, at zero lag (Dixon, 1975).

Pseudorange

The time shift required to align (correlate) a replica of the GPS code generated in the receiver with the received GPS code, scaled into distance by the speed of light. This time shift is the difference between the time of signal reception

(measured in the receiver time frame) and the time of emission (measured in the satellite time frame).

Pseudorange difference

See carrier beat phase.

Receiver channel

See channel

Reconstructed carrier phase

see Carrier Beat Phase

Relative positioning

The determination of relative positions between two or more receivers which are simultaneously tracking the same radiopositioning signals (e.g. from GPS).

Restart capability

The proprerty of a sequential processing computer program, that data can be processed rigorously in a sequence of computer runs, rather than only in one long run.

S-code

The Standard GPS code (formerly the C/A, Coarse/Acquisition, or Clear/Access code) -- a sequence of 1023 pseudorandom binary biphase modulations on the GPS carrier at a chip rate of 1.023 MHz, thus having a code repetition period of one millisecond.

Satellite constellation

The arrangement in space of the complete set of satellites of a system like GPS.

Satellite configuration

The state of the satellite constellation at a specific time, relative to a specific user or set of users.

Simultaneous measurements

Measurements referred to time frame epochs which are either exactly equal, or else so closely spaced in time that the time misalignment can be accomodated by correction terms in the observation equation, rather than by parameter estimation.

Slow switching channel

A switching channel with a sequencing period which is too long to allow recovery of the integer part of the carrier beat phase.

Spread spectrum systems

A system in which the transmitted signal is spread over a frequency band much wider than the minimum bandwidth needed to transmit the information being sent (Dixon, 1975).

Squaring-type channel

A GPS receiver channel which multiplies the received signal by itself to obtain a second harmonic of the carrier, which does not contain the code modulation.

Standard positioning service (SPS)

The level of kinematic positioning accuracy that will be provided by GPS based on the single frequency S-code (U.S. DoD/DOT, 1982).

Static positioning

Positioning applications in which the positions of points are determined, without regard for any trajectory they may or may not have.

Switching channel

A receiver channel which is sequenced through a number of satellite signals (each from a specific satellite and at a specific frequency) at a rate which is slower than, and asynchronous with, the message data rate.

Translocation

See relative positioning.

User equivalent range error (UERE)

The contribution to the range measurement error from an individual error source, converted into range units, assuming that error source is uncorrelated with all other error sources (Martin, 1980).

Z-count word

The GPS satellite clock time at the leading edge of the next data subframe of the transmitted GPS message (usually expressed as an integer number of 1.5 second periods) (van Dierendock et al., 1980).